université de BORDEAUX

THÈSE PRÉSENTÉE

POUR OBTENIR LE GRADE DE

DOCTEUR DE

L'UNIVERSITÉ DE BORDEAUX

ÉCOLE DOCTORALE des Sciences de la vie et de la santé

SPÉCIALITÉ : Biologie végétale

Par Marc LABADIE

DECIPHERING SPATIO-TEMPORAL DEVELOPMENT OF STRAWBERRY PLANT

Sous la direction de : Béatrice DENOYES
(co-directeur : Yann GUÉDON)

Soutenue le 21 décembre 2017

Membres du jury :

M. LAURI, Pierre-Eric	Ingénieur de Recherche, INRA Montpellier	Rapporteur
M. SAKR, Soulaiman	Professeur, AgroCampus Ouest d'Angers	Rapporteur
M. HERNOULD, Michel	Professeur, Université de Bordeaux	Président du Jury
Mme. OLLAT, Nathalie	Ingénieure de Recherche, ISVV Bordeaux	Examinateur
Mme. DEMENÉ, Marie-Noëlle	Ingénieure, Invenio	Invitée
Mme. DENOYES, Béatrice	Ingénieure de Recherche, INRA Bordeaux	Directrice de thèse
M. GUÉDON, Yann	Directeur de Recherche, CIRAD Montpellier	Co-directeur de thèse

Résumé

Chez le fraisier la balance entre floraison et développement végétatif incluant la production de stolons (tiges allongées portant les plants filles) conditionne le rendement du plant. L'objectif de la thèse était d'obtenir une meilleure compréhension des processus de développement du fraisier, la floraison, le développement végétatif des axes et le stolonnage, grâce à une étude spatio-temporelle. Trois approches complémentaires ont été développées sur six variétés non-remontantes plantées en conditions « hors-sol » : (1) la modélisation des profils d'émergence hebdomadaire de fleurs, feuilles et stolons par une analyse de segmentation longitudinale, (2) l'analyse spatio-temporelle de l'architecture des plants durant une saison de production et (3) le suivi de l'expression de gènes clés liés à la floraison.

(1) Les modèles univariés de détection de ruptures appliqués à chaque variable phénologique étaient basés sur l'hypothèse que les changements de phases sont synchrones entre les individus d'une même variété. Ces modèles ont permis d'identifier des phases pour chacune des variétés et chacun des trois types d'organe. Les modèles de détection de ruptures multivariés combinant les trois types d'organes ont permis de mettre en évidence une forte structuration du développement du fraisier par la floraison et le stolonnage. De plus, les variétés se regroupent autour de deux profils de floraison avec la présence ou pas d'un deuxième pic de floraison. Enfin, les modèles d'émergence de stolon montrent un synchronisme suggérant un fort effet environnemental.

(2) L'analyse spatio-temporelle de l'architecture s'est basée sur un modèle de graphe arborescent multi-échelle, permettant une représentation visuelle et une analyse de la topologie du plant au cours de son développement. Cette analyse a permis de mettre en évidence des différences topologiques précoces ainsi que différentes stratégies de développement entre les variétés. Ces différences de développement expliquent en partie les différents profils de floraison.

(3) Parmi les gènes étudiés pour leur expression au cours de la culture des plants de fraisier, *SUPPRESSOR OF OVEREXPRESSION OF CONSTANS1* (*SOC1*) apparait comme un marqueur de développement végétatif et de l'émergence des stolons. Une approche architecturale a également été initiée sur le fraisier diploïde. Les premiers résultats ont permis de mieux préciser le devenir des méristèmes axillaires.

En conclusion, ce travail a permis d'évaluer les variétés en condition de production et d'identifier des critères de sélection pour le développement de nouvelles variétés. Il a également permis de développer de nouveaux outils qui pourront être utilisés par les sélectionneurs et les expérimentateurs.

Mots clés : Fraisier, Développement, Phénologie, Architecture, Modélisation, Floraison

Abstract

In strawberry, the balance between flowering and vegetative development, including the production of stolons (elongated stems carrying the daughter plants), conditions the yield of the plant. The objective of the thesis was to better understand the developmental processes of strawberry plant, namely flowering, the vegetative development of axes and runnering, through a spatio-temporal study. Three complementary approaches have been developed on seasonal flowering varieties planted in "soilless" conditions: (1) modeling the weekly emergence of flowers, leaves and stolons by a longitudinal segmentation analysis, (2) spatio-temporal analysis of plant architecture during a seasonal production and (3) expression of key genes related to flowering.

(1) Univariate multiple change-point models applied to each phenological variable were based on the assumption that phase changes were synchronous between individuals of a given variety. These models allowed to identify phases for each variety and each type of organ. Multivariate multiple change-point models combining the three types of organ highlighted a strong structuring of strawberry development by flowering and runnering. Moreover, the varieties can be grouped into two profiles of flowering with the presence or not of a second period of flowering. Finally, the stolon emergence models show a synchronism suggesting a strong environmental effect.

(2) Spatio-temporal analysis of the architecture relied on a multi-scale tree graph allowing visual representation and topological analysis of plant development. This analysis revealed early topological differences as well as different strategies of development between varieties. These differences in development partially explain the different flowering patterns.

(3) Among the genes studied for their expression during the cultivation of strawberry plants, SUPPRESSOR OF OVEREXPRESSION OF CONSTANS1 (SOC1) appears as a marker of vegetative development and stolon emergence.

An architectural approach was also initiated on the diploid strawberry. First results allowed to better specify the fate of axillary meristems.

In conclusion, this work allowed to evaluate the varieties in production condition and to identify selection criteria for the development of new varieties. It has also allowed the development of new tools that can be used by breeders and experimenters.

Keywords: Strawberry, Development, Phenology, Architecture, modeling, flowering

Acknowledgment

Après trois ans j'arrive (enfin!) au bout de cette thèse. Malgré les difficultés, les coups de blues et de nombreuses notations et architectures. Cette thèse restera dans mon esprit comme le premier projet que j'ai eu en main du début à la fin, MON projet. Et quelle joie, quand, après de nombreuses heures d'analyse et d'écriture devant l'ordinateur, de réussir à donner un sens à toutes ces données cumulées.
Néanmoins, je n'ai pas pu réaliser cette thèse seul, et sans le soutien et l'aide des nombreuses personnes qui m'ont entouré pendant ces trois années je ne serais sans doute pas arrivé au bout. Je tiens donc ici à les remercier pour tout ce qu'elles m'ont apporté.

Tout d'abord, mes directeurs de thèse, Béatrice Denoyes et Yann Guédon, pour leur disponibilité et l'aide apportée dans la rédaction et la relecture de ce manuscrit. Je les remercie également pour tous les échanges que nous avons pu avoir aussi bien professionnels que personnels ainsi que pour leur patience. Je remercie Béatrice, pour sa confiance et son soutien tout au long de la thèse, mais également pour toutes les connaissances supplémentaires que j'ai pu accumuler au cours de cette thèse en particulier sur le fraisier. Je remercie Yann, pour sa confiance et son soutien tout au long de la thèse, mais également de m'avoir appris la rigueur nécessaire dans les analyses statistiques et m'avoir permis de découvrir de nouvelles méthodes d'analyse qui m'étaient inconnues jusqu'à présent.

Je souhaiterais également remercier mes 2 rapporteurs, Mrs Soulaiman Sakr et Pierre-Eric Lauri, qui ont accepté de relire et corriger ce mémoire de thèse, ainsi que pour le délai supplémentaire qu'ils m'ont gentiment accordé, ainsi que M. Michel Hernould, Mmes. Nathalie Ollat et Marie Noëlle Demené qui ont accepté d'être examinateur lors de la soutenance de thèse. J'adresse mes remerciements également aux membres de mon comité de thèse Mmes Catherine Rameau et Christine Granier, ainsi qu'à ma tutrice de thèse Fatma Lecourieux, pour les éclairages et les idées qu'elles m'ont apportés pour la poursuite de mes travaux de thèse.

Ce projet n'aurait pas été réalisé sans le soutien de la Région Aquitaine et de l'INRA pour le financement de cette thèse ainsi que les professionnels de la fraise, Invenio et le Ciref, qui m'ont fait confiance et qui ont mis à ma disposition les moyens nécessaires dans la réalisation de mes travaux. Je voudrais également remercier tous les membres d'Invenio et du

Ciref pour leur accueil et leur gentillesse, mais particulièrement Karine Guy pour l'aide apportée ainsi que ses conseils lors des notations en serre ainsi que les notations d'architecture.

Evidemment, je souhaite remercier tous les membres de l'équipe OrFE (Organogenèse du fruit et endoréplication), de l'UMR BFP pour leur aide, leur soutien et les plaisanteries que nous avons eus ensemble ainsi que les parties de babyfoot que nous avons pu partager et les enguelades pour la paillasse sale notamment avec les Freds. Mais également l'équipe Génomique fonctionnelle du développement du fruit de l'UMR BFP, pour les moments partagés au cours de nombreux repas le midi, et pour les fêtes et les repas de fin d'année. Parmi les membres de l'équipe je tiens particulièrement à remercier Flavie Metais pour son travail sur l'expression des gènes de clefs de floraison incorporer dans ce travail.

Je tiens également à remercier tous les membres de mon équipe du CIRAD de Montpellier, équipe M2P2, pour tous les moments partagés ensemble lors de mes nombreux déplacements dans les locaux. Parmi ces membres, je tiens tout particulièrement à remercier Christophe Pradal, pour ces longues heures de conseil et de formation au langage Python et au développement du package strawberry sur OpenAléa. Je tiens également à remercier Yves Caraglio de l'UMR AMAP du CIRAD pour son aide, les nombreuses discussions et conseils, et son implication dans ma thèse.

Merci également à tous mes camarades de galère et de bureau, de colocation et de pauses cigarette parfois : Léa, Isma, Tracey, ainsi que les autres thésards, amis et confidents de déprime de Bordeaux et Montpellier : Aurélia, Jean-Phillipe (JP), Rémi, Moogly, Arthur, Adrien. Parmi toutes ces personnes, je tiens tout particulièrement à remercier Clémence De Jaham qui est devenu ma compagne pendant la thèse, pour son soutien dans la vie de tous les jours, mais également dans l'écriture de la thèse

Pour finir, je voudrais remercier tous les membres ma famille sans qui je ne serais pas là. Mes parents pour m'avoir fait confiance, soutenu durant toutes mes années d'étude. Mes grands-parents pour leurs nombreux coups de fil et leurs déplacements lors des moments difficiles. Mes frères, pour les nombreuses taquineries et bêtises qui m'ont permis de décompresser durant cette thèse.

Résumé en français de la thèse

Contexte :

Chez le fraisier, 3ième production fruitière en termes de chiffre d'affaire en France, la multiplication végétative via les stolons (tiges allongées portant les plants filles) et la reproduction florale via les fleurs se produisent successivement ou conjointement selon le génotype, la technique culturale et l'environnement. Ces deux processus sont importants dans la culture de la fraise car ils déterminent respectivement la production de plants en pépinière et la production de fruits dans les champs, les tunnels ou les serres. Cependant la multiplication végétative se fait au détriment du rendement en fruits. La compréhension de la balance entre la reproduction végétative et florale est donc un enjeu majeur dans la fraisiculture. C'est pourquoi de nombreuses études ont été menées pour comprendre les mécanismes physiologiques, génétiques et environnementaux impliqués dans cette balance. Cependant peu d'études concerne la dynamique de ces processus au cours du temps.

Dans ce contexte l'objectif de ce travail de thèse a été d'approfondir la compréhension du développement du plant par une analyse spatio-temporelle.

Méthodes :

Trois approches complémentaires ont été développées sur six variétés non-remontantes plantées en conditions de production « hors-sol » : (1) la modélisation des profils d'émergence hebdomadaire de fleurs, feuilles et stolons par une analyse longitudinale de segmentation en phases, (2) l'analyse spatio-temporelle de l'architecture des plants durant une saison de production et (3) le suivi de l'expression de gènes clés liés à la floraison.

(1) La modélisation des profils d'émergence hebdomadaire a été réalisée sur trente-deux plants par variété durant vingt-huit semaines. Cette modélisation appliquée à chaque variable phénologique était basée sur l'hypothèse que les changements de phases sont synchrones entre les individus d'une même variété. Une analyse trivariée, c'est-à-dire combinant les trois variables phénologiques étudiées a également été réalisée afin de réaliser une synthèse du développement du plant et d'identifier les processus majeurs qui conditionne le développement du plant.

(2) L'analyse spatio-temporelle de l'architecture du plant a été réalisée sur cinquante-quatre plants par variété par un prélèvement mensuel de neuf plants pour chaque variété au cours de cette même saison de production Elle s'appuie sur un modèle arborescent multi-échelle (MTG) permettant de stocker les informations spatiales et temporelles de chaque entité

décrite (ex. feuilles, inflorescences), de lui associer des propriétés variables selon la nature de cette entité (ex. longueur, nombres de fleurs) et *in fine* de représenter graphiquement la plante dans son entier, ou une portion de cette plante, en 3D ou en 2D. Ce modèle permet ainsi une analyse de la topologie du plant au cours de son développement.

(3) L'analyse de l'expression des gènes impliqués dans la floraison au cours du temps a été réalisée sur des prélèvements de disques foliaires de la dernière feuille la plus étalée identifiée lors de l'analyse de l'architecture des plants sur trois des six génotypes étudiés. Cette analyse d'expression a été réalisée sur trois gènes connus comme étant activateur de la floraison chez le fraisier, *FT1*, *FT2*, et *FT3*, sur le gène *TFL1* connu comme étant un répresseur de floraison et *SOC1* jouant un rôle central dans le contrôle de la balance entre reproductions végétative et florale.

Résultats :

Les analyses phénologiques univariées ont porté sur la floraison, la croissance végétative et l'émergence des stolons. Ces analyses faites pour chacun des génotypes et chaque processus permettent d'une part de montrer que l'ensemble de ces processus peut être décrit sous forme de phases successives bien différenciées et d'autre part de comparer les variétés pour chacun des processus. Ces analyses nous ont permis de grouper les variétés selon leur profil : en deux groupes pour la floraison avec des variétés ayant un pic de floraison suivi d'une production stationnaire jusqu'à la fin de la saison de production, ou deux pics de floraison séparés par une phase de production moins intense ; en trois groupes pour la croissance végétative avec des variétés ayant une production continue de feuilles, un ou deux pics de production de feuilles. Pour l'émergence des stolons un seul pattern a été identifié pour l'ensemble des variétés avec une production de stolons synchrone en fin de période de production.

L'analyse trivariée a permis de mettre en avant une forte structuration des phases de développement du fraisier par la floraison et le stolonnage. Cette analyse a permis de mettre en avant 3 types de comportement avec des variétés ayant : i) deux pics de floraison, deux pics de croissance végétative et 1 pic d'émergence de stolons concomitant avec le second pic de floraison et de croissance végétative ; ii) un pic de floraison, un pic de croissance végétative et un pic d'émergence de stolons concomitant avec le pic de croissance végétative et iii) un seul pic de floraison et un pic d'émergence de stolons avec une croissance végétative continue.

L'analyse exploratoire de l'architecture a été basée sur une analyse exploratoire visuelle 3D et 2D de l'architecture permettant l'identification de cinq variables d'intérêt différenciant les variétés, suivie par une analyse exploratoire statistique de ces cinq variables. Cette analyse exploratoire statistique a permis d'identifier des différences de croissance via l'apparition des modules successifs au cours du temps, des différences de complexité de l'inflorescence, de ramifications, ainsi que des spécificités du rang du module notamment des premiers rangs de modules pour le nombre de feuilles, la complexité de l'inflorescence, le type de ramification et la localisation des stolons.

La mise en parallèle de ces deux études, phénologique et spatio-temporelle de l'architecture, nous a permis *in fine* d'expliquer les différences de profils identifiés lors de l'analyse phénologique par l'architecture. De plus, ces deux études complémentaires nous ont permis d'identifier et d'associer des critères de sélection tels que la complexité de l'inflorescence, la vitesse d'apparition des modules au cours du temps et le type de ramification en fonction des profils de floraison attendus par les producteurs.

Parmi les gènes étudiés pour leur expression au cours de la culture des plants de fraisier, aucune différence d'expression n'a pu être identifiée entre les variétés. Cependant cette étude nous a permis d'identifier l'expression de *SOC1* comme un marqueur du développement végétatif et de l'émergence de stolons.

Conclusion :

Au final ce travail a permis une meilleure compréhension du développement d'un plant de fraisier au travers du développement de méthodes et d'outils d'analyse phénologique et architecturale. Ce travail permet également de mettre en avant de nombreuses perspectives dans la compréhension du développement du fraisier notamment le transfert de la méthodologie ainsi que des outils aux professionnels pour une meilleure évaluation et sélection des variétés. A plus long terme ce travail permettra une meilleure caractérisation des réseaux de gènes impliqués dans la balance entre développement végétatif et floral et particulièrement du devenir du méristème par l'identification au niveau architectural de zones spécifiques du devenir des méristèmes en stolons, ramifications ou en inflorescences. *In fine*, ce travail via l'utilisation de modèle généralisé pourrait permettre aussi bien aux scientifiques qu'aux producteurs de disposer d'un modèle structure-fonction du développement du fraisier permettant de prédire son développement.

Summary

Figures

Tables

Abreviations

AGL24: Agamous-Like 24
AO: Apparent Branching Order
AP1: APETALA 1
BO: Branching Order
bt: Terminal bud
BTC1: Bolting Time Control 1
CO: Constans
DN: Day Neutral
F: Expanded leaf
f: Primordia leave
FAO: Food Agricultural Organization
FLC: Flowering Locus C
FT: Flowering Locus T
GA: Gibberellin
GA20ox4: GA 20-Oxidase 4
GI: GIGANTEA
GU: Growth Unit
HT : Terminal Inflorescence
ht : terminal floral bud
IGP: Indication Géographique Protégée
LD: Long Days
LFY: LEAFY
PEBP: Phosphatidyl Ethanolamine-binding Protein
PF: Perpetual Flowering
QTL: Quantitative Trait Locus
R: Runnering Locus
r: Runnerless
s: Stolon
SD: Short Days
SF: Seasonal Flowering
SFL: SF Locus
SOC1: Suppressor of CO
SVP: Short Vegetative Phase

Chapter 1: Bibliographic synthesis

In this bibliographic synthesis, I chose to present first the two main concepts used in my work, phenology and architecture and their interests. Secondly, I described the current knowledge in strawberry. Thirdly, I will present the context of my PhD study and the approaches and objectives.

1 Phenology: definition, concept, regulation and interest

In this part we will describe after a definition, the concept and short history of phenology, the factors influencing the phenology of plants as well as different interests of the study of phenology in plants.

1.1 Definition, concept and short history of phenology

The word phenology is derived from the Greek word *phainein* meaning to appear. Phenology is defined as the study of periodic life-cycle events during plant or animal life cycle (Forrest and Miller-rushing, 2010). This term was used for the first time in a public lecture at the *Académie royale des Sciences et des Beaux arts de Belgique* in Brussels, 16 December 1849 by Charles Morren (Demarée and Rutishauser, 2011). The concept of phenology is based on recurrent observations and recording of life-history events such as the first opening leaves or flowers, the hatching and the migration of birds (Bussière *et al.*, 2015).

Documenting and recording these regular observations along time and at different scales was of high interest for the mankind knowledges and activities, whether for agriculture or simply as indicator of the succession of cycles across seasons a. As an example, seasons are defined by phenological events: e.g. autumn is associated with leaf fall, winter with dormancy, which is visible by a cessation of plant growth, spring with flowering and summer with fructification. Ancient Greeks recognized phenology as a reliable indicator of local weather. For example, they used the leaf fall as an indicator for sowing winter crops (Bostock *et al.*, 1855; cited by Forrest and Miller-rushing, 2010). In Japan, the date of the cherry festival is related to the full flowering of cherry tree since the 9th century (Yasuyuki Aono and Kazui, 2008; Demarée and Rutishauser, 2011). In Europe, the record of phenological events is a long tradition, which enabled the creation of the unique phenological network in Europe in 1957 by F. Schnelle and E. Volkert, International Phenological Garden (IPG) (Menzel, 2003). The idea of IPG is to make large-scale and standardized phenological observations through a network of gardens. Research within this network is focused on possible impacts of climate changes on forest ecosystems. In all gardens, genetically identical trees and shrubs are planted in order to

compare different developmental stages of plants (phenological phases) along time. During the last 40 years (1959-1998) more than 65.000 observations of 23 plant species with different varieties and provenances have been collected (Menzel and Fabian, 1999).

1.2 Factors influencing the phenology

1.2.1 Environmental factor influencing phenology

The plants, which are sessile organisms, are subjected during their life cycle to seasonal variations. Among these environmental conditions: temperature, photoperiod and water availability are the main factors influencing phenology.

- Effect of temperature on phenology

Recently, one of the most studied effects of temperature on the development of the plant is global warming. Numerous studies carried out on the impact of global warming show that the increase in temperature from the 50s causes a shift of phenological events (Cleland *et al.*, 2007; Ibáñez *et al.*, 2010; Korner and Basler, 2010). Study conducted by Pañelas and collaborators in 2002 is a good example. In their study, they showed that an increase of 1.4°C of the temperature between 1952 and 2000 led to leaf emergence on average 16 days earlier, and fall on average 13 days later in 2000 compared to 1952. Flowers and fruits appear on average 6 days and 9 days earlier than in 1952 and 1974 respectively (Peñuelas *et al.*, 2002). Moreover phenology is not impacted only by warm temperatures. The cold temperatures also affect phenology. For example, in artic area, extended effect of winter icing on the three dominant dwarf shrub species (*Empetrum nigrum*, *Vaccinium vitis-idaea* (both evergreen) and *Vaccinium myrtillus* (deciduous)) leads to a flowering reduction of 57%. Furthermore, they showed that the bud burst was earlier following an icing treatment (Preece *et al.*, 2012).

Numerous reviews and articles on phenology showed that one of the major effect of temperature on plant phenology is related to dormancy (Rathcke and Lacey, 1985; Wilczek *et al.*, 2010; Legave *et al.*, 2015). In temperate regions, many trees and perennial plants including fruit species are dormant in autumn and winter (Luedeling *et al.*, 2013). The dormancy of buds requires an accumulation of chill temperatures in winter in order to overcome the endodormancy phase. It is followed by an ecodormancy phase in which an accumulation of heat temperatures is needed to resume growth and to bloom in spring (Legave *et al.*, 2015). This is

why changes in temperature modify the rate of development of plants. However, identification of these temperatures (chill and heat requirements) is difficult and requires controlled experiments on large scales. The chill and heat requirements are therefore not always available (Luedeling *et al.*, 2013).This is why numerous studies on cultivated varieties of plants such as wheat or cherry tree produce optimum, minimum and maximum temperature for each of the phenological phases in order to optimize the culture potential. For example, the effect of optimum temperatures on the various phenological events was identified and reported in the review of Porter and Gawith (Table 1, reproduced from Porter and Gawith, 1999).

Table 1: Base (Tmin), optimum (Topt) and maximum (Tmax) temperatures for different phenological phases and stages in wheat (issue from Porter and Gawith, 1999)

Phenological stage/ phase	Literature source	*T*min (°C)	*T*opt (°C)	*T*max (°C)	Cultivar
Sowing	Russell and Wilson (1994)	5–7	7.1–20	20.1–30	
Germination/emergence	Petr (1991)	3–4.5	25	35	
	Petr (1991)	1–2	24–28	36–38	
	Petr (1991)	3.9–4.4	25	30–32.2	
	Wilsie (1962)	3.9–4.4	25	30–32.2	
	Ali et al. (1994)	0–2	22.1–29.8	>32	
	Slafer and Rawson (1995b)	<0	<22		
	Gupta (1978)	1	20	>30	Bread wheat
	Narciso et al. (1992)	<2	15–25	>30	S. European
	Petr (1991)	10	12.5–13.5		
	Blum and Sinmena (1994)			>35	Bread wheat
Vernalization	Petr (1991)	<−3–0	2–6	>10	
	Narciso et al. (1992)	<−1	0–3	>12	S. European
	Halevy (1985)	0	7	11	
	Chujo (1975)	<5	4–12	>15	Winter wheat
	Hänsel (1955)	−5	1–6	15	
	Lumsden (1980)	−4	3–10	17	
	Evans et al. (1975)			>30	
Tillering	Narciso et al. (1992)	<3	6–9	>9	S. European
Double ridges	Slafer and Rawson (1995b)		20		
	Slafer and Savin (1991)	4			
Spikelet Initiation	Qu and Wang (1982)		<10.5[a]		
	Halevy (1985)		15		
	Kirby (1985)	0		20–25	
Terminal spikelet	Qu and Wang (1982)		<7.5[b]		Winter wheat
	Qu (1989)				
	Petr (1991)	3	8–12		
Shoot elongation	Narciso et al. (1992)	<12	15–22	>40	S. European
Heading	Slafer and Savin (1991)	3.9	24.3		
Anthesis	Slafer and Savin (1991)	9.5			
	MacDowell (1973)	<10		>30	
	Russell and Wilson (1994)	<10	18–24	>32	
Pollination	Petr (1991)	>10	18–24	32	
Grain-filling	Jenner (1991,b)		20		
	Hawker and Jenner (1993)			>40	
	Slafer and Rawson (1995b)	7	>25		
	Stone et al. (1995)			30–40	
	Hunt et al. (1991)	4.7±0.6			Mean of 10 cultivars
	Wardlaw (1974)		15–18		cv. Crako
	Angus et al. (1981)	8.9			Spring wheat
	Pararajasingham and Hunt (1991)	7.8–8.8			
	Russell and Wilson (1994)	12	20	35	
Maturity	Narciso et al. (1992)	<15	22–25	>32	S. European

[a]Between floret initiation and terminal spikelet.
[b]Between single ridge and glume differentiation.

- Effect of photoperiod on phenology

In addition to temperature, the effects of photoperiod, i.e. daylight duration (and consequently of night), on plant growth and development are well known, notably on growth and flowering. The decrease in the duration of the daylight in winter is a reliable indicator of the end of the growth of temperate plants. Conversely, the increase in duration of the daylight indicates the arrival of spring and the resumption of growth followed by flowering (Wilczek *et al.*, 2010).

The first impact of photoperiod on plant development was identified by Garner and Allard in 1920. During experiments on many species, they realized that in the absence of favorable duration of daylight for some species, vegetative development continued more or less indefinitely causing a phenomenon of gigantism. Conversely, suitable conditions of duration of daylight could lead to an early flowering and maturation of fruits. Species exposed to duration of daylight favorable to growth and sexual reproduction have shown a tendency to ever-blooming and ever-bearing type of development. During temperate plant development in response to short day (SD), signal induces the growth cessation and bud-set associated with the decrease of daylight duration at the end of summer (Rohde *et al.*, 2011; Ding and Nilsson, 2016). The critical daylight duration that is considered to represent a SD varies with latitudinal origin. For poplar, trees growing at northern latitudes have longer critical daylight duration than trees from more southern locations. This ensures that vegetative growth and the induction of dormancy and cold hardiness occur before winter arrival at northern latitudes. In plant model *Arabidopis thaliana,* some experiments showed that an exposure of plants to long photoperiod of 16h promotes flowering whereas an exposition to short photoperiod of 10h leads to a delay of flowering (Ratcliffe *et al.*, 2003). These experiments were conducted to classify plants according to their ability to bloom according to the daylight duration (Garner, 1933):

i) Short Day (SD) plants, which bloom only if the duration of daylight is less than a threshold called critical photoperiod or ten hours in increments of 24 hours
ii) Long Day (LD) plants, who require a duration of daylight greater than the critical photoperiod (12 or 14 hours per day) to flower
iii) Day-neutral plants (DN), which don't require minimum illumination. Instead, they may initiate flowering after attaining a certain overall developmental stage or age, or in response to alternative environmental stimuli, such as vernalization.

- Impact of water availability on phenology

Water availability is important and affects both plant survival and growth (Wilczek *et al.*, 2010). For this reason, water availability has an indirect impact on phenology. Some studies in various plants showed that drought stress is indirectly responsible of late flowering, namely a drought escape strategy. As an example, in *Brassica rapa* and *Avena barbata* plants, the impact of drought period was evaluated by modification of water availability, i.e. well-watered and water-limited conditions (Sherrard and Maherali, 2006; Franks, 2011). In these two articles, results showed that those plants prefer to escape drought by reduction of their life cycle (earlier flowering) rather than to avoid drought by an increase of water use efficiency. In order to escape drought, the response mechanisms of these both species were an increase in transpiration and an inefficient water use.

Plants can also use other mechanisms than earlier flowering to cope with water stress. In a review on the effect of drought stress, Farooq *et al.* (2009) summarized different effects of the drought stress on several crops at different growth stages and its impact on yield (Table 2). For example, they reported that plants adapt their development by a reduction of their growth rate and a reduction of their yield capacity at different development stages. In a study on pea, drought stress impaired the germination and the early seedling. In rice, they reported that drought stress reduces vegetative development and plant growth. Moreover, they reported that a drought stress applied on post-anthesis reduces the grain yield of barley due to a reduction of the anthesis duration (Farooq *et al.*, 2009).

We have seen that phenology is influenced by the environment. However, phenology and its response to the environment are also controlled by genetic mechanisms.

Table 2: Economic yield reduction by drought stress in some representative field crops (from Farooq *et al.*, 2009)

Crop	Growth stage	Yield reduction	References
Barley	Seed filling	49–57%	Samarah (2005)
Maize	Grain filling	79–81%	Monneveux et al. (2005)
Maize	Reproductive	63–87%	Kamara et al. (2003)
Maize	Reproductive	70–47%	Chapman and Edmeades (1999)
Maize	Vegetative	25–60%	Atteya et al. (2003)
Maize	Reproductive	32–92%	Atteya et al. (2003)
Rice	Reproductive (mild stress)	53–92%	Lafitte et al. (2007)
Rice	Reproductive (severe stress)	48–94%	Lafitte et al. (2007)
Rice	Grain filling (mild stress)	30–55%	Basnayake et al. (2006)
Rice	Grain filling (severe stress)	60%	Basnayake et al. (2006)
Rice	Reproductive	24–84%	Venuprasad et al. (2007)
Chickpea	Reproductive	45–69%	Nayyar et al. (2006)
Pigeonpea	Reproductive	40–55%	Nam et al. (2001)
Common beans	Reproductive	58–87%	Martínez et al. (2007)
Soybean	Reproductive	46–71%	Samarah et al. (2006)
Cowpea	Reproductive	60–11%	Ogbonnaya et al. (2003)
Sunflower	Reproductive	60%	Mazahery-Laghab et al. (2003)
Canola	Reproductive	30%	Sinaki et al. (2007)
Potato	Flowering	13%	Kawakami et al. (2006)

1.2.2 Genetic mechanisms regulating plant phenology

Plant phenological events are triggered by environmental cues taking place during the year. These phenological events result in intricate genetic networks that dictate a fine tuning of timing. These networks perceive and integrate not only environmental signals such as photoperiod and temperature but also endogenous signals, such as carbohydrate and hormonal status. A number of contemporary models exploit the growing knowledge of the molecular pathways in response to environmental cues. In these models, the incorporation of genetic and molecular information improved their predictive power and eased to decipher network behaviour (Chew *et al.*, 2012).

Flowering is the best characterized of these pathways regulating phenology. Recent advances in plant genome analysis have revealed a remarkable conservation of the genetic pathways controlling flowering time in *Arabidopsis* and regulating phenology in perennial such as *Populus* and the pathways (Andrés and Coupland, 2012; Ding and Nilsson, 2016). In *A. thaliana*, over the past four decades, many key regulators of flowering time have been identified by isolating and characterizing early and late flowering mutants. Flowering is affected by the photoperiod, ambient temperature, plant hormones and plant age, and approximately six genetic pathways for the promotion or repression of flowering have been identified in Arabidopsis, including photoperiod, temperature, vernalization, gibberellin (GA) biosynthesis, autonomous and aging pathways (Fornara *et al.*, 2010; Dorca-Fornell *et al.*, 2011). In addition, light quality and biotic and abiotic stresses can contribute to floral induction in plants (Amasino and Michaels, 2010; Song *et al.*, 2013) (Figure 1).

Genes that integrate the floral transition pathways have been named floral integrators (reviewed by Parcy, 2005; cited by Dorca-Fornell *et al.*, 2011). *FLOWERING LOCUS T* (*FT*) is such a floral integrator, as it integrates signals from the autonomous and vernalization pathways through its repression by the MADS box factor *FLOWERING LOCUS C* (*FLC*) and its activation by the photoperiod pathway through the B-box transcriptional regulator *CONSTANS* (*CO*) (Searle *et al.*, 2006; cited by Dorca-Fornell *et al.*, 2011). FT belong to the family of phosphatidyl ethanolamine-binding proteins (PEBPs), which is an evolutionarily conserved group of proteins that occur in all taxa from bacteria to animals and plants (see below focus on this family) (Banfield *et al.*, 1998). In long days, which accelerate flowering in Arabidopsis, *CO* codes for a zinc finger and CCT domain- containing transcription factor that accumulates under long day conditions in leaves as a result of the combination of the rhythmic expression of *CO* mRNA and the stabilization of CO protein by light (de Montaigu *et al.*, 2010)

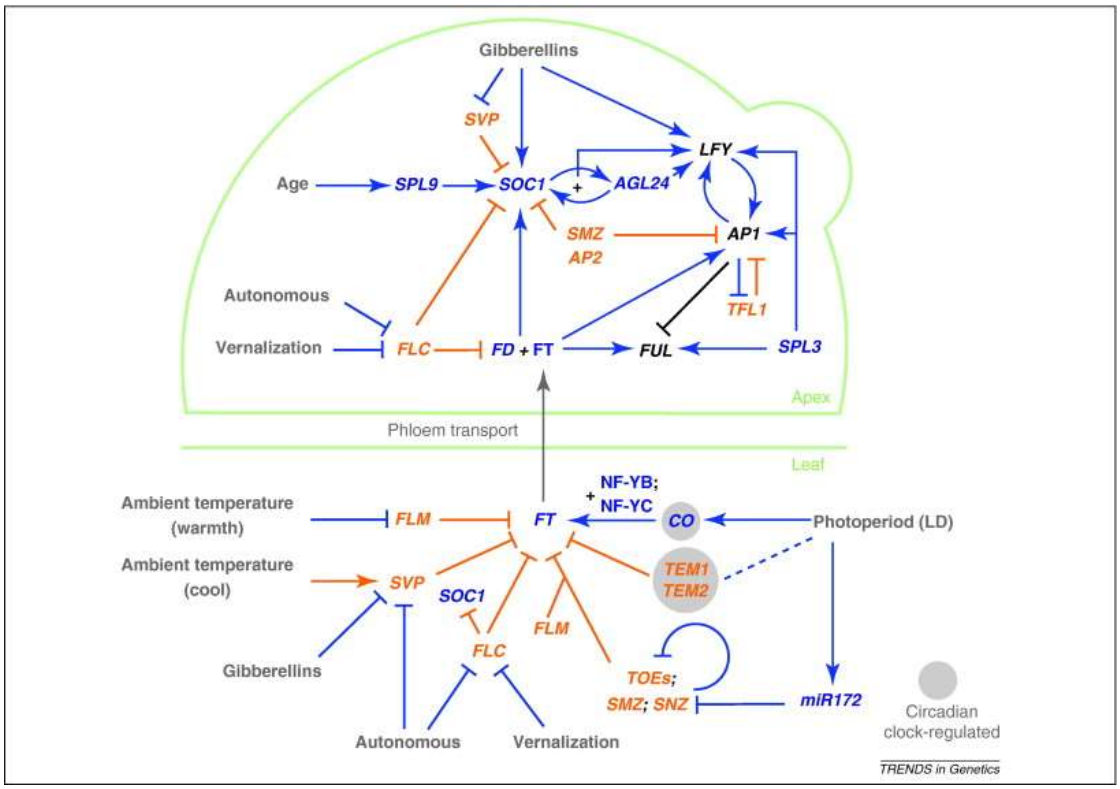

Figure 1: Schematic diagram of the genetic pathways that regulate flowering time in Arabidopsis.
Different pathways respond to various external (photoperiod, vernalization, ambient temperature) and internal (autonomous, age, gibberellins) conditions to regulate the floral transition through an elaborate genetic network. Inductive signals have first to overcome the activity of several repressors of the floral transition (genes indicated in orange), for activators (genes indicated in blue) to eventually turn on the meristem identity genes (*APETAL1 (AP1)* and *LFY*). The pathways operate on different network components (genes) and on different tissues, but the genetic network integrates their inputs through changes in expression of many of its genes. (From Wellmer and Riechmann, 2010)

Another floral integrator is the MADS-box gene *SUPPRESSOR OF OVEREXPRESSION OF CO 1* (*SOC1*). FLC has been shown to bind to regulatory sequences of *SOC1*, and this binding is necessary for its repression (Hepworth *et al.*, 2002). *SOC1* is also activated by FT at the SAM (Searle et al., 2006). Moon *et al.*, 2003 showed that the GA pathway promotes *SOC1* expression. It has also been shown that SOC1 promotes the expression of *LEAFY (LFY)* (Lee *et al.*, 2008). *LFY* is also considered to be a floral integrator since it integrates the photoperiod and the GA pathways through separate cis elements in its promoter (Blázquez and Weigel, 2000). After the floral transition *LFY* is the first meristem identity gene to be expressed and it promotes floral meristem development (Ratcliffe *et al.*, 1999). The other two genes involved in floral meristem identity determination, which play roles in the floral

transition, are the MADS-box genes *SHORT VEGETATIVE PHASE* (*SVP*) and *AGAMOUS-LIKE 24* (*AGL24*) (Gregis *et al.*, 2008). Genetic and molecular evidence revealed that SVP binds to the same promoter regions of *SOC1* and *FT* as *FLC* (Lee *et al.*, 2007).

In plants, members of the PEBP gene family (or *FT/TFL1* family for plants) have been shown to act as key regulators of the transition from the vegetative to the reproductive phase as well as being involved in determining plant architecture (Karlgren *et al.*, 2011). Consequently, these members have been intensively studied in *Arabidopsis thaliana*; in particular, FT and TERMINAL FLOWER1 (TFL1) are among the most thoroughly investigated PEBP proteins. Despite an amino acid identity of over 98%, these two proteins have antagonistic functions: FT promotes flowering by mediating both photoperiod and temperature signals, while TFL1 represses it (Karlgren *et al.*, 2011).

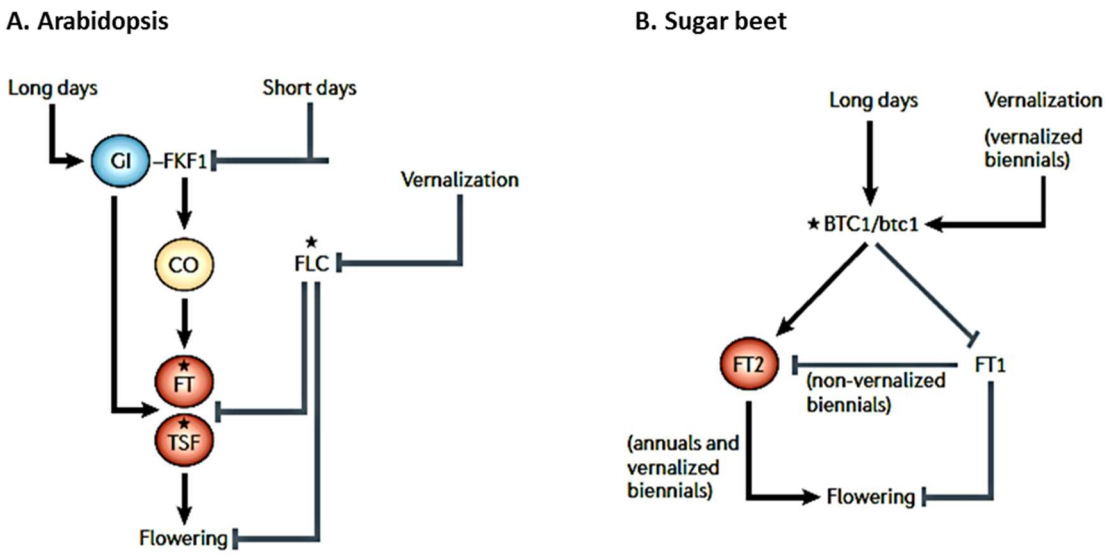

Figure 2: Comparison of flowering time regulation by day length and vernalization in different aradidopsis (a), sugar beet (b).
Grey and black lines represent repression and induction, respectively. Genes marked with a star present allelic diversity associated with natural variation of flowering time. Red shapes indicate homologues of *FT*, yellow shapes indicate homologues of *CONSTANS* (CO) and blue shapes indicate homologues of *GIGANTEA (GI)*. (Modified from Andrés and Coupland, 2012)

If these functions are conserved in numerous flowering plants, different controls of flowering time could be observed such as in beet (Figure 2). In *Beta vulgaris*, two genes belong to the *FT*-like clade, *BvFT1* and *BvFT2*, have been described with antagonist function (Pin *et al.*, 2010). *BvFT2* is the functional *FT* ortholog in beets. Transgenic expression of *BvFT2* in

both *Arabidopsis* and sugar beet strongly promoted flowering. At contrary, *BvFT1* repressed flowering when ectopically expressed in transgenic sugar beet and *Arabidopsis* plants. These data suggest that an *FT*-like gene, evolutionarily more related to *FT* than to *TFL1/CEN*, has evolved into a true flowering repressor.

In *Populus*, two *FT* paralogs, *FT1* and *FT2*, have been described. Sub-functionalization of these *FT*s have been hypothesized based on a year round transcript profiling studies of adult field-grown trees. Hsu and co-authors (2011) proposed that reproductive onset is determined by *FT1* in response to winter temperatures, whereas vegetative growth and inhibition of bud set are promoted by *FT2* in response to warm temperatures and long days in the growing season (Figure 3).

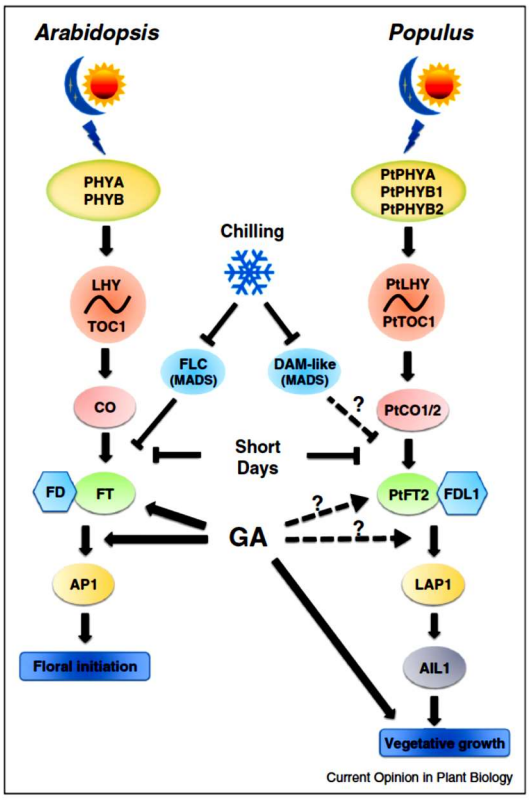

Figure 3: Schematic diagram showing similarities in the proposed regulatory networks controlling floral initiation in *Arabidopsis* (left panel) and vegetative growth in *Populus* (right panel) (from Ding and Nilsson, 2016).
Arrows indicate activation, whereas flat-ended arrows indicate repression.

Research within the past revealed also clear differences between the molecular mechanisms that regulate floral transition (Blümel *et al.*, 2015). Dally *et al.*, (2014) identified *BvBBX19* in sugar beet (*Beta vulgaris L.*) as a floral promoter involved in bolting regulation by fine-tuning the two beet *FT* paralogs. Soon afterwards, *BBX19* was functionally characterized

in *Arabidopsis* and described as a direct interaction partner of *CO* and a repressor of *FT* (Chia *et al.*, 2008). Since no true *CO* ortholog has been identified in beet so far (Chia *et al.*, 2008; Dally *et al.*, 2014), a divergent, CO-independent pathway may be active in which *BvBBX19* interacts with the bolting promoting gene *BOLTING TIME CONTROL 1* (*BTC1)* to regulate the beet *FT* paralogs (Dally *et al.*, 2014).

PEBP (or FT/TFL1 proteins) encoding genes are involved in the development of reproductive tissues, control of shoot meristem identity, and flowering time. Therefore, this family of genes is of critical interest when studying flowering.

In conclusion, the key regulator genes for flowering and morphology in plant species have diverged and evolved to uniquely adapt to different environmental conditions. The flowering transition and inflorescence architecture are modulated by two homologous proteins, FT and TFL1. The florigen FT promotes the transition to reproductive development and flowering, while TFL1 represses this transition. Both *FT* and *TFL1* belong to the *FT/TFL1* family encoding genes involved in the development of reproductive tissues, control of shoot meristem identity, and flowering time. Therefore, *FT/TFL1* gene family is a major target of floral initiation studies.

1.3 Interest of phenology in plant community

In the previous section (1.2), we were able to see that the phenological traits vary according to genetic and environmental factors. These variations allow a better understanding of the development of plants and prediction of plant development in response to climate change.

Thus, combining physiological and phenological studies allowed to highlight the mechanisms involved in the development of plants such as hormonal control. Ecophysiological studies have been able to demonstrate the different pathways involved in the survival and development of plants face to abiotic stresses such as transpiration, opening and closing of stomata acting directly on light gathering, photosynthesis, the availability of water. Finally, genetic studies have been able to demonstrate the pathways of genetic signalling as shown by the various models of signalling in plant model species such as *Arabidopsis, Populus*, etc. for flowering.

Studying plant phenological patterns allows characterizing, evaluating and classifying plants (populations or varieties). The identification of the phenological pattern is done by comparing the growth or flowering curves according to a time index. In the case of flowering

phenology, i) the frequency of occurrence of flowering during the life cycle of the plant allows the plants to be classified as continuous (flowering with sporadic brief break), sub-annual (more than one cycle per year), annual (only one cycle major per year), supra annual (Newstrom *et al.*, 1994). ii) the time of occurrence which include the starting date of the earliest individuals and the date of peak activity, iii) the duration of event, iv) the magnitude (both the mean and variability), and v) the degree of synchrony both within and between species

2 Plant architecture definition, concept and interest

In this part, we will describe after a definition and short history of architecture, the concept of architectural studies and interest of architecture studies in plants. For this, this part were strongly inspired to review of Barthélémy and Caraglio, 2007.

2.1 Plant architecture definition and history

Plant architecture is defined as the three-dimensional organization of the plant (Hallé and Oldeman, 1970; Hallé *et al.*, 1978). This organization at a given time is described by the connections between plant components (e.g. the different phytomers at a fine scale and the axes at a more macroscopic scale either built by the same meristem or deriving one from another by branching), named topology and the geometry of the plant such as its shape, or dimensions, and the localization of each component in space (Godin and Caraglio, 1998). However, this organization changes along time with apparition of different components of the plant such as leaves, flowers or branches. This organization also depends on temporal components such as the date of flowering and on the environment. In sum, it depends on the phenology. The architecture of a plant relies on the nature and the relative arrangement of each of its parts. It is, at any given times, the expression of an equilibrium between endogenous processes of growth and exogenous constraints exerted by the environment (Edelin, 1984). The aim of architectural study is, by means of observations and sometimes experimentations, to identify and understand these endogenous processes and to separate them from the plasticity of their expression resulting from external influences (Edelin, 1984; Barthélémy and Caraglio, 2007). These observations can be made at different scales, e.g. at the bud, leaf, stem or entire plant scale making the architectural observations complex. The analysis of the architecture consists in considering the plant in its globality and detecting the simplest elements of its organization, thus maintaining the structural information of the plants (Edelin, 1984).

Plant architecture plays a major role in agronomy. The best-known example is the selection of varieties of wheat with short and robust stems during the Green revolution (1960-1970). These criteria allowed these varieties to withstand winds and rains while carrying bigger grain yield (Peng *et al.*, 1999). Since the Green revolution years, numerous studies on the architecture of the plants and more particularly on their analysis have emerged (Hallé and Martin, 1968; Hallé and Oldeman, 1970; Hallé *et al.*, 1978; Tomlinson, 1983). In 1968, Hallé and Martin studied the rhythmic of growth of *Hevea* by describing foliar variation, the growth curve and the mitotic activity of the apex (Hallé and Martin, 1968). In 1970, the concept of architectural model was introduced for the first time by Hallé and Oldman (1970) following observations of the structure and mode of development of tropical plants. These two authors found that despite the species diversity, the architecture of plants could be summarized in a limited number of fundamental forms which they called "architectural models". Since the discovery of the concept of architectural model, the study of architecture rapidly developed and diversified.

2.2 Concept of architectural model

Studies based on these concepts were extended to the temperate species, herbs, lianas and root systems (Edelin, 1984; Barthélémy and Caraglio, 2007). Among all the plants studied to date, only 23 architectural models have been identified (Hallé *et al.*, 1978). Each architectural model bears the name of a botanist who particularly illustrated himself in the description of species with a related developmental pattern. The architectural model is the plant growth pattern which determines the successive architectural phases. It is an inherent growth strategy that defines both the manner in which the plant elaborates its form and the resulting architecture.

The identification of architectural models is based on the four simple morphological criteria (Edelin, 1984; Barthélémy and Caraglio, 2007):

1) Growth pattern: determinate vs indeterminate, rhythmic vs continuous
2) Branching pattern: monopodial vs sympodial, immediate (sylleptic) vs delayed (proleptic)
3) Morphological differentiation of axes: orthotropy vs. plagiotropy
4) Position of sexuality: lateral vs terminal flowering

2.2.1 The growth pattern

The growth of plant is the result of several processes that can be grouped in two morphological events coordinate and distinct, the organogenesis and the elongation.

- Rhythmic vs continuous growth

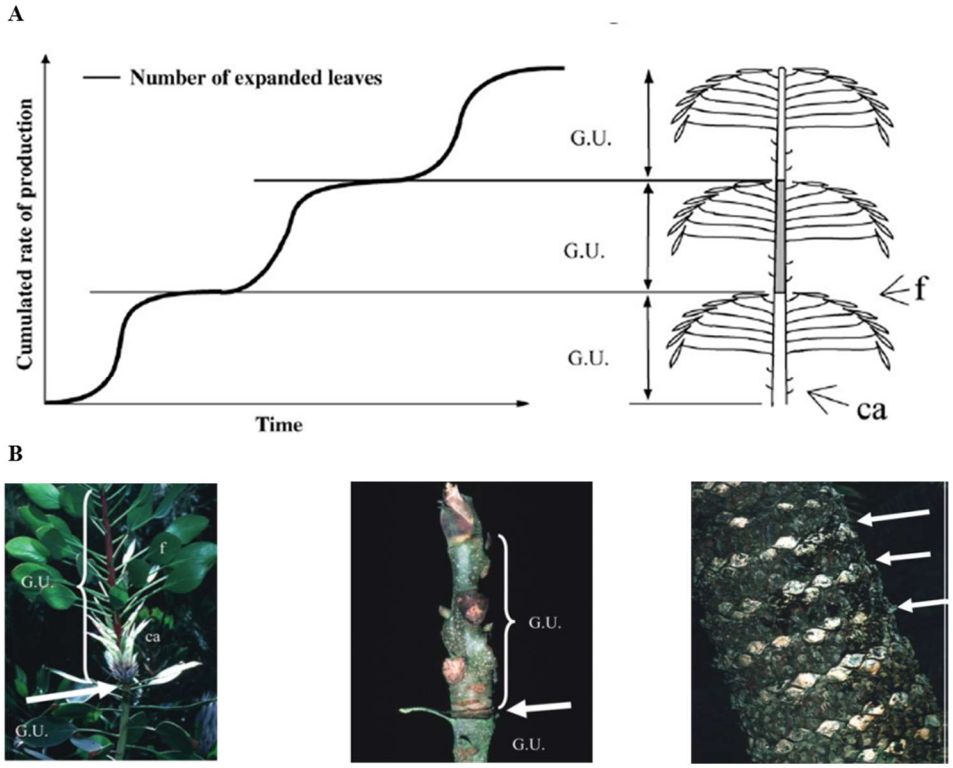

Figure 4: Rhythmic cumulative rate of leaf extension of *Hevea brassiliensis* (A), and morphological markers of rhythmic extension in *Protea cynaroïdes*, *Carya laciniosa* and *Cycas pectinate* (B).
Growth cessation phases (arrow) and delimitation of successive growth units (GU) as revealed a posteriori by the cataphylls (ca) and photosynthetic leaves (f) or their scars (from Barthélémy and Caraglio 2007)

Rhythmic growth is characterized by alternative periods of elongation and rest. Conversely a continuous growth is defined by a growth without resting period (Hallé *et al.*, 1978; Edelin, 1984; Barthélémy and Caraglio, 2007). This rhythmic or continuous growth could be determined by the observation of the apparition of vegetative organs (leaves), called phyllochron. In architecture, a rhythmic pattern is defined by the "growth units" (GU). This term emerged from the study of Hallé and Martin on *Hevea* (Hallé and Martin, 1968) as the portion of an axis which develops during an uninterrupted period of extension. The limit between two GUs can be easily identified by a perceptible slow-down of growth marked by a

zone of short internodes, and/or by a zone of scale leaves (cataphylls) (Barthélémy and Caraglio, 2007) (Figure 4).

- Determinate vs indeterminate growth

Growth could also be described as determinate or indeterminate growth. Axis growth is considered as determinate, when the meristem ceases all function after an activity period (death, abscission, or abortion) or when it transforms into a specialized structure such as flower or inflorescence, stopping the extension capacity of axis (Figure 5A). Conversely, axis growth is considered as indeterminate when the meristem maintains indefinitely its organogenetic activity until the end of plant life cycle (Figure 5B).

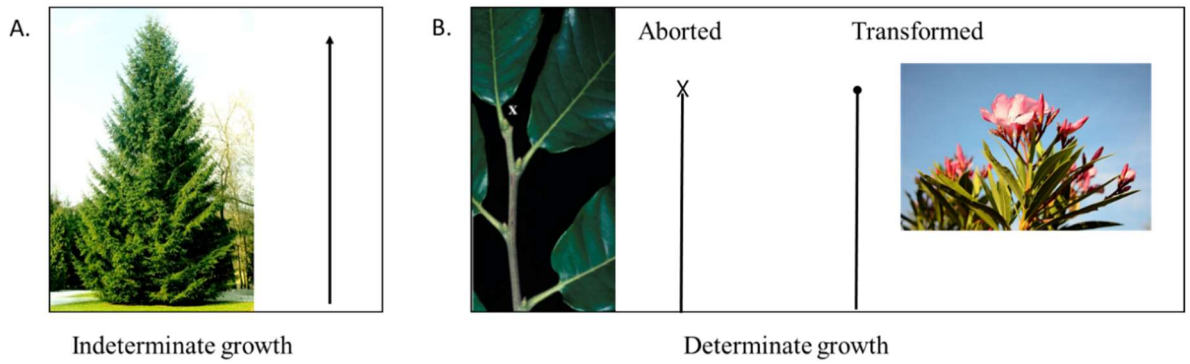

Figure 5: Indeterminate and Determinate growths
Indeterminate growth (A) corresponding to permanent apical meristem functioning and determinate growth (B) corresponding to a stopping of apical meristem activity (death, abscission or abortion) or to a transformation of the apical meristem into a flower, an inflorescence or a spine (modified from Barthélémy and Caraglio, 2007)

2.2.2 The branching pattern

- Monopodial vs sympodial

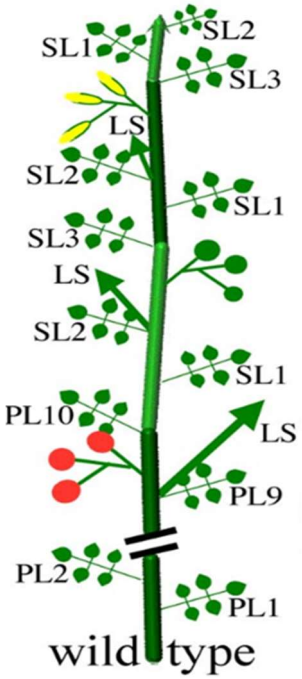

Figure 6: A scheme of a WT main shoot of the tomato plant composed of the primary shoot (leaves 1–10) and reiterated SUs (SL1–3). LS, lateral shoot; PL, primary leaf; SL. (from Shalit *et al.*, 2009)

Sympodial and monopodial developments are important criteria in plant architecture (Edelin, 1984) depending on the indeterminate and determinate growth pattern of axis (Barthélémy and Caraglio, 2007). In sympodial development, death, abscission, abortion or transformation of the apical meristem leads to the development of one, two or more branches on the uppermost positions of the parent shoot leading to a mono-, di- or polychasial branching pattern. In 1967, Prévost qualified the growth unit deriving from sympodial branching, i.e. the portion of an axis edified by a single terminal meristem, as “a module” or “a sympodial unit”. In some cases, a sympod may imply a linear succession of modules and then looks like a monopodial structure. This structure mimics an axis build up by a single meristem with indeterminate growth (Caraglio Y. and Edelin C., 1990). Tomato offers a good model for this type of structure. In this species, growth of the primary shoot emerging from the seed is terminated by the initiation of the first inflorescence, and growth of the plant continues from the active development of the bud at the axil of the last leaf formed before the reproductive structure. This bud produces a shoot segment bearing some leaves before initiating a new

inflorescence, which is once again rejected laterally by the active outgrowth of an axillary bud, and the process is indefinitely reiterated in indeterminate tomatoes (Shalit *et al.*, 2009) (Figure 6). On plane tree, Caraglio and Edelin shows that architectural analysis highlights an apparent very strong monopodial organization despite its sympodial functioning generating successions of linear orthotropic modules (Figure 7A-B).

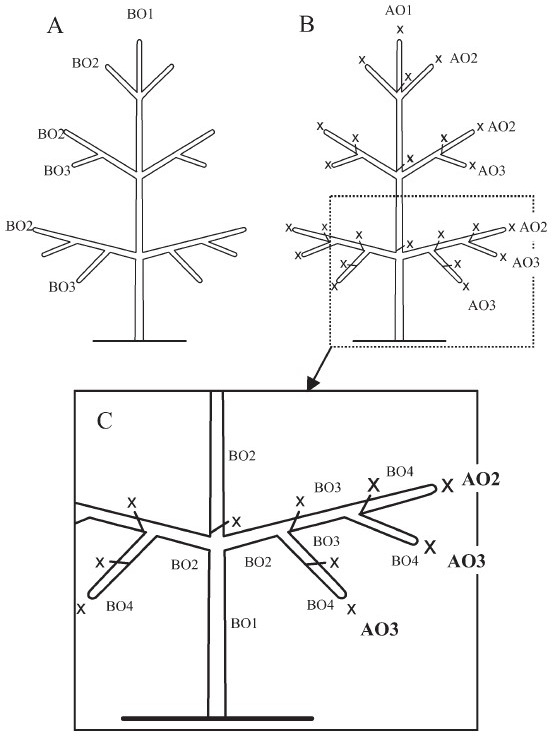

Figure 7: Illustration of branching order in a monopodial (A) and in a sympodial (B and C) system issue from Barthélémy and Caraglio, 2007
Spatial succession of axes is referred as branching order (BO). The first axis, branching order 1 (BO1), bears a lateral one, branching order 2 (BO2), and so on. In a sympodial branching system (B and C), when successive units are in a more or less rectilinear disposition, the general spatial direction of such a succession constitutes an apparent branching order (AO) as in monopodial system (A).

- Immediate vs delayed

In plant, each organ results from developmental and growth processes (Dambreville, 2012). Hence, branching pattern depends on the timing of development of branches, i.e. if the branching occurs immediately or with delay with respect to the parent node establishment date. A lateral axis can develop immediately after initiation of axillary meristem or after a period during which lateral meristem stays dormant. This branching pattern is referred as immediate (sylleptic) and delayed (proleptic) branching respectively (Barthélémy and Caraglio, 2007). This phenomenon is observed at *posteriori* by periodical observations and measurements of the

stage of lateral meristems, bud size and number of leaves primordia (Hallé *et al.*, 1978; Sabatier and Barthelemy, 1999; Barthélémy and Caraglio, 2007).

- Branching order

Describing a branching system is complex because branching does not occur at the same time (immediate vs delayed). Thus, analysis of branching system needs a precise terminology called the branching order. This latter consists of identifying branching using consecutive integers. The main stem is considered as a reference with order 0 or 1 (Hallé *et al.*, 1978; Barthélémy and Caraglio, 2007). The following axes, rising from the main stem, are referred as order 1 or 2, respectively, and so on. In a sympodial system, successive sympodial units would be referred as order 1, 2, 3, etc. However, a sympod with a successive module is considered as an "apparent" axis and is represented by an apparent branching order (a single order branching) (Figure 7B-C).

2.2.3 Morphological differentiation of axis

- Orthotropic vs plagiotropic

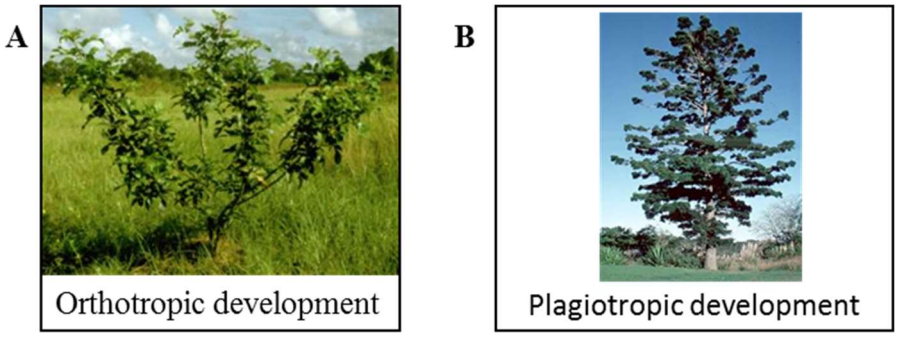

Figure 8: Illustration of (A) orthotropic development and (B) Plagiotropic development. Orthotropic development (A) refers to axes whose development is vertical, with radial symmetry and spiral, opposite or verticilliate disposition of leaves. Plagiotropic development refers to axes which have a horizontal development, with bilateral symmetry.

During their development, plants can take different forms relative to their environment and endogenous processes of growth. Thus orthotropic and plagiotropic terms allow to differentiate spatial occupancy of plant (Edelin, 1984). Orthotropic refers to axes whose development is vertical, with radial symmetry and spiral, opposite or verticilliate disposition of leaves (Hallé *et al.*, 1978) (Figure 8A). The lateral branches are arranged in all spatial directions.

Conversely, plagiotropic refers to axes which have a horizontal development, with bilateral symmetry. Lateral branches are generally arranged in a plane (Hallé *et al.*, 1978; Barthélémy and Caraglio, 2007) (Figure 8B).

2.2.4 Position of sexuality (Lateral vs terminal flowering) (Edelin, 1984; Barthélémy and Caraglio, 2007)

The formation of the reproductive organs is a key step in the life of plant. It depends on the irreversible transformation of the vegetative meristem into floral meristem, also called floral transition. According to its position, this floral transition plays an important role in the establishment of plant architecture. It has a direct impact on the growth and branching processes.

Two types of position of sexuality are distinguished: terminal and lateral. The establishment of sexuality in the terminal position definitely arrests the growth of the axis. This stopping of growth can lead either to mortality of the plant after maturation of the fruit, as for example in annual species such as wheat, or to the development of a new axis, in the case of a sympodial growth such as in tomato or in plane tree (Caraglio and Edelin, 1990). The lateral flowering does not affect the growth of a plant, it is generally found in the monopodial plant of indeterminate growth.

2.2.5 Notion of organization levels, architectural unit and reiteration

Thanks to these criteria, the concept of architectural model allows to describe the main growth strategy of the plant. These descriptions allow to relate roughly the processes of growth, branching and the position of the reproductive organs. The architecture of the plant can also be seen as a hierarchical sequence at different levels of organization that changes along time. Architecture model can be seen as a repetition of elementary botanical entities or construction units at the first level, which form axes. Those axes are organized in an architectural unit, and reiteration of this architectural unit forms the whole plant (Figure 9).

- Notion of organization levels and architectural unit

The elementary botanical entities correspond to the smallest scale of the plant and can be defined by their morphological traits or functions. Among these entities, we can distinguish:

i) the internodes which are stem portions between two nodes (= insertion zones of leaves), ii) leaves, iii) buds, iv) flowers. At the same scale, one construction unit which can be considered is the metamer or phytomer. This unit of construction corresponds to a complex composed of internodes, with buds localized on the axil of leaves (Figure 9). Moreover, this scale can be combined with temporal unit to describe dynamic growth using the GU or the annual shoot unit, typically for climates with contrasted growing seasons. GU and annual shoot unit, specific to monopodial system, can be defined by a succession of phytomers or leaves during a period of growth in a rhythmic growth or during one year respectively. For sympodial system, unit used as unit of construction is the module or sympodial unit.

The following scale is the axis scale. This scale is defined by a succession of GU, annual shoot units or modules forming an axis. Those axes can be then grouped into categories according to their morphological, anatomical or functional distinctive features. The main stem or trunk is issued from the seed or the runner, and roots, leaves and ramifications are formed on this main stem. It originates from the first meristem activity. The trunk is generally the most imposing axis in plants and supports the entirety of its structure. The second axis category includes the branches. Branches are defined by whole axis linked directly or indirectly to the trunk. In tree, different type of branches such as branchelets and twigs define other categories of axes.

The architecture of a plant can then be seen as a hierarchical branched system in which the axes can be grouped into categories. The hierarchical organization of the axes in the plant forms the architectural unit. Architectural unit (or diagram architectural) represents the fundamental, architectural and functional elementary unit of any given species, and thus defines the specific elementary architecture of each plant species according to the main rule of architectural concept seen previously (Figure 10) (Edelin, 1984; Barthélémy and Caraglio, 2007).

- Notion of reiteration

In architecture, the reiteration is defined as a morphological process in which the plant duplicates totally or partially its own architecture or architectural unit (Edelin, 1984). The concept of reiteration can thus take various forms. For example, whatever the level of organization, axes are formed of a succession of phytomers. *Stricto sensu*, this repetition of morphological entities such as internodes, leaves, buds or phytomers can be considered as a

reiteration. This reiteration is qualified as “automatic” or “sequential” and is common to all plants and constitutes the base of architectural description. However, in architecture, these reiterations are not really considered as a reiteration but rather as a parameter describing a part of sequence observed during the whole developmental sequence of plant (Barthélémy and Caraglio, 2007). Then, reiteration of the architectural unit forms the whole plant.

Growth process, branching pattern, position of sexuality, levels of organization, architectural unit and reiteration form a set of criteria that allows to describe plant in its entirety (Figure 9). This description of the plant architecture is specific of a given plant species and is used to have a better understanding of the complex processes which lead to this particular architecture.

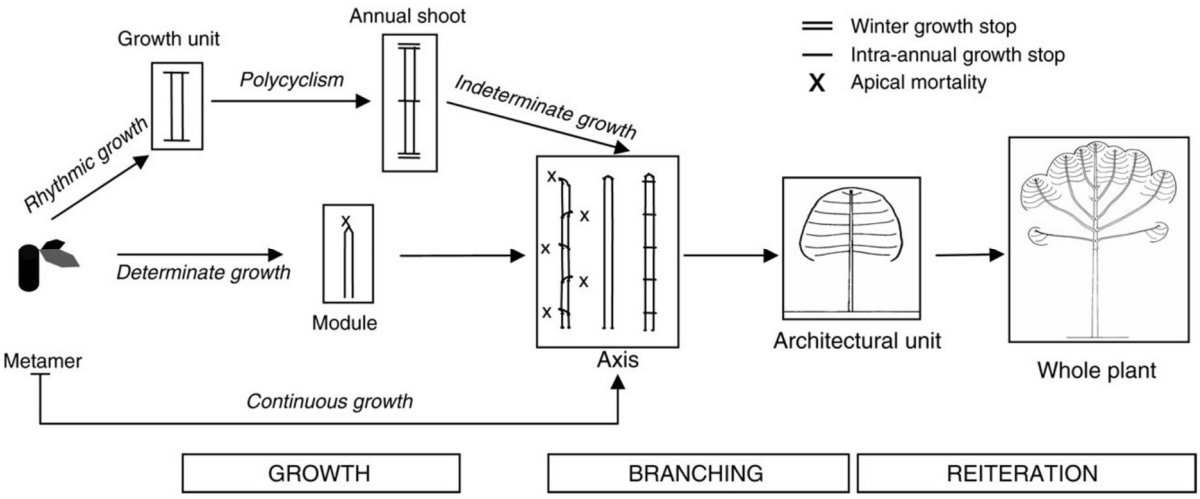

Figure 9: Diagram of the various organization levels which defined plant architecture and of repetition phenomena (in italics). (issue from Barthélémy andCaraglio, 2007)

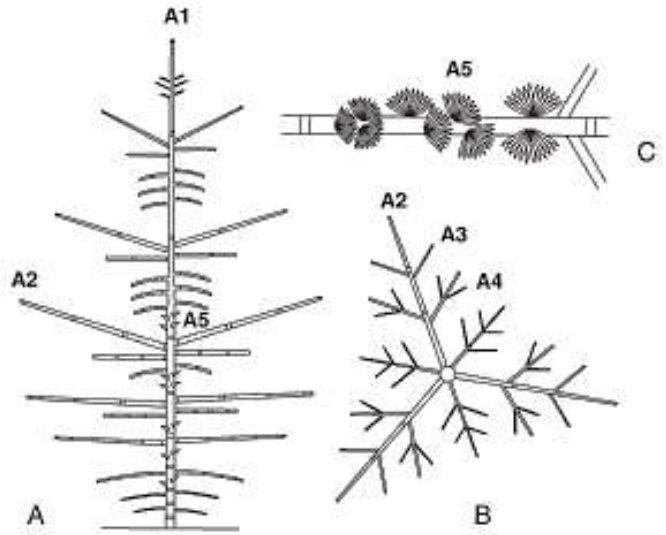

Trunk (A1)	Branches (A2)	Branchlets (A3)	Twigs (A4)	Brachyblasts (A5)
Indeterminate growth	Long term determinate growth	Long term determinate growth	Medium term determinate growth	Short term determinate growth
Rhythmic growth	Rhythmic growth	Rhythmic growth	Rhythmic growth	Rhythmic growth
Vertical growth direction	Horizontal to slanted growth direction	Horizontal growth direction	No precise growth direction	No precise growth direction
Rhythmic delayed and immediate branching	Rhythmic delayed and immediate branching	Rhythmic delayed and immediate branching	Rhythmic delayed branching	Unbranched
No reproductive structures	No reproductive structures	No reproductive structures	No reproductive structures	Terminal male or female cones
Spiral phyllotaxis	Spiral phyllotaxis	Spiral phyllotaxis	Spiral phyllotaxis	Spiral phyllotaxis

Figure 10: Architectural unit of *Cedrus atlantica* (*Pinaceae*) is composed of five axis categories (A1 to A5) (from Barthélémy and Caraglio, 2007)
A: Diagrammatic representation of the tree (view in elevation) representing the relative position of the main axis categories; B: diagrammatic representation of a tier of branches (view from above); C: diagrammatic representation of a twig annual shoot bearing several short shoots. The break symbol indicates the limit between two successive annual shoots. The table summarizes the morphological features of all axes categories.

2.3 Interest of architecture

Plant architecture is the result of the combination of the endogenous growth processes and of the exogenous constraints from its environment. Then, the aim of architecture analysis is to identify and understand these endogenous processes and to separate then from the plasticity of their expression linked to the environment. For example, architecture analysis led to a better understanding of crown construction in trees (Barthélémy and Caraglio, 2007).

Furthermore, in a more practical point of view, architecture analysis can be used to predict the yield. For example, Bosc *et al.* (2012) tried to predict strawberry plant yield by analyzing plant architecture before chilling. Even if they didn't find a correlation between this architecture and fruit yield, they found that the architecture before chilling could be used to predict the earliness of the production. Moreover, a correlation between architecture of coffee trees and their yield capacity could be find and led to the definition of ideotypes (Cilas *et al.*, 2006).

Architecture can also be used to have a better understanding of pathosystems and then, could lead to the identification of new strategies of crop protection. Indeed, architecture can be used to model pathosystems by functional-structural plant models (Garin *et al.*, 2014). These models can be used to simulate the interactions between plant structure and epidemic. For example, it can help to characterize the interactions between pathogens and the tissue they colonized or to characterize the spore dispersal from the localized infected tissues to the localized healthy tissues.

3 Strawberry

3.1 Taxonomy, domestication and economical context

3.1.1 Taxonomy

The strawberry belongs to the *Rosaceae* family. This family takes its name from the rose and represents one of the largest plant families of economic importance. The *Rosacea* family includes more than 3000 species spread over more than 100 genera (Shulaev *et al.*, 2008) Among the economically important species belonging to this family, we find: i) fruit trees such as apple, pear, cherry, peach, almonds (belonging to *Malus*, *Pyrus* and *Prunus* genus respectively):ii) Fruit herb species such as strawberry, raspberry, blackberry (belonging to *Fragaria* and *Rubus* genus); iii) horticultural crops such as rose, *Potentilla* and *Pyrachantha* (Potter *et al.*, 2007).

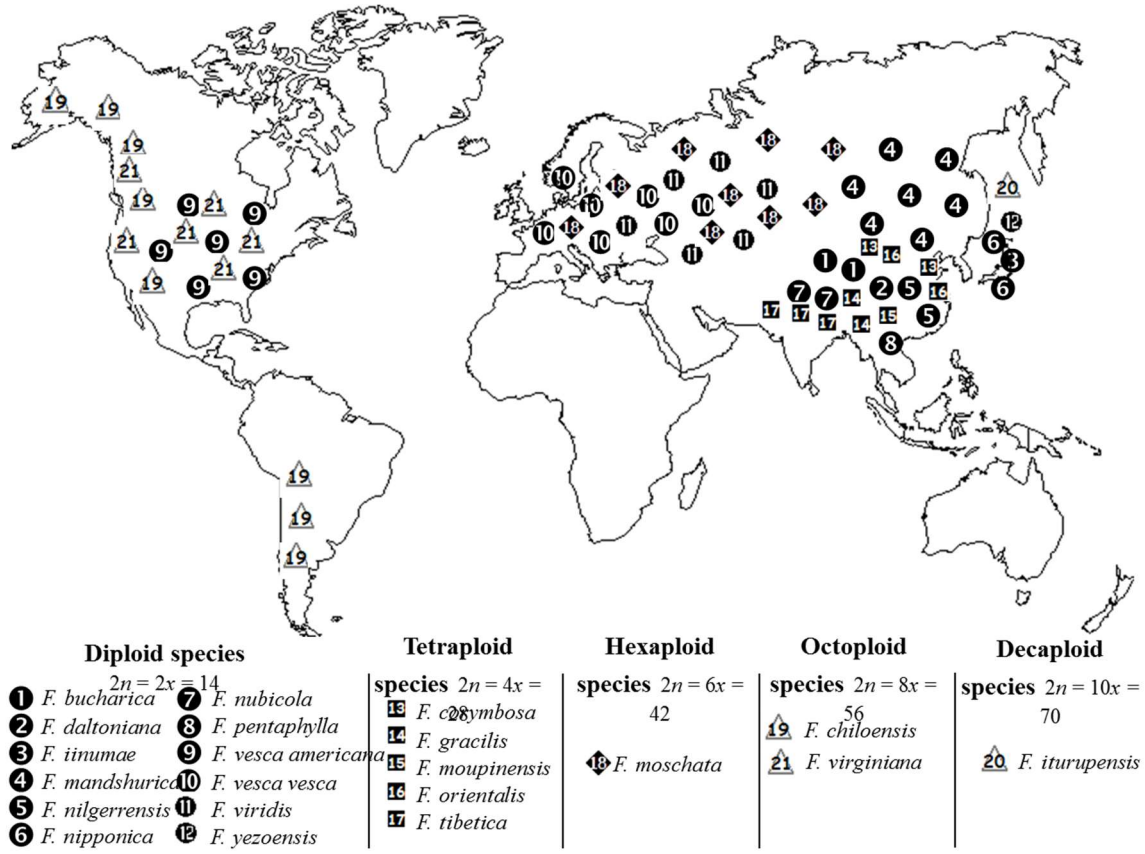

Figure 11: Geographic repartition of wild *Fragaria* species and sub-species

The basic chromosome number in *Fragaria* is x = 7 (Ichijima, 1926). This genus comprises about 22 species, and includes different ploidy levels of diploids, tetraploids, hexaploid, octoploids (Staudt, 1989) and decaploid (Hummer *et al.*, 2009). The wild species of *Fragaria* are distributed throughout the Holarctic zone with a few endemic zones into the tropics. All species are restricted to single continents or specific areas (Figure 11) (Rousseau-Gueutin *et al.*, 2009), except the diploid species *F. vesca*, which is found in both Eurasia and America (Staudt, 1962, 1989). Ten diploid species are distributed in Eastern, South Eastern and Central Asia and the three others in Europe and Western Siberia (described by Staudt from 1962 to 2008 with references cited in Rousseau-Gueutin *et al.*, 2009). Five tetraploid species ($2n=4x=28$) are restricted to Eastern and South-Eastern Asia (described by Staudt 2001 and 2003 with references cited in Rousseau-Gueutin *et al.*, 2009), while the hexaploid species ($2n=6x=42$), *F. moschata*, occurs in Europe and Western Siberia (described by Staudt from 1962 to 2008 with references cited in Rousseau-Gueutin *et al.*, 2009). Concerning the two octoploid species, *F. chiloensis and F. virginiana*, are present in America with different distributions in South and North America (Staudt, 1962, 1989). Recently, a decaploid number ($2n=10x=70$) has been reported for three accessions of *F. iturupensis* originating from Mount Atsunupuri (Hummer *et al.*, 2009). Synthetic octoploids have been constructed via controlled, interspecific hybridizations accompanied by chromosome doubling, in an effort to broaden the octoploid gene pool available to strawberry breeders (Evans, 1977; Bors, 2000)

3.1.2 Domestication

Consumption of strawberries was present from the Roman period and until the Middle Ages. Fruits of the woodland strawberry, *F. vesca*, were appreciated for their fragrance and they were also used by Romans for their medicinal properties and their cosmetic properties. It was only in the 14th century that the strawberry was actually grown, becoming a 'crop' species. King Charles V asked his gardener to plant 1200 strawberry plants in the royal gardens of Louvres, in Paris. Subsequently, the cultivation of the three species present in Eurasia, *F. vesca*, *F. moschata* and *F. viridis*, has spread throughout Europe from the 15th century onwards. However this latter species were little cultivated because these fruits were less interesting due to a high acidity compared to the two other varieties. At the 17th century, the octoploid strawberry (2n = 2x = 56) *F. virginiana* named also Scarlet for the bright red color of its fruits was introduced from Virginie, North America. Probably due to its polyploidy, its fruits were much larger than the ones of the three European species. At the 17th century, another octoploid

strawberry, *F. chiloensis*, already cultivated by the pre-Columbian Amerindians, was brought back to Europe in 1716 by Captain Frézier, who inadvertently had harvested male sterile plants. These plants were then spread by vegetative multiplication (runnering) and grown in many botanical gardens. However, outside Great Britain, this species was not popular in Europe because it required the intervention of a pollinator.

In the *Fragaria* genus, the most economically relevant species is the octoploid cultivated strawberry, *F.* × *ananassa* (2n=8x=56). This species results from a hybridization by chance between two related species, North American origin scarlet strawberry (*F. virginiana* Mill.) and South American domesticated *F. chiloensis* (L.) Mill (Darrow, 1966; Hancock *et al.*, 1999). This hybridization occurred in a European garden in the early 1700s, resulting in a new cultivated fruit species, *F.* ×*ananassa*. Strawberry breeding began in England in the late 1700s, followed by France and Germany. The first selected European cultivars were used as genitors in early American breeding programmes, together with American native cultivars (Darrow, 1966). The origin of strawberry and these early breeding practices reduced initial genetic variability. As an example, pedigrees of 134 North American cultivars were traced and shown to originate from only 17 cytoplasmic sources (Dale and Sjulin, 1990). Recently, sequence variation of chloroplast DNA revealed three maternal lineages among traditional strawberry cultivars, separating North American cultivars, which mainly have the *F. virginiana* haplotype, from Japanese cultivars, which are characterized by the *F. chiloensis* haplotype (Honjo *et al.*, 2009).

During the 200 years of strawberry breeding, initial diversity increased thanks to introgression of wild strawberry germplasm or using unrelated progenitors in breeding programmes (Darrow, 1966). However, these introgressions did not compensate for the loss of diversity observed in modern strawberry cultivars (Gil-Ariza *et al.*, 2009; Horvath *et al.*, 2011). Today there are more than 600 varieties of strawberries all confused, of which 154 varieties are inscribed in the official French catalog of varieties (http://www.gnis.fr/catalogue-varietes).

3.1.3 Economic context and evolution in cultural techniques

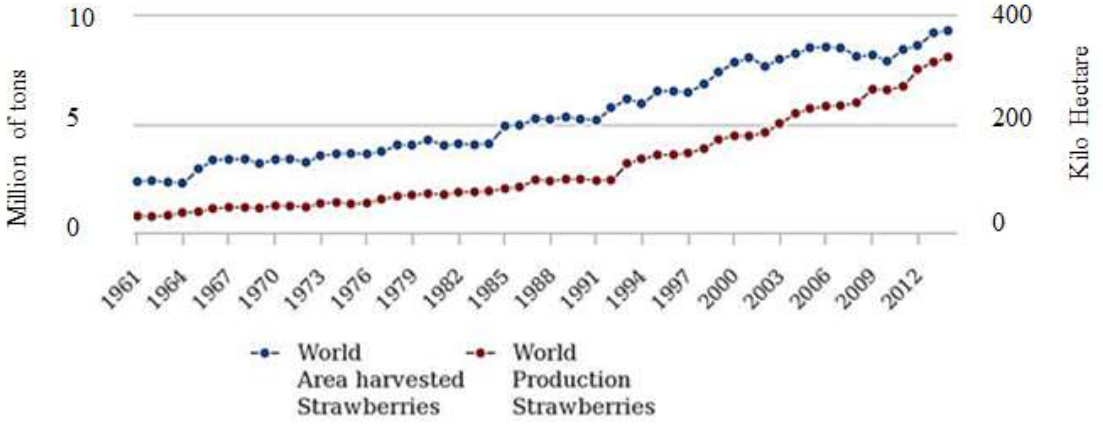

Figure 12: Yield (in tons) and Area (in kilo hectare) production of strawberry on the world between 1961 and 2014 (source FAO)

According to the Food and Agricultural Organization of the United Nations (source FAO), in 2014, strawberry is the most important berry crops (not considering grape), with a world production of more than 8 million of tons, on a cultivable area reaching almost 400 thousand hectares. Used in direct consumption, called "mouth strawberry", or processed (jams, syrups, yogurts), called "industrial strawberry", its production has multiplied by 10 and its cultivated surface by 4 since the 1960s (Figure 12). The top three strawberry producing countries are China (over 3 million of tons), the United States (more than 1 million of tons) and Mexico (with just under 400 thousands of tons). At continent scale, Europe is the third largest producer of strawberries, covering 19.7% of the world market, behind Asia (48.9%) and America (25.4%) (Figure 13). In Europe the first producers of strawberries are Spain and Belgium representing respectively 76% and 10% of European production in 2015.

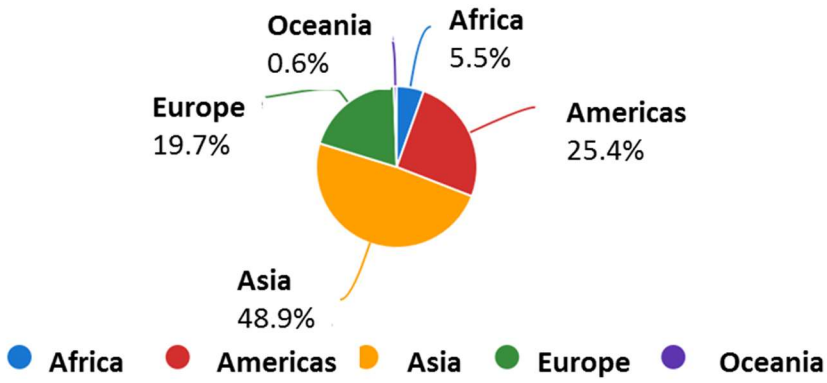

Figure 13: Repartition of strawberry production by continent (source FAO, 2014)

France is oriented towards the production of "strawberry of mouth". It is placed 17th worldwide ranks and 6th in Europe, with a production of around 59,000 tons, spread over 3 major production areas, South West (39.6% of national production), South East (22.1% of national production) and Center West (8.5% of national production) (Figure 14). The production of French strawberries relies on taste and nutritional quality to tackle the competition with strict specifications as evidenced by 'Red labels' and the IGP, the Périgord strawberries.

Strawberry is a perennial herbaceous plant forming a rosette. It multiplies vegetatively with production of daughter plants carried by stolons, which are elongated stems, as well as sexually with inflorescences bearing flowers and therefore fruits. Thus, strawberry culture is structured around two industries, nurseries and fruit producers.

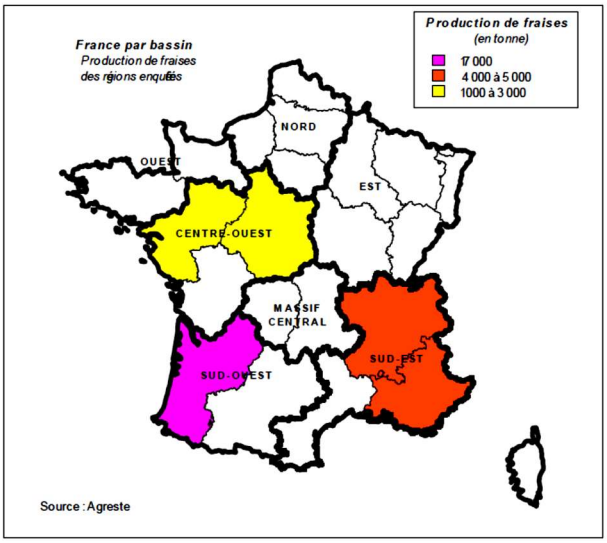

Composition des bassins de production

Bassin	Région
Centre-Ouest	Centre, Pays-de-la-Loire, Poitou-Charentes
Est	Alsace, Bourgogne, Champagne-Ardenne, Franche-Comté, Lorraine
Massif-Central	Auvergne, Limousin
Nord	Haute-Normandie, Ile-de-France, Nord-Pas-de-Calais, Picardie
Ouest	Basse-Normandie, Bretagne
Sud-Est	Corse, Languedoc-Roussillon, Provence-Alpes-Côte d'Azur, Rhône-Alpes
Sud-Ouest	Aquitaine, Midi-Pyrénées

Figure 14: Area of strawberry production in France (source Agreste, April 2011)

In strawberry, the yield is partially set up in nursery where the floral initiation occurs in young daughter plants and partially in fruit production where the floral initiation followed by organogenesis are expressed with the emergence of inflorescences and then fruits. In nursery, plants of a same genotype can display floral initiation at different times and with different intensities due to environmental conditions such as temperature, nutrition *etc* (Battey *et al.*, 1998). As an example, high temperatures during the summer 2006 led to a delay of floral initiation and then to a decrease of yield the following year, in 2007 (Ollat *et al.*, 2013). In fruit production, environmental conditions can affect inflorescence development and fruit quality

During the last two decades, the cultivation of strawberries has undergone major technical changes. In the 1980s, fruit production was carried out in the field, or small tunnels, and the plants were kept several years for fruit production. Today, plants are renewed each year, and they are grown mainly under large tunnel of 9m and in soilless culture. This last cultural technique, by maintaining plants at 1m high, get easier fruit harvest and suppress soil diseases. In addition, it allows a range of date of plantations, including early plantation in middle December when the tunnel is heated (temperature above 8 ° C). With this type of plantation, the plant is maintained in conditions favorable to floral initiation, which leads to enlarge the period of flowering and therefore the period of fruit production.

3.2 Structural description and growth habit

The strawberry structure has been described in different reviews and articles (Guttridge, 1955; Savini *et al.*, 2006; Heide *et al.*, 2013; Hytönen, 2014). The strawberry consists of a stem called crown, stipulated trifoliate leaves which are assembled in rosette and an inflorescence (Figure 15A) and axillary buds which can developed in stolon, lateral crowns (extension or branch crown) or stay dormant

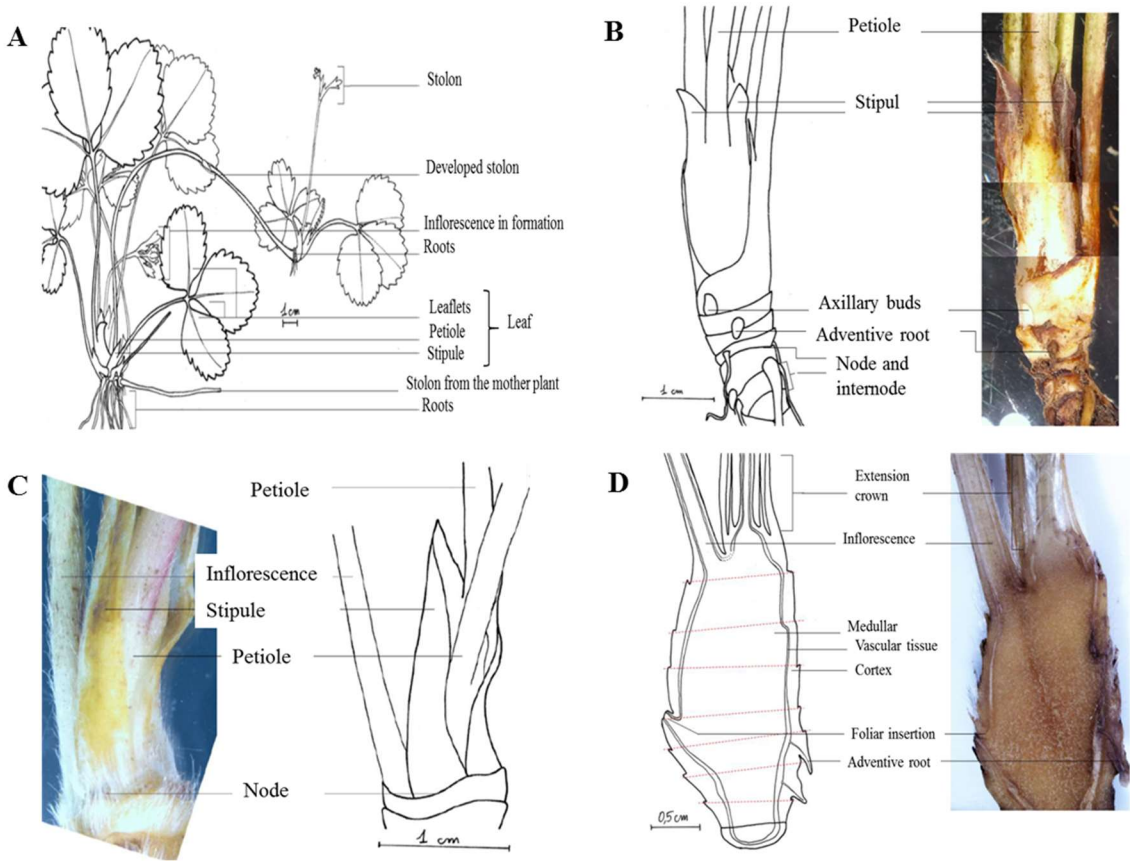

Figure 15: Pointwise on strawberry structural description
(A) Strawberry issue from runner reproduction, (B) Primary crown the basal part is exposed to distinguish nodes, internodes and adventive roots, (C) Primary crown apex terminated by a inflorescence. A vegetative relay is in place at the same node giving monopodial growth development and (D), longitudinal section of strawberry primary crown highlighting sideway displacement of the inflorescence and extension crown development. Red dotted line delimit the internodes (from Maltaite and Caraglio, 2016)

The stem of strawberry (crown) derived from apical meristem activity following germination or stolon development is called primary crown. It is characterized by short internodes, bearing roots, leaves and stolons. The root system, resulting from germination or from development of stolon, disappears rapidly in favor of adventitious root which ensures the function of water nutrition (Figure 15B). Leaves are trifoliate and stipulated. It follows a spiral phyllotaxy of type 2/5 (Savini *et al.*, 2006), that is to say that there are 5 leaves of 2 revolutions before finding two leaves aligned on an axis parallel to the stem. The leaves have long petioles and are attached to the stem by the stipule which helps to protect the axillary bud located at the axil of the leaves. When conditions are favorable for flowering, the apical meristem becomes floral followed by organogenesis to give inflorescence. The growth of the strawberry is therefore determinate in accordance with the description of the architectural model concept described above (§2.2.1).

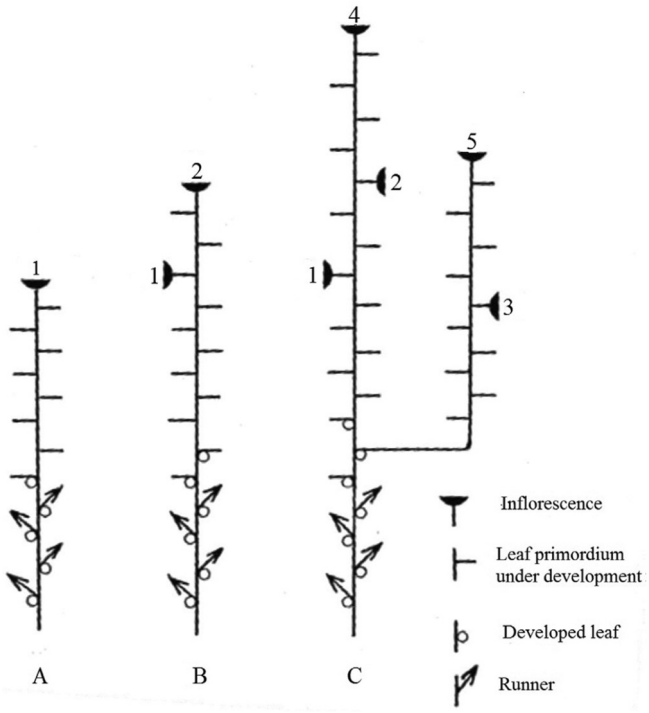

Figure 16: Architectural development of strawberry by Guttridge in 1955, (from Heide *et al.*, 2013)

To compensate the arrest of the growth of its main stem, the strawberry sets up a vegetative relay resulting from the activity of the uppermost lateral meristem, which resumes dominance over lower laterals and displaces the inflorescence to one side. This lateral meristem allows the extension of the growth of the strawberry forming a lateral branch called extension crown. The growth habit is thus sympodial, although the sideway displacement of the inflorescence is superficial, giving the impression that the growth is monopodial (Figure 15C-D) (Jahn *et al.*, 1970; Heide *et al.*, 2013). After the initiation of some leaves, three or four leaves (Jahn *et al.*, 1970; Bosc *et al.*, 2012), and a new inflorescence, this extension crown can form a new extension crown on the main axis and so on until the end of the life cycle of the plant. Along crowns (primary, branch or extension crowns), axillary buds remain dormant, or develop either a stolon or a new crown called branch crown. Therefore, branching can occurred through extension crowns and branch crowns. The new branch crown will have the same development as the main axis, a sympodial growth, and will be determined. This branching crown is orthotropic and the growth can be considered as discontinuous because bud giving a branch crown can stay dormant several months. Guttridge (1955) proposed the first architectural development of the strawberry development and took into account the sympodial growth of this species (Figure 16).

Stolon is a particular branch of strawberry. Compare to branch crown, it is characterized by two long internodes which allow it to colonize space horizontally without the constraint of sexual reproduction, and it represents a complete reiteration of the plant by producing daughter plants with roots (Figure 15A). Stolon shows a sylleptic development, without a rest phase, starting immediately after initiation of axillary meristem (Massetani *et al.*, 2011). The first node of the stolon has a pre-leaf α, which generally remains dormant but which sometimes develops a second stolon. On the second node, adventive roots develop and form the anchor point of the development of the daughter plant clone. Along the crown, axillary buds leading to stolons or to branch crowns can be visually identified at early stages since the buds of a stolon are flat, elongated and show conical shape.

Flowering can be summarized by three successive phases: the floral induction when the meristem is susceptible to environmental or internal factors, the floral initiation when the meristem becomes floral and the organogenesis when the inflorescence and then flower is formed. Floral transition has been well described using light microscopy (Jahn *et al.*, 1970) and scanning electronic (Taylor *et al.*, 1997). Initiation of an inflorescence was first evident as a raising and enlargement of the apical meristem. Initiation of the primary flower began after the bracts of the inflorescence were evident. Floral initiation is centripetal, the sepals appearing first, followed by petals, stamens and pistils.

The phyllotaxy of the crown continues in the bracts of the main axis of the inflorescence. The inflorescence of strawberry is basically a dichasial cyme, i.e. the inflorescence is composed of one primary flower, then under this primary flower two flowers are formed on each secondary branches and two flowers are formed in each tertiary branch and so on. The flowers are composed of five white petals, five green sepals, twenty stamens and numerous carpels.

3.3 Growth cycle of strawberry and environmental cues controlling this development

The growth and development in strawberry and its environmental control will be focus on the seasonal flowering (SF) strawberry also called June-bearing strawberry. Some information will be given on the perpetual flowering (PF), which is able to flower all along the growth cycle.

June-bearing strawberries display a perennial growth behavior characterized by an annual cycling between flowering, growth and dormancy. Compare to forest trees, which show

a multiple-year delay in flowering, strawberry is able to flower the second year of the plant life. Whatever the strawberry, diploid or octoploid, its plant cycle can be summarized into five phases (Figure 17):

1) A phase of floral initiation, which takes place in autumn, when temperature and photoperiod decrease (September-October);
2) A phase of growth cessation named dormancy in winter during which the growth of the plant decreases due to cold temperatures (November-February);
3) A phase of resumption of the growth of the plant, after satisfying chilling requirements, when temperatures and photoperiod increase (February -Mars);
4) A phase of flowering (April-May) and following fruiting (May-June) in spring;
5) A phase of vegetative multiplication via stolon production, when temperatures and photoperiod are high in summer (July-August).

The length and the occurrence date of these phases may vary according to the type of genotypes, SF or PF, and environment. PF strawberries are able to initiate flowers all along the vegetative plant cycle. Therefore, the flowering period can be extended in long days (summer) leading to an extension of the fruit production period and may lead to a difference of architecture development (Costes *et al.*, 2014)

By offering an extension of flower/fruit production period and therefore by possibly increasing the flower/fruit production, this trait represents one of the main objectives of numerous breeding programs (de Camacaro *et al.*, 2002; Albani and Coupland, 2010).

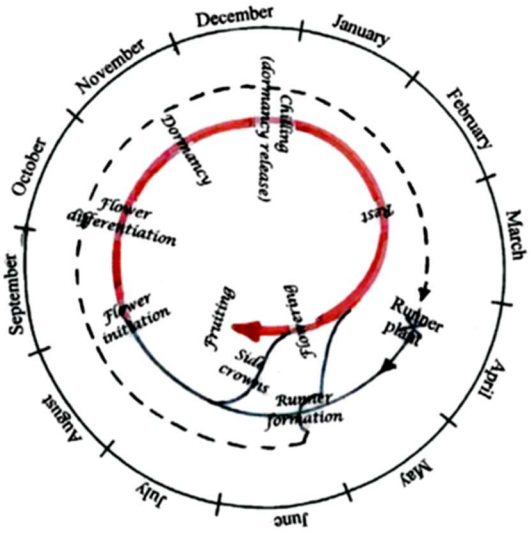

Figure 17: Annual growth life cycle of seasonal strawberry plant. The red color highlights the reproductive phase of plant development. Dotted line highlight the development of plant issue from a newly-formed runner (from Heide et al., 2013)

3.3.1 Environmental cues of floral induction/initiation

Temperature, photoperiod and their interaction are the most important environmental factors that regulate the transition from vegetative to floral growth in strawberries (Figure 18) (Ito and Saito, 1962; Darrow, 1966; Manakasem and Goodwin, 1998; Battey, 2000; Watson *et al.*, 2002; Massetani *et al.*, 2011).

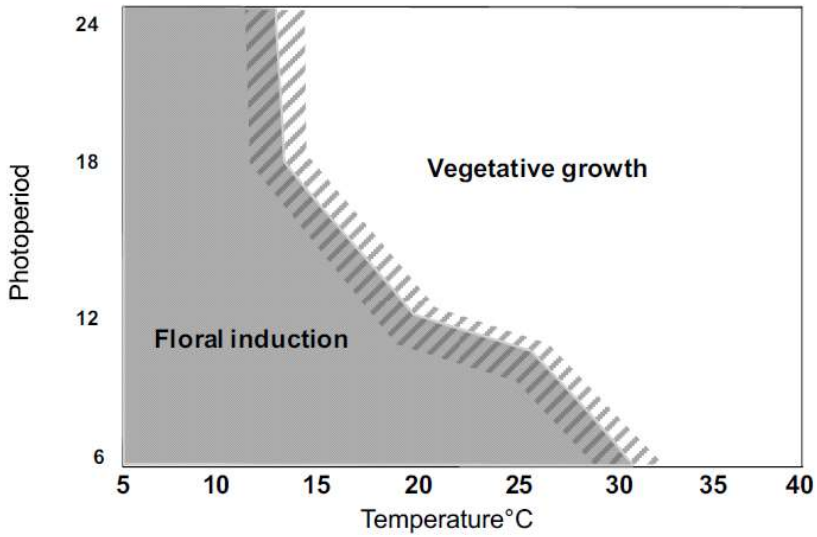

Figure 18: Relation between photoperiod and temperature to induce reproductive (flower induction) or vegetative growth (from Massetanni, 2011 modified from Ito and Saito 1962)

In SF strawberries, the period in inductive conditions required for floral initiation occurs has been studied only under controlled climatic chambers conditions (e.g. 14h of daylight and 16¨C). According to studies, one week until five weeks (Battey *et al.*, 1998; Sonsteby and Heide, 2008*b*) are necessary to promote flowering in plants. Interaction between varieties, temperature and number of inductive cycles has been described showing the complexity of network for floral initiation to be released (Sonsteby, 1997).

In SF strawberries, flower initiation is promoted by shorts days and low temperatures (Leshem and Koller 1964), such as at 15-18°C during short days (< 14h of daylight) (Battey *et al.*, 1998). In contrast, with colder temperatures, e.g. 12 ° C, a longer day length up to 16h remains inducible (Verheul *et al.*, 2006, 2007; Opstad *et al.*, 2011). However, high temperatures (> 20°C) delay floral initiation or suppress it when temperatures are above 26-30°C, regardless of the photoperiod (Ito and Saito, 1962; Verheul *et al.*, 2006, 2007). In SF varieties, with floral initiation occurring in autumn and stopping with dormancy, flowering occurs once a year in the following spring leading to a single harvest period (Heide, 1977; Verheul *et al.*, 2007; Bradford *et al.*, 2010; Opstad *et al.*, 2011; Heide *et al.*, 2013). In Europe, the floral initiation starts at the

end of August in the South-West in France or at the middle of September in Germany. In France with climate global changing, summer and autumn temperature will increase and delay the date of floral initiation such as observed in 2006, leading to a decrease of yield the spring 2007 (Ollat *et al.*, 2013).

On the opposite, PF genotypes generate flower buds cyclically regardless of photoperiod if temperatures are at least moderate (< 28°C) (Durner *et al.*, 1984; Galletta and Maas, 1990; Battey *et al.*, 1998). For these PF varieties, LD promotes flowering rather than SD (Sonsteby and Heide, 2008*a*).

Beside interaction between photoperiod and temperature, intensity of light also plays a crucial role in induction / initiation of flowering. In the cultivated strawberry, lower luminous intensity will lead to earlier floral initiation (Darnell *et al.*, 2003). Spectral characteristics is also of importance. Low red/far-red ratios in enabling short-day plants to flower in long days (Collins, 1966). In the diploid perpetual-flowering strawberry, which did not express the floral repressor (see paragraph 'Genetic mechanism'), the end-of-day far-red and blue light activate flowering but not red treatments (Rantanen *et al.*, 2014). However, results are not always clear since the spectral dependence changed markedly with time (Vince-Prue and Guttridge, 1973; Vince-prue *et al.*, 1976). Floral initiation in the SD strawberry cv. Cambridge Favourite was inhibited by a daylength extension with red light during the second half of a 16-hour night but not during the first half, and by far-red light in the first half but not during the second. Mixed red plus far-red light was inhibitory to flowering at both times (Vince-Prue and Guttridge, 1973).

3.3.2 Chilling requirement

In addition, to express their full potential, strawberry often requires a chilling period (<7 ºC), although the cultivars developed for warm regions do not always need a chilling period (Darrow, 1966). During vegetative growth, the reduction of photoperiod (at the end of summer), cause the reduction of the petiole length and this reduction is the first sign of decrease of growth rate (growth cessation) (Guttridge and Thompson, 1959; Hytönen *et al.*, 2009). Varieties varied a lot for their chilling requirements from approximatively 200 hours for Floridian varieties until 1500 hours for Northern-European varieties such as Florence. A modeling approach allowed to quantifying chilling units required for flowering and fruit yield potential (Tanino and Wang,

2008). Results showed that flowering time correlated with accumulative chilling hours using either a simple accumulation model or a weighted accumulation model.

3.3.3 Hormonal cues in strawberry growth cycle

Gibberellic acid (GA) has been shown to inhibit flower initiation in genotypes ranging from the day-neutral for flower induction (perpetual fruiting) to short-day genotypes very sensitive to photoperiod (Guttridge and Thompson, 1959; Hytönen *et al.*, 2009). This growth regulator also promotes runner formation and induces internode elongation. In summary, this growth-regulating substance(s) promotes vegetative growth and inhibits flower initiation.

3.4 Genetic mechanism regulating growth and development of strawberry

Thanks to recent advances in strawberry genetics (Shulaev *et al.*, 2011), genetic factors underlying variations in flowering and runnering begin to be deciphered (Figure 19). In diploid F.*vesca*, perpetual flowering is controlled by a recessive allele SEASONAL FLOERING LOCUS (SFL) (Albani *et al.*, 2004). The gene underlying the SFL locus was identify as a homolog of TERMINAL FLOWERING LOCUS 1 (*FveTFL1*), a floral repressor (Iwata et al. 2012), A deletion of 2pb in the *sfl* allele leads to an inactive protein and therefore to the absence of floral repressor. In absence of floral repressor, the woodland strawberry flowers continuously, likely with the presence of a floral activator, which could be a *FLOWERING LOCUS T* (*FT*). The runnering is controlled by a different dominant locus, the *RUNNERING* locus (*R*) (Brown and Wareing, 1965), and is due to a mutation on the *GA20ox4* gene involved in GA pathway (Tenreira *et al.*, 2017). The deletion of 9 nucleotide occurs in the active site of the enzyme, which is likely enable to transform GA inactive into GA active. When *FveGA20ox4* is mutated, axillary meristems remain dormant or produce crowns terminated by inflorescence, increasing thus the number of inflorescences on the plant.

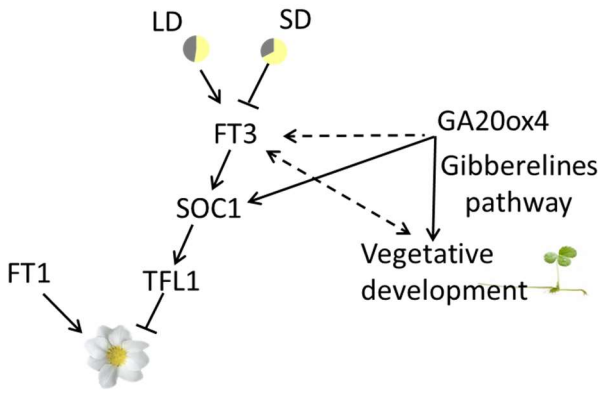

Figure 19: Model showing the photoperiodic regulation of flowering and stolon formation in strawberry. Arrows indicate activation and bars indicate repression. (from Mouhu et al. 2013 and Gaston comm. pers.)

In the cultivated octoploid *F. x ananassa*, no clear conclusions was reached concerning the perpetual flowering trait. According to study, flowering was either controlled by a single dominant locus (Shaw and Famula, 2005; Sugimoto *et al.*, 2005) or was under quantitative inheritance (Serce and Hancock, 2005) and controlled by numerous QTL (Quantitative Trait Locus) with various additive effects (Weebadde *et al.*, 2008). These conflicting results can be due to the use of different set of parents in inheritance studies and to different environments (Maltoni *et al.*, 1996). Gaston *et al.* (2013) reported the identification of a major QTL named *FaPFRU*. This locus affects both the flowering and the runnering, the latter being related to the balance of flowering and vegetative development. The *FaPFRU* QTL is not orthologous to the loci affecting perpetual flowering (*SFL*) and runnering (*R*) in *F. vesca*, therefore suggesting different genetic controls of flowering and runnering in the diploid and octoploid *Fragaria* species. Furthermore, the *FaPFRU* QTL displays opposite effects on flowering (positive effect) and on runnering (negative effect), indicating that both traits are genetically linked and share common physiological control. Fine mapping of this QTL (Perrotte *et al.*, 2016) suggested that this locus could be controlled by a FT gene (*FaFT1*).

Beside genes belonging to the FT/TFL1 family, *SUPPRESSOR OF OVEREXPRESSION OF CONSTANS1* (*FvSOC1*) has been shown as a repressor of flower initiation under inductive short days (Mouhu *et al.*, 2013). Its silencing causes continuous flowering in both short days and non-inductive long days, similar to mutants in the floral repressor FvTFL1.

4 Aim and approach of phD

Through this introduction we have seen that the development of a plant could be described temporally by its phenology but also spatially by its architecture. These two types of phenotypic description result from the different exogenous (e.g. environmental) factors and endogenous (e.g. genetic) factors of the plant.

In strawberry, a plant of important economic interest, the understanding of the development of the plant and particularly of the flowering and the runnering processes is a major issue both for the production of fruits and of new plants. Therefore, several studies (Battey *et al.*, 1998; Darnell *et al.*, 2003; Heide *et al.*, 2013; Kurokura *et al.*, 2013) have been conducted in order to understand the environmental and genetic control of the flowering and runnering processes. Little is known concerning these developmental processes along time and even less concerning the ontogenetic processes (Massetani *et al.*, 2011; Bosc *et al.*, 2012).

The aim of this work was to get a better understanding of strawberry plant development integrating phenology and architecture.

This work mainly focused on the development of six seasonal octoploid varieties in culture production conditions. The first objective of this work was to develop a method to identify phenological phases within the flowering, vegetative development and runnering processes. The second objective was to develop a method to study the architectural development along time, and the third objective was to establish a link between phenology, architecture and the expression of key flowering genes.

For this, during one cycle of fruit production for each variety:

1) Plant phenology was phenotyped recording the number of weekly emerged flowers, leaves and stolons and analyzed using dedicated statistical models. We introduced a new framework of longitudinal data analysis, based on multiple-change point models, for identifying developmental phases for each process and consensus phases combining the three processes. The univariate multiple change-point models applied to each phenological variable were based on the assumption of phases synchronous between individuals of a given variety. These models allowed to identify phases for each variety and each type of organ and were used to group varieties on this basis.

2) Architectural development was characterized every month and analyzed using multiscale tree graphs, allowing visual representation and topological analysis of plant architectural development. This analysis allowed us to identify specific architectural characteristics of strawberry plants which explain phenological patterns.

3) Because several key flowering genes (FT/TFL1 families and SOC1) were identified in previous studies, during this work, a third approach of molecular expression was conducted on these genes in order to identify genes responsible from the flowering pattern

Beside the core of this thesis dealing with octoploid seasonal varieties, a preliminary study of plant development in the diploid model of strawberry was initiated using seedlings. One of the limitations of the study of the octoploid varieties was the lack of knowledge concerning the plant development in the nursery phase (e.g. the floral initiation during this phase). In this respect, the use of seedlings enable to study the whole plant development. Therefore, the second objective of my thesis was to initiate experiments on the diploid woodland *Fragaria*, *F. vesca*, as a model of plant development in Rosaceae. One objective was to identify the floral transition, when the shoot apical meristem becomes reproductive in order to work further on events before floral transition and floral induction. Another objective was to establish when and where stolons emerge in order to have a better understanding of the fate of the axillary meristems that can become a branch crown, a stolon or stay dormant. In order to fulfill these objectives, phenological and architecture approaches were used.

Chapter 2: Material and Methods

A. Green house at minimal Temperature of 8°C

B. Schematic representation of experimental plan

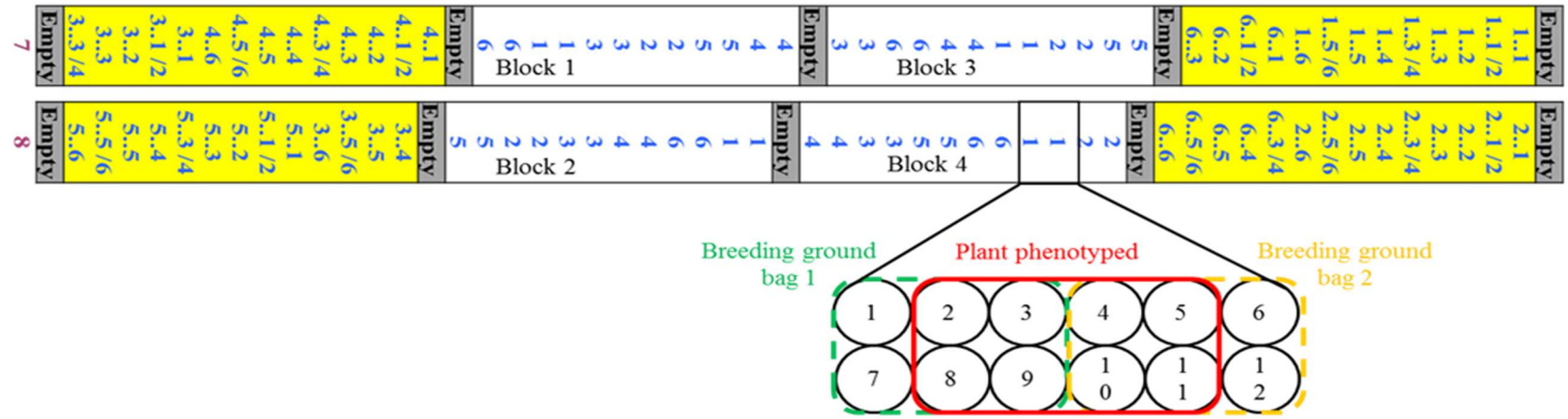

Figure 20: Experimental design.
Phenological study was performed in randomized blocks (block 1-4) separated by empty places (grey). Each block was composed of 12 plants per genotype (annotated 1-6)*, allocated in two breeding grounds. Eight plants per block were studied. On each side of this experiment (yellow), a total of 54 plants per genotype were planted for architectural study.
*(1) Gariguette, (2) Ciflorette, (3) Clery, (4) Capriss, (5) Darselect, (6) Cir107

1 Field site and plant material

1.1 Field site and plant material for the study of plant development in production condition

Six seasonal flowering varieties (Capriss, Ciflorette, Cir107, Clery, Darselect and Gariguette) of the cultivated octoploid strawberry were studied. These varieties differ by their chilling requirement (between 300 and 500 hours of chilling for Capriss and Cir107, 700 hours for Ciflorette, 800 hours for Gariguette and 900 hours for Clery and Darselect), flowering earliness (Ciflorette and Gariguette have the earliest flowering followed by Clery, Capriss and Cir107 (1/2 flowering earliness), and Darselect which has the least early flowering) and yield dynamic (Table 3). Cold stored plants were obtained from Invenio nursery (Douville, France 0° 61' E and 45° 02' N, altitude 150 m).

In nursery cold stored plants received their chilling requirement in autumn 2014 by placing them into a climatic chamber at 2°C. Afterwards, all the varieties were planted on 12th December except Ciflorette (4th December) into breeding ground bag (ORGAPIN) of 10L with drip irrigation and fertilization in greenhouse at a minimal temperature of 8°C (Figure 20A). The experiment was conducted in randomized blocks with four blocks. Each block consisted of two breeding ground bags per variety placed side by side, each containing 6 plants, i.e. 12 plants per genotype and block. However, only the height most central plants per block (a total of 32 plants per variety) were phenotyped in order to avoid possible interaction effects between varieties on plant development such as spatial and light competition. In addition, 54 plants per variety located in the outermost part of the banks were planted at the same date and in the same conditions for the study of the architecture (Figure 20-B). In total; 612 plants were studied (96 plants per variety).

Table 3: Chilling requirement, flowering earliness and Yield dynamic for the six seasonal strawberry varieties

	Chilling requirement	**Flowering earliness**	**Yield dynamics**
Capriss	300-500 hours	½ earliness	No peak of production, Yield ≥ Gariguette
Ciflorette	700 hours	Earliness	-
Cir107	300-500 hours	½ flowering earliness	High yield, extension of cropping flowering
Clery	900 hours	½ earliness	High Yield
Darselect	900 hours	lateness	No selected for 2nd peak of flowering
Gariguette	800 hours	Earliness	1st high peak of flowering + 2nd peak of flowering

1.2 Field site and plant material for seedling development in the diploid strawberry model

Plant development of the woodland strawberry *F. vesca*, was studied using three genotypes that differed according to their type of flowering, seasonal flowering (SF) or perpetual flowering (PF) and their capacity to produce stolons, runnering (R) or runnerless (r) (Table 4). 'Reine des Vallées' is a perpetual flowering and runnerless variety (PF and r), and therefore was easily commercialized by seeds for more than 20 years. Sicile is a wild genotype sampled in Sicile by CRA (Italy) and is seasonal flowering and runnering (SF and R). NIL-2.39.63 ('Fb2', PF and R) resulted from the introgression of the runnering WT allele from *F. bucharica* (R) into *F. vesca* 'Reine des Vallées' ('RdV', PF and r) to create the Near-Isogenic Line (NIL) (Urrutia *et al.*, 2015).

For each genotype, Fb2, RdV and Sicile, 80 seeds were sown the 12th November 2015 in box containing substrate composed of 1/4 of sand and 3/4 of fertile ground. Then seedlings at two unifoliate leaves and one trifoliate emerging leaf were directly transplanted to plates including 28 pots of 7 cm diameter the 7th January 2016. We decided to skip the intermediate step with transplantation into plates with small pots (3 cm diameter) to keep the development in the same environment from transplantation to flowering. This experiment was performed in a greenhouse at 22°C day and a photoperiod of 16h. These conditions did not allow the floral initiation in SF genotypes but in PF genotypes.

Table 4: Characteristics of diploid genotypes

	Seasonal flowering (SF)	**Perpetual flowering (PF)**
Runnering (R)	Sicile	NIL 2.39.63 (Fb2)
Runnerless (r)	-	RdV (Reine des Vallées)

2 Phenological study: Characterization of strawberry developmental process along time

2.1 Phenological data

For the six seasonal varieties, 32 plants per variety were phenotyped during seasonal production. During 27 weeks, from 16 December 2014 to 24 June 2015, the number of newly emerged leaves, flowers and stolons were counted. To facilitate the counting of newly emerged leaves, the leaves with a petiole of about 0.5 cm were ringed. At each measurement occasion,

the new emerged leaves corresponded to the leaves without ring. They were counted and ringed and so on until the end of the experiment. The stolons, with a length above 1 cm, were counted. Once counted, the stolons were cut to the base according to the crop route in production conditions. The total number of flowers was counted at each measurement occasion for each plant. The number of newly emerged flowers thus corresponds to the difference of the total number of flowers between two consecutive measurement occasions. The day of plantation (DAP) was chosen as the time origin of the phenological series which were indexed by day. The interval between two successive measurement occasions was between 5 and 10 days, this interval being a week in more than half of the cases (14 intervals among 26). Because of the unevenly spaced measurement occasions, the data were standardized and each element of a phenological series consisted of the number of weekly emerged organs.

In order to identify flowering, vegetative (for leaves) and stolon patterns, a longitudinal data analysis was performed using categorical multiple change-point models, a statistical model dedicated to the synchronous segmentation of longitudinal data.

2.2 Statistical models: Synchronous segmentation of phenological series for each genotype using multiple change-point models and its illustration on the flowering series of Gariguette.

We assumed that the phenological pattern of a genotype took the form of a succession of well-differentiated stationary phases where the distribution of the number of weekly emerged organs did not change substantially within each phase, but changed markedly between phases. These phenological patterns have been analyzed using segmentation models applied to each genotype. We thus assumed that the phenological phases were common for the different plants measured for a given genotype and used multiple change-point models for the synchronous segmentation of the phenological series of the different plants; see Appendix A for a formal definition of multiple change-point models and associated statistical methods. For each genotype, the data to be segmented thus consisted of a sample of series of length 27 (the number of measurement dates) where each series corresponded to a plant. Univariate series for each type of organ (either flower, leaf or stolon) and trivariate series combining flowers, leaves or stolons were considered. The statistical methodology for univariate multiple change-point models directly generalizes to multivariate multiple change-point models since the different observed variable are assumed to be mutually independent within each phase.

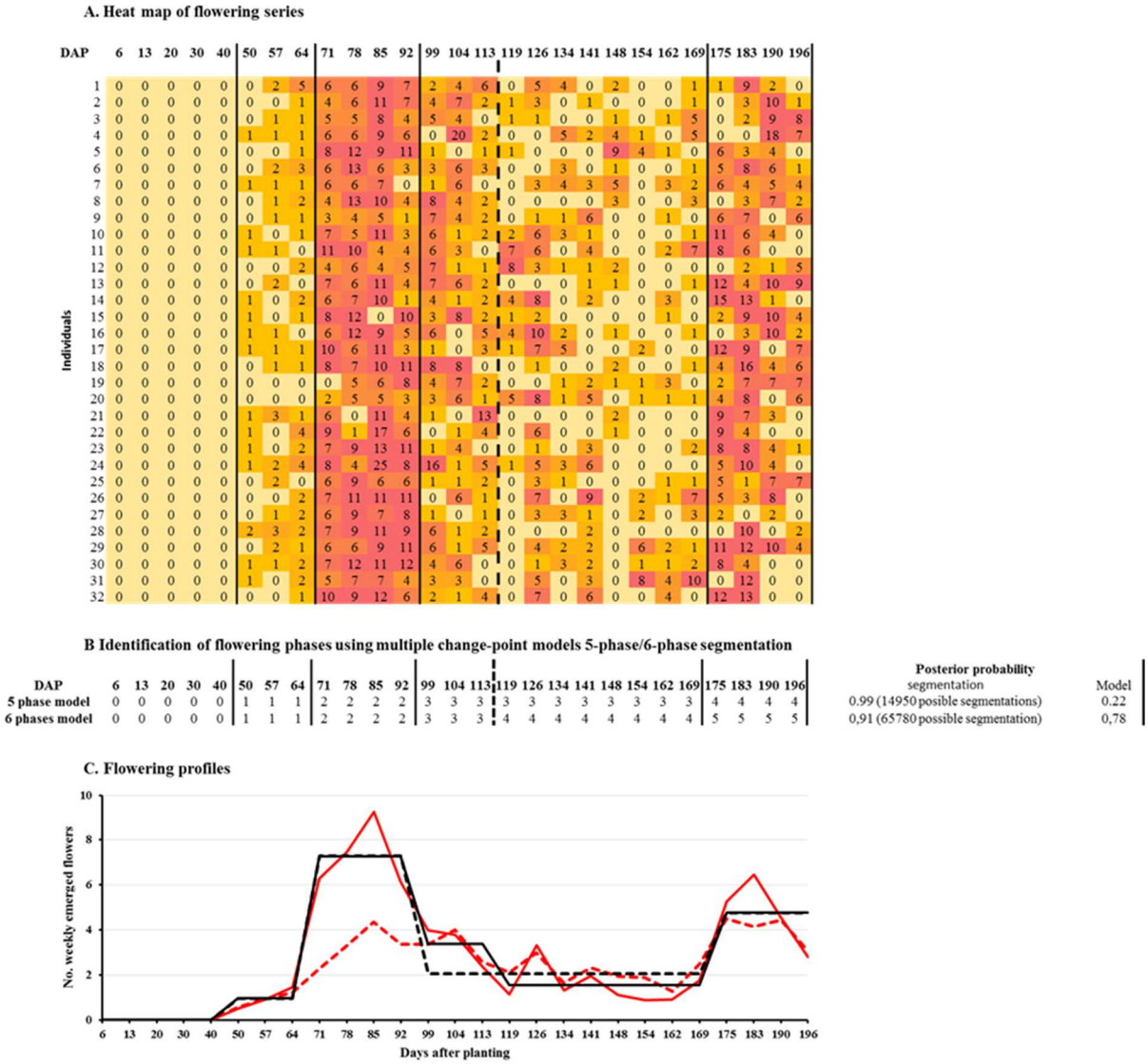

Figure 21: Identification of flowering phases for Gariguette using categorical multiple change-point models.
(A) Heat map of flowering series, (B) Identification of flowering phases using categorical multiple change-point models, (C). Profiles of flowering: segmentations represented as step functions (black solid line for the optimal 6-phase segmentation and dashed black line for the alternative 5-phase segmentation) and pointwise mean number of weekly emerged flowers (solid red line) with associated standard deviations (dashed red line).

In Gariguette, the heat map representation of the series of the number of weekly emerged flowers for all individuals (Figure 21A) show that flowering can be divided in successive well-differentiated roughly stationary phases common to all the individuals. These phases can be identified by differences in color from light orange (low intensity: 0) to red (high intensity: 25). A first phase without flowering can be identified between 6 and 40 DAP (light orange). This phase is followed by a phase corresponding to the beginning of flowering between 50 and 64 DAP (mostly orange) and a phase of intense flowering between 71 and 113 DAP (majority dark

orange). These two phases of flowering production were followed by a phase with lower flowering production between 119 and 169 DAP followed by another phase of high flowering until the end of the experiment.

Because the number of weekly emerged organs was between 0 and 25 for flowers, 0 and 9 for leaves, and, 0 and 11 for stolons and the frequencies were low for the highest values (Figure 22), we chose to consider these variables as categorical and to group the categories corresponding to the highest values above a given threshold. Furthermore, the frequency distributions for the flowers and the stolons were zero inflated and standard parametric assumptions for count distributions (e.g. Poisson and negative binomial distributions) were not adapted to our case. The number of categories was seven for the leaves, the last one corresponding to the grouping of the values ≥ 6 (the frequency of more than 6 weekly emerged leaves was only 125 to be compared to a sample size of 5184 –i.e. the cumulative length of the 192 phenological series–) for multiple change-point model estimation. The number of categories was four for the stolons, the last one corresponding to the grouping of the values ≥ 3 (the frequency of more than 3 weekly emerged stolons was only 238 to be compared to a sample size of 5,184). For the flowers, because the values were more dispersed, we chose to keep alone the value 0 because of its high frequency (between 38% and 46% for the different genotypes), to group by two the following values up to 10 and to group the values ≥ 11 (the frequency of more than 11 weekly emerged flowers was only 165 to be compared to a sample size of 5,184). We thus directly estimated probability masses for the possible categories within a given flowering phase. The rather large sample sizes (32 plants for each genotype to be multiplied by the length of the phase in observation dates) justified the direct estimation of probability masses for the possible categories.

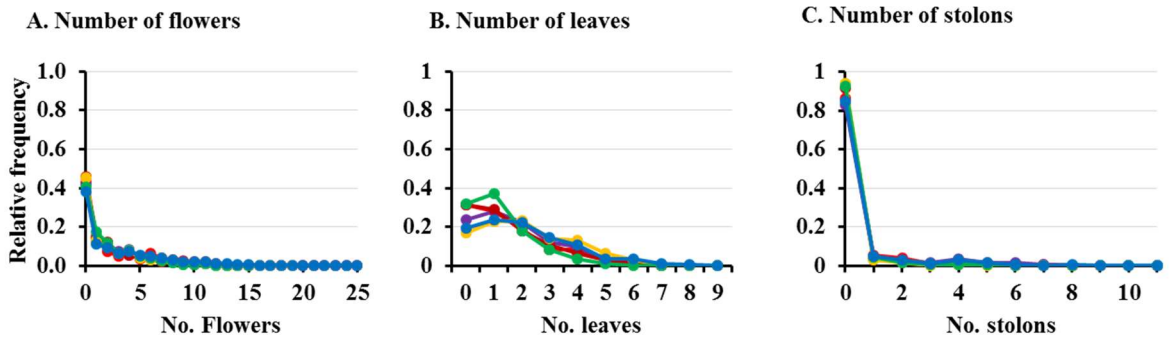

Figure 22: Relative frequency distributions of the number of (A) flowers, (B) leaves and (C) stolons for each variety
Each variety is indicated by one color: yellow for Capriss, purple for Ciflorette, blue for Cir107, marron for Clery, green for Darselect and, red for Gariguette.

We adopted a retrospective or off-line inference approach whose objective was to infer the number of phases *J*, the positions of the $J-1$ change points $\tau_1, \ldots, \tau_{J-1}$ (with the convention $\tau_0 = 1$ and$\tau_J = T+1$) and the within-phase probability masses for each number of organs. For the selection of the number of phases, we used the slope heuristic proposed by Guédon (2015). The principle of this kind of penalized likelihood criterion consists in making a trade-off between an adequate fitting of the model to the data and a reasonable number of parameters to be estimated. Once the number of phases *J* had been selected for a given genotype, the series were optimally segmented into *J* phases using the dynamic programming algorithm proposed by Auger and Lawrence (1989). The assessment of multiple change-point models relied on two posterior probabilities (see Appendix A):

- posterior probability of the selected *J*-phase model i.e. weight of the *J*-phase model among all the possible models. This posterior probability is an output of the slope heuristic.
- posterior probability of the optimal segmentation in *J* phases i.e. weight of the optimal segmentation among all the possible segmentations in *J* phases.

These two posterior probabilities reflect the hierarchical nature of the inference with two successive steps: (i) selection of the number of phases using the slope heuristic considering all the possible segmentations in *J* phases for $J = 1, \ldots, J_{\max}$ and (ii) computation of the optimal segmentation in the number of phases previously selected.

We used different diagnostic tools and in particular, the dynamic programming algorithm for computing the top *N* most probable segmentations in *J* phases proposed in Guédon (2013), to

assess the synchronous segmentation assumption; see an illustration with alternative segmentations in Figure 21. It is often of interest to quantify the uncertainty concerning change-point positions. To this end, we computed uncertainty interval for each change point using the smoothing algorithm proposed by Guédon (2013). All these quantities used for diagnostic are formally defined in Appendix A.

For Gariguette flowering, the slope heuristic favors two models (Figure 21B), the optimal model with 6 phases (posterior probability of 0.78) and an alternative model with 5 phases (posterior probability of 0.22). The optimal segmentations in 5 and 6 phases are nested with a supplementary change point between 113 and 119 in the case of 6 phases. These segmentations are non-ambiguous with very high associated posterior probabilities (0.99 and 0.91 to be related to 14950 and 65780 possible segmentations for 5 and 6 phases respectively). The limits between flowering phases are consistent with abrupt changes in color along the time axis of the heatmap. The step functions corresponding to the successive mean number of weekly emerged flowers within each of the 6 and 5 phases is consistent with the pointwise average number of flowers per week extracted from data (Figure 21C).

For diploid genotypes, phenological study consisted of recording every week during 4 months (from 13th January 2016 to 20th April 2016) the number of leaves (unifoliate leaves (one leaflet) and trifoliate leaves (three leaflets)), stolons and crowns, until the apparition of inflorescence on 50 plantlets. It should be noted that segmentation models were not used in this study which rather consisted in an exploratory analysis. That is why this study is based on cumulative number of leaves, stolons and crowns.

3 Architectural study: representation of the strawberry architecture and analysis of the spatio-temporal development of strawberry

3.1 Architectural data

The core of the architecture description of a plant is its topology, i.e. the adjacency of plant components and its geometry, i.e. the form of the plant components.

For the six seasonal varieties, in order to characterize the spatio-temporal development of varieties the architecture of nine plants per variety was described approximatively once per month at the same date. Topological structure of this plant was described by dissection during which position of leaves, buds, stolons and inflorescences were noted on the main crown as well as on branch crowns. The position and branching order of each crown was also implicitly incorporated in the topological notation (Figure 23A). In addition to the plant topology, several measurements were performed:

i) Petiole length, height and width of left and central leaflets on the last fully expanded leaf to determine the leaf area.

ii) The numbers of opened, closed and aborted flowers of each inflorescence were counted. The total number of flowers by inflorescence was thus obtained. The developmental stages of terminal and axillary meristems were identified by binocular observation. These stages followed a scale from 17 to I used by Invenio and based on the work of Dana and Neri (Jahn *et al.*, 1970; Neri, 2002) for meristem dissection before apparition of inflorescence (Figure 23B). Once inflorescence has appeared, stages of inflorescence follow a BBCH scale (Meier *et al.,* 1994).

The full architecture data was encoded in a spreadsheet file and converted into a Multiscale Tree Graph (MTG) (Figure 24A and B). MTG is a model dedicated to the representation of plant architecture (Figure 24C) at different scales and potentially at successive stages of development along time (Godin and Caraglio, 1998).

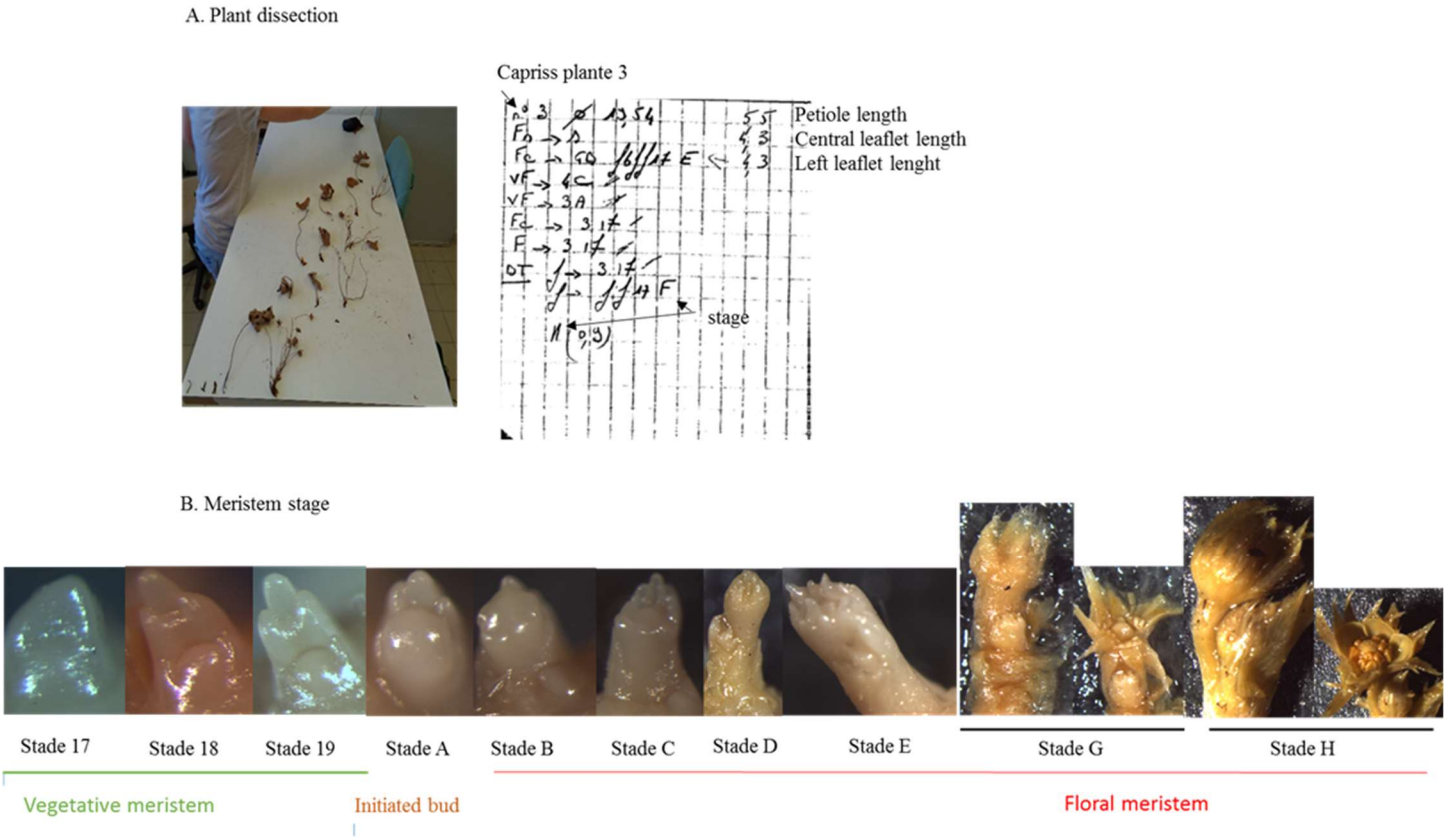

Figure 23: Illustration of (A) plant architecture notations and (B) meristem stage from 17 to H.
In plant architecture notations, each organ is represented by a label, F (leaf), f (primordium), s (stolon), b (vegetative bud), and BT (terminal bud). Stages of meristem are noted from 17 to I: stages F and I are not represented, stages from 17 to 19 represent meristem at vegetative stages, stage A represents floral initiation, and stages from B to H represents floral differentiation steps of meristem.

3.2 Principle of Multiscale Tree Graph models

At a given time, plant architecture can be defined by topological and geometrical information (Balduzzi *et al.*, 2017). Topology deals with the physical connections between plant components, while geometry includes shape, size, orientation and spatial location of the components.

The topology of the plant can be described using a mathematical graph such as the Multiscale Tree Graph (MTG) (Godin and Caraglio, 1998) (Figure 24B). An MTG is a set of trees, which are composed of vertices and labeled edges. A vertex represents a biological modularity (e.g. a plant, a crown, an axis, a leaf or a bud), which can be described at different scales. The multiscale organization of the plant is represented as a quotiented graph, where a vertex contains itself a tree. For instance, a plant (named vertex P) contains several crowns,

each one is defined by a set of connected phytomers, inflorescences, stolons and buds. The connection between entities is represented by an edge in the graph. Branching relationships are represented by an edge labeled '+', while succession of entities by an edge labeled '<'. This simple formalism allows to represent and to encode various architectures including those of cereals/grasses, horticultural plants or forest trees, as well as root system architecture.

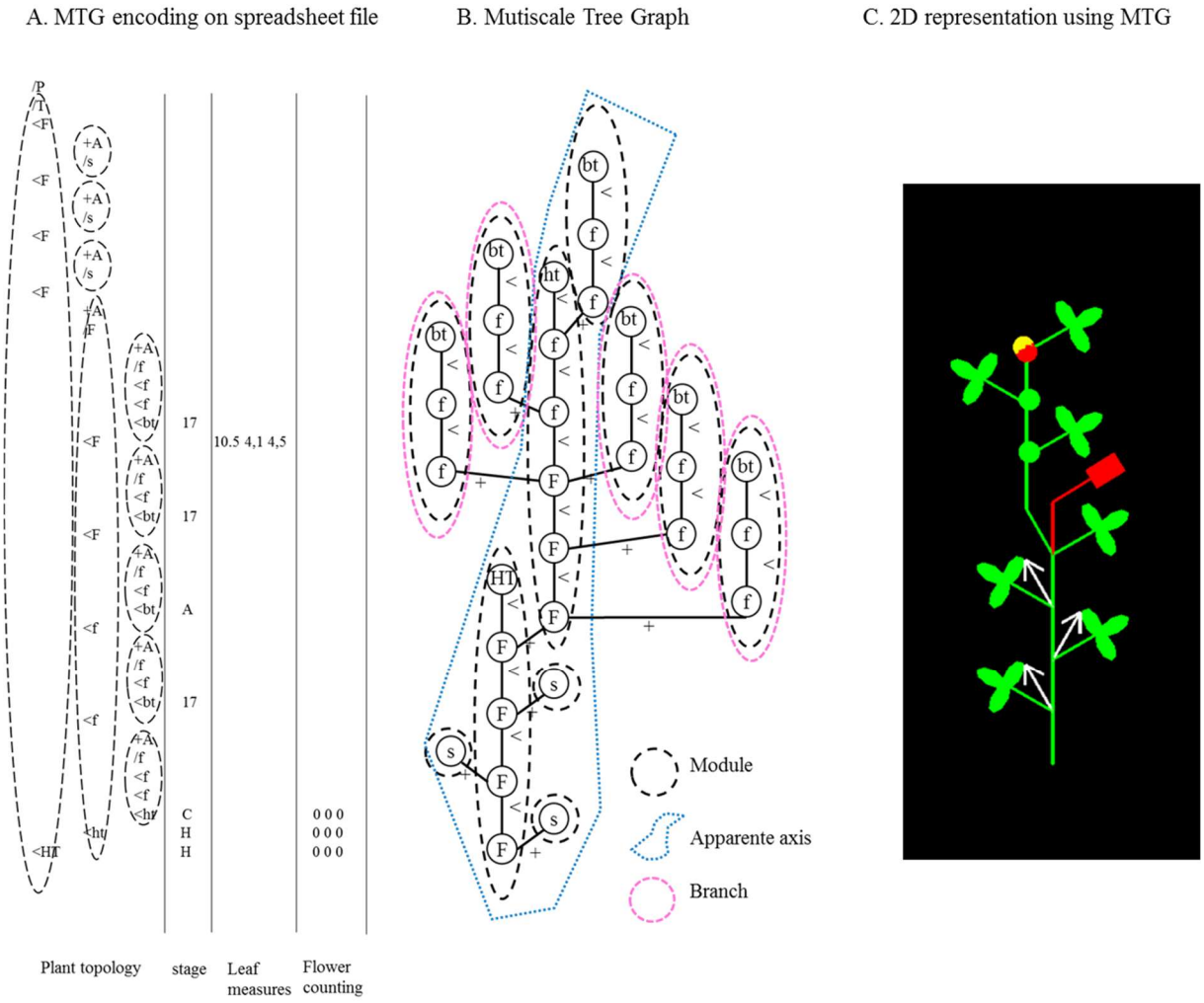

Figure 24: Illustration of strawberry MTG. (A) encoding of a MTG in a spreadsheet file, (B) representation of the topological structure at multiple scale using a MTG and (C) 2D representation
Modules are surrounded by black dashed circles A and B. The main apparent axis is surrounded by a blue dotted line and branches by rose dotted lines in B.

Moreover, the MTG is also a property graph. A set of properties can be associated with each vertex such as, geometrical shape (i.e. cylinder, box, disc…), and measurements (length, height, width …), categorical information (i.e. developmental stage), as well as quantitative information (e.g. number of flowers). While the topology is stored using the structure of the

MTG itself, all the other information (geometry and properties) are stored as properties associated to each vertex.

Because the MTG is a universal formalism to store any plant architecture, it has been used both to encode and analyze architecture in a generic way, but also to model plant structure and function. It is central in the OpenAlea software platform, where each model use MTG as a data structure to communicate in a modular way (Garin *et al.*, 2014).

3.3 MTG applied to strawberry

3.3.1 MTG encoding of strawberry architecture

Because of the genericity of the MTG model, it is necessary to specify the MTG corresponding to a given measurement protocol. Different scales were thus chosen to encode strawberry architecture in MTG (Table 5, Figure 24A and B).

The lowest scale, the organ or entity scale, represent the plant organs: leaf primordia, expanded leaves (internode, petiole and leaflets), axillary and terminal buds, stolons, inflorescence primordia and developed inflorescences. Variables measured for the last fully expanded leaf (length of petiole, central and left leaflet areas), bud stages from 17 to A, and inflorescence stages (from B to H for primordia inflorescences and from I to 87 for expanded inflorescences) were explicitly included. Successions of leaves until inflorescence constitute crowns at module scale. Coding by successor edge label '<' and branching edge label '+' allowed to distinguish two types of crowns: primary crowns (T) and lateral crowns (+A). The distinction of lateral crowns in extension crowns and branch crowns will be implicitly determinate by the crown position with respect to the terminal inflorescence. The crown localized immediately below the terminal inflorescence will be considered as an extension crown while the other crowns in less distal positions will be considered as branching crowns. The coarsest scale chosen to encode strawberry architecture was the plant scale.

Table 5 : Summarize of Strawberry MTG encoding (Symbol, scale and associate properties)

Definition (Symbol)	Scale (range scale)	Properties
Plant (P)	Plant (1)	Date, Varieties, Plant number (explicitly)
Primary Crown (T)	Axis/module (2)	-
Lateral Crown (A)	Axis/module (2)	Branch or Extension Crown (implicitly)
Leaf (F)	Organ (3)	Length of petiole, central and left leaflet areas
Primordia leaf (f)	Organ (3)	-
Bud (b)	Organ (3)	Stage from 17 to A
Stolon (s)	Organ (3)	-
Inflorescence (HT)	Organ (3)	Stage from I to 87, Total No. flowers, No. opened flower, No. aborted flowers
Primordia inflorescence (ht)	Organ (3)	Stage from B to H

3.3.2 Visualization of strawberry architectures using MTGs

Plant architectures are often highly structured and dedicated visualization techniques are a natural complement of exploratory analyses based on statistical summaries. This visual analysis is particularly useful for the identification of the architectural scheme consisting of summarizing all the architectural observations. This visual representation is designed to bring out both the structure of the plant at a given time in its development and the mode of growth leading to its establishment (Edelin, 1984). In our case, two types of representation were designed:

The 3D realistic representation of the plants (Figure 25A) highlights:

(i) The true spatial organization of the plant in three dimensions including phyllotaxis.

(ii) The rank of the modules using a color scale ranging from green to purple (order 0, 1, 2, 3, 4 or 5 are respectively in green, red, blue, yellow, magenta and purple).

(iii) The timing and intensity of flowering by a representation of the inflorescence using light blue boxes. In order to represent the flowering intensity, the box shape is modified according to the inflorescence complexity. The box size is proportional to the number of flowers of the inflorescence and the box is more or less conic according to the proportion of opened/ aborted and closed flowers.

(iv) Stage of buds. Buds are represented by a green or orange sphere when their meristems are vegetative or initiated. When meristems are floral, buds are represented by an orange cube.

The 2D schematic representation (Figure 24C and Figure 25B) of the plant architecture is in accordance with the architectural model, and thus highlights the growth rules described

above as well as the different structures of the plant. This representation makes it possible to highlight sympodial growth, and apparent axes distinguishing the main axis (succession of extension crowns from the primary crown) from the branches (succession of extension crowns from a branch crown). In this representation, the leaf primordia are not visualized. Developmental stages of vegetative, initiated and floral buds are represented by spheres respectively in green, orange and red. Inflorescences are represented by red rectangles.

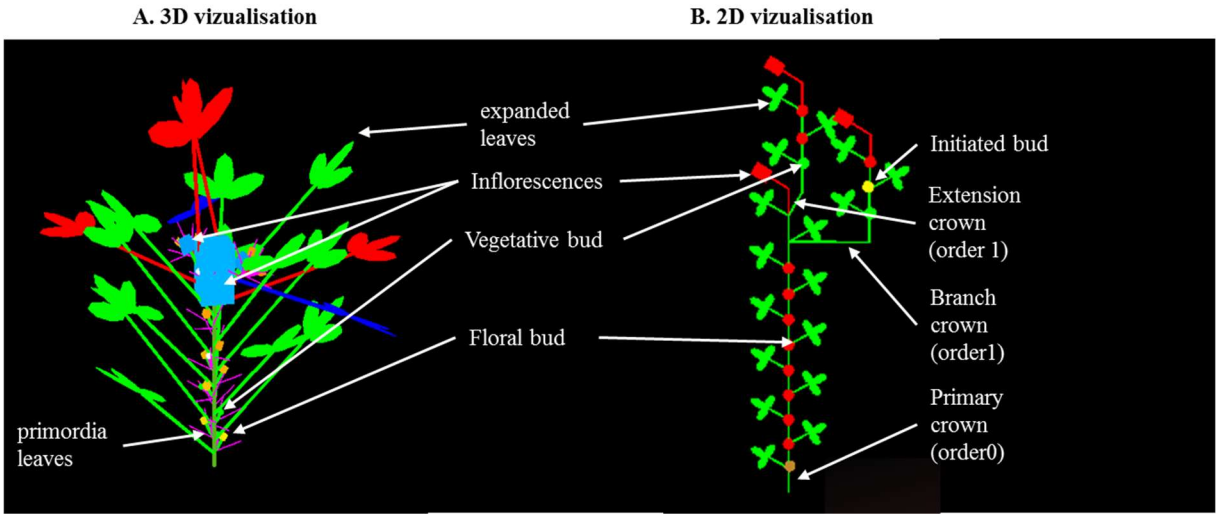

Figure 25: Visualization of strawberry architectures using MTG: (A) 3D realistic representation and (B) 2D schematic representation.
In 3D visualization, leaf and crown order modules are represented by specific color: first order module (order 0 in green), second order module (order 1 in red) and third order module (order 2 in blue). Inflorescence shape (light blue box) changes according to proportion of total and opened, aborted or close flowers. Leaf primordia are represented by purple segments and floral and vegetative buds by green sphere and orange box, respectively. 2D visualization shows sympodial growth and apparent axis: here the main axis consists of a single primary crown followed by a single extension crown and the branch crown is identified by a horizontal shift.

In order to summarize the architecture of strawberry varieties over time, an architectural scheme based on representative individuals for each successive date of observation was build. The representative individual for each date of observation was the most central individual among nine found using a standardization procedure that relies on the number of leaves, flowers, stolon, maximum module order and branching (number of extension and branch crowns).

3.3.3 Standardization procedure for selecting the most central individual for schematic representation (2D)

In the architectural study, we had only 9 individuals described at each successive date of observation. Regarding the potential high structural complexity of the architecture and the small sample size, we chose to extract a representative individual for each genotype and each observation date. To this end, we ordered the 9 individuals within each sample from the most central to the most outlying using a robust standardized distance d_i based on few global variables $(x_{i,1}, \dots, x_{i,j}, \dots)$ (e.g., number of flowers, number of leaves, number of stolons, maximum module order and number of branch and extension crown):

$$d_i = \sum_j \frac{\left| x_{i,j} - \bar{x}_j \right|}{\text{mad}_j},$$

$$d_i = \sum_j \frac{\left| x_{i,j} - \tilde{x}_j \right|}{\text{mad}_j},$$

where $\text{mad}_j = \sum_i \left| x_{i,j} - \tilde{x}_j \right|$. is the mean absolute deviation from the median $\bar{x}_j$ $\tilde{x}_j$ for the variable *j*. Since different individuals were sampled destructively at each date, we did not systematically select the most central individual but in some cases a well-supported (in terms of centrality) alternative individual to show series of individuals at the successive dates which were reasonably consistent in terms of architectural development.

3.3.4 Exploration of architectural data: Module sequencing

In complement to the visual analysis, an exploratory analysis of the plant architecture was made. Due to the small sample size for each variety at a given date and in order to keep part of the structural information of the plants, an extraction in the form of sequences indexed by the order of the successive modules has been made.

Each sequence corresponds to an apparent axis, i.e. a sequence is a succession of extension crowns having for origin the principal crown or a branch crown until the most distal crown. A total of 908 sequences were extracted from 54 plants by varieties, 241, 296, 263, 361, 367, 246 sequences for Gariguette, Ciflorette, Clery, Capriss, Cir107 and Darselect respectively.

The sequences are indexed by the order of the module and incorporated several variables characterizing these modules.

i) Count variables such as the number of leaves, flowers and runners.

ii) Categorical variables such as the type of crown (1: primary crown, 2: extension crowns, 3: branch crown) and the crown status (1: terminal vegetative bud (bt, stage

17, 18, 19, None), 2: terminal bud initiated (bt, stage A), 3: terminal floral bud (ht), 4: inflorescence (HT)).

The exploratory analysis of the strawberry architecture at the module scale consisted in comparing the frequency distributions of five main variables of interest: i) module order as a function of the date observation, ii) number of leaves as a function of the module order, iii) number of flowers as a function of the module order, iv) number of stolons as a function of the module order and v) crown type as a function of the module order. Standard statistical methods were applied (ANOVA based on ranks with post hoc tests for count and categorical ordinal variables and contingency tables for nominal variables) for the exploration of these frequency distributions.

For diploid genotypes, only three plantlets were sampled for architecture at different stages (3, 5, 8, 10, 12 and 14 trifoliate adult leaves). Each plantlet was described for their number and size of leaves and their position on the axis. To record easily the surface of the leaves, they were organized on a scorecard in the order they appeared on the plantlet. This scorecard was digitized to make geometric measures of leaves such as leaf area, leaf shape (height and width of each leaflet) or petiole length thanks to the ImageJ image analysis software (Rasband WS. U.S. National Institutes of Health, Bethesda, MD, USA) (Figure 26A). In addition to the plant architecture study, the stage of each terminal and axillary meristem was identified under binocular optic (Figure 26B) and scored according to Jahn (Jahn *et al.*, 1970; Neri, 2002). This scale ranges the meristem as vegetative (stages 17 or 19) or floral (A when the first observation of floral transition with the mounding of the meristem and letters from B to H, for organogenesis of flower and then inflorescence).
In addition of this genotype, three more plants of Alpine were studied for their architecture at 5.5 months old and incorporate in Tenreira *et al.*, (2017).

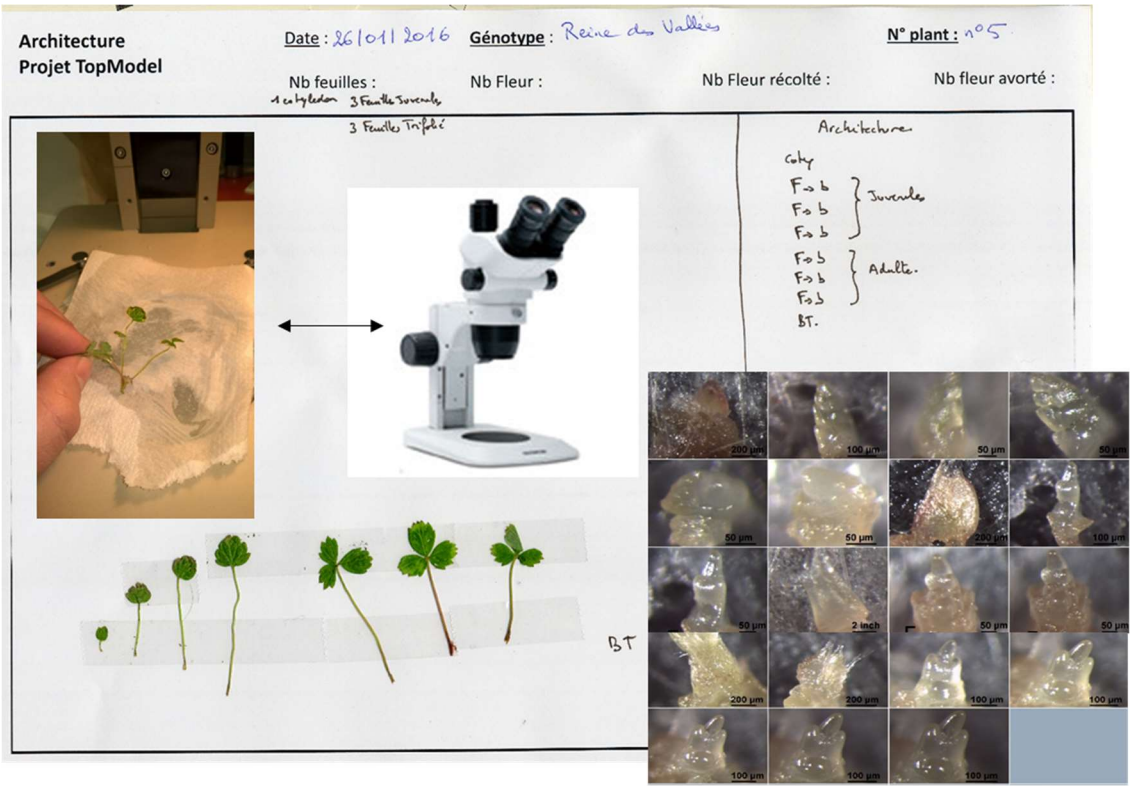

Figure 26: Illustration of architectural notations: (A) architecture of the plant and (B) meristem dissection

4 Molecular expression of flowering key genes

Beside architecture, plants of three out of the six varieties were analyzed for flowering gene expression: Cir107, Darselect and Gariguette. Three replicates, consisted in three foliar discs sampled on three plants with one disc per plant, were obtained for each variety and each date. Foliar discs were maintained in Eppendorf tubes and were placed at 80°C before RNA extraction. Dates of sampling were the same than for architecture: 10/12/2014 (T0 plantation), 08/01/2015 (T4), 11/02/2015 (T8), 04/03/2015 (T12), 02/04/2015 (T16), 20/05/2015 (Tf last date of architecture).

Total RNA was developed based on the CTAB method with modifications, including more PVP, and beta-mercaptoethanol to prevent oxidation of phenolic complexes (Liao *et al.*, 2004). After the last step of ethanol 70 % cleaning, RNA was resuspended in DEPC water. RNA quality and quantity were checked by spectrophotometer (concentration, A260/280 value (more than 1.8), A260/230 value (more than 1.8) and Qubit titration (Qubit® 3.0 Fluorometre RNA High Sensibility kit). cDNA synthesis was carried out with 1µg of total RNA with iScript™ cDNA Synthesis Kit (Bio-Rad) following manufacturer's instructions. Real-time

PCR reactions were performed using 3 µL of resultant cDNA product (1/50 dilution), and 10mM of each primer in a final volume of 20µL with GoTaq® qPCR Master Mix (Promega). Three biological replicates and three technical replicates per biological replicate were analyzed using CFX96 Real-Time System (Bio-Rad). *FveMSI* (Mouhu *et al.*, 2013) and *FveEF1* were used as reference gene.

Analysis of flowering genes expression focused on the three *FT, FT1, FT2* and *FT3*, and *TFL1*, already described (Iwata *et al.*, 2012). Published primers were used for this analysis. In addition to these genes, expression of SOC was also analyzed considering its pivotal role in the balance between vegetative and flowering development (Mouhu *et al.*, 2013). Primer efficiency and qPCR conditions were previously tested for a European project GoodBerry (Metais, comm. pers.).

Chapter 3: Results

Table 6: Univariate flowering models for each variety: Mean number of flowers per phase and limits between phases with the associated uncertainty interval in brackets, Number of phases and posterior probabilities of the optimal segmentation and optimal multiple change-point model.

	Mean numbers of flowers per phase and limits between phases												Posterior probability	
	Mean	Limit	Mean	Limit	Mean	Limit	Mean	Limit	Mean	Limit	Mean	No. phases	Segmentation	Model
Gariguette	0	50 (50,50)	0.96	71 (71,71)	7.27	99 (99,99)	2.04	-	-	175 (175,175)	4.76	5*	0.99	0.22
Gariguette	0	50 (50,50)	0.96	71 (71,71)	7.27	99 (99,99)	3.36	119 (113,119)	1.54	175 (175,175)	4.76	6	0.91	0.78
Clery	0.19	57 (57,57)	1.49	78 (78,78)	4.39			113 (113,113),	1.35	175 (175,175)	3.28	5	1	0.9
Cir107	0.06	57 (57,57)	2.3	78 (78,78)	6.39			113 (113,113)	3.38	-	-	4	0.97	0.99
Capriss	0.02	57 (57,57)	1.14	78 (78,78)	4.66			113 (113,113)	2.39	-	-	4	0.99	0.98
Ciflorette	0.03	56 (56,56)	1.83	77 (77,77)	4.6			105 (105,105)	2.5	-	-	4	1	1
Darselect	0.17	64 (57,64)	1.23	78 (68,85)	4.01			113 (113,113)	2.33	-	-	4	0.51	0.99

(*) well-supported alternative model.

Table 7: Univariate vegetative models for each variety: Mean number of leaves per phase and limits between phases with the associated uncertainty interval in brackets, Number of phases and posterior probabilities of the optimal segmentation and optimal multiple change-point model.

	Mean numbers of leaves per phase and limits between phases												Posterior probability	
	Mean	Limit	Mean	Limit	Mean	Limit	Mean	Limit	Mean	Limit	Mean	No. phases	Segmentation	Model
Gariguette	0.63			40 (40,40)	2.10	92 (92,99)	0.62			154 (154,154)	2.26	4	0.86	1
Clery	1.42									154 (154,154)	2.43	2 *	1	0.17
Clery	0.42			40 (40,40)	1.32					154 (154,154)	2.42	3	1	0.53
Clery	0.42			40 (40,40)	1.62			113 (113,113)	0.83	154 (154,154)	2.42	4 *	0.65	0.29
Cir107	1.71									154 (154,154)	3.72	2	0.99	0.82
Cir107	0	13 (13,13)	1.8							154 (154,162)	3.24	3 *	0.97	0.18
Darselect	0.97									162 (162,162)	2.01	2 *	1	0.24
Darselect	0	13 (13,13)	1.02							162 (162,162)	2.01	3	1	0.76
Ciflorette	1.7											1	1	0.99
Capriss	0	13 (13,13)	2.27									2	1	0.97

(*) well-supported alternative model.

Table 8: Univariate runnering models for each variety: Mean number of stolons per phase and limits between phases with the associated uncertainty interval in brackets, Number of phases and posterior probabilities of the optimal segmentation and optimal multiple change-point model.

	Mean numbers of stolons per phase and limits between phases								Posterior probabilities	
	Mean	Limit	Mean	Limit	Mean	Limit	Mean	No. phases	Segmentation	Model
Gariguette	0			162 (162,162)	1.47			2	1	0.98
Clery	0.01			169 (169,169)	1.09			2*	1	0.39
Clery	0	154 (119,169)	0.14	169 (169,175)	1.09			3	0.32	0.52
Capriss	0			169 (169,175)	0.64			2	0.76	0.82
Capriss	0			162 (141, 169)	0.14	175 (175,190)	0.74	3*	0.62	0.18
Ciflorette	0			160 (160,168)	2.27			2	0.97	0.99
Cir107	0			162 (154,162)	0.67	175 (169,190)	2.81	3	0.62	0.93
Darselect	0			162 (162,162)	0.67			2	0.99	0.6
Darselect	0	154 (134,162)	0.11	169 (162,190)	0.76			3*	0.64	0.4

(*) well-supported alternative model.

Part 1: Plant development of six cultivated strawberries in production conditions

1 Phenological study: identification of developmental patterns on cultivated strawberry varieties in production conditions

For longitudinal data analysis, we assumed that the flowering, vegetative and runnering patterns were common for all the 32 individuals of a given variety and that these patterns took the form of a succession of stationary well-differentiated phases. The analysis of these flowering, vegetative and runnering patterns broke down in two steps:

i. Segmentation in successive flowering, vegetative or runnering phases, synchronous between the individuals, for each variety. For this analysis of the flowering, vegetative and runnering patterns of each variety, we focused in particular on the selection of the number of flowering, vegetative and runnering phases and on the assessment of the synchronous segmentation assumption.
ii. Comparison of the segmentations in successive flowering, vegetative or runnering phases of the variety in order to identify commonalities and differences between the flowering, vegetative and runnering patterns of these varieties.

1.1 The segmentation in phases using univariate multiple change-points model is well defined

The assumption of synchronous segmentation between individuals for a given variety is strongly supported by: i) the high posterior probabilities of both the selected number of phases and the optimal segmentation in this number of phases and ii) the narrow uncertainty intervals for each limit between phases (Table 6-Table 8).

The flower series were segmented in four (Capriss, Ciflorette, Darselect and Cir107), five (Clery) or six flowering phases (Gariguette) with an associated posterior probability of the optimal model above 0.78 (Table 6). The leaf series were segmented in one (Ciflorette), two (Capriss, Cir107, Darselect), three (Clery) or four vegetative phases (Gariguette) (Table 7) with an associated posterior probability of the optimal model above 0.53. The stolon series were

segmented in two (Capriss, Ciflorette, Darselect and Gariguette) or three runnering phases (Cir107, Clery) with an associated posterior probability of the optimal model above 0.52 (Table 8). Moreover the low ambiguity of segmentation is confirmed by the high posterior segmentation probability (Table 6-Table 8) with a probability above 0.9 for all varieties and developmental processes (flowering, vegetative and runnering) except for Darselect ($p = 0.51$) flowering, and Cir107 and Capriss runnering with probability of 0.62 and 0.76 respectively.

Segmentation in flowering, vegetative and runnering phases shows some well-supported alternative models.

Concerning flowering, only one alternative model is well supported for Gariguette (posterior probability of 0.22 for the 5-phase model instead of 0.78 for the optimal 6-phase model). The corresponding 5-phase segmentation is nested within the 6-phase segmentation of the optimal model (merging of the fourth and fifth phases). This can be explained by a not too abrupt decrease of the flower production or by some asynchronisms between individuals at the end of the first flush (fourth phase in the optimal model). (Figure 27, example illustrated with Gariguette).

Concerning vegetative development, two alternative models are well supported for Clery (posterior probabilities of 0.29 for 4-phase model and 0.17 for 2-phase model instead of 0.53 for the optimal 3-phase model) and one alternative model for Cir107 (posterior probability of 0.18 for the 3-phase model instead of 0.82 for the optimal 2-phase model) and Darselect (posterior probability of 0.27 for the 2-phase model instead of 0.76 for optimal 3-phase model). For Clery, the 3-phase segmentation of the optimal model is nested within the 4-phase segmentation of the alternative model (merging of the third and fourth phases). The 2-phase segmentation of the alternative model is nested within the 3-phase segmentation of the optimal model (merging of the first and second phases). For Cir107 and Darselect, the 2-phase segmentation of the optimal model for Cir107 and alternative model for Darselect is nested within 3-phase segmentation of the alternative model for Cir107 and optimal model for Darselect (merging of the first and second phases). These can be mainly explained by the low amplitude of the jump of the number of weekly emerged leaves between these phases (Figure 28, example illustrated with Clery).

Concerning runnering, one alternative 3-phase model is well supported for Capriss (posterior probability of 0.18 instead of 0.82 for optimal 2-phase model) and Darselect (posterior probability of 0.4 instead of 0.6 for optimal 2-phase model), and one alternative 2-phase model for Clery (posterior probability of 0.38 instead 0.52 for optimal 3-phase model).

For Capriss and Darselect, the 2-phase segmentation of the optimal model is nested within the 3-phase segmentation of the alternative model (merging of the second and third phases), while for Clery, the 2-phase segmentation of the alternative model is nested within the 3-phase segmentation of the optimal model (merging of the second and third phases). This can be explained by the high dispersion of stolon production and some asynchronisms between individuals. (Figure 29, illustrated with Darselect).

Whatever the model considered (optimal or alternative), we only consider the optimal segmentation for the selected number of phases because the associated posterior probabilities were most often very high (Table 6-Table 8) and used expressions such as “the optimal/alternative 4-phase segmentation” as a shortcut for “the optimal segmentation of the optimal/alternative 4-phase model”. Segmentation in phases is thus well defined for flowering and a little less for leaves and stolons as highlighted by the alternative models.

To compare varieties, we mainly used optimal univariate flowering, vegetative and runnering models. However for vegetative models (Table 7), the optimal model incorporates a very short first phase consisting of a single date of measurement for Capriss, Darselect, and Cir107. We did not consider that this first phase represents a biologically meaningful phenomenon and thus chose to merge it with the following phase for further analyses. Merging the two first phases for Darselect and Cir107 led us to select a well-supported alternative model, whereas, for Capriss, merging the two first phases led us to select a 1-phase model with a mean of 2.19 weekly emerged leaves. For Clery, we consider both the alternative 2-phase and 4-phase models in order to simplify the comparison between varieties, the optimal model corresponding to an intermediate nesting between these two alternative models.

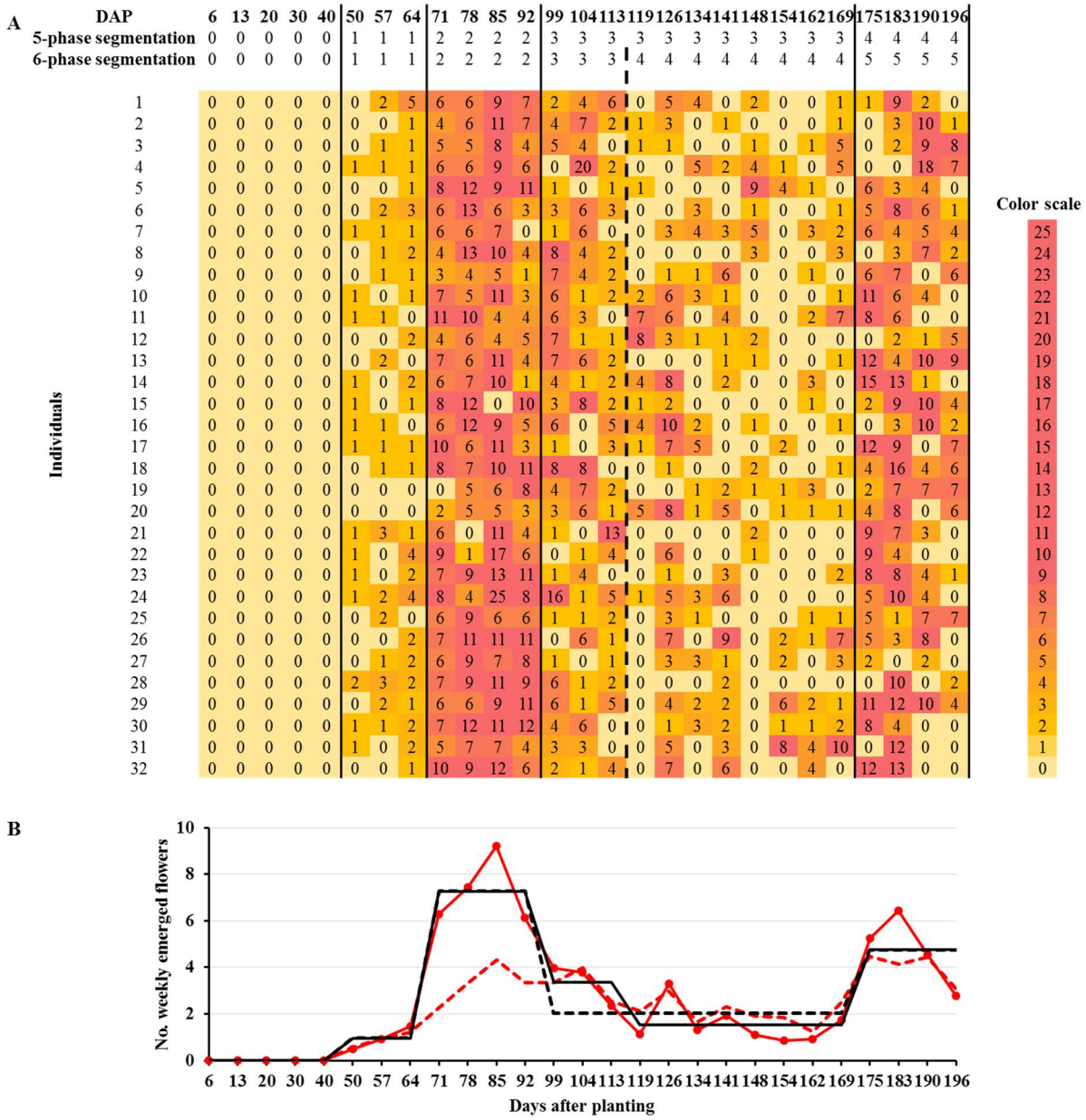

Figure 27 Heat map of the series of the numbers of weekly emerged flowers and univariate flowering models for Gariguette during seasonal production

(**A**) The numbers of weekly emerged flowers for successive dates (Days After Planting, DAP) are represented on the heat map by a color scale from light orange (low intensity) to red (high intensity). Phases are delimited by solid and dotted black lines. Solid black lines represent limits between phases common to the optimal 6-phase and alternative 5-phase segmentations, and the dotted black line represents the additional limit between phases of the optimal segmentation. (**B**) The optimal 6-phase and alternative 5-phase segmentations are represented as step functions (solid black lines for the optimal model and dotted black lines for the alternative model), the level of each step corresponding to the mean number of weekly emerged flowers in the phase. Pointwise means and associated standard deviations of the number of weekly emerged flowers are represented by solid and dotted red lines respectively.

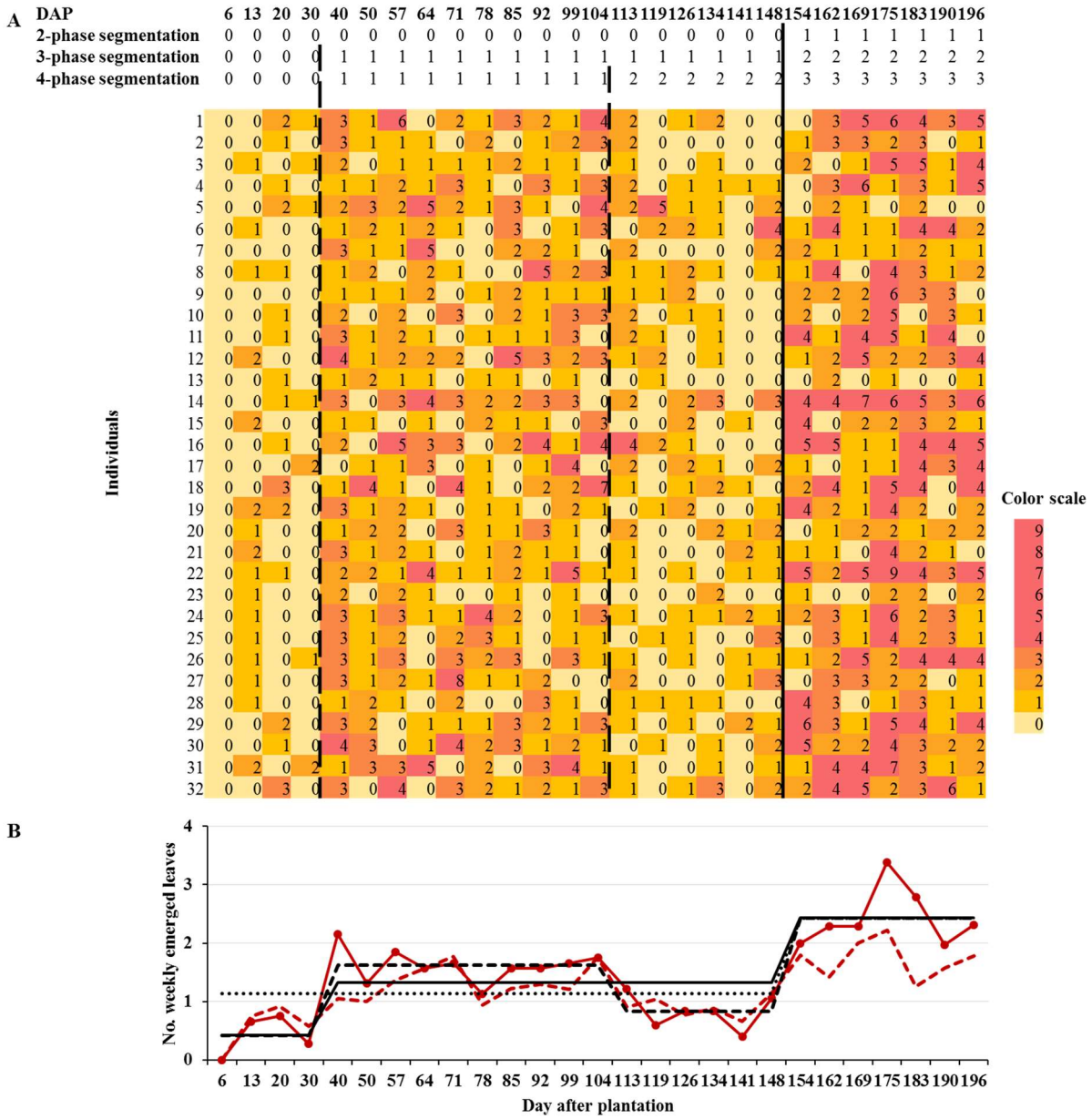

Figure 28: Heat map of the series of the numbers of weekly emerged leaves and univariate flowering models for Clery during seasonal production.

(**A**) The numbers of weekly emerged leaves for successive dates (Days After Planting, DAP) are represented on the heat map by a color scale from light orange (low intensity) to red (high intensity). Phases are delimited by solid and dotted black line. The solid black lines represents the limit between phases common to the optimal 3-phase and alternative 4-and 2-phase segmentations. The first dotted black line represents the limit between phases common to the optimal 3-phase and alternative 4-phase segmentations, and the second dotted black lines represents the additional limit between phases of the alternative 4-phase segmentation. (**B**) The optimal 3-phase and alternative 2- and 4-phase segmentations are represented as step functions (solid black lines for the optimal 3-phase segmentation, dotted black line for alternative 4-phase segmentation and point line for the alternative 2-phase segmentation), the level of each step corresponding to the mean number of weekly emerged leaves in the phase. Pointwise means and associated standard deviation of the number of weekly emerged leaves are represented by a solid and dotted maroon lines.

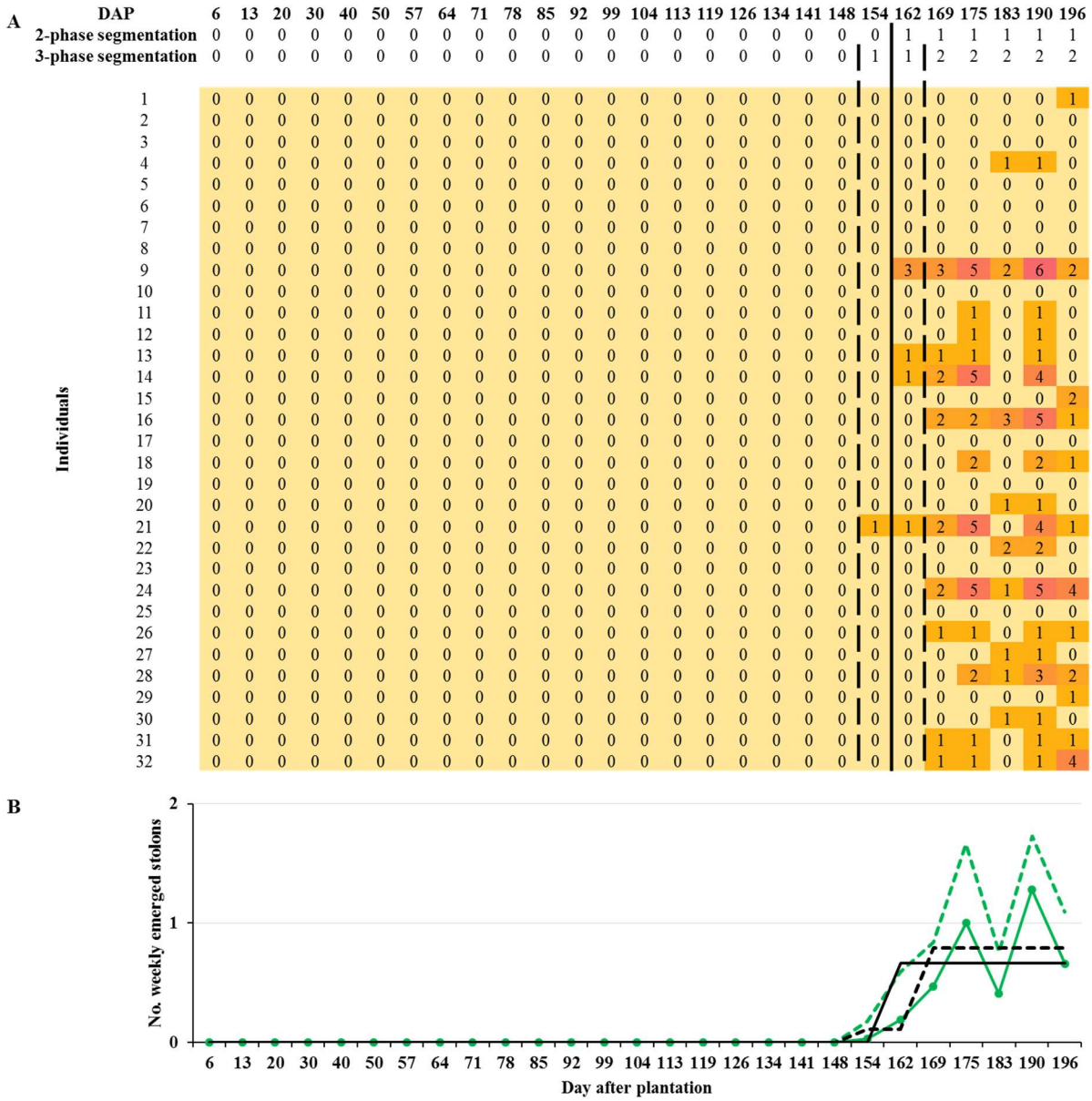

Figure 29: Heat map of the series of the numbers of weekly emerged leaves and univariate stolon models for Darselect during seasonal production.

(**A**) The numbers of weekly emerged stolons for successive dates (Days After Planting, DAP) are represented on the heat map by color scales from light orange (low intensity) to red (high intensity). Phases are delimitated by solid and dotted black lines. The solid black line represents the limit between phases of the 2-phase optimal segmentation and the dotted black lines represent limits between phases of the alternative 3-phase segmentation. (**B**) The 2-phase optimal and 3-phase alternative segmentations are represented as step functions (solid line for the optimal segmentation and dotted line for the alternative segmentation), levels of each step corresponding to the mean number of weekly emerged stolons in the corresponding phase. Pointwise means and associated standard variation of the number of weekly emerged stolons are represented by solid and dotted green lines.

1.2 Comparison of flowering, vegetative and runnering patterns between varieties

1.2.1 Comparison of flowering patterns between varieties

The main differences between varieties concern (i) the occurrence of a second flowering flush in June for Clery and Gariguette, (ii) the higher intensity of the flowering flushes for Gariguette and Cir107, and (iii) for the varieties without a second flush, the higher intensity of the phase of lower flower production for Cir107 (Figure 30).

All the varieties present a common first flush between February and April with a short phase in end January/begin February between the initial non-flowering phase and the phase corresponding to the peak of flowering intensity of the first flush. It can be explained either by the asynchronous increase of flowering for the different individuals of a variety or by some progressivity in the synchronous increase of flowering for the different individuals of a variety, or by a combination of these two reasons (Figure 30A). The first common flush differs between varieties essentially by the intensity of its flowering peak, Gariguette having the highest flowering peak with a mean number of weekly emerged flowers of 7.37, followed by Cir107 with a mean number of weekly emerged flowers of 6.39. The other varieties have relatively similar flowering peaks with a mean number of weekly emerged flowers around 4. These intensities of the flowering peak are significantly different between varieties according to the Kruskal Wallis test (ANOVA based on ranks). Gariguette which shows the highest peak of flowering intensity for the first flush has also a short phase intermediate between this peak and the phase of lower flower production. This phase is less well-defined since, in the well-supported alternative model with one less phase, this phase is merged with the phase of lower flower production (Figure 30B).

From April, flowering differs between varieties by their pattern and intensity. For Gariguette and Clery flowering is characterized by two successive phases of flowering. First phase shows a lower production of flower with a mean number of weekly emerged flowers between 1.5 and 2 from early April to end May. It is followed by a second flowering flush until the end of experiment in July with a mean number of weekly emerged flowers of 4.76 and 3.28 respectively. The other varieties (Capriss, Ciflorette, Cir107 and Darselect) are characterized by a single phase of flower production from April to July. For Cir107, flower production within this phase is higher than for the other varieties, with a mean number of weekly emerged flowers

of 3.38 compare to a mean number of weekly emerged flowers around 2.4 for Capriss, Ciflorette and Darselect varieties (confirmed statistically by Kruskal Wallis test).

To summarize, comparison between varieties allows grouping varieties according to their flowering pattern: (i) Gariguette and Clery with two flushes of flowering separated by a phase of lower production of flowers, (ii) Capriss, Ciflorette, Cir107 and Darselect with one flush of flowering followed by a single phase of lower flower production. Within these two patterns, differences of intensity are observed with a higher intensity of flowering within the two flushes for Gariguette compared to Clery, and a higher intensity of flowering for Cir107 compared to Capriss, Ciflorette and Darselect.

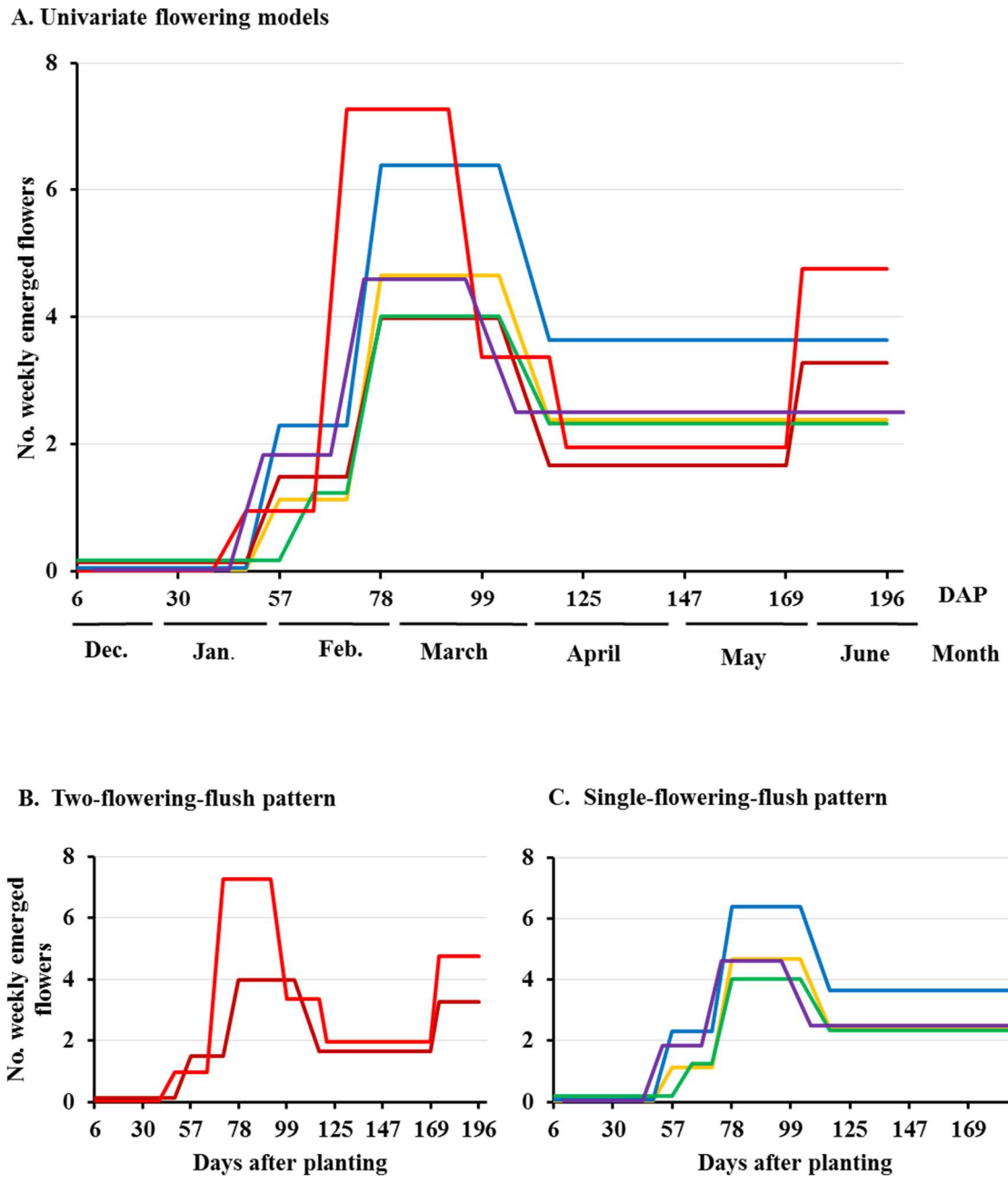

Figure 30: (A) Univariate flowering models represented as step functions, each step corresponding to the mean number of weekly emerged flowers within the corresponding phase. (B) two-flowering-flush pattern of Gariguette and Clery, (C) Single-flowering-flush pattern of Cir107, Capriss, Ciflorette and Darselect

Each variety is represented by one color: yellow for Capriss, purple for Ciflorette, blue for Cir107, brown for Clery, green for Darselect and red for Gariguette. Time is in Days after plantation (DAP) with corresponding months in Figure 30A.

1.2.2 Comparison of vegetative patterns between varieties

The main differences between varieties concern (i) the number of vegetative flushes (zero for Capriss and Ciflorette, one flush for Cir107, Darselect and alternative 2-phase model of Clery or two flushes for Gariguette and alternative 4-phase model of Clery), (iii) the intensity of leaf production which is higher for Capriss compared to Ciflorette (stationary production pattern) and for Cir107 compared to Darselect and alternative 2-phase model of Clery (Figure 31A).

For varieties without a vegetative flush (Figure 31D), the intensity of leaf production is higher for Capriss than for Ciflorette with a mean number of weekly emerged leaves of respectively 2.27 and 1.7.

For varieties with vegetative flush (Figure 31B, C), all the varieties (Cir107, Clery, Darselect and Gariguette) present a common flush from early May. This vegetative flush differs between varieties by its intensity which is higher for Cir107 (mean number of weekly emerged leaves of 3.72), intermediated for Gariguette and Clery (mean number of weekly emerged leaves of 2.42) and lower for Darselect (mean number of weekly emerged of 2.01). Furthermore, Gariguette and the alternative 3-phase model of Clery are characterized by an additional first vegetative flush between mid-January and early April. This first vegetative flush is higher and less extended for Gariguette than for Clery with a mean number of weekly emerged leaves of 2.1 and from early January to early March and 1.6 from early January to early April respectively. At the opposite, Cir107, Darselect and the alternative 2-phase model of Clery are characterized by an initial phase of low leaf production from mid-December to end April, with a higher intensity for Cir107. The identification for Clery of an alternative 2-phase model similar to Cir107 and Darselect and of another alternative 4-phase model similar to Gariguette shows that Clery has a leaf production pattern intermediate between Cir107/Darselect and Gariguette.

To summarize, comparison between varieties allows grouping varieties according to their vegetative patterns (Figure 31B-D): i) Capriss and Ciflorette without vegetative flush, ii) Darselect and Cir107 with a single flush starting in early-May and iii) Gariguette with two flushes, Clery is being intermediate between Cir107/Darselect and Gariguette. However, because the alternative 4-phase model has a higher posterior probability than the alternative 2-phase model, we chose to group Clery with Gariguette. This grouping is reinforced by the optimal 3-phase vegetative model exhibiting 2 vegetative flushes.

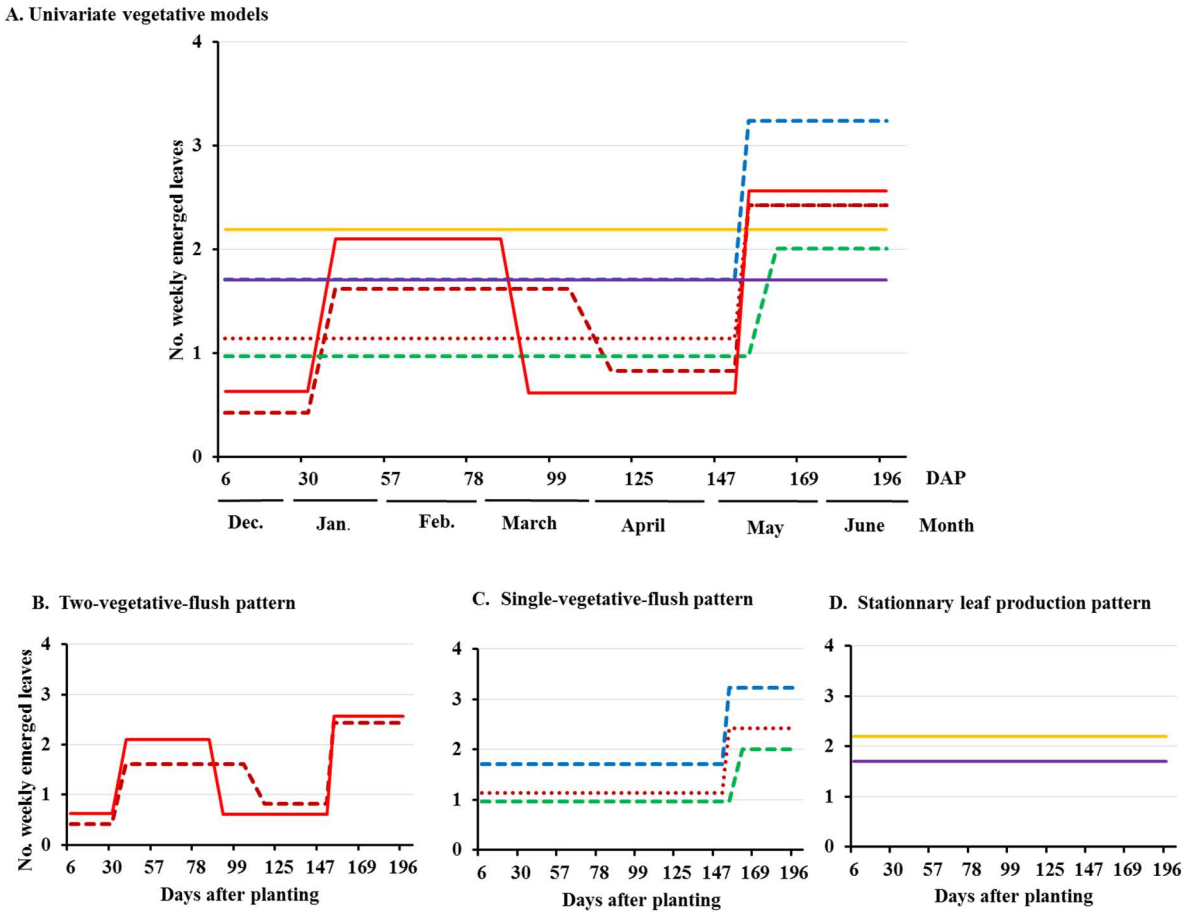

Figure 31: (A) Univariate vegetative models represented as step functions, each step corresponding to the mean number of weekly emerged leaves within the corresponding phase. (B) two-vegetative-flush pattern of Gariguette and Clery, (C) Single-vegetative-flush pattern of Clery, Cir107 and Darselect (D) stationary/steady leaf production pattern of Capriss and Ciflorette .

Each variety is represented by one color: yellow for Capriss, purple for Ciflorette, blue for Cir107, brown for Clery, green for Darselect and red for Gariguette. Optimal models are represented by solid lines and alternative models are represented by dotted or point lines. Time is in Days after plantation (DAP) with corresponding months in Figure 31A.

1.2.3 Comparison of runnering patterns between varieties

All the varieties present a flush of stolon from May to the end of the experiment after a non-stolon production phase from planting to May. The main differences between varieties concern: (i) the starting date of the flush, (ii) the presence or not of a short intermediate phase between the phase of non-stolon production and the phase corresponding to the peak of production and (iii) the intensity of the peak of production (Figure 32).

The runnering flush differs between varieties by a lag of 2 weeks between the early varieties Ciflorette and Clery, with emergence of stolons from early May (154 DAP), and the latest Capriss, with emergence of stolons from mid-May (169 DAP). Gariguette and Clery are intermediate with a lag of 1 week (162 DAP) with respect to Ciflorette and Clery. Because of the overlap between the uncertainty intervals for this limit between phases (Table 8), we can consider that the flush of stolon production is roughly synchronous between varieties. Furthermore, for Cir107 and Clery, a short intermediate phase of low stolon production was identified between the phase of non-stolon production and the phase corresponding to the peak of production. This short phase was also identified in the alternative 3-phase model in Capriss and Darselect (Table 8 and Figure 29 for Darselect). This result shows that this short phase is less well defined. This can be explained by the asynchronism between individuals for some variety, by the not too abrupt increase of stolon production or by the fact that stolon emergence occurred lately during a short period (4 weeks).

The varieties differ also by their intensity of stolon production with the highest production for Cir107 followed by Ciflorette with a mean number of weekly emerged stolons of respectively 2.81 and 2.27. Capriss and Ciflorette present a lower intensity of stolon production than the other varieties with a mean number of weekly emerged stolons of respectively 0.74 and 0.67, while Gariguette and Clery present intermediate intensities with a mean number of weekly emerged stolons of respectively 1.47 and 1.09.

In summary, a single runnering pattern was identified for all the varieties with one synchronous flush of stolons which appeared lately in seasonal production. This pattern differs mainly between varieties by its intensity.

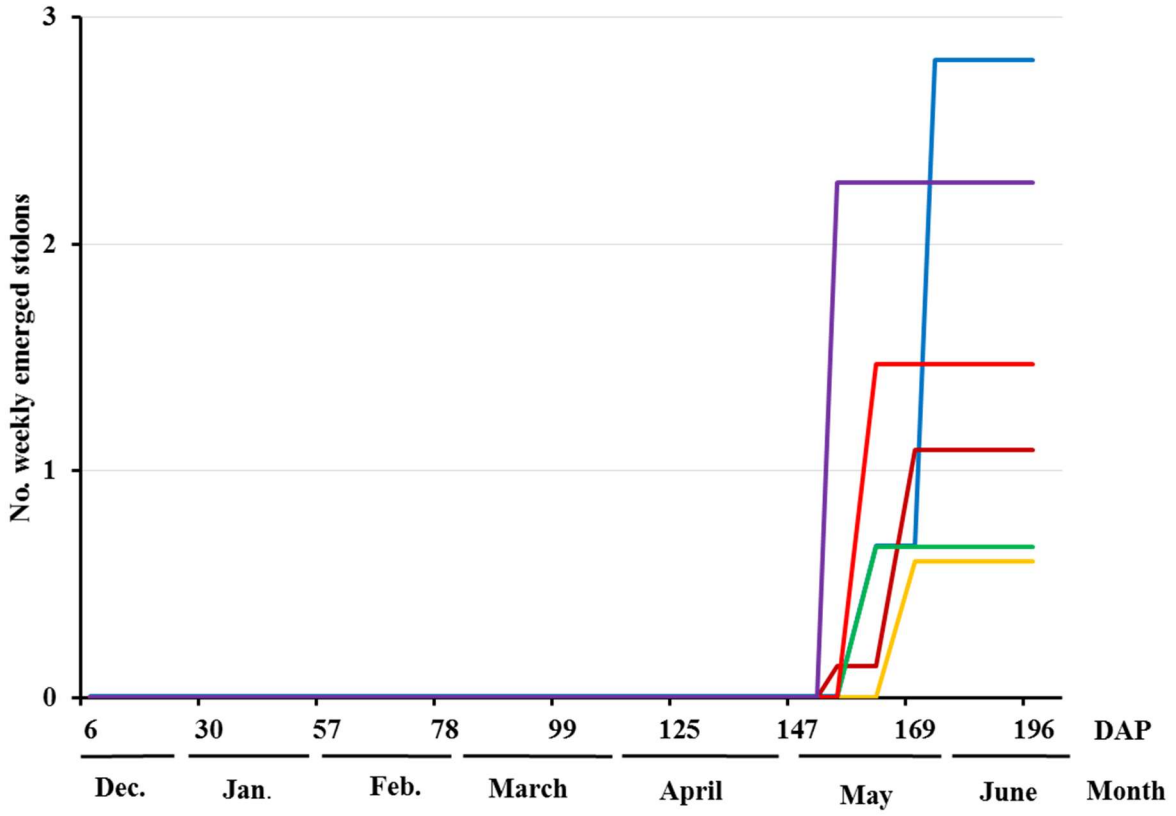

Figure 32: Univariate stolon model represented as step functions, each step corresponding to the mean number of weekly emerged stolons within the corresponding phase

Each variety is represented by one color: yellow for Capriss, purple for Ciflorette, blue for Cir107, brown for Clery, green for Darselect and red Gariguette. Times is in Days after plantation (DAP) with corresponding months.

1.3 Comparison of developmental phases combining flowering, vegetative and runnering patterns

In order to summarize the different phases of plant development based on the three developmental processes, we jointly analyzed the flowering, vegetative development and runnering processes using a trivariate multiple change-points model for each variety. These trivariate multiple change-point models highlighted the changes of highest amplitudes for one or several of the three processes (assuming in this latter case that they are synchronous).

Limits between phases identified by trivariate models called consensus limits are represented by black lines in the heat map representing flowering, vegetative and runnering phases deduced from univariate optimal models (Figure 33). For all the varieties, the first consensus limit between phases corresponds to the beginning of the first flowering flush (i.e. beginning of the first low-intensity flowering phase within this flush), except for Darselect (beginning of the second high-intensity flowering phase within this flush). For Gariguette and Clery additional consensus limits were identified within this flush: at the beginning of the second high-intensity flowering phase for Gariguette and at the end of this phase for the two varieties. Furthermore, for all the varieties, the last consensus limit identified using the trivariate models corresponds to the beginning of the runnering flush. The non-detection of some limits identified using univariate models (corresponding in particular to vegetative phases) can be explained by the lower amplitude of the jump (in number of weekly emerged organs) between successive phases.

Furthermore, three main phases were identified at a macroscopic scale using trivariate models: a first macroscopic phase corresponding to a vegetative phase, a second macroscopic phase beginning with the first flowering flush and ending just before the runnering flush and a third macroscopic phase corresponding to the runnering flush. This third phase is concomitant with the vegetative flush at the end of production for all the varieties except Capriss and Ciflorette and with the second flowering flush for Gariguette and Clery.

These results show that the developmental pattern of strawberry is mainly structured by the flowering and runnering processes and suggest different hierarchies between the three developmental processes along plant development.

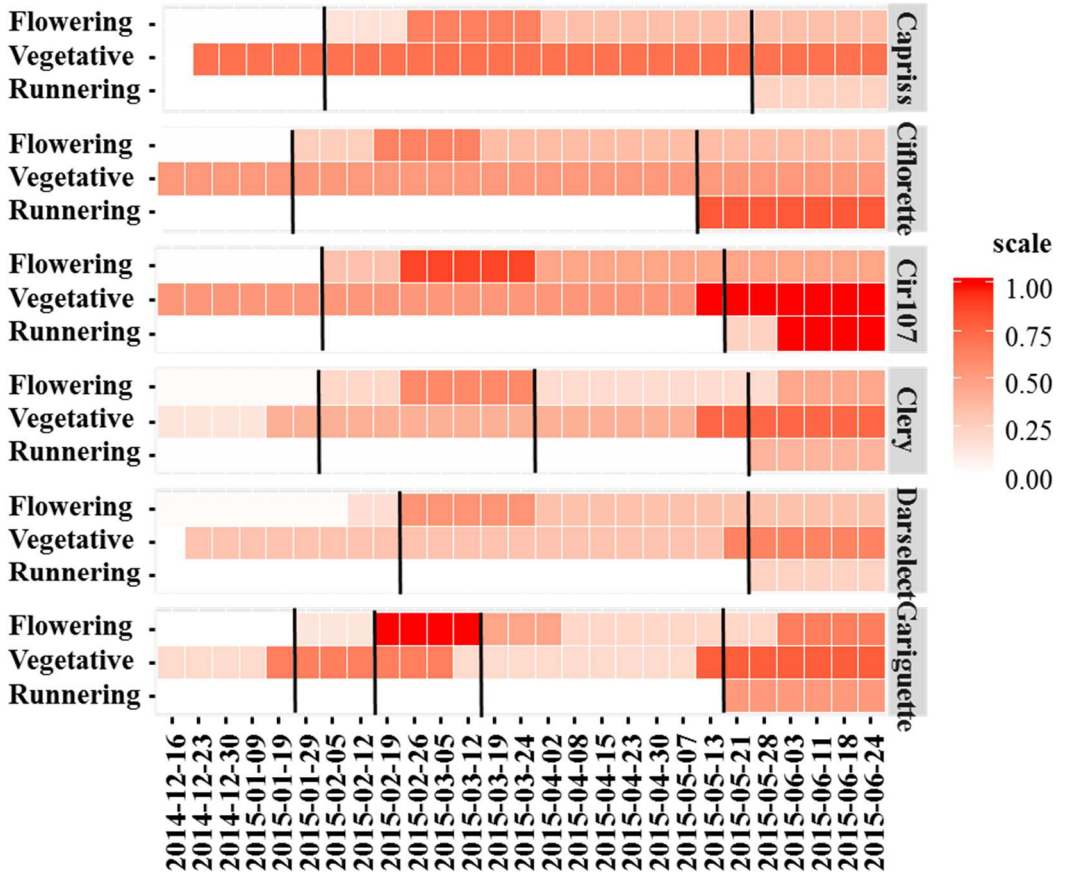

Figure 33: Heat map representation of flowering, vegetative and stolon patterns for all varieties.

The color scale represents the intensity of each phase normalized by the maximal intensity of each developmental process (flowering, vegetative development and runnering) for all the varieties. Vertical black lines represent the consensus limits identified using trivariate multiple change-point models.

To conclude, the longitudinal analysis of flowering, vegetative and runnering processes using univariate multiple change-point models allows identifying:

i. Two flowering patterns: a first one, corresponding to Gariguette and Clery, characterized by two flowering flushes and a second one, corresponding to Capriss, Cir107, Ciflorette, and Darselect, characterized by a single flowering flush followed by a phase of lower flower production. Within these two patterns, differences of flowering intensity were observed with high intensity of the two flushes for Gariguette compared to Clery, and high intensity of flower production for Cir107 compared to the Capriss, Ciflorette and Darselect.
ii. Three vegetative patterns: a first one, corresponding to Gariguette and Clery, characterized by two vegetative flushes, a second one, corresponding to Darselect and Cir107, characterized by a single flush, and a third one, corresponding to Capriss and Ciflorette, characterized by a stationary leaf production. Within each pattern, varieties differ by their intensity of leaf production.
iii. A runnering pattern common to all the varieties with a single flush at the end of the seasonal production which differs by the intensity of stolon production.

Trivariate multiple change-point models show that the developmental patterns are highly structured mainly by the flowering and runnering processes. Based on this hierarchy, varieties can be grouped on the basis of the three developmental processes in the following way (Figure 34):

- Gariguette and Clery: two flowering flushes, two vegetative flushes and at the end of the experiment the runnering flush concomitant with the second flowering flush and the second vegetative flush;
- Cir107 and Darselect: a single flowering flush, and at the end of the experiment the runnering flush concomitant with the single vegetative flush;
- Capriss and Ciflorette: a single flowering flush and, at the end of the experiment, the runnering flush.

Moreover trivariate multiple change-point models confirm the synchronous emergence of stolons for all the varieties and a potential delay of flowering for Darselect.

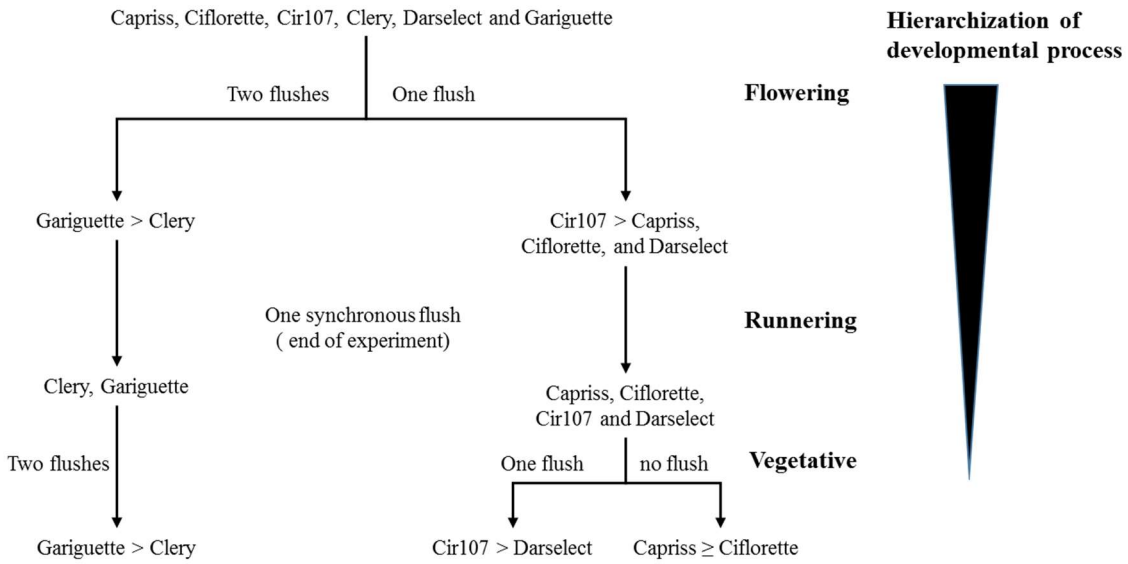

Figure 34: Developmental patterns of strawberry varieties summarized as a hierarchy of developmental processes

2 Architectural study: spatio-temporal analysis of strawberry architecture

The main objective of this architectural exploratory analysis was to characterize the ontogeny of strawberry individuals and its modulation by the genotype. This, analysis combined schematic 2D and realistic 3D representations of individual architectures at successive dates and exploratory architectural data analysis.

2.1 Visualization of plant architecture

Strawberry is a perennial rosette-forming herbaceous plant. At plantation, the plant consists of a primary crown (zeroth-order module) composed of leaves, axillary meristems at the axils of leaves and a terminal inflorescence. When the shoot apical meristem becomes floral, the meristem at the axil of the uppermost leaf below the terminal inflorescence develops into a shorter secondary crown (first-order module). This sympodial branching thus produces an extension crown. Axillary meristems along the primary crown (zeroth-order module) can develop into either a branch crown (another first-order module) or a stolon, or stay dormant. During the plant development, new higher-order crowns (i.e. sympodial units corresponding to determinate growth and classified either as extension or branch crown depending on their positions with respect to the apical inflorescence) develop on the extension and/or branch crowns. In summary, sympodial growth habit can be represented by a succession of incremental order modules. Based on this description, we explored the spatio-temporal architecture of strawberry using two types of visualization, i) A “realistic” 3D representation of all plants along tunnel culture for each variety; ii) A schematic 2D representation of the most central individual highlighting median plant structure at successive dates for each variety.

2.1.1 Realistic 3D representation

We choose for this 3D representation to focus on two architectural criteria, module order and flowering earliness and intensity. Module order is rendered by the color of leaves carried by the module, when leaves are figured in the representation (Figure 35) or by the color of the petioles when leaves are removed from the representation (Figure 36). Earliness and intensity of flowering are represented by a box whose size is proportional to the number of opened flowers of the inflorescence when leaves (except their petioles) are removed from the representation (Figure 36). The 3D representations illustrate that the plant develops through the

establishment of new modules at higher orders and by different flowering intensities (Figure 35-Figure 36).

Visually, the 9 individuals of each variety at each successive dates of observation show a homogenous development, with similar module order distributions (Figure 35). For example, all the Gariguette individuals at planting (mid-December) consisted of a single zeroth-order (green) module. Then, first-order (red) and second-order (blue) modules appeared respectively in mid-February and early April. Third-order (yellow) and fourth-order (purple) modules appeared the last date of observation (early June). Despite this homogeneous development, the varieties differed by their earliness of module development. For Gariguette, Clery and Ciflorette, first-order modules appeared in mid-February while they appeared in early January for Capriss and Cir107 and in mid-December for Darselect. Second-order modules appeared in early March for Capriss, Gariguette, Clery and Ciflorette, while they appeared in mid-February for Cir107 and Darselect. Third- and fourth-order modules appeared the last date of observation (early June) except for Darselect, for which third-order modules appeared in early April.

Using the representation without leaflets (Figure 36), the 9 individuals of each variety at each successive dates of observation show a homogenous flowering represented by the light blue boxes, with similar earliness and intensity. Varieties showed marked differences in intensity of flowering. For Gariguette and Cir107, flowering was already intense for all plants in early March while at this date, flowering started for the four other varieties.

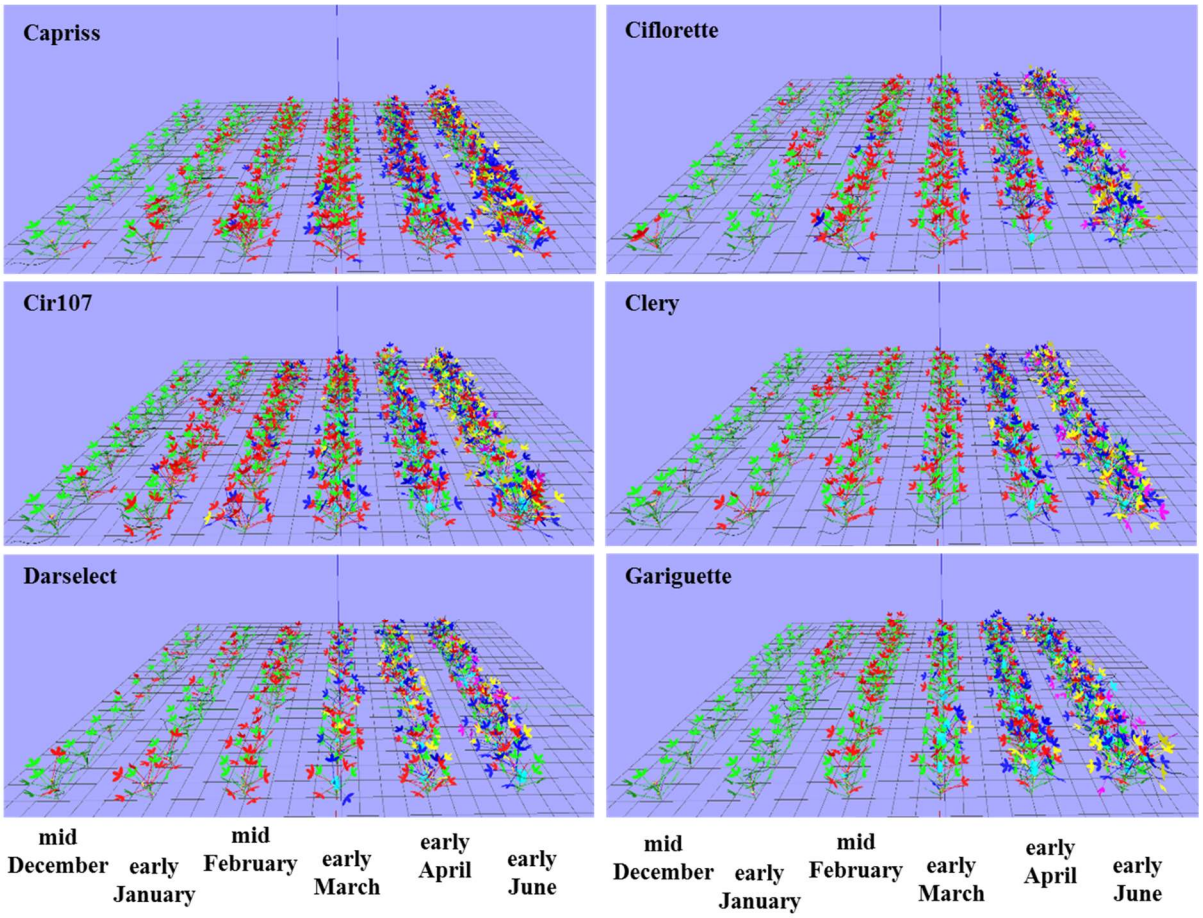

Figure 35: 3D representation with leaflets of the 9 plants of each variety for the successive dates of observation

Colors from green to purple represent module orders (green for order 0; red for order 1, blue for order 2, yellow for order 3, and purple for order 4)

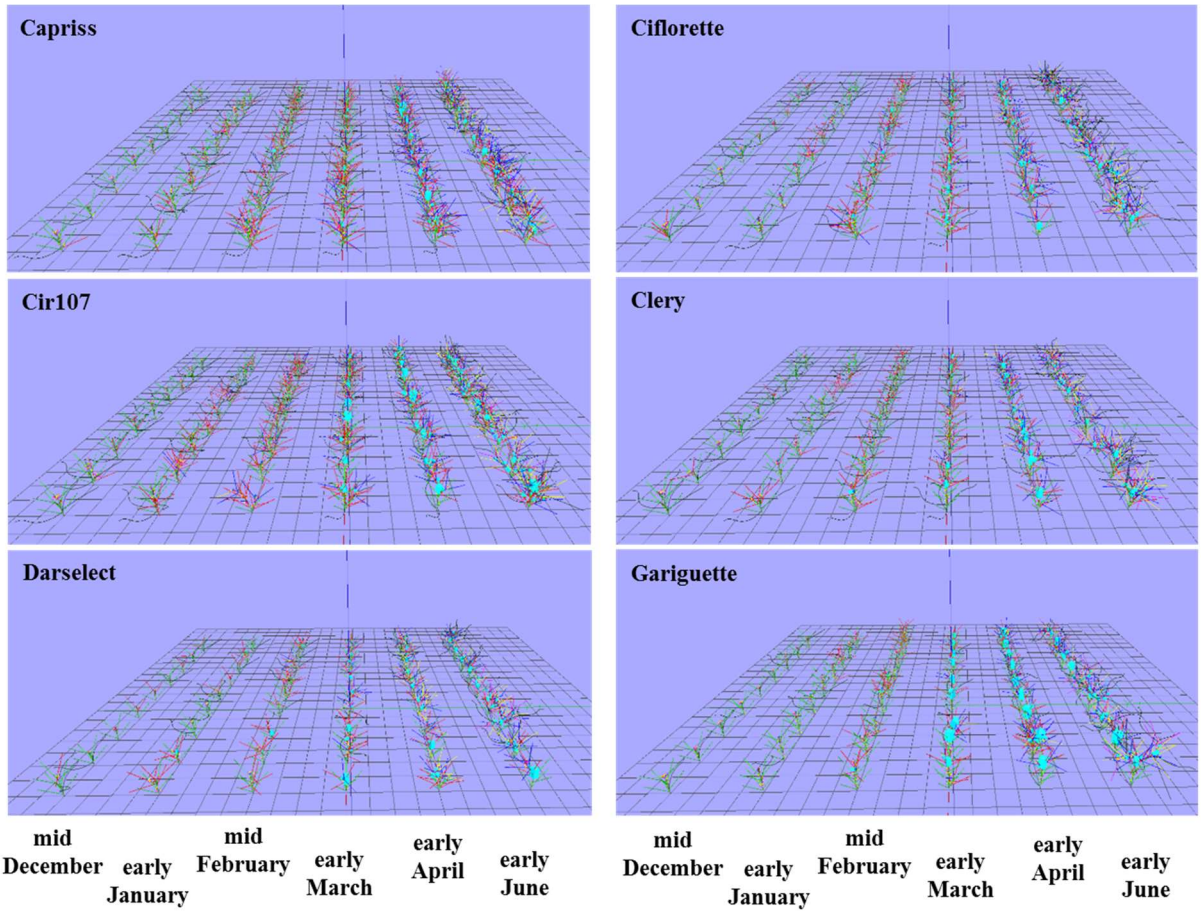

Figure 36: 3D representation without leaflets of the 9 plants of each variety for the successive dates of observation.

Colors from green to purple represent module orders (green for order 0, red for order 1, blue for order 2, yellow for order 3, and purple for order 4) and light blue boxes represent inflorescences. The size of boxes is proportional to the number of opened flowers.

2.1.2 Schematic 2D representation

In addition, we designed a schematic 2D representation similar to botanical diagrams in order to identify structural differences between varieties.

For this 2D schematic representation (Figure 37), we identified among the 9 plants the most central for each variety at each date. This central plant was determined on the basis of the median of the total number of developed leaves, inflorescences, stolons, flowers and branching (number of branches and extension crowns). Then a schematic 2D representation of this central plant at each date and for variety was realized. In this representation, successive extension crowns (modules) along apparent axes were individualized through a slight offset between modules. This representation allowed us to separate the primary apparent axis (primary crown + successive extension crowns issued from the uppermost axillary meristem) from secondary axes (branch crowns + successive extension crowns issued from branch crowns). In addition, inflorescences were represented by red boxes, stolons by arrows and we summarized the status of a bud by the stage of its uppermost meristem (since a bud may contain a non-elongated branching system).

For the six varieties, the zeroth-order modules (8-10 leaves and 12-15 flowers for all the variety except Darselect with 6 leaves and 12 flowers) show a far higher number of leaves and flowers compared to the higher-order modules, which have about 2-4 leaves and 3-8 flowers. The number of leaves and flowers is roughly constant from order 1 onward.

Comparison of architectures between varieties shows that they differ by their complexity and in particular by their branching behavior. This difference in branching leads to different numbers of secondary axes. In early June, Gariguette has developed only a single secondary axis, Ciflorette, Clery, Darselect, two secondary axes, and Capriss, Cir107 four secondary axes (Figure 37). In addition, distribution of secondary axes along the primary crown differed between varieties. The four secondary axes of Capriss and Cir107 were distributed from the bottom to the top of the primary crown while the single secondary axis of Gariguette was at the top of the primary crown. Regulation of apical dominance could be responsible from these differences. The role of apical dominance is reinforced by observation of lateral buds, which did not developed or even aborted from planting date (mid-December) to the last observation (early June).

We can observe that stolons (white arrows) are distributed on zeroth-order module (primary crown) and on the highest-order modules, i.e. on the top of plants, for all varieties. Stolons were absent on first-order modules and rare on second-order modules. Stolons observed

on the highest-order modules appeared in early June at the end of experiment, when day length was about 15 hours. Moreover we can observe that Ciflorette exhibited more stolons than other varieties with 6 stolons compared to 3-4 stolons for other varieties. In zeroth-order module, stolons emerged before planting during the cultivation in nursery.

To summarize, the use of various rules of internode length upscaling within 2D and 3D representations was very useful to introspect the plant structure at successive dates of observation. Realistic 3D representation of plant architecture allows us to observe differences in plant development (module order appearance) and flowering intensity. Schematic 2D representation shows that varieties differ by their structure with differences in vegetative development (given by the number of leaves), branching and inflorescence complexity (given by the number of flowers) according to module order. Thereby, these representations will be appropriate tools for strawberry breeders or scientists to identify the main differences between varieties. Moreover, they also help to communicate complex architectural rules.

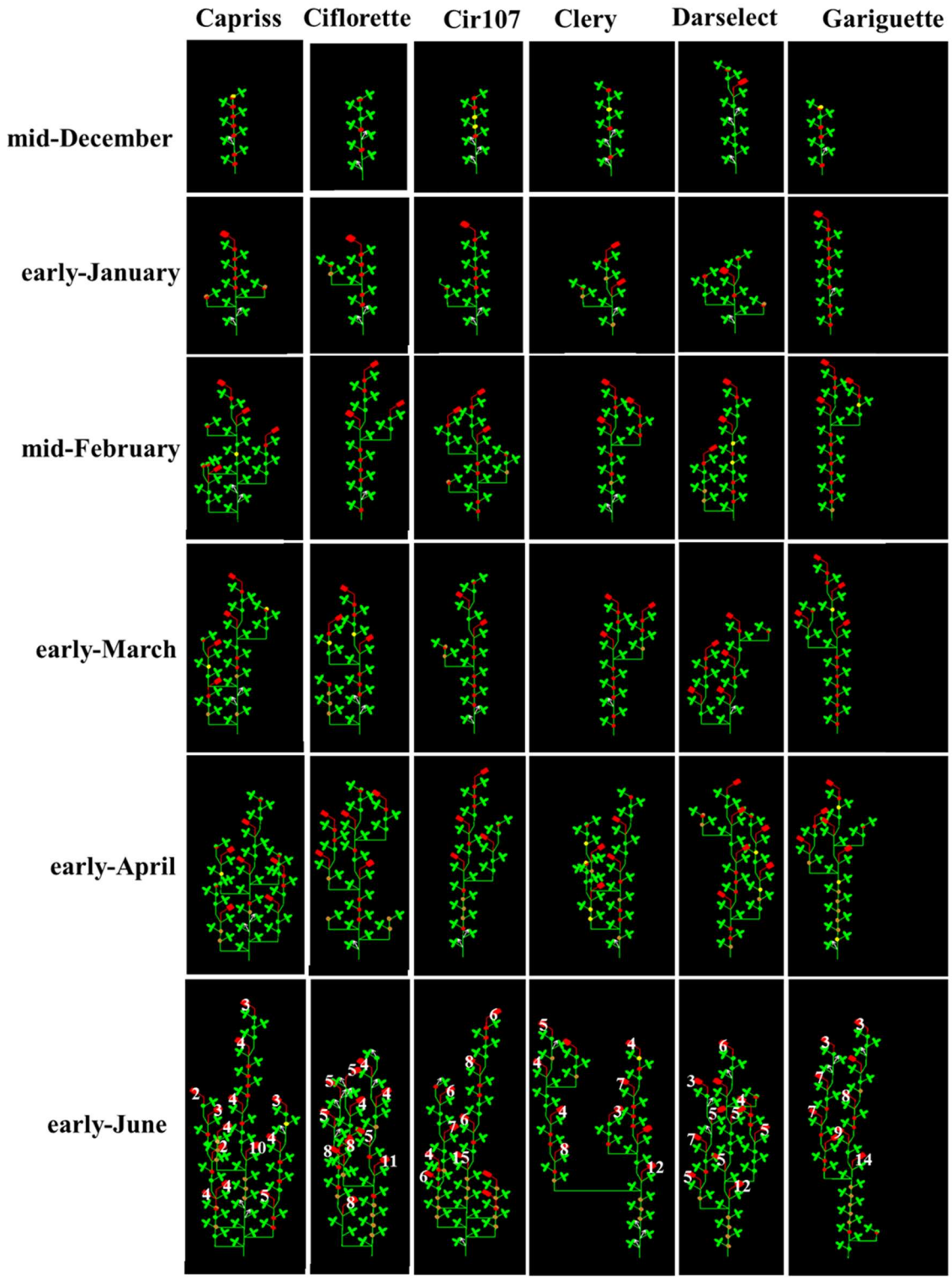

Figure 37: 2D schematic representation of the most central plant architecture according to sympodial development and apparent axes for the six varieties over time

Each organ is represented by a geometrical shape, inflorescence by a red box, phytomer (internode + petiole + 3 leaflets) by a green cylinder terminated by 3 discs and buds by a sphere whose color changes according to their stage: green, yellow and red respectively for vegetative, initiated and inflorescence stage. For the last date (early June), the number of opened flowers for each inflorescence was included.

2.2 Analyses of plant architectural data

In complement to visual analysis, an exploratory analysis of plant architectural data was conducted. Because of the small sample size (9 individuals per genotype and date) and the protocol of experiments with individuals sampled destructively at each date, we chose to focus the exploratory analysis mainly on the modules which were rapidly quite numerous along growth.

The main objective of this exploratory analysis of architectural data was to characterize the ontogeny of strawberry individuals and its modulation by the genotype. In our cultivation system, there was very marked changes of the module characteristics with the few first orders. Afterwards, the characteristics of the modules stabilized. We thus explored these trends for different modules characteristics.

We focused this exploratory analysis on five variables: (i) occurrence of module orders for successive dates, (ii) number of leaves, flowers and stolons per module for successive orders and (iii) crown types (chosen among primary, extension and branching crown) for successive orders. The exploratory analysis consisted in the comparison of the frequency distributions of these variables for the successive dates (first variable) and successive module orders (other variables).

The count variables i.e. the number of leaves, flowers and stolons per module were analyzed using ANOVA on ranks (Kruskal Wallis test with associated post hoc tests). Crown types (categorical variable) were analyzed using contingency tables. We chose to group the highest-order modules because of the small sample sizes (Table 9) using a recursive pooling of samples from the highest order downward if sample size $\leq$ 8, (Table 10).

Table 9: Number of modules for the successive orders before grouping

	Order 0	Order1	Order2	Order 3	Order 4	order 5
Capriss	54	190	102	31	4	0
Ciflorette	54	115	78	31	17	3
Cir107	54	154	110	41	8	0
Clery	54	98	63	34	14	0
Darselect	54	87	57	39	8	1
Gariguette	54	94	62	21	9	1

Table 10: Number of modules for the successive orders after grouping for each variety

	order 0	Order1	Order2	Order 3	Orders 4-5
Capriss	54	190	102	35	0
Ciflorette	54	115	78	31	20
Cir107	54	154	110	41	8
Clery	54	98	63	34	14
Darselect	54	87	57	39	9
Gariguette	54	94	62	21	10

2.2.1 Analysis of the appearance of the successive module orders at the successive dates of observation

We here focus on the appearance of the successive module orders along plant development. Because of the sparse time sampling with only six unevenly spaced dates of observation and the potentially small frequencies for the higher-order modules (Table 11-Table 16), we chose to define thresholds on module orders using high-quantile criterion (0.75- and 0.9-quantile). The quantile is the inverse function of the cumulative distribution function. For instance, the 0.9 quantile divides the range of possible module orders in two contiguous intervals such that the probability of the left interval is 0.9 and the probability of the right interval is 0.1. We chose to present the results of the 0.75-quantile (3rd quartile) and 0.9-quantile that give complementary views on the appearance of the successive module orders along plant development. The 0.75-quantile is sometimes delayed from one date with respect to the 0.9-quantile while this latter may correspond to the highest module order at the final date of observation (early June) for some varieties (Table 17). This approach is more robust that the choice of the highest module order which may correspond to an outlier individual while the quantile criteria rely on the overall distribution of module order at a given date of observation.

Table 11: Capriss module order frequency distribution (with cumulative distribution function in brackets) for the successive dates of observation. The cumulative frequencies for each order and each date are given respectively in the last column and row

Order	mid December	early January	mid-February	early March	early April	early June	Frequency
0	9 (0.8)	9 (0.26)	9 (0.17)	9 (0.14)	9(0.1)	9(0.07)	54
1	2 (1)	24 (0.97)	38 (0.87)	39 (0.74)	44(0.58)	43(0.41)	190
2		1 (1)	7 (1)	17(1)	37(0.99)	40(0.73)	102
3					1(1)	30(0.97)	31
4						4(1)	4
Frequency	11	33	54	65	91	126	380

Table 12: Ciflorette module order frequency distribution (with cumulative distribution function in brackets) for the successive dates of observation. The cumulative frequencies for each order and each date are given respectively in the last column and row

Order	mid December	early January	mid-February	early March	early April	early June	Frequency
0	9 (0.69)	9 (0.64)	9 (0.2)	9 (0.18)	9 (0.14)	9 (0.09)	54
1	4 (1)	5 (1)	30 (0.85)	25 (0.68)	25 (0.52)	24 (0.31)	113
2			7 (1)	15 (0.98)	29 (0.96)	27 (0.56)	78
3				1 (1)	3 (1)	27 (0.81)	31
4						17 (0.97)	17
5						3 (1)	3
Frequency	13	14	46	50	66	107	296

Table 13: Cir107 module order frequency distribution (with cumulative distribution function in brackets) for the successive dates of observation. The cumulative frequencies for each order and each date are given respectively in the last column and row

Order	mid December	early January	mid-February	early March	early April	early June	Frequency
0	9 (0.64)	9 (0.31)	9 (0.16)	9 (0.13)	9 (0.12)	9 (0.08)	54
1	5 (1)	17 (0.9)	33(0.74)	33 (0.58)	31 (0.52)	35 (0.38)	154
2		3 (1)	14(0.98)	28(0.96)	30 (0.91)	35 (0.68)	110
3			1(1)	3(1)	7 (1)	30(0.93)	41
4						8(1)	8
Frequency	14	29	57	73	77	117	367

Table 14: Clery module order frequency distribution (with cumulative distribution function in brackets) for the successive dates of observation. The cumulative frequencies for each order and each date are given respectively in the last column and row

Order	mid December	early January	mid-February	early March	early April	early June	Frequency
0	9 (0.82)	9 (0.47)	9 (0.31)	9 (0.24)	9 (0.14)	9 (0.09)	54
1	2 (1)	10 (1)	20 (1)	21 (0.79)	24 (0.51)	21 (0.29)	98
2				7 (0.97)	27 (0.92)	29 (0.58)	63
3				1 (1)	5 (1)	28 (0.86)	34
4						14 (1)	14
Frequency	11	19	29	38	65	81	263

Table 15: Darselect module order frequency distribution (with cumulative distribution function in brackets) for the successive dates of observation. The cumulative frequencies for each order and each date are given respectively in the last column and row

Order	mid December	early January	mid-February	early March	early April	early June	Frequency
0	9 (0.6)	9 (0.45)	9 (0.31)	9(0.24)	9(0.14)	9(0.12)	54
1	6 (1)	11 (1)	17 (0.9)	15(0.63)	20(0.44)	18(0.35)	87
2			3(01)	10(0.89)	20(0.74)	24(0.66)	57
3				4(1)	17(1)	18(0.89)	39
4						8(0.9)	8
5						1(1)	1
Frequency	15	20	29	38	66	78	246

Table 16: Gariguette module order frequency distribution (with cumulative distribution function in brackets) for the successive dates of observation. The cumulative frequencies for each order and each date are given respectively in the last column and row

Order	mid December	early January	mid-February	early March	early April	early June	Frequency
0	9 (1)	9 (0.56)	9 (0.27)	9 (0.24)	9 (0.14)	9 (0.11)	54
1		7 (1)	24 (1)	17 (0.68)	26 (0.53)	20 (0.36)	94
2				11 (0.97)	28 (0.95)	23 (0.65)	62
3				1(1)	3 (1)	17 (0.87)	21
4						9 (0.99)	9
5						1 (1)	1
Frequency	9	16	33	38	66	79	241

Table 17: Highest module order according to the 0.75-quantile and the 0.9-quantile for successive dates of observation. The colors for each module order are the ones used in the 3D representation (Figure 25)

	Capriss		Ciflorette		Cir107		Clery		Darselect		Gariguette	
	0.75 quantile	0.9 quantile	0.75 quantile	0.9 quantile	0.75 quantile	0.9 quantile	0.75 quantile	0.9 quantile	0.75 quantile	0.9 quantile	0.75 quantile	0.9 quantile
mid December	0	1	1	1	1	1	0	1	1	1	0	0
early January	1	1	1	1	1	2	1	1	1	1	1	1
mid February	1	2	1	2	2	2	1	1	1	2	1	1
early March	2	2	2	2	2	2	1	2	2	3	2	2
early April	2	2	2	2	2	2	2	2	3	3	2	2
early June	3	3	3	3&4	3	3	3	3&4	3	4	3	3&4

We mainly focused on the 0.9-quantile to define the highest module order at successive dates of observation (Table 18 and Figure 38). In mid-December all varieties were composed of zeroth- and first-order modules except Gariguette for which the first-order modules appeared in early January. Second-order modules appeared early for Cir107 (early January), at an intermediate date for Capriss, Ciflorette and Darselect (mid-February) and later for Clery and Gariguette (mid-March) (Cir107 > Capriss, Ciflorette, Darselect > Gariguette, Clery). Third-order modules appeared earlier for Darselect (mid-March) than for the other varieties (early-June) (Darselect > Cir107, Capriss, Ciflorette, Gariguette, Clery). At the last date of observation (early-June), the highest module order was 3 for Capriss and Ciflorette, and 4 for Gariguette, Clery, Ciflorette and Darselect (Ciflorette, Gariguette, Clery, Darselect > Cir107, Capriss). This reflects different rates of development between early April and early June (2 months) with a gain of two module orders (3 and 4) for Ciflorette, Clery and Gariguette and a gain of only one module order (3 or 4) for Capriss, Cir107 and Darselect.

In summary Capriss and Cir107 which have fast development from planting to April, have the slowest development from April until the end of the experiment. Conversely, Clery and Gariguette, which have slow development from planting to April, have fast development from April until the end of the experiment. Ciflorette have an intermediate development rate while Darselect show the fastest development during all the experiment. We thus ordered the varieties as followed:

From planting to April: Darselect > Cir107, Capriss, ≥Ciflorette > Gariguette, Clery

From April to end of experiment: Darselect > Gariguette, Clery≥ Ciflorette > Capriss, Cir107

Table 18: Highest module orders for each date of observation and each variety according to 0.9 quantile. The colors for the module orders are the ones used in the 3D representation (Figure 25)

	Capriss	Ciflorette	Cir107	Clery	Darselect	Gariguette
mid-December	1	1	1	1	1	0
early-January	1	1	2	1	1	1
mid-February	2	2	2	1	2	1
early-March	2	2	2	2	3	2
early-April	2	2	2	2	3	2
early June	3	3&4	3	3&4	4	3&4

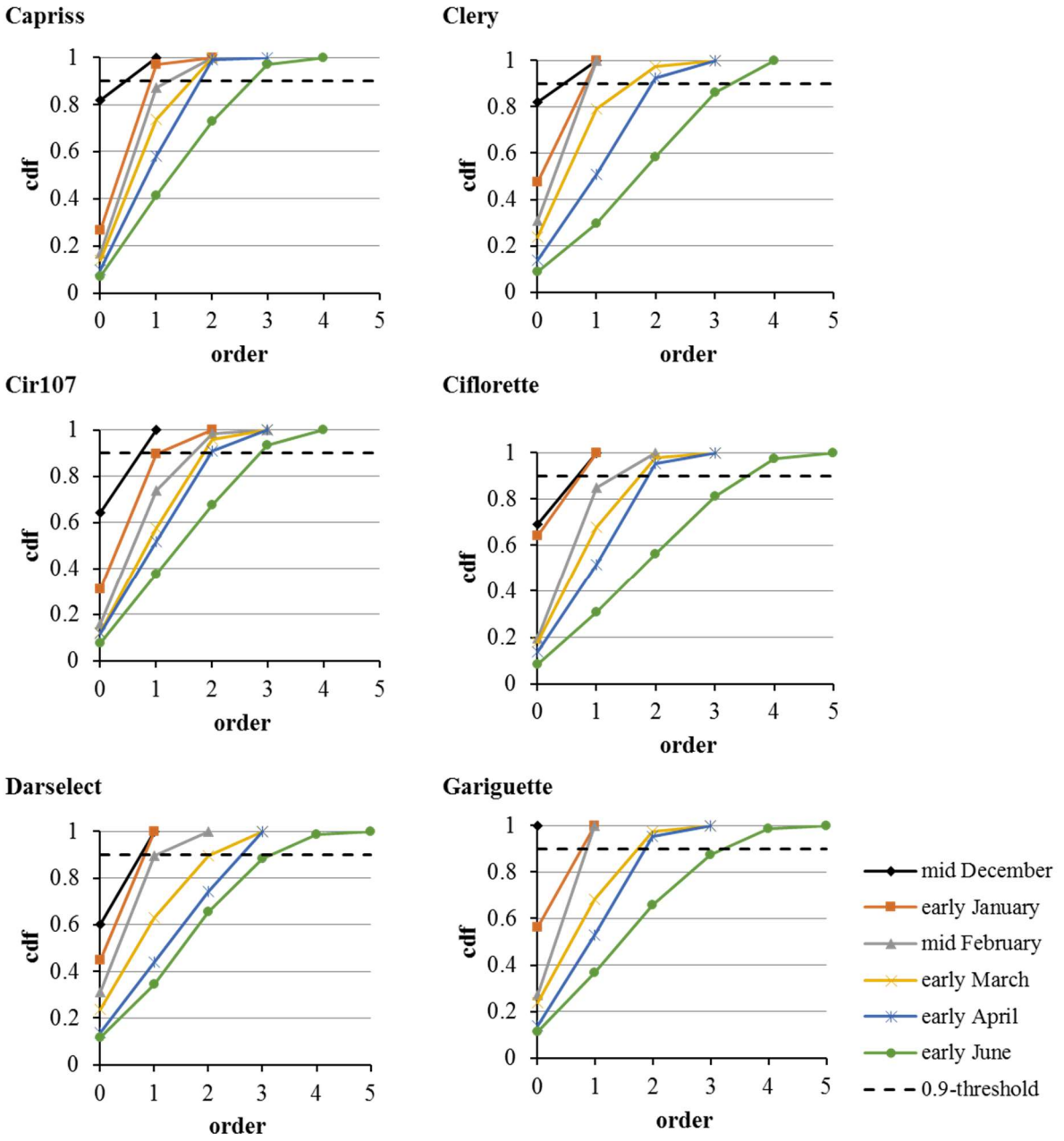

Figure 38 Cumulative distribution function (cdf) of the module order for each date of observation and each variety.
Each date is represented by one color (black for mid-December, orange for early January, grey for mid-February, yellow for early March, blue for early April and green for early June). 0.9 quantile thershold is represented by dotted black lines.

2.2.2 Analysis of the frequency distributions of the number of leaves and the number of flowers per module as a function of the module order

Before examining if varieties showed differences in their number of leaves and flowers according to the module order, the frequency distributions of these count variables were explored and compared.

- Frequency distributions of the number of leaves and the number flowers

For Gariguette, the zeroth-order modules displayed 7 to 18 leaves while first- and second-order modules displayed 2 to 6-8 leaves and third- and fourth-order modules only 2-3 leaves (Figure 39, Gariguette No. leaves). The lower variability for the orders 3 and 4 can be explained by their occurrences at the end of the experiment (early June) (Table 16) and a smaller number of modules (21 and 9 for respectively third- and fourth-order modules) compared to the number of modules at lower orders (54, 94 and 62 for respectively zeroth-, first- and second-order modules) (Table 16). Despite the dispersion of the number of leaves of zeroth-, first- and second-order modules, the frequency distribution of the number of leaves of zeroth-order modules is clearly separated from the ones of higher-order modules (Figure 39, Gariguette no. leaves). Zeroth-order modules were thus generally composed of a far higher number of leaves than modules of higher orders with a mean of 10 leaves compared to a mean of 3-4 leaves for the higher-order modules (Figure 40A). This result indicates that Gariguette developed a primary crown (zeroth-order module) with a mean of 10 leaves while subsequent crowns (branch or extension crowns) had only 3-4 leaves (almost constant number of leaves for module of order ≥ 1). This exploratory analysis of data detailed for Gariguette was applied to the other varieties (Figure 39 and Figure 40A): i) zeroth-order modules were clearly separated from higher-order modules and ii) the higher–order modules exhibit similar frequency distribution (Figure 39) with a mean number of leaves between 3 and 4 leaves for all the varieties (Figure 40A). Moreover, difference in mean number of leaves of zeroth-order module can be observed between varieties with a mean number of leaves around 10 leaves for Capriss, Gariguette and Cir107, around 7-8 leaves for Clery and Ciflorette and 5 for Darselect (Figure 40A).

Frequency distributions of the number of flowers for the successive module orders show that, as shown previously for the number of leaves, zeroth-order modules are separated from the higher-order modules (Figure 39, Number of flowers). The inflorescence complexity

measured by the number of flowers decrease abruptly after the zeroth-order module (Figure 40B).

For zeroth-order modules, Gariguette produced the most complex inflorescences with a mean of 18 flowers and Capriss the less complex inflorescences with a mean of 8 flowers (Figure 40B). The other varieties, Cir107, Clery, Ciflorette and Darselect, displayed intermediate complexity inflorescence with means between 10 and 15 flowers. Contrary to the number of leaves of modules, the number of flowers of inflorescences did not stabilize at order 1 but rather at order 2 (Figure 39, Number of flowers).

For first-order modules, Cir107 had the most complex inflorescences with a mean of 8 flowers, Capriss exhibited the less complex inflorescences with a mean of 3 flowers (Figure 40B). The four other varieties, Clery, Ciflorette, Darselect and Gariguette, showed inflorescences of intermediate complexity with a mean of 6-7 flowers. Modules of order ≥ 2 displayed similar frequency distributions of the number of flowers within variety (but not between varieties) (Figure 39, Number of flowers). For modules of order ≥ 2, Gariguette has the most complex inflorescences with a mean of 6 flowers, Capriss has the less complex inflorescences with a mean of 3 flowers. The number of flowers varies between 4 and 5 for the other varieties (Figure 40B).

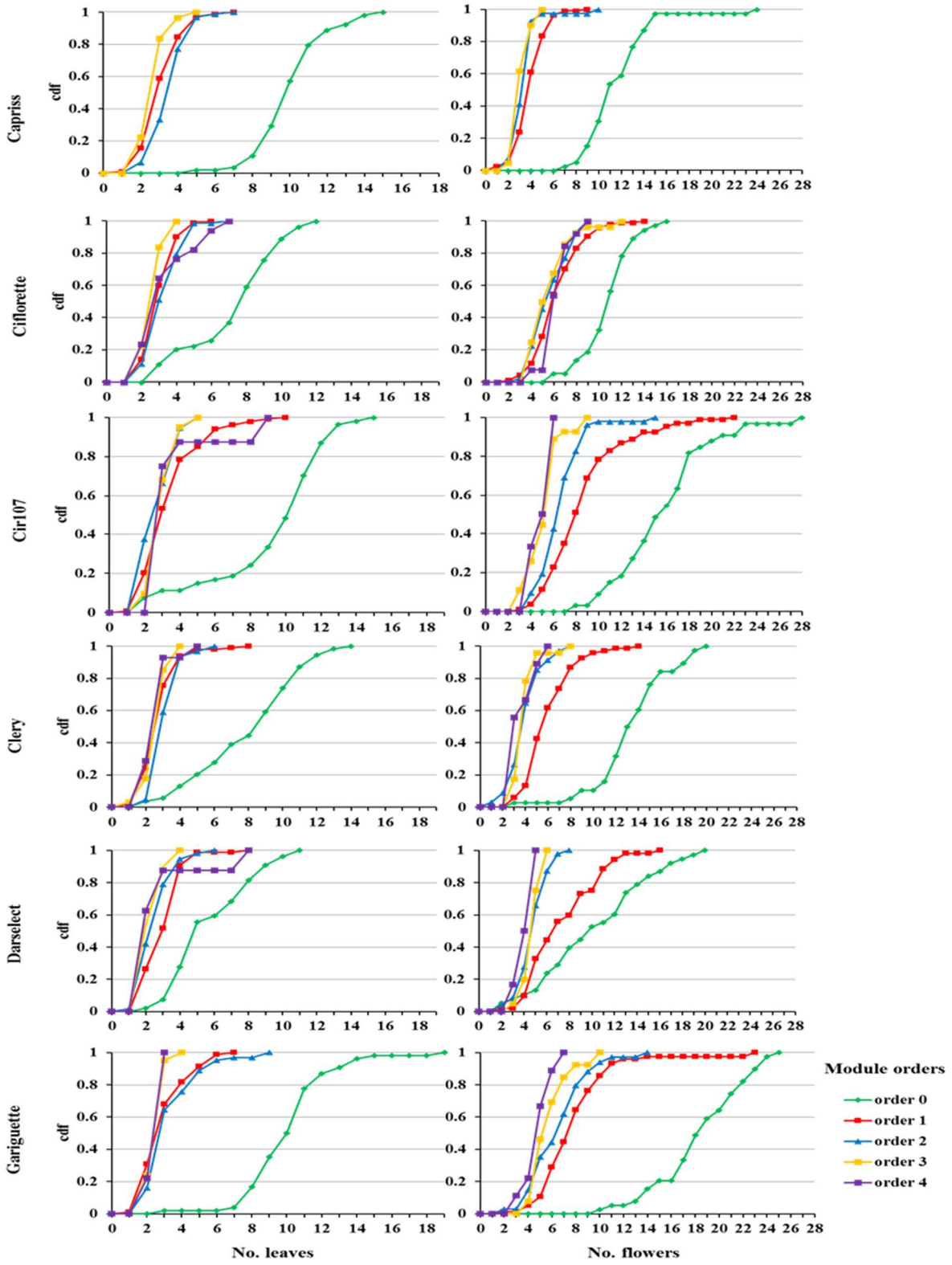

Figure 39: Cumulative distribution function (cfd) of the number of leaves and the number of flowers for each module order.
Each modules order is represented by one color (green for order 0, red for order 1, blue for order 2, yellow for order 3 and, purple for order 4).

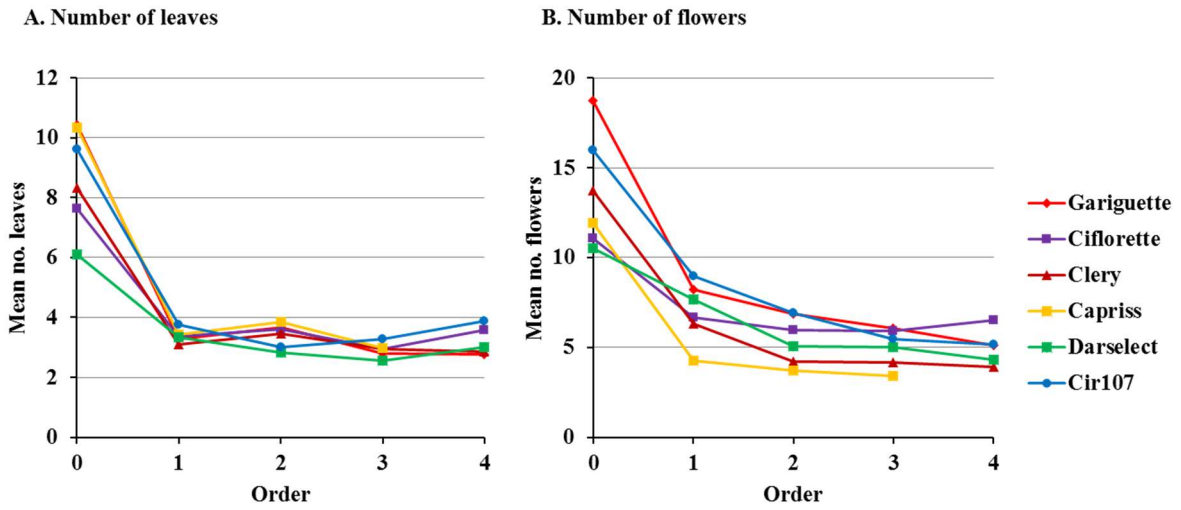

Figure 40: Pointwise mean number of leaves (A) and flowers (B) of modules for successive orders and for each variety
Each variety is represented by a color: yellow for Capriss, purple for Ciflorette, blue for Cir107, marron for Clery, green for Darselect and red for Gariguette

- Comparison of the numbers leaves and the numbers of flowers for successive orders between varieties

In order to compare the number of leaves and the number of flowers between varieties, we aimed at identifying from which module order the number of leaves or flowers was roughly constant for each variety using a linear trend regression. In particular, we tested the zero value of the slope parameter. The number of leaves was constant from order 1 onward except for Cir107 and Darselect (Table 19). However, this non-zero slopes were explained by the increase of variability for the highest orders (Figure 41, see the 95% confident intervals) and we concluded that the number of leaves was almost constant. Similarly the number of flowers was constant from order 2 onward (Table 20). This approach thus allowed us to compare between varieties the number of leaves for zeroth-order (order 0) and from first-order module onward (orders ≥ 1) and the number of flowers for zeroth- order module, first-order module (orders 1) and from second-order module onward (orders ≥ 2) (Figure 42 and Table 21-Table 22).

Table 19: Linear trend (estimate slope and 95% confidence interval−IC95%−) for the number of leaves as function of the module order for zeroth-order onward (orders ≥ 0) and for first-order onward (orders ≥ 1)

	Order ≥ 0		**Order ≥ 1**	
	Slope	IC 95%	Slope	IC 95%
Capriss	-1.89	[-2.15, -1.62]	-0.06 n.s.	[-0.21, 0.10]
Ciflorette	-0.91	[-1.11, -0.71]	0.05 n.s.	[-0.08, 0.18]
Cir107	-1.62	[-1.87, -1.36]	-0.24	[-0.43, -0.05]
Clery	-1.28	[-1.52, -1.04]	-0.05 n.s.	[-0.18, 0.08]
Darselect	-0.96	[-1.14, -0.78]	-0.30	[-0.46, -0.14]
Gariguette	-2.00	[-2.32, -1.68]	-0.12 n.s.	[-0.33, 0.10]

n.s. indicates that the slope is non-significantly different from zero

Table 20: Linear trend (estimate slope and 95% confidence interval−IC95 %−) for the number of flowers as function of the module order for zeroth-order onward (orders ≥ 0), for first-order onward (orders ≥ 1) and for the second-order module onward (orders ≥ 2)

	Order ≥ 0		**Order ≥ 1**		**Order ≥ 2**	
	Slope	IC 95%	Slope	IC 95%	Slope	IC 95%
Capriss	-2.61	[-3.02, -2.20]	-0,51	[-0.75, -0.27]	-0,47 n.s.	[-0.97, 0.03]
Ciflorette	-1.07	[-1.36, -0.79]	-0,15 n.s	[-0.44, 0.13]	0,33 n.s.	[-0.14, 0.79]
Cir107	-2.86	[-3.33, -2.40]	-1,65	[-2.14, -1.17]	-1,13	[-1.73, -0.53]
Clery	-2.63	[-3.04, -2.22]	-1,01	[-1.34, -0.68]	-0,14 n.s.	[-0.58, 0.30]
Darselect	-1.85	[-2.28, -1.42]	-1,26	[-1.69, -0.82]	-0,22 n.s.	[-0.59, 0.15]
Gariguette	-3.46	[-4.06, -2.85]	-0,99	[-1.49, -0.48]	-0,68 n.s.	[-1.36, 0]

n.s. indicates that the slope is non-significantly different from zero

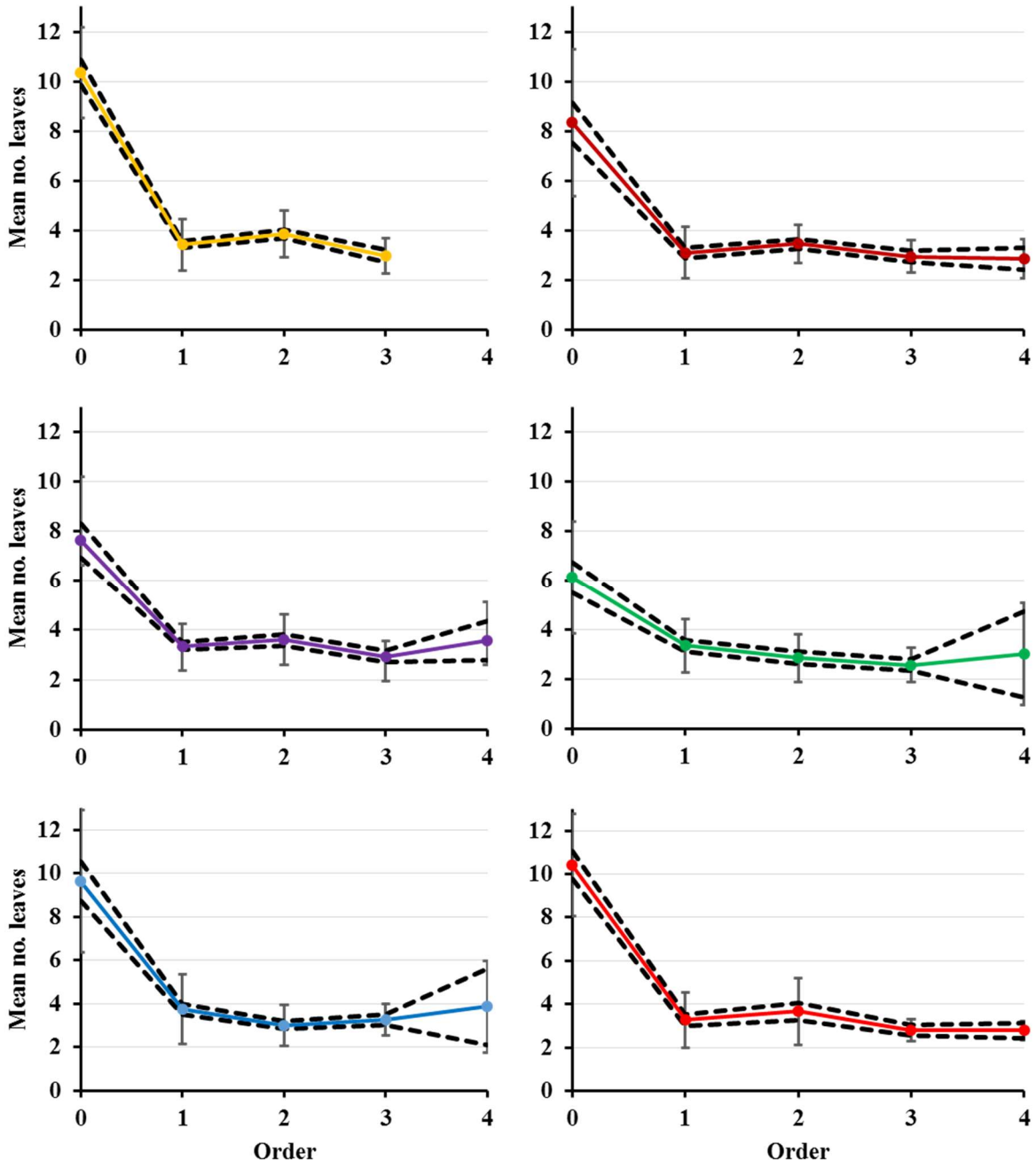

Figure 41: Pointwise mean number of leaves per module with associated 95% confidence intervals, and associated standard deviations for each variety

Mean number of leaves are represented by solid lines, confidence intervals by dotted lines and standard deviations by bars. Each variety is represented by one color: yellow for Capriss, purple for Ciflorette, blue for Cir107, marron for Clery, green for Darselect and red for Gariguette.

ANOVA on ranks shows that varieties can be grouped according to their number of leaves for the zeroth order module. First group includes Gariguette, Capriss and Cir107 with the highest number of leaves, followed in the second group by Clery and Ciflorette, and then in the last group by Darselect: Gariguette, Cir107, Capriss > Clery, Ciflorette > Darselect. For modules of order ≥ 1, no marked differences can be detected except for the two extreme varieties, Capriss with the highest number of leaves and Darselect with the lowest. Varieties can be ordered as follow: Capriss ≥ Cir107, Ciflorette, Clery, Gariguette ≥ Darselect.

ANOVA on ranks show that varieties can be ordered according to their number of flowers for the zeroth-order module as follow: Gariguette > Cir107 > Clery, Ciflorette, Darselect > Capriss. For first-order modules, results show that Cir107, Gariguette and Darselect are grouped with the highest number of flowers followed by Ciflorette and Clery, and then by Capriss (Cir107, Gariguette, Darselect >Ciflorette, Clery > Capriss). For modules of order ≥ 2, results show that Gariguette, Cir107, Ciflorette are grouped with the highest number of flowers, followed by Darselect and then, Clery and Capriss (Gariguette, Cir107, Ciflorette > Darselect > Clery, Capriss).

In summary, these results allow us to order varieties according to their number of leaves of zeroth-order module (Gariguette, Cir107, Capriss > Clery, Ciflorette > Darselect). Overall, the varieties can be ordered according to the number of flowers per module as followed: Gariguette > Cir107 > Clery, Ciflorette, Darselect > Capriss. Gariguette displays the most complex inflorescences for all the module orders, followed by Cir107 while Capriss displays the less complex inflorescences for all the module orders. Ciflorette, Clery and Darselect display inflorescences of intermediate complexity between Cir107 and Capriss.

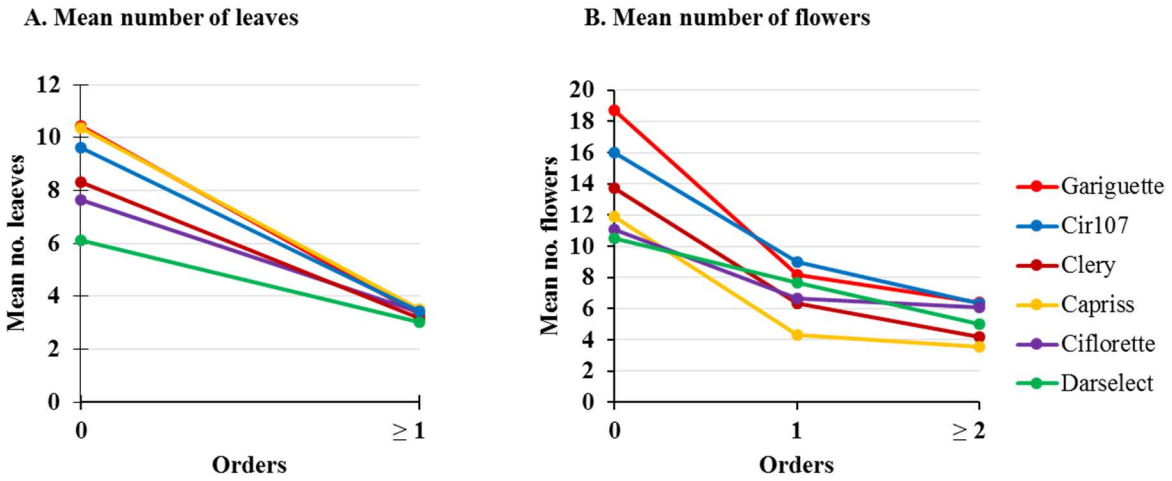

Figure 42: Mean numbers of leaves (A) and flowers (B) of modules for the successive orders for each variety
Varieties are represented by different colors: yellow for Capriss, purple for Ciflorette, blue for Cir107, marron for Clery, green for Darselect and red for Gariguette.

Table 21: Mean number of leaves with standard deviation (S.d.) and grouping of varieties using ANOVA on ranks (Kruskal-Wallis test and associated post-hoc tests) represented by letters for zeroth-order module (Order 0) and from first-order modules onward (Order ≥ 1)

	Order 0			**Order ≥ 1**		
	Mean	S.d.	Group	Mean	S.d.	group
Capriss	10.35	1.82	a	3.51	1.02	a
Cir107	9.63	3.29	a	3.43	1.36	ab
Gariguette	10.43	2.35	a	3.33	1.31	bc
Ciflorette	7.63	2.57	b	3.4	1.01	ab
Clery	8.33	2.97	b	3.16	0.91	bc
Darselect	6.11	2.29	c	3.02	1.07	c

Table 22: Mean number of flowers with standard deviation (Sd) and grouping of varieties using ANOVA on ranks (Kruskal-Wallis test and associated post-hoc tests) represented by letters for zeroth-order module (Order 0), first-order modules and from second-order modules onward (Order ≥ 2)

	Order 0			**Order 1**			**Order ≥ 2**		
	Mean	S.d.	Group	Mean	S.d.	Group	Mean	S.d.	Group
Gariguette	18.74	3.68	a	8.20	3.25	ab	6.40	2.15	a
Cir107	16.00	4.20	b	8.98	3.46	a	6.32	1.87	a
Clery	13.71	3.34	c	6.34	2.13	c	4.17	1.27	c
Ciflorette	11.08	2.19	d	6.64	2.07	c	6.06	1.68	a
Darselect	10.50	4.77	d	7.69	3.03	b	5.00	1.12	b
Capriss	11.92	2.87	d	4.28	1.28	d	3.56	1.11	c

2.2.3 Comparison of the frequency distributions of the number of stolons per module for successive module orders

Zeroth-order modules bore several stolons while first-order modules did not bear stolon and second-order modules no or very few stolons (Figure 43-Figure 44). The number of stolons per module then increased gradually with the module order from order 1 onward. Because of these systematic changes of the frequency distributions of the number of stolons per module as a function of the module order, we compared these frequency distributions between varieties for each module order using ANOVA on ranks (Kruskal-Wallis test) (Table 23).

Results of these comparisons show that Capriss and Cir107 can be grouped and display a higher number of stolons than the other varieties for zeroth-order modules, with a mean between 1.8 and 2 stolons, while Darselect and Gariguette can be grouped and display the lowest numbers of stolons with a mean of 0.6 and 0.9 respectively. Ciflorette and Clery are intermediate with a mean between 1 and 1.7 stolons for zeroth-order module. There are no difference between varieties for order 1 (no stolon) and order 2 (no or very few stolons).
Ciflorette exhibits higher numbers of stolons than the other varieties with a mean of 0.9 and 1.8 respectively for third- and fourth-order modules. For the other varieties, the mean number of stolons is between 0.2 and 0.4 stolons for third-order modules. For fourth-order modules, for all the varieties except Capriss, we observe an increase of the mean number of stolons with a mean between 0.7 and 1.2. The ANOVA on ranks show that Darselect and Clery can be grouped and display a lower number of stolons with a mean between 0.7 and 0.8 while Ciflorette display the highest number of stolons with a mean of 1.8, Cir107 and Gariguette are intermediate with a mean number of stolons between 1 and 1.2. Stolons born by zeroth-order module were present at planting (Figure 37), then new stolons emerged during the experiment only on the third- and fourth-order modules.
This comparison shows that Ciflorette exhibits a higher number of stolons than the other varieties, followed by Cir107, Gariguette and Clery and then Darselect. Capriss exhibits a small number of stolons compared to the other varieties (Ciflorette > Cir107 > Gariguette, Clery > Darselect).

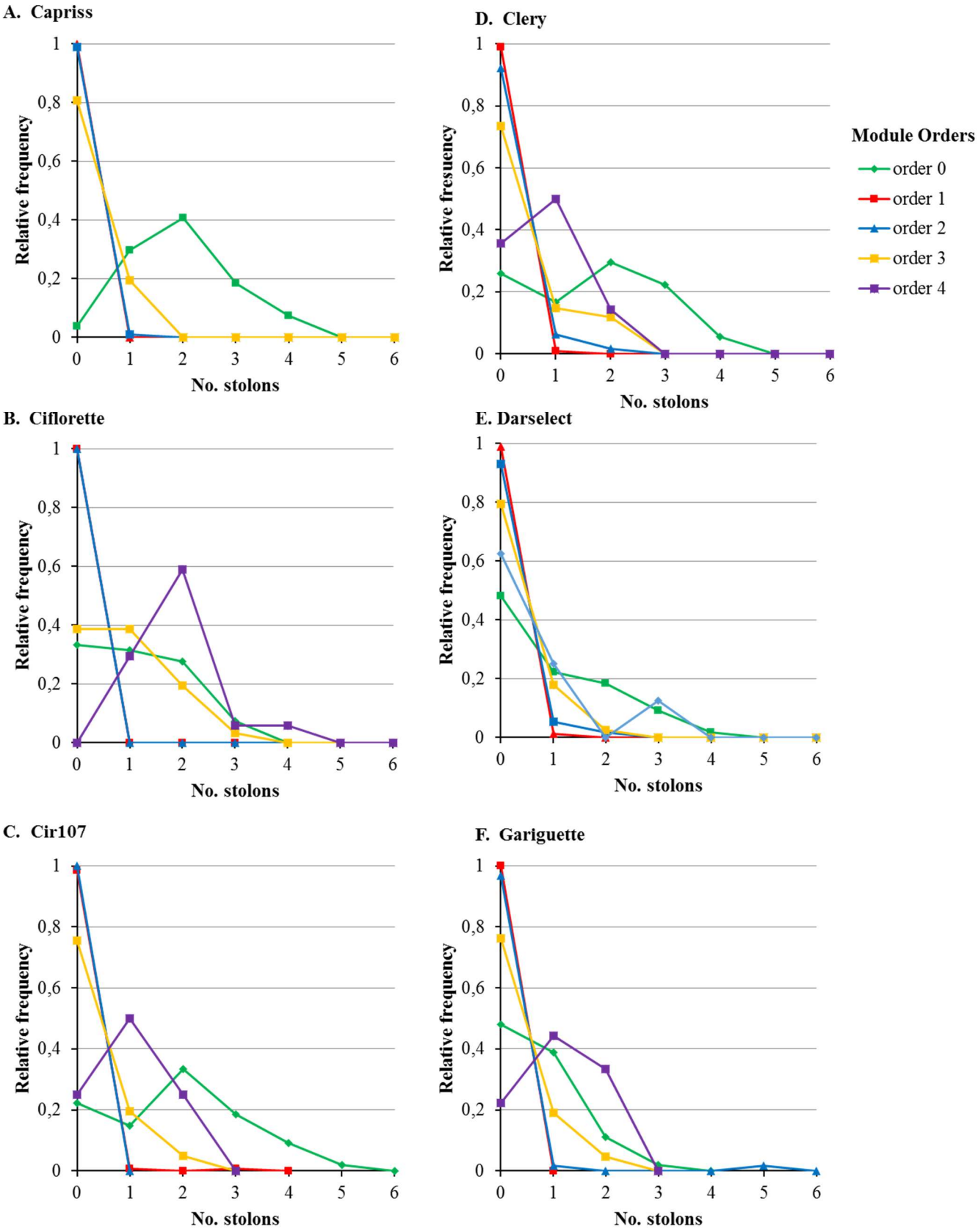

Figure 43: Relative frequency distributions of the number of stolons per module for successive orders and for each variety (A-F)

The module orders are represented by different colors: green for order 0, red for order 1, blue for order 2, yellow for order 3, and purple for order 4.

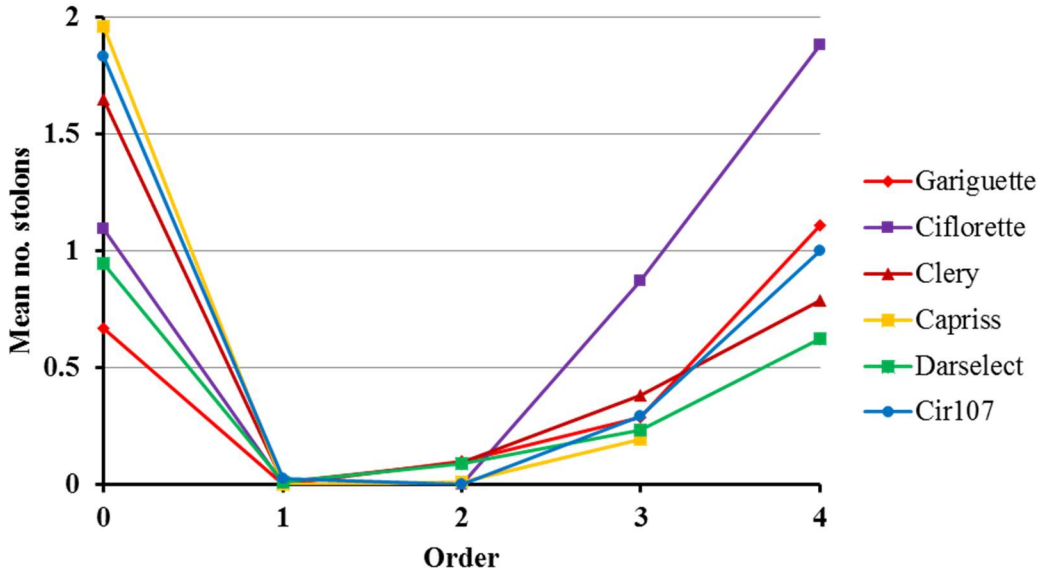

Figure 44: Pointwise of mean number of stolons per module for successive orders and for each variety
The varieties are represented by different colors: yellow for Capriss, purple for Ciflorette, blue for Cir107, marron for Clery, green for Darselect and red for Gariguette.

Table 23: Mean number of stolon with standard deviation (S.d.) and grouping of varieties using ANOVA on ranks (Kruskal-Wallis test and associated post-hoc tests) represented by letters for successive module orders (Order 0, Order 1, Order 2, Order 3, and Order 4)

	Order 0			Order 1			Order 2			Order 3			Order 4		
	Mean	Sd	group	Mean	Sd	group	Mean	Sd	group	Mean	Sd	group	Mean	Sd	group
Ciflorette	1,09	0,96	bc	0,00	0,00	a	0,00	0,00	a	0,87	0,85	a	1,80	0,77	a
Cir107	1,83	1,33	a	0,03	0,25	a	0,00	0,00	a	0,29	0,56	b	1,00	0,76	ab
Gariguette	0,67	0,00	c	0,00	0,00	a	0,10	0,65	a	0,29	0,56	b	1,20	0,79	ab
Clery	1,65	1,25	ab	0,01	0,10	a	0,10	0,35	a	0,38	0,70	b	0,79	0,70	b
Darselect	0,94	1,11	c	0,01	0,11	a	0,09	0,34	a	0,23	0,48	b	0,67	1,00	b
Capriss	1,96	0,97	a	0,00	0,00	a	0,01	0,10	a	0,20	0,41	b			

2.2.4 Proportion of branch crowns and extension crowns as a function of the module order

For all the varieties, relative frequencies of branch crowns per module (Figure 45A), show that the proportion of branch crowns was far higher in first-order modules (45% and 80%) than in higher-order modules (0 to 20%). In addition, relative frequencies of branch crowns (and conversely proportions of extension crowns) (Figure 45B) were similar for order 2 onward for each variety as confirmed by chi2 tests (Table 24).

Comparison of proportions of branch crowns for first-order modules allowed to order varieties (Figure 46A and Table 25). Capriss and Cir107 exhibit the highest proportions of branch crowns (75-80% of branch crowns) followed by Gariguette and Clery (60-63% of branch crowns), then Ciflorette (65% branch crowns) and finally Darselect (45% branch crowns).

Comparison of proportions of branch crowns produced from order ≥ 2 (Figure 46B and Table 25) shows that Capriss plants produced very few or even no branch crowns (3% of branch crowns), compared to other varieties (10-20% branch crowns~~)~~

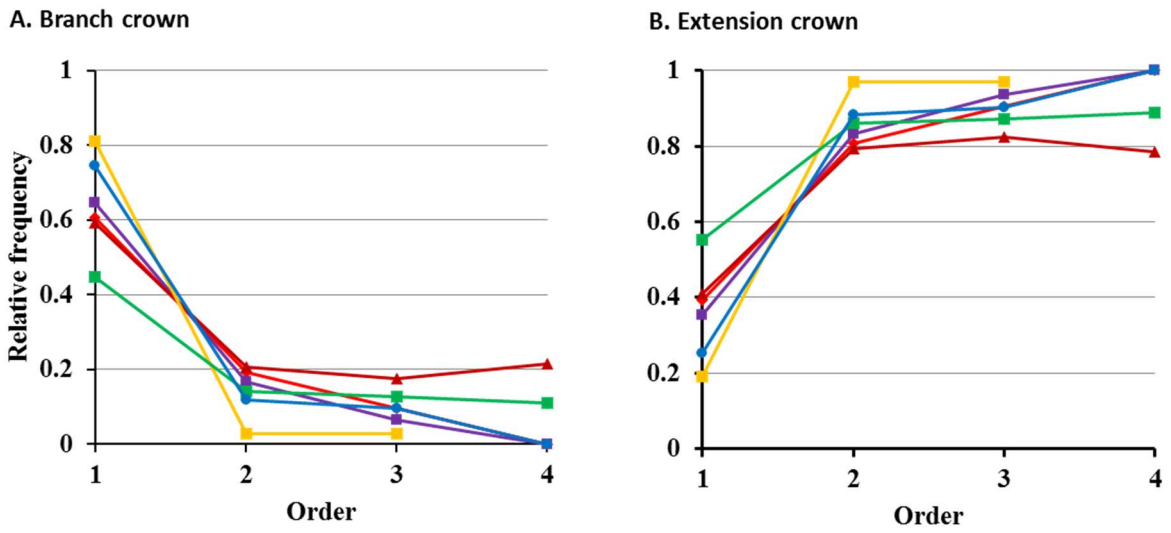

Figure 45: Relative frequencies of branch crowns (A) and extension crowns as a function of the module order for each variety
Each variety is represented by a color: yellow for Capriss, purple for Ciflorette, blue for Cir107, marron for Clery, green for Darselect and red for Gariguette

Table 24: Chi2 comparison of proportions of branch versus extension crown for successive module order from order ≥ 1 and from order ≥ 2 for each variety (P-values of the Chi2 tests for these contingency tables)

	Order ≥ 1	Order ≥ 2
Capriss	<2.2e-16	1 n.s.
Ciflorette	<2.2e-16	0.09 n.s.
Cir107	<2.2e-16	0.68 n.s
Clery	1.766e-07	0.93 n.s.
Darselect	2.947e-05	0.96 n.s.
Gariguette	2.501e-09	0.2 n.s.

n.s. indicates non-significant differences for successive module orders

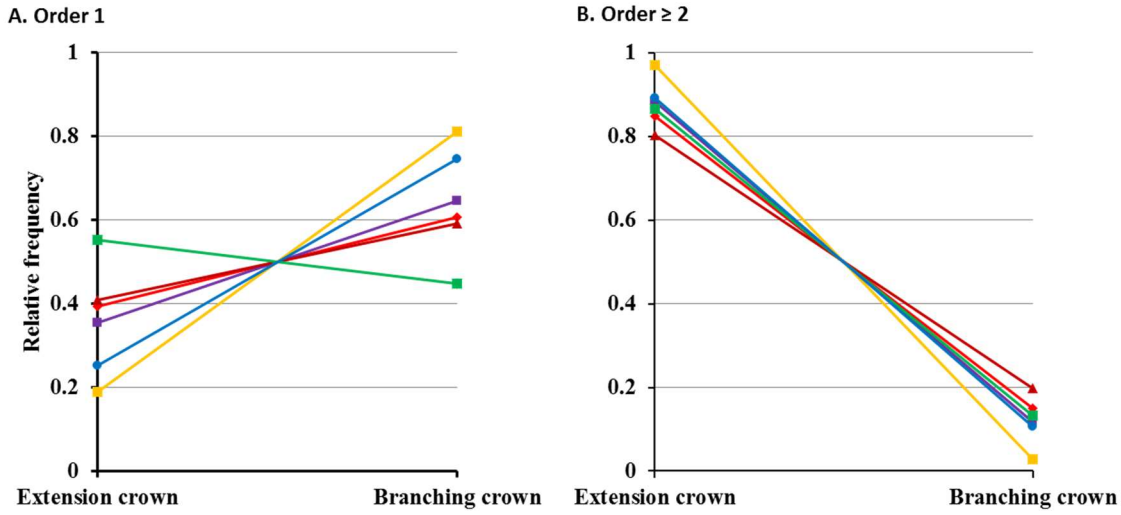

Figure 46: Relative frequencies of branch crowns and extension crowns for first-order modules (A) and higher-order modules (B) for each variety
Each variety is represented by one color: yellow for Capriss, purple for Ciflorette, blue for Cir107, marron for Clery, green for Darselect and red for Gariguette

Table 25: Chi 2 comparison of proportion of branch crown versus extension crown between varieties for first-order module (Order 1) and from second-order module onwards (Order ≥ 2)

	Order 1			Order ≥ 2		
	Extension crown	Branch crown	group	Extension crown	Branch crown	group
Capriss	0.19	0.81	a	0.97	0.03	a
Cir107	0.25	0.75	a	0.89	0.1	b
Ciflorette	0.35	0.65	ab	0.88	0.12	b
Gariguette	0.39	0.61	b	0.87	0.13	b
Clery	0.59	0.41	b	0.85	0.15	b
Darselect	0.55	0.45	c	0.80	0.2	b

To conclude exploratory analysis by visualization and exploratory analysis of architectural data allowed us to highlight:

i) Very marked changes of the module characteristics such as the inflorescence complexity and the number of leaves as well as a specificity of location of branch crowns and stolons;

ii) Comparison between varieties allows to identify variety specific traits and difference of plant development.

For all the varieties we observed there were very marked changes of the module characteristics according to the order. The few first orders and particularly zeroth-order module showed higher numbers of leaves and flowers than the higher-order modules. Afterwards module characteristics were almost stabilized from first-order modules for the number of leaves and from second-order modules for the inflorescence complexity. In addition, we observed a specificity of axillary meristem fate. For varieties which are branched (Capriss, Cir107 and Ciflorette), the branching concerned mainly axillary meristem of first-order modules (born by primary crown) while stolons were present on zeroth-order module and third-and four-order modules (sole module growing during the period of emergence of stolon).

In addition, these architectural studies allowed us to identify specific traits for each variety.

The number of flowers per module order allowed ordering varieties according to inflorescence complexity (Gariguette > Cir107 > Clery, Ciflorette, Darselect > Capriss). Gariguette and Cir107 are the varieties with the most complex inflorescences whatever the module order while Capriss exhibits the less complex inflorescences. For the three other varieties with intermediate inflorescence complexity (Ciflorette, Clery and Darselect), the inflorescence complexity varies according to the module order.

Study on the number of leaves per module order showed that mainly difference concerned zeroth-module order, few differences being observed from first-order module onwards. This difference conducted us to order varieties according to the following order: Gariguette, Capriss, Cir107> Clery, Ciflorette> Darselect.

Results on proportions of branch crown and extension crown highlighted differences of branching. Capriss, Cir107 are more bushy varieties than Clery, Darselect and Gariguette, while Ciflorette is intermediate regarding this criterion (Capriss, Cir107 > Ciflorette > Clery, Darselect and Gariguette)

The analysis of the appearance of successive module orders at successive dates suggested a difference of development rate between varieties. As zeroth- and first-order modules were present for each variety from planting, the difference of development rate is perceptible from second-order module onwards. According to this observation, comparison between varieties of the appearance of successive module orders showed that from planting to early April, Cir107, Ciflorette, Capriss and Darselect developed more rapidly than Clery and Gariguette. Afterwards until the end of the experiment we observed an inversion of development rate for some varieties. Capriss and Cir107 which belong to varieties developing the fastest at the beginning of experiment show the slowest development rate at the end of experiment and inversely for Gariguette and Clery. This observation allowed to order varieties as followed:
From planting to April: Darselect, Cir107, Capriss ≥ Ciflorette, > Gariguette, Clery
From April to the end of the experiment: Darselect > Gariguette, Clery≥ Ciflorette > Capriss, Cir107

3 Molecular expression of flowering key genes

RNA extracted from each sample showed and average of 600 ng/µL with good ratios of A260/280 and A260/230 (average of 2.00 and 1.9 respectively). The average of RIN from Agilent analyses was 6.9, which showed a good quality of RNA for strawberry. Reference genes, *FveMSI* and *FveEF1*, were detected in all samples with same intensity as expected. *FveMSI* gave more homogeneous results than *FveEF1* and was further used for qPCR analyses.

Bands issued from PCR were observed on agarose gel to confirm the success of amplification and the expected size. In addition, amplifiats were send for sequencing to be sure amplification was the target gene. According to the intensity of the amplifiats, a scale from 0 (absence of amplifiat) to 5 (visualization of an intense band) was assigned to each replicate. In addition, the number of biological replicates with amplifiats was also scored and included in Table 26. Results showed that *TFL1* was sporadically expressed and its expression was clearer in February. This gene showed alternative splicing and could not be analyzed by qPCR.

Results of qPCR were available for *FT1, FT3* and *SOC. FT1* (Figure 47) was very low expressed at almost all dates confirming that this gene is not photoperiodic (Gaston pers. com.). *FT3* and *SOC* expressions increased along time confirming that both genes are long day expressed genes (Mouhu *et al.*, 2013, Gaston pers comm.). In our conditions, it was difficult to detect differences between varieties. Further expression analyses could be done on samples that

include replicates within plants to take into account the position of the leaf in the plant architecture.

Table 26: Results of cDNA amplification for TFL1, FT1, FT3, SOC and MSI genes on Cir107, Darselect and Gariguette at different dates.
For each gene, the number of amplified replicates are shown by number and amplification intensity is indicated by color scale from yellow to red

Genotype	Date	Timing	TFL1 qKSN1-2	FT1 qFT2d	FT3 NnFaFT1	SOC TiRTSOC1 f + TiSOC2 r	MSI TiMSI
Cir107	10/12/2014	T0	2+?	3		2	3
Darselect	10/12/2014	T0	1	2		1	3
Gariguette	10/12/2014	T0		1		1	3
Cir107	08/01/2015	T04	1	2		3	3
Darselect	09/01/2015	T04		1		2	3
Gariguette	08/01/2015	T04		3		3	3
Cir107	11/02/2015	T08	1		2	3	3
Darselect	11/02/2015	T08	3	2		1	3
Gariguette	12/02/2015	T08	1	3		3	3
Cir107	04/03/2015	T12		3		2	3
Darselect	06/03/2015	T12		2	3	3	3
Gariguette	06/03/2015	T12		3	1	3	3
Cir107	02/04/2015	T16		3	3	3	3
Darselect	03/04/2015	T16		3		3	3
Gariguette	02/04/2015	T16		3	3	3	3
Cir107	20/05/2015	Tfinal		3	2	3	3
Darselect	20/05/2015	Tfinal	1	3	1	3	3
Gariguette	19/05/2015	Tfinal		3		3	3
Positive control (ADNg)			3	3	3	3	3

intensity of bands on agarose gel

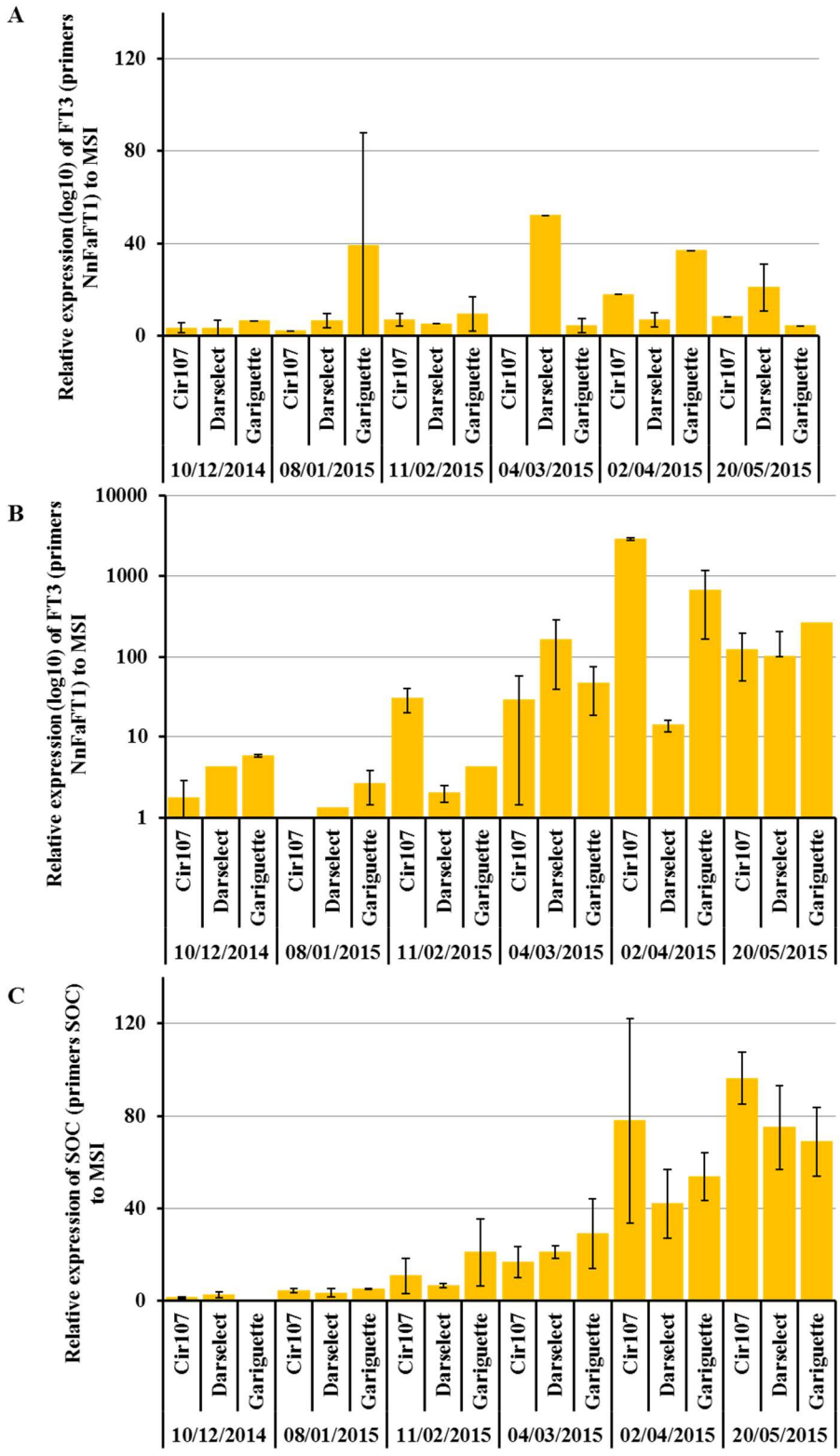

Figure 47: Relative expression of FT1 (A), FT3 (B) and SOC1(C) for Cir107, Darselect and Gariguette varieties with their standard deviation.

Part 2: Preliminary results on diploid strawberry varieties (*F. vesca*)

In strawberry, having morphological time scale rather than chronological age will provide a useful tool for further molecular studies. Therefore, the second part of my PhD was to initiate a study (i) to identify phenotypic markers at plant scale, which can be correlated with the meristem stage and (ii) ultimately, to study the relationship between these phenotypic markers and the expression of flowering and runnering genes.

1 Occurrence of organs over time in strawberry plantlets

Mean numbers of leaves (unifoliate and trifoliate), runners, crowns and flowers were extracted for each of the three genotypes, NIL 2.39.63 (Fb2), Reine des Vallées (RdV) and Sicile (Figure 48).

The number of trifoliate leaves showed a continuous increase, concomitant with the senescence of unifoliate leaves (Figure 48A and B). Moreover, leaf emergence rates were similar between all genotypes until 29th March, with almost emergence of one leaf by week. Sicile developed a lower number of leaves than Fb2 and RdV, which were similar as expected since they display both an RdV genetic background. At 10 leaves (29th March), we observe a strong increase of the number of trifoliate leaves of RdV compared to the two other genotypes. This increase is explained by the emergence of new crowns at the same date, linked to branching (Figure 48D).

As expected, only Sicile and Fb2 genotypes (runnering genotypes) produced stolons (Figure 48C). Stolons appeared four-five weeks (16-22th February) after transplantation when plantlets displayed 5-6 and 4-5 trifoliate leaves for respectively Fb2 and Sicile. From this stage, all the axillary meristems of the new leaves produced runners (Figure 49).

The first inflorescence was visually observed at the same date, the 18th April, for perpetual genotypes, RdV and Fb2, despite the fact that they displayed different numbers of leaves, 12 and 14 respectively, which are similar to the number of leaves of primary crown observed in strawberry octoploid varieties (see previously). This result suggests that the number of leaves of primary crowns could be an approximate marker of the time of emergence of inflorescence. As expected, in these cultural conditions, no flower was observed in Sicile, which is a seasonal flowering variety.

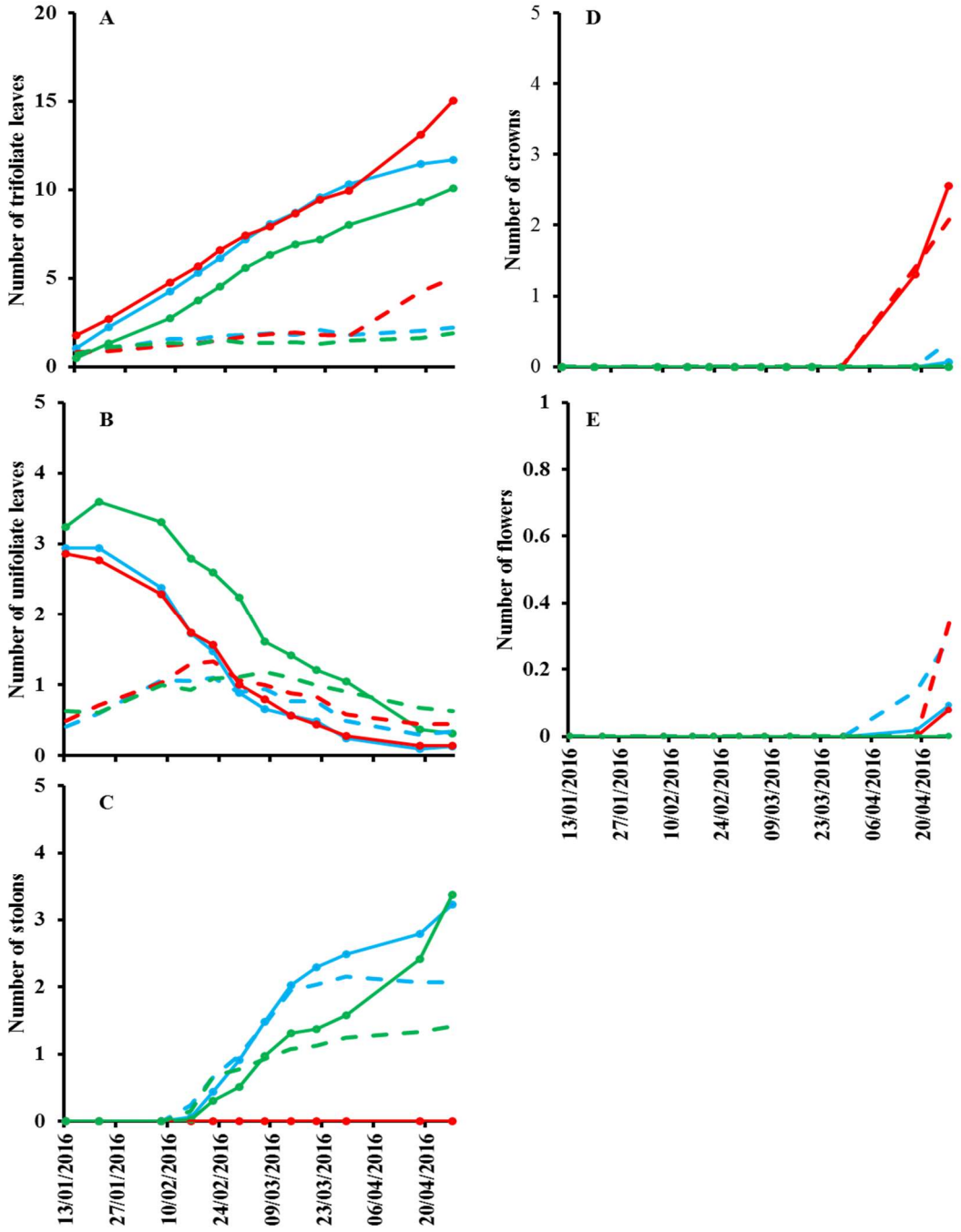

Figure 48: Development of plantlets of three genotypes belonging to F. vesca.
Cumulative mean numbers (in solid lines) of trifoliate leaves (A), unifoliate leaves (B), stolons (C), crowns (D) and (E) flowers, for Fb2 (blue), RdV (red) and Sicile (green).Dotted lines represent the standard deviations (n=80 at the beginning of experiment).

2 Plant architecture

Results of plant architecture are illustrated in Figure 49. Meristem stage for terminal and axillary buds were all at the stages 17-19 whatever their genotype, their position and the date of observation except for terminal meristem of Fb2 and RdV at the last date of observation.

Fb2 and RdV showed a floral transition in their terminal meristem between 10- and 12-leaf stages for Fb2 and 12- and 14-leaf-stages for RdV. This transition was followed by the vegetative development of the axillary bud just below the terminal floral meristem.

These observations suggest that meristems can stay a long time at a vegetative stage while floral transition could be a fast occurring event. In addition, comparison of architecture and meristem dissection between Fb2 and RdV suggest that the runnering process does not fundamentally change the time of floral transition, 12- and 14-leaf stages, in perpetual flowering genotypes.

Moreover, the emergence of stolons was visually observed from the 5-leaf stage on both Sicile and Fb2. At microscopic level, the extension of the axillary meristem was not observed before this stage. However, for the stolons which were macroscopically observed the 8-leaf stage, extension of the axillary meristem was observed the 5-leaf stage. This apparition only on the fifth-leaves and not before suggests that position of lateral buds could influence meristem fate. This hypothesis should be confirmed by another experiment

In addition to meristem dissection, leaf area and petiole length (data not shown) were measured at different stages of plant development (Figure 50). In perpetual flowering genotypes Fb2 and RdV, leaf area increased with the position of the leaf until the seventh or the eighth adult leaf. Between the seventh leaves until the tenth leaf, the surface was constant. From the 11^{th} leaf and over, we cannot conclude without the observation of stage above14 leaves since the leaves could continue to grow. In the genotype Sicile, the leaf area of the leaves continue to increase with the position of the leaf on the first axis.

The resulted plateau for the leaf area was visible at 10-trifoliate-leaf stage for perpetual flowering genotypes RdV and Fb2. This stage is the one that should correspond to the beginning of the floral transition. We can hypothesize that the plateau of leaf area from the eighth trifoliate leaf and visible at 10-trifoliate-leaf stage is due to resource mobilization from vegetative process to reproduction process. This phenotypic trait at plant scale could be an indicator of floral initiation at meristem scale. To confirm this hypothesis, another experiment has to be set up with a higher number of plants per genotype.

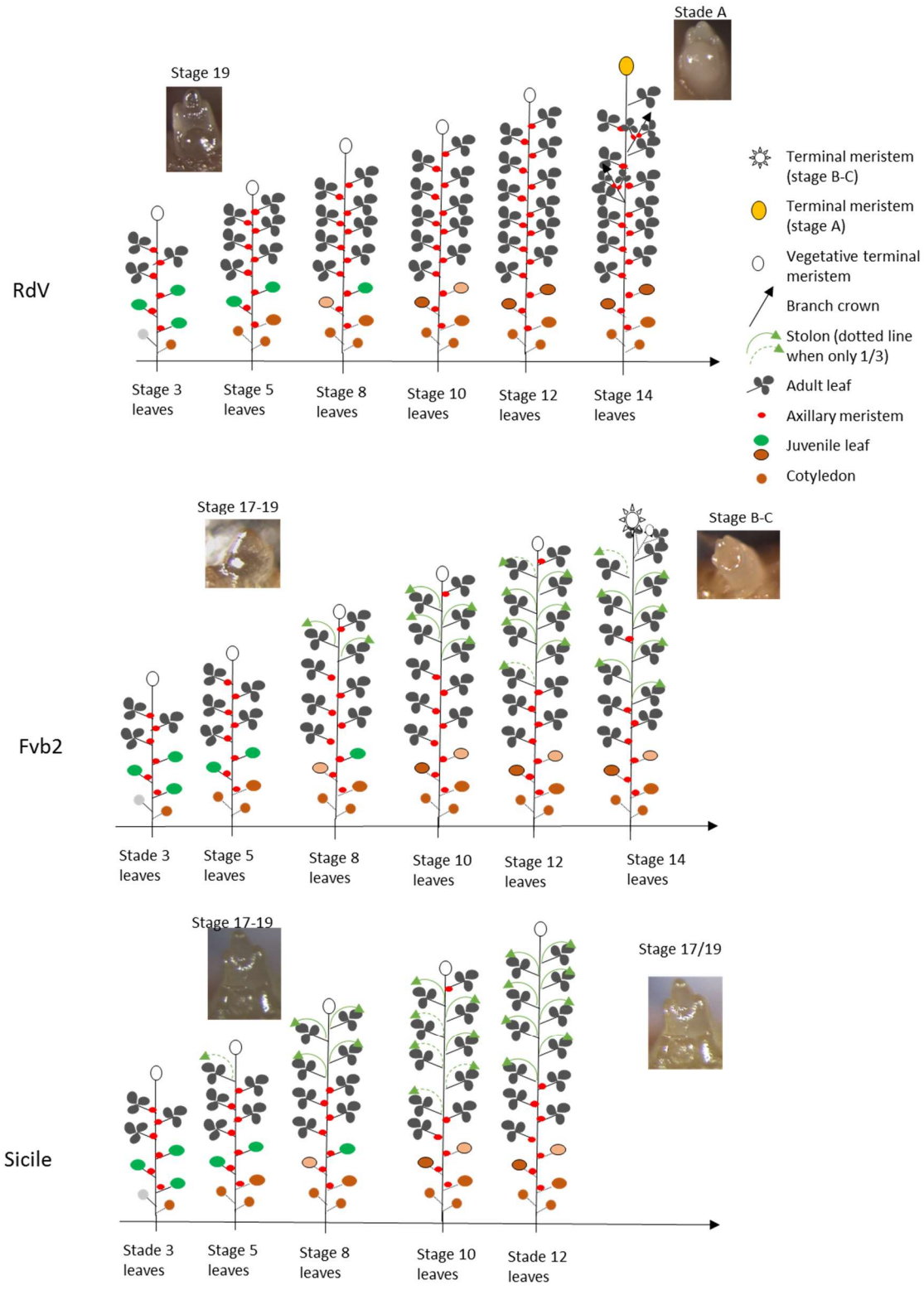

Figure 49: Dynamic of architecture of diploid strawberry plantlets for NIL 2.39.63 (Fb2), perpetual flowering and runnering (A), RdV, perpetual flowering and runnerless (B) and Sicile, once flowering and runnering (C).
On the top of the schematic 2D representation of architecture at each stage, photos and stages of meristem dissection.

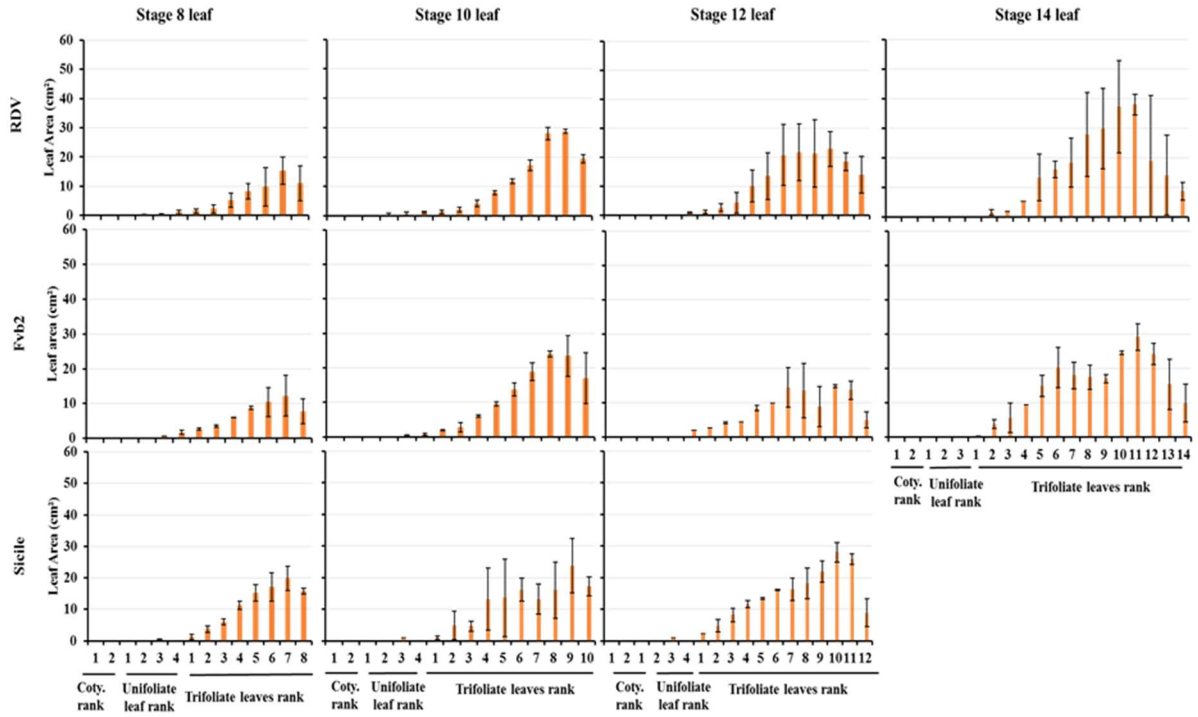

Figure 50: Leaf areas of plantlets of strawberry at stage 8, 10, 12 and 14 trifoliate leaves for RDV, Fvb2 (Nils) and Sicile varieties

3 Architecture consequences of runnering

To see the consequences of perpetual flowering versus seasonal flowering on genotypes and runnering versus runnerless on genotypes, three 5.5-month-old plants at were studied for their architecture. In addition to the three genotypes described above, Alpine, a perpetual and runnerless genotype was added to the study. Alpine and Sicile were the parents of an F_2 population that segregates for runnering and flowering behavior.

Results allowed to examine the fate of axillary meristems in runnerless and runnering genotypes (Figure 51). In Fb2 and Sicile, axillary meristems at the 6th leaf and above produced stolons while the uppermost axillary meristem produced a branch crown in Fb2 after the floral transition of the terminal meristem. In RdV and Alpine, all axillary meristems produced branch crowns or remained dormant. We further examined axillary meristems in more detail in RdV and Fb2. Regardless of their fate, axillary meristem morphology and shape were similar between Fb2 and RdV.

Thus, in the runnerless mutant, the fate of an axillary meristem that does not produce stolon is to remain dormant or to generate a branch crown terminated by an inflorescence. This information concerning architecture was used to study the cause of the trade-off between

runnering and flowering. These results were included in the paper published in *Plant Cell* (ANNEXE) in which it is showed that this trade-off is controlled by the *gibberellin* (GA) *20-oxidase* (*GA20ox*) gene.

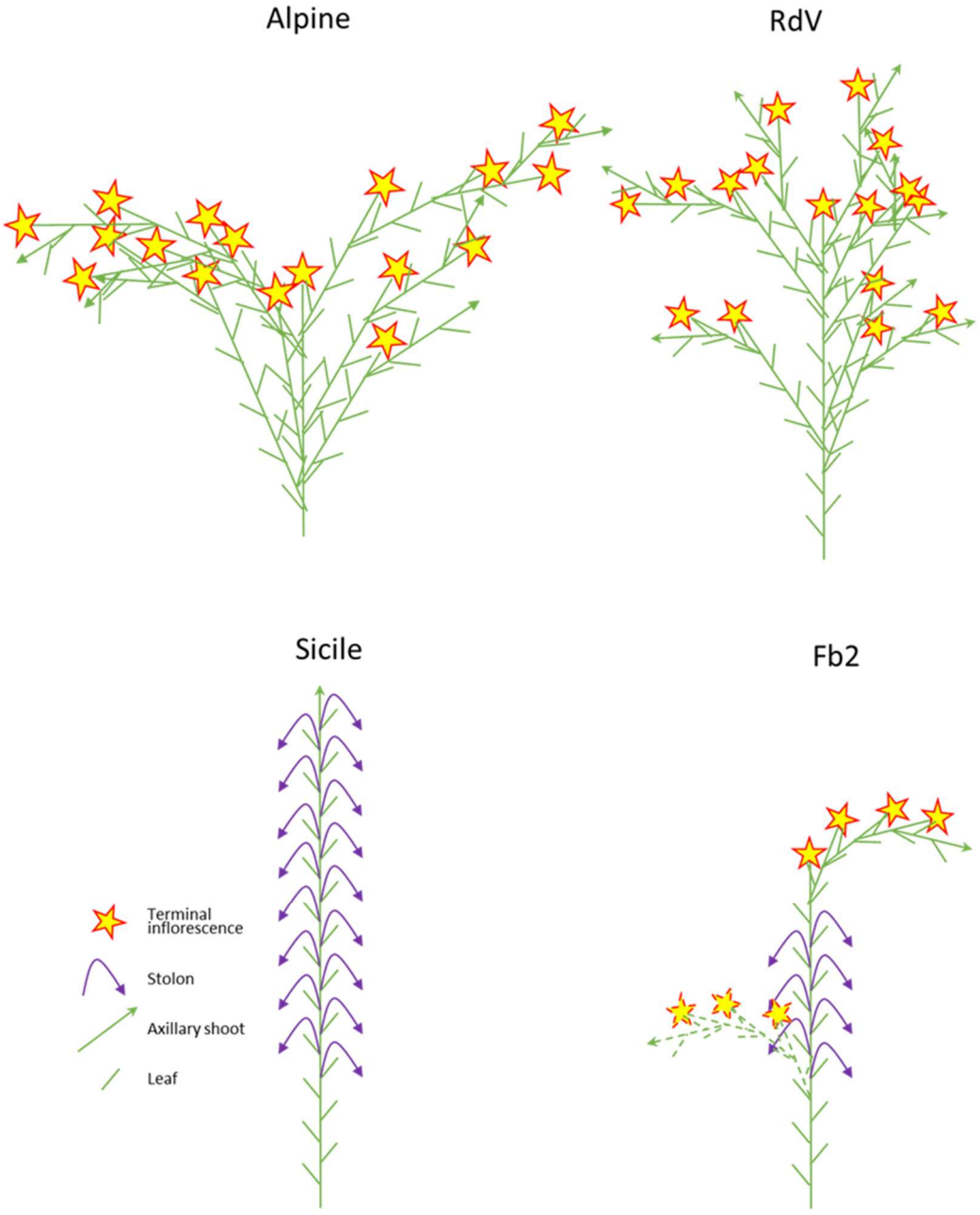

Figure 51: Illustration of four genotypes that differ for their flowering and runnering behaviors. Alpine and Reine des Vallées (RdV) are perpetual flowering and runnerless, Sicile (wild type) seasonal flowering and runnering and NIL 2.39.63 (Fb2) perpetual flowering and runnering.

Chapter 4: Discussion and perspectives

The link between phenology and plant architecture is a major issue in developmental biology for better understanding plant development. Plant developmental is defined as a combination of ontogenetic processes modulated by environmental and genetic factors (Hallé and Oldeman, 1970; Hallé *et al.*, 1978; Barthélémy and Caraglio, 2007).

In strawberry, vegetative reproduction with stolons and sexual reproduction with inflorescences occur successively or jointly according to genotype, cultural technique and environment. These two processes are important in strawberry culture because they determine plant production in nurseries and fruit production in fields, tunnels or greenhouses. However, vegetative propagation could occur at the expense of fruit yield (Tenreira *et al.*, 2017). Therefore, several studies (Battey *et al.*, 1998; Darnell *et al.*, 2003; Heide *et al.*, 2013; Kurokura *et al.*, 2013) have been conducted in order to understand environmental and genetic control influencing both flowering and runnering processes. Little is known concerning these developmental processes along time and even less including ontogenetic process during plant development that can influence the development of the plant (Massetani *et al.*, 2011; Bosc *et al.*, 2012).

The aim of my PhD consisted in getting a better understanding of plant development integrating phenological and architectural development in strawberry. This work mainly focused on the development of octoploid plants placed under culture production. Beside this work, study of plant development in the diploid model of strawberry was initiated using seedlings.

My PhD project has led (1) to the development of univariate and multivariate segmentation models to identify, in production conditions, patterns in the form of successive phases for the flowering, vegetative development and runnering processes and, (2) to identify which structures explain the different flushes of flowering using an architectural approach based on destructive observation. (3) In addition, my project allowed to initiate the first characterization of the development of strawberry seedlings.

1 Relevance of analysis methods for investigating developmental processes: longitudinal data analyses and architectural analyses using MTGs

Usually developmental processes are investigated on the basis of on-off measures even if they are highly structured in time and space. For example, the on-off measures allow to determine the time of first flowering occurrence (date of flowering) and flowering duration as

the number of weeks of half or full flowering (Sonsteby and Heide, 2007; Honjo *et al.*, 2011; Rahman *et al.*, 2014). These on-off measures allow taking a snapshot at a given time of the flowering status but not to take into account the flowering process along time, whereas longitudinal data analysis does. This analysis can be based either on the cumulative number of organs or on the number of newly emerged organs at successive dates of observation.

Cumulative numbers of organs at successive dates of observation are often analyzed using sigmoidal functions (e.g. logistic functions) (Sonsteby and Heide, 2008*b*; Opstad *et al.*, 2011). Abrupt changes in the production of organs cannot be reliably estimated within such smoothed functions. The shortcoming of this approach is that it exclusively focuses on the slowly varying component while ignoring the rapidly varying components (e.g. abrupt changes or local fluctuations in the production of organs) (Chatfield, 2003). That is why we chose to analyze the series of weekly emerged organs for successive observation periods which correspond to the first-order differencing of the series of cumulative numbers of organs. It was possible in this way to detect in a reliable way phenological phases corresponding to abrupt changes in the number of weekly emerged organs using segmentation models.

In this segmentation model, we assumed that the phenological pattern of a variety took the form of a succession of well-differentiated stationary phases, where the distribution of the number of weekly emerged organs (either flower, leaf or stolon for the univariate analysis) did not change substantially within each phase, but changed markedly between phases. This approach was successfully used for identifying a QTL specific to the last flowering phase in strawberry perpetual flowering genotypes (Perrotte *et al.*, 2016). In my PhD work, we applied this approach to identify flowering, vegetative and runnering patterns. It should be not, that contrarily to the segmentation models used in mango (Dambreville *et al.*, 2014) and Arabidopsis (Lièvre *et al.*, 2016) that rely on an assumption of asynchronous phases between individuals, we chose here to assume that phases were synchronous between individuals.

Furthermore, we developed a new multivariate segmentation model in order to summarize the three developmental processes i.e., the flowering, vegetative development and runnering processes. If the assumption of well-differentiated stationary phases is reasonably valid in the univariate case, it is far less in the multivariate case where both the number of weekly emerged flowers, leaves and stolons are integrated in multiple change-point models at three observed variables. We indeed did not expect systematic synchronous changes of these three variables. But the model behavior is a bit more subtle since a change of high amplitude on a single variable may be sufficient to define a limit between phases. This was in particular illustrated by the stolons for which the well-defined runnering phase was detected for the six

varieties even if we incorporate the flower and leaf variables. We thus exploited this behavior in the meta-analysis to help defining a hierarchy between the different phenological phases identified for each organ using the univariate multiple change-point models. In my PhD study, results of this meta-analysis showed a hierarchy between the three developmental processes with first flowering, then runnering and finally vegetative development. In further discussion below, we will therefore focus mainly on the two first processes, flowering and runnering, which are also the two key processes for fruit and stolon productions.

Once the phenological phases were identified, it was interesting to understand which structure in the strawberry plant is involved in these phases. Therefore, we developed an architectural approach to study the role developmental processes in the spatio-temporal development of the plant structure. Plant architecture describes the spatial distribution of vegetative and reproductive organs and their developmental phases (Massetani *et al.*, 2011). Architecture description is often summarized by schemas or drawings, which differs according authors (Guttridge, 1955; Bosc *et al.*, 2012; Costes *et al.*, 2014), and the exploration of plant architectures often does not incorporate statistical analyses. When these analyses are done, they only concern a set of measurements at a given scale, such as the analysis of the primary crown in Bosc *et al.*, (2012). My PhD project has led to the development of MTG in strawberry. This MTG was used for the representation of plant architecture development and for the statistical analysis at different scales of the developmental processes.

MTG is a model, which represents the development of plant architecture along time at different scales. Thus, MTG allows to investigate the rules of development of plant architecture and to visualize plant architecture along time (Godin and Caraglio, 1998; Balduzzi *et al.*, 2017). Because the MTG is a universal formalism to store any plant architecture, it has been used both to encode and analyze architecture in a generic way, but also to model plant structure and function. It is central in the OpenAlea software platform, where each model use MTG as a data structure to communicate in a modular way (Garin *et al.*, 2014). In my PhD work, we chose to study strawberry architecture by developing a strawberry package relying on MTG within the OpenAlea software platform.

2 Flowering, vegetative and runnering patterns differed according to variety and their architecture

Segmentation models allowed us to identify flowering, vegetative and runnering patterns.

Concerning flowering, all the varieties showed a first common flush that differed in intensity (high intensity for Gariguette and Cir107) and in less extent earliness (Gariguette). This first common flowering flush was followed by a phase of moderate flowering, more moderate for Gariguette and Clery that showed a second flowering flush than for Capriss, Cir107, Ciflorette and Darselect for with this phase extends up to the end of the experiment. Taking together these results allowed us to identify two patterns of flowering based on the flowering intensity of the phase following the first flush and the presence or not of a second flowering flush. Although these patterns were not described in the literature, they were in accordance with observations of growers (Demené pers. comm.). Varieties differed also by their architecture and more precisely by the occurrence of module orders along time, the complexity of inflorescences and the branching pattern. Because all varieties were grown in the same conditions, differences in patterning or plant architecture rely on differences in genetic controls of flowering such as flower initiation or plant development (Savini *et al.*, 2006; Iwata *et al.*, 2012; Gaston *et al.*, 2013; Mouhu *et al.*, 2013). The absence of differences in expression of flowering genes between varieties in our study could be due to the low efficiency of our experiment because of the limited number of samples or studied genes. All of these results were synthesized in Figure 52 proposing a model of development of varieties combining the phenological, architectural and genetic results.

Superposition of occurrences of module orders along time with phenological pattern suggests that the first flowering flush is mainly located on the zeroth- and first-order modules (Figure 52). Architecture just after dormancy (1st date of architecture description at plantation) showed that only these two module orders were present for almost all varieties (Gariguette first-order module clearly appeared in January). This suggests that only zeroth- and first-order modules were subjected to inductive floral conditions in previous autumn, when temperatures and photoperiod decreased (Battey *et al.*, 1998; Heide *et al.*, 2013). This hypothesis is reinforced by similar results obtained in Gariguette (Bosc *et al.*, 2012). After flowering of zeroth- and first-order modules, a decrease of flowering was observed and this decrease was more severe for Gariguette and Clery (Figure 52A). This decrease of flowering at the end of the

first flush could result from the end of flowering on the zeroth- and first-order modules. The subsequent phases of flowering after the first flush were thus due to the occurrence of higher-order modules. The commonality of the first flush could be due to the cultural system used in the study, in which the greenhouse was warmed allowing resumption of growth development for all varieties (Massetani *et al.*, 2011) and thus a similar expression of inflorescence emergence.

Differences in the first flowering flush intensity could be due either to the complexity of inflorescences (Darrow, 1929; Battey *et al.*, 1998) or to the number of modules terminated by inflorescences (Hytonen *et al.*, 2004; Tenreira *et al.*, 2017).

As an example, Elsanta produces a first inflorescence with a maximum of 15 flowers (Battey *et al.*, 1998), while Gariguette is well known for the complexity of its first inflorescence which can reach 30 flowers (Demené pers comm). In our study, Gariguette and Cir107 showed the inflorescences of higher complexity for all the module orders compared to the four other varieties (Table 22, in results). Complexity of inflorescences could be controlled genetically as suggested by Darrow, who reported breeding selection pressure on inflorescence complexity (Darrow, 1929). For all the angiosperm species, inflorescences originate from small groups of stem cells in shoot apical meristems (SAMs), which transform into inflorescence meristems (IMs) upon perceiving a combination of environmental and endogenous signals (Andrés and Coupland, 2012). Inflorescences of angiosperms can be simple or highly complex (Prusinkiewicz *et al.*, 2007). Molecular control of inflorescence morphology has been described for species such as Arabidopsis, rice, maize (Wang and Li, 2006; Liu *et al.*, 2013) or in tomato (Xu *et al.*, 2016). These data are not available on strawberry.

A high number of modules leads to a high number of inflorescences since each module is terminated by an inflorescence under favorable environmental conditions. In our study, differences between varieties of branching on first-order modules was observed, with Capriss, Cir107 and Ciflorette producing more branch crowns than other varieties. However, this hypothesis is not well supported since Ciflorette and Capriss did not display a more intense first flowering flush and the hypothesis of inflorescence complexity is therefore more relevant.

Gariguette showed also difference in the first flowering flush for its earliness (one week of earliness) (Figure 52A). Earliness difference could result from differences between timings of floral initiation (Sonsteby, 1997; Opstad *et al.*, 2011). Terminal shoots will be more often differentiated into inflorescences in a variety with an earlier timing of flower initiation. After

dormancy, these inflorescences will emerge. Beside control of floral initiation by environmental conditions (Heide *et al.*, 2013), timing of this process is also dependent on varieties (Sonsteby, 1997; Opstad *et al.*, 2011). This genetic effect should underline molecular control with notably the involvement of the FTs/TFL1 family, which are known to be involved in the flowering process (Iwata *et al.*, 2012). The study focused on culture production and no data was available for the development of plants in nursery before plantation. To confirm this hypothesis, plants should be followed for their expression of *FT1*, the activator of flowering, and *TFL1*, the repressor of flowering (Iwata *et al.*, 2012; Koskela *et al.*, 2016), during the plant development in nursery.

After this first flush between end January/early February and April, all varieties showed flowering until the end of experience (end of June). Usually, floral initiation occurs in short day conditions (< 12-14 h day) when temperatures are low (< 12-16°C) (Ito and Saito, 1962; Heide, 1977; Heide *et al.*, 2013). In our culture conditions in South West of France, 14 h day correspond to end of April when the temperature was 15-16°C in 2015 and therefore still inductive in our study. Assuming that the time lag between floral initiation of apical meristem and visual emergence of inflorescences was between 8 and 10 weeks in strawberry [e.g. about 10 weeks for the SF 'Frida' variety (Sonsteby and Heide, 2008*a*), and 9 weeks for the SF 'Elsanta' variety (Battey *et al.*, 1998)], we should have the emergence of inflorescences at the end of June. Because we observed at the end of June inflorescences on third- or fourth-order modules, we can hypothesize that they were issued from floral initiation that occurred approximatively until April. Because the architectures were measured approximately every month and the last measurement occurred in early June, we are not able to determine the end of the floral inductive period.

Expression of *FT1*, which is the florigene in strawberry, is not photoperiodic (Gaston et al. in preparation), which is confirmed by our results with the low expression of this gene at almost all dates of analysis. On the contrary, *SOC1*, which activates the floral repressor *TFL1*, is photoperiodic and expressed in long days (Mouhu *et al.*, 2013). In long days, expression of TFL1 overcomes the expression of FT1, which leads to vegetative development (Gaston comm. pers.). *FT3*, which is upstream to both *SOC1* and *TFL1*, is also strongly expressed in long days without any expression in short days. In our results, we observed an increase of the level of expression of *SOC1* and *FT3* along the experiment, which suggests their role in vegetative development such as stolons. Analyzing their expression after June in summer should give more

information on the function of these genes. Expression of TFL1 showed two bands. New primers should be developed for analyzing this gene.

From April, varieties showed different patterns of flowering based on the presence of a second flowering flush after a phase of moderate flowering (Gariguette and Clery for pattern 1, Figure 52A) or a single phase of flower production (Capriss, Ciflorette, Cir107 and Darselect for pattern 2, Figure 52B). Differences between these patterns could be due to differences of occurrence of module orders. Kurokura *et al.* (2005) hypothesized that it is necessary to shorten the intervals between differentiations of each inflorescence that terminates module to avoid gap of flowering. Based on this hypothesis, we can suggest that the absence or presence of second flush of flowering leading to difference of flowering patterns is due to the rapid or slow occurrence of second-order module. This hypothesis fits with our observation. In varieties of pattern 2 ((varieties without a second flush), Figure 52B, Module order occurrence), occurrence of second-order module appeared early before the first flowering flush (caused by zeroth- and first-order modules) while it occurred later, only in mid-first flowering flush, for varieties of pattern 1 ((varieties with a second flowering flush) Figure 52A, Module order occurrence).

In varieties of pattern 2, flowers emerged continuously leading to a single phase of flowering. This continuous flowering can be explained either by branching or rapid occurrence of module of higher orders. High-order of branching associated to continuous flowering was already observed in perpetual flowering genotypes versus seasonal flowering (Hytonen *et al.*, 2004; Tenreira *et al.*, 2017), and the perpetual flowering can constitute a single phase of flowering (Perrotte *et al.*, 2016). In our study, we observed a higher proportion of branch crowns in the first-order modules for Capriss, Cir107, Ciflorette (65-81%) but not for Darselect (45%) (Table 25, in results). This high proportions of branch crowns within first-order modules entail a higher number of third- and fourth-order modules for Capriss, Cir107 and Ciflorette compared to other varieties (Tables 11-16, in resulst). For Darselect, the single phase of flowering could be explained by the early occurrence of the third-order modules (mid-March) compared the Capriss, Cir107 and Ciflorette (June). As we previously reported, this rapid occurrence leads to shorten the intervals between differentiations of inflorescences (Kurokura *et al.*, 2005).

As observed for the first flowering flush, variation in flowering intensity is mainly explained by difference in inflorescence complexity whatever the flowering pattern of the variety. Complexity of inflorescences of Cir107 and Gariguette led to a higher flowering intensity than for the other varieties.

In summary, varieties showed either second flowering flush after a moderate phase (pattern 1) or a stationary flowering after the first flush (pattern 2). These two patterns differ mainly by the occurrence of the second-order modules. Varieties could also differ within each pattern according to their third-order module occurrence, their complexity of inflorescences or their branching. This last process is a critical event in plant development and is linked to apical dominance.

Apical dominance is the term used to describe the control of the shoot apical meristem over axillary bud outgrowth (Cline, 1997). In strawberry, the floral transition occurs at the shoot apical meristem and the inflorescence is then initiated. Then, apical dominance is released and axillary buds just below the inflorescence develop into extension crowns (Guttridge, 1955; Kurokura *et al.*, 2005). Kurokura (2005) observed concomitance between appearance of uppermost axillary bud and flower initiation at the first inflorescence, which suggested that the release of apical dominance may trigger the differentiation of the uppermost axillary bud leading to the second inflorescence. This apical dominance is partly caused by auxin transport from terminal bud to axillary buds (basipetal transport of auxin) which are maintained dormant (Thiman and Skoog, 1933 cited by Costes *et al.*, 2014). Recent studies suggest another hormonal control by strigolactone (Brewer *et al.*, 2009), which could be independent to auxin control (Brewer *et al.*, 2015). Strigolactone could either directly inhibit bud outgrowth or impede the ability of buds to export auxin into the main stem, and hence inhibit their outgrowth (Domagalska and Leyser, 2011).

Beside the controls on apical dominance by auxins and strigolactone, gibberellin and cytokinin were also reported for their action on branching. Waithaka *et al.* (1980) showed that these two hormones are responsible of strawberry vegetative *in vitro* development. A low concentration of cytokinin promoted a single shoot development while high concentration of cytokinin promotes production of multiple shoots. Black, (2004) and Hytönen *et al.*, (2009) show that gibberellin is responsible of meristem fate and Tenreira *et al.* (2017) demonstrated it. Indeed, inhibition of gibberellin or mutation in its pathway allows to promote crown development while expression of gibberellin promotes stolon production.

Concerning stolon occurrence, only one pattern was observed in our experiment. This pattern showed a synchronous emergence of stolons and differences in runnering intensity according to varieties.

Synchronous occurrence in May was observed in our experience and corresponded to long day photoperiod (15h of day) as previously reported (Guttridge and Thompson, 1959; Hytönen *et al.*, 2009). Architectural study showed that stolons appeared only on the third- and fourth-order modules. These modules were the only ones growing at this period.

Runnering has been shown to be controlled by gibberellin (Guttridge and Thompson, 1959; Hytönen *et al.*, 2009). As an example, Black (2004) showed that in 'Chandler' variety, a treatment of Prohexadione-Calcium (P-Ca), an inhibitor of gibberellin, reduced stolon production. Application of different concentration of this molecule showed that it is necessary to have a high concentration (240mg.L^{-1}) of P-CA to reduce the formation of stolons and increase the formation of crowns, while a low concentration of P-CA (60mg.L^{-1}) has no effect on stolon production.

Genetic control of runnering started to be deciphered in the diploid strawberry, *F. vesca*. Molecular analysis revealed that SOC1 regulates the differentiation of axillary buds to runners or axillary leaf rosettes, probably through the activation of gibberellin biosynthetic genes (Mouhu *et al.*, 2013). The role of gibberellin genes was confirmed by Tenreira and co-authors. They showed using a runnerless (r) natural mutant, that this trait was due to a deletion in the active site of a gibberellin 20-oxidase (GA20ox) gene, which is expressed primarily in the axillary meristem dome and primordia and in developing stolons. When FveGA20ox4 is muted, axillary meristems remain dormant or produce secondary shoots terminated by inflorescences, thus increasing the number of inflorescences in the plant. This study showed that the regulation of axillary meristem fate (branching versus stolon) by gibberellins governed the trade-off between flowering and runnering. In our study, we can hypothesize that difference of runnering intensity between varieties could result from a difference of gibberellin accumulation, that can be governed by different allelic expression of gibberellin biosynthetic pathway.

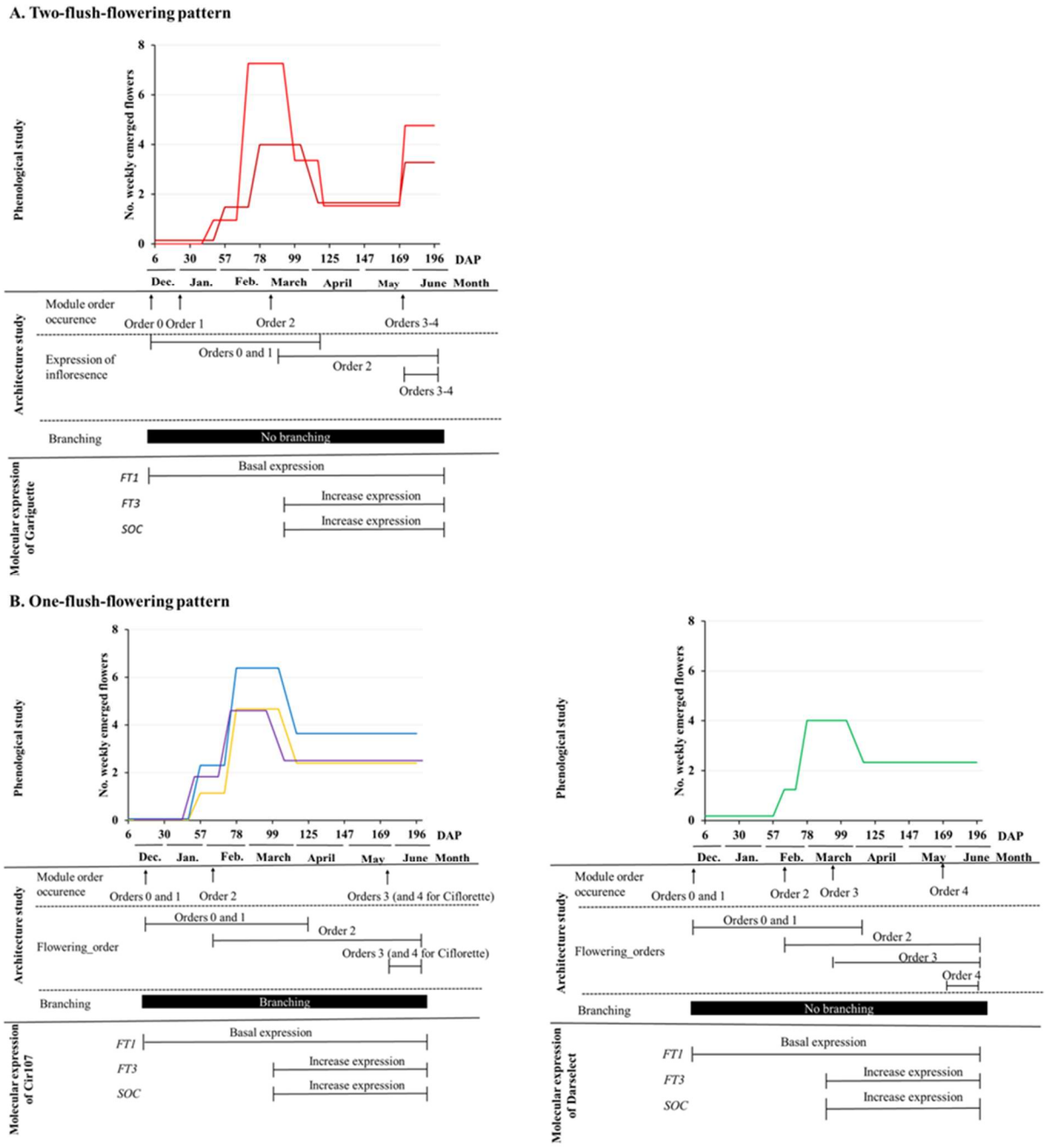

Figure 52: Model combining phenological, architectural and genetic results according to flowering patterns, (A) two-flushes-flowering pattern (Pattern1), (B) and single-flush-flowering patterns (Pattern 2).

Two-flushes-flowering and single-flush-flowering patterns pattern differ according to the occurrence of second-order module. Flowering_order represents the period of flowering for each order module). Among the pattern 2, varieties differ according the occurrence of high-order module. Along the culture production, expression of *FT1* is basal while *FT3* and *SOC* increase in long days from March to the end of experiment, end-May.

3 Perspectives

We have developed a statistical approach to integrate three developmental processes of plant, namely flowering, vegetative development and runnering. Our results demonstrate that, using this approach, it was possible to differentiate varieties according to their development.

How these results can be used by breeders and technicians from experimental centers?

In a breeding program, one of the objectives is to produce fruits early because of the highest prices of marketable strawberry fruits occur in the first month of fruiting. The identification of flowering phases within the production season could simplify the evaluation of varieties for this trait. Considering the flowering patterns identified in this study, a first measurement of the number of flowers could be made in March corresponding to the first flowering flush. This measurement would allow to evaluate the differences in intensity between the varieties corresponding to this first flowering flush. Another objective of a breeding program is to extend the fruit production without pause of fruiting in order to keep all pickers. To achieve this objective, a second measurement point could be made mid-April to separate genotypes according to the presence of an abrupt decrease of flowering or to a stability of flowering (marked by a moderate decline in flowering). This second measurement could be confirmed by a third and last measurement in June, that would allow to check either the stability of flowering, or the resumption of flowering (2^{nd} flowering flush), but also to check the emergence of stolons as well as to evaluate a difference in intensity of runnering. The runnering trait is important for nursery as well as for maintaining genetic resources.

A second perspective for breeders would be to use plant architecture in their breeding program. Whereas the architecture is time consuming, it produces an accurate way to characterize genotypes according to branching habit and inflorescence complexity. This architecture could be described during the third year of the breeding program when evaluation is performed on 10-20 breeding lines and at two measuring occasions. Three varieties could be selected and then evaluated in production condition in the 6th year (Figure 53). The architecture could be described in April after the first flush of flowering to select varieties that (1) show a complex inflorescence in zeroth- and first-order modules, (2) growth quickly after plantation to produce new branching. These varieties should produce a first intense flowering flush because of complex inflorescences and then, flower continuously until at least the end of June thanks to their new branches. A second measurement could be made at the end of production to evaluate

the presence or not of stolons on the varieties, or a change of rhythm or not in the growth rate, or to confirm the complexity of branching of the varieties. These architectural measurements made at two occasions would allow to identify the ideotypes that show a spread production or a second flush of flowering.

In experimental centers, the cultivated strawberry is subjected to numerous assays. To evaluate the plasticity of strawberry, the architecture is a powerful approach that summarizes all modifications in plant development. Therefore, the transfer of the methods of analysis and representation of the architecture developed during this thesis would be an asset to describe in a standardized way, store, and analyze the architecture of varieties subjected to different assays. The standardization provided by the MTGs would allow to re-analyze previous assays several years later and to compare the results with those of current assays. In this way, the assays would be far better exploited in breeding programs.

Another longer-term perspective that could be of interest to growers, breeders and technicians would be to also take into account the fruiting process in plant development and especially fruit size and flower abortion rate in order to predict yield of varieties.

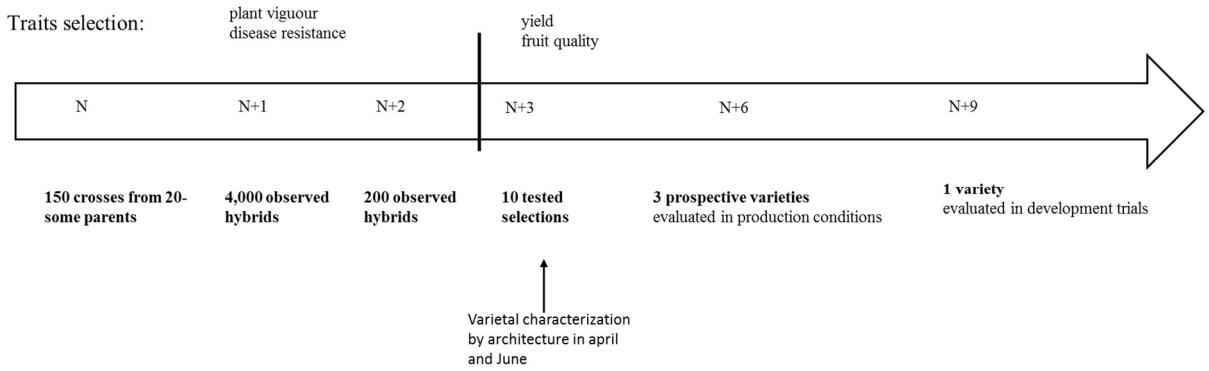

Figure 53: Schematic representation of CIREF breeding program and trait selection with adequate possible timing for architectural characterization of varieties

Which perspectives for research?

The design of an architectural model that would spatially and temporally structure the plant development of diploid strawberry is critical for establishing molecular networks of developmental processes in this species. As an example, a seedling architectural model from seed to first inflorescence would provide a better understanding of the fate of the terminal and

axillary meristems. Indeed, it would make it possible to study more precisely the genetic, physiological and environmental regulation mechanisms that take place during floral initiation, stolon emergence or branching. Our preliminary study strongly suggested that the stolon appeared only from the 5th leaf. Sampling axillary buds at the 5th leaf before and after stolon initiation for performing RNAseq analysis would allow to characterize gene expression during stolon initiation. It will highlight the gene network involved in the initiation of the axillary meristems generating stolons.

In addition, the architectural model of a diploid seedling using MTGs will make possible to study the impacts of environmental factors on the development of the plant. For example, integrating the Caribu model of light interception (Chelle and Andrieu, 1998) could be done. Subsequently, we could move to functional structure models that would allow in the longer term to predict the development of the plant.

Chapter 5: Bibliography

Albani MC, Battey NH, Wilkinson MJ. 2004. The development of ISSR-derived SCAR markers around the SEASONAL FLOWERING LOCUS (SFL) in Fragaria vesca. Theoretical and Applied Genetics **109**, 571–579.

Albani MC, Coupland G. 2010. Comparative Analysis of Flowering in Annual and Perennial Plants. In: Timmermans MCP, ed. Current Topics in Developmental Biology. Plant Development. Academic Press, 323–348.

Amasino RM, Michaels SD. 2010. The Timing of Flowering. Plant Physiology **154**, 516–520.

Andrés F, Coupland G. 2012. The genetic basis of flowering responses to seasonal cues. Nature Reviews Genetics **13**, 627–639.

Auger I, Lawrence C. 1989. Algorithms for the optimal identification of segment neighborhoods. Bulletin of Mathematical Biology **51**, 33–54.

Balduzzi M, Binder BM, Bucksch A, Chang C, Hong L, Iyer-Pascuzzi AS, Pradal C, Sparks EE. 2017. Reshaping Plant Biology: Qualitative and Quantitative Descriptors for Plant Morphology. Frontiers in Plant Science **8**, 1–15.

Banfield MJ, Barker JJ, Perry ACF, Brady RL. 1998. Function from structure? The crystal structure of human phosphatidylethanolamine-binding protein suggests a role in membrane signal transduction. Structure **6**, 1245–1254.

Barthélémy D, Caraglio Y. 2007. Plant Architecture: A Dynamic, Multilevel and Comprehensive Approach to Plant Form, Structure and Ontogeny. Annals of Botany **99**, 375–407.

Battey NH. 2000. Aspects of seasonality. Journal of Experimental Botany **51**, 1769–1780.

Battey N., Miere P, Tehranifar A, Cekic C. 1998. Genetic and environmental control of flowering in strawberry. Genetic and environnemental manipulation of horticultural Crops, 111–130.

Baudry JP, Maugis C, Michel B. 2012. Slope heuristics: Overview and implementation. Statistics and Computing **22**, 455–470.

Black BL. 2004. Prohexadione-calcium decreases fall runners and advances branch crowns of 'Chandler' strawberry in a cold-climate annual production system. Journal of the American Society for Horticultural Science **129**, 479–485.

Blázquez MA, Weigel D. 2000. Integration of floral inductive signals in Arabidopsis. Nature **404**, 889–892.

Blümel M, Dally N, Jung C. 2015. Flowering time regulation in crops—what did we learn from Arabidopsis? Current Opinion in Biotechnology **32**, 121–129.

Bors RH. 2000. *A Streamlined Synthetic Octoploid System that Emphasizes Fragaria Vesca as a Bridge Species*. National Library of Canada.

Bosc JP, Neri D, Massetani F, Bardet A. 2012. Relationship between plant architecture and fruit production of the short-day strawberry cultivar Gariguette. Journal of Berry Research **2**, 105–111.

Bostock J, Pliny, Riley HT, Riley HT. 1855. *The natural history of Pliny / translated,*

with copious notes and illustrations by John Bostock and H.T. Riley. London : H.G. Bohn,.

Bradford E, Hancock JF, Warner RM. 2010. Interactions of Temperature and Photoperiod Determine Expression of Repeat Flowering in Strawberry. **135**, 102–107.

Brewer PB, Dun EA, Ferguson BJ, Rameau C, Beveridge CA. 2009. Strigolactone Acts Downstream of Auxin to Regulate Bud Outgrowth in Pea and Arabidopsis. Plant Physiology **150**, 482–493.

Brewer PB, Dun EA, Gui R, Mason MG, Beveridge CA. 2015. Strigolactone Inhibition of Branching Independent of Polar Auxin Transport. Plant Physiology **168**, 1820–1829.

Brown T, Wareing PF. 1965. the Genetical Control O F the Everbearing Habit a N D Three Other Characters. Geology **14**.

Bussière EMS, Underhill LG, Altwegg R. 2015. Patterns of bird migration phenology in South Africa suggest northern hemisphere climate as the most consistent driver of change. Global Change Biology **21**, 2179–2190.

de Camacaro MEP, Camacaro GJ, Hadley P, Battey NH, Carew JG. 2002. Pattern of Growth and Development of the Strawberry Cultivars Elsanta, Bolero, and Everest. Journal of the American Society for Horticultural Science **127**, 901–907.

Caraglio Y., Edelin C. 1990. Architecture et dynamique de la croissance du platane, Platanus hybrida Brot. (Platanaceae) fsyn. Platanus acerifolia (Aiton) Willd.g. Bulletin de la Société Botanique de France, Lettres Botaniques **137**, 279–291.

Chatfield C. 2003. *The Analysis of Time Series: An Introduction, Sixth Edition (Chapman & Hall/CRC Texts in Statistical Science)*. Chapman and Hall/CRC.

Chelle M, Andrieu B. 1998. The nested radiosity model for the distribution of light within plant canopies. Ecological Modelling **111**, 75–91.

Chew YH, Wilczek AM, Williams M, Welch SM, Schmitt J, Halliday KJ. 2012. An augmented Arabidopsis phenology model reveals seasonal temperature control of flowering time. New phytologist **194**, 654–665.

Chia TYP, Müller A, Jung C, Mutasa-Göttgens ES. 2008. Sugar beet contains a large CONSTANS-LIKE gene family including a CO homologue that is independent of the early-bolting (B) gene locus. Journal of Experimental Botany **59**, 2735–2748.

Cilas C, Bar-Hen A, Montagnon C, Godin C. 2006. Definition of architectural ideotypes for good yield capacity in Coffea canephora. Annals of Botany **97**, 405–411.

Cleland EE, Chuine I, Menzel A, Mooney HA, Schwartz MD. 2007. Shifting plant phenology in response to global change. Trends in Ecology and Evolution **22**, 357–365.

Cline MG. 1997. Concepts and terminology of apical dominance. American Journal of Botany **84**, 1064–1069.

Collins WB. 1966. Floral Initiation In Strawberry And Some Effects Of Red And Far-Red Radiation As Components Of Continuous White Light. Canadian Journal of Botany **44**, 663–668.

Costes E, Crespel L, Denoyes B, Morel P, Demene M-N, Lauri P-E, Wenden B. 2014. Bud structure, position and fate generate various branching patterns along shoots of closely related Rosaceae species: a review. Frontiers in Plant Science **5**, 666.

Dale A, Sjulin TM. 1990. Few cytoplasm contribute to North American strawberry cultivars. HortScience **25**, 1341–1342.

Dally N, Xiao K, Holtgrawe D, Jung C. 2014. The B2 flowering time locus of beet encodes a zinc finger transcription factor. Proceedings of the National Academy of Sciences **111**, 10365–10370.

Dambreville A. 2012. Croissance et développement du manguier (Mangifera indica L .) in natura : approche expérimentale et modélisation de l ' influence d ' un facteur exogène , la température, et de facteurs endogènes architecturaux.

Dambreville A, Lauri P-É, Normand F, Guédon Y. 2014. Analysing growth and development of plants jointly using developmental growth stages. Annals of botany, 1–13.

Darnell RL, Cantliffe DJ, Kirschbaum DS, Chandler CK. 2003. The physiology of flowering in strawberry. In: Janick J, ed. Hoticultura Reviews. John Wiley & Sons, 325–349.

Darrow GM. 1929. Inflorescence Types of Strawberry Varieties. American Journal of Botany. Botanical Society of America, 571–585.

Darrow GM. 1966. *The Strawberry* (Holt, Rinehart, and Winston, Eds.). The New England Institute for Medical Research.

Demarée GR, Rutishauser T. 2011. From 'Periodical Observations' to 'Anthochronology' and 'Phenology' - the scientific debate between Adolphe Quetelet and Charles Morren on the origin of the word 'Phenology'. International Journal of Biometeorology **55**, 753–761.

Ding J, Nilsson O. 2016. Molecular regulation of phenology in trees-because the seasons they are a-changin'. Current opinion in plant biology **29**, 73–79.

Domagalska MA, Leyser O. 2011. Signal integration in the control of shoot branching. Nature Reviews Molecular Cell Biology **12**, 211–221.

Dorca-Fornell C, Gregis V, Grandi V, Coupland G, Colombo L, Kater MM. 2011. The Arabidopsis SOC1-like genes AGL42, AGL71 and AGL72 promote flowering in the shoot apical and axillary meristems. Plant Journal **67**, 1006–1017.

Durner E, Barden J, Himelrick D, Poling EB. 1984. Photoperiod and temperature effects on flower and runner development in day-neutral, junebearing and everbearing strawberries. J. Amer. Soc. Hort. Sci., 396–400.

Edelin C. 1984. L'architecture monopodiale: l'exemple de quelques arbres d'Asie tropicale.

Evans WD. 1977. The use of synthetic octoploids in strawberry breeding. Euphytica **26**, 497–503.

Farooq M, Wahid A, Kobayashi N, Fujita D, Basra SMA. 2009. Plant drought stress: effects, mechanisms and management. Agronomy for Sustainable Development **29**, 185–212.

Fornara F, de Montaigu A, Coupland G. 2010. SnapShot: Control of flowering in arabidopsis. Cell **141**, 3–5.

Forrest J, Miller-rushing AJ. 2010. Toward a synthetic understanding of the role of phenology in ecology and evolution. , 3101–3112.

Franks SJ. 2011. Plasticity and evolution in drought avoidance and escape in the annual plant Brassica rapa. New Phytologist **190**, 249–257.

Galletta GJ, Maas JL. 1990. Strawberry genetics. Hortscience **25**, 871–879.

Garin G, Fournier C, Andrieu B, Houlès V, Robert C, Pradal C. 2014. A modelling framework to simulate foliar fungal epidemics using functional-structural plant models. Annals of Botany.

Garner WW. 1933. Comparative responses of long-day and short-day plants to relative length of day and night. Plant physiology **8**, 347.

GARNER WW, ALLARD HA. 1920. EFFECT OF THE RELATIVE LENGTH OF DAY AND NIGHT AND OTHER FACTORS OF THE ENVIRONMENT ON GROWTH AND REPRODUCTION IN PLANTS 1. Monthly Weather Review **48**, 415–415.

Gaston A, Perrotte J, Lerceteau-Köhler E, Rousseau-Gueutin M, Petit A, Hernould M, Rothan C, Denoyes B. 2013. PFRU, a single dominant locus regulates the balance between sexual and asexual plant reproduction in cultivated strawberry. Journal of Experimental Botany **64**, 1837–1848.

Gil-Ariza DJ, Amaya I, Lopez-Aranda JM, Sanchez-Sevilla JF, Angel Botella M, Valpuesta V. 2009. Impact of Plant Breeding on the Genetic Diversity of Cultivated Strawberry as Revealed by Expressed Sequence Tag-derived Simple Sequence Repeat Markers. J. Amer. Soc. Hort. Sci. **134**, 337–347.

Godin C, Caraglio Y. 1998. A multiscale model of plant topological structures. Journal of theoretical biology **191**, 1–46.

Gregis V, Sessa A, Colombo L, Kater MM. 2008. AGAMOUS-LIKE24 and SHORT VEGETATIVE PHASE determine floral meristem identity in Arabidopsis. Plant Journal **56**, 891–902.

Guédon Y. 2013. Exploring the latent segmentation space for the assessment of multiple change-point models. Computational Statistics **28**, 2641–2678.

Guédon Y. 2015. Slope heuristics for multiple change-point models. 30th International Workshop on Statistical Modelling . **2**, 103–106.

Guttridge CG. 1955. Observations on the Shoot Growth of the Cultivated Strawberry Plant. Journal of Horticultural Science **30**, 1–11.

Guttridge, Thompson. 1959. Effect of gibberellic acid on the initiation of flowers and runners in the strawberry. Nature **184**, 72–73.

Hallé F, Martin R. 1968. Etude de la croissance rythmique chez l'hévéa (Hevea brasiliensis) (Müll. Arg., Euphorbiacées, crotonoïdées). Adansonia **8**, 475–503.

Hallé F, Oldeman RAA. 1970. *Essai sur l'architecture et la dynamique de croissance des arbres tropicaux*. Masson.

Hallé F, Oldeman Roelof A. A., Tomlinson PB. 1978. *Tropical trees and forests : an architectural analysis*. New York : Springer-Verlag Berlin.

Hancock JF, Lavin A, Retamales JB. 1999. Our southern strawberry heritage: Fragaria chiloensis of Chile. HortScience **34**, 814–816.

Heide OM. 1977. Photoperiod and Temperature Interactions in Growth and Flowering of Strawberry. Physiologia Plantarum **40**, 21–26.

Heide OM, Stavang JA, Sønsteby A. 2013. Physiology and genetics of flowering in cultivated and wild strawberries - A review. Journal of Horticultural Science and Biotechnology **88**, 1–18.

Hepworth SR, Valverde F, Ravenscroft D, Mouradov A, Coupland G. 2002. Antagonistic regulation of flowering-time gene SOC1 by CONSTANS and FLC via separate promoter motifs. EMBO Journal **21**, 4327–4337.

Honjo M, Kataoka S, Yui S, Morishita M, Kunihisa M, Yano T, Hamano M, Yamazaki H. 2009. Maternal lineages of the cultivated strawberry, Fragaria ×ananassa,

revealed by chloroplast DNA variation. HortScience **44**, 1562–1565.

Honjo M, Kataoka S, Yui S, Morishita M, Yano T, Hamano M, Yamazaki H. 2011. Varietal Differences and Selection Indicators for Flowering Pattern in Everbearing Strawberry. Journal of the Japanese Society for Horticultural Science **80**, 38–44.

Horvath A, Sánchez-Sevilla JF, Punelli F, *et al.* 2011. Structured diversity in octoploid strawberry cultivars: Importance of the old European germplasm. Annals of Applied Biology **159**, 358–371.

Hsu C-Y, Adams JP, Kim H, *et al.* 2011. FLOWERING LOCUS T duplication coordinates reproductive and vegetative growth in perennial poplar. Proceedings of the National Academy of Sciences **108**, 10756–10761.

Hummer KE, Nathewet P, Yanagi T. 2009. Decaploidy in fragaria iturupensis (rosaceae). American Journal of Botany **96**, 713–716.

Hytönen T. 2014. *Regulation of strawberry growth and development*.

Hytönen T, Elomaa P, Moritz T, Junttila O. 2009. Gibberellin mediates daylength-controlled differentiation of vegetative meristems in strawberry (Fragaria x ananassa Duch). BMC plant biology **9**, 18.

Hytonen T, Palonen P, Mouhu K, Junttila O. 2004. Crown branching and cropping potential in strawberry (Fragaria ananassa Duch.) can be enhanced by daylength treatments. The Journal of Horticultural Science and Biotechnology **79**, 466–471.

Ibáñez I, Primack RB, Miller-Rushing AJ, Ellwood E, Higuchi H, Lee SD, Kobori H, Silander JA. 2010. Forecasting phenology under global warming. Philosophical transactions of the Royal Society of London. Series B, Biological sciences **365**, 3247–60.

Ichijima K. 1926. Cytological and genetic studies on Fragaria. Genetics **11**, 590–604.

Ito H, Saito T. 1962. Studies on the Flower Formation in the Strawberry Plants I. Effects of Temperature and Photoperiod on the Flower Formation. Tohoku journal of agricultural research **13**, 191–203.

Iwata H, Gaston A, Remay A, Thouroude T, Jeauffre J, Kawamura K, Oyant LH Saint, Araki T, Denoyes B, Foucher F. 2012. The TFL1 homologue KSN is a regulator of continuous flowering in rose and strawberry. Plant Journal **69**, 116–125.

Jahn OL, Dana MN, American S, Jul N. 1970. Crown and Inflorescence Development in the Strawberry , Fragaria Ananassa. American Journal of Botany **57**, 605–612.

Karlgren A, Gyllenstrand N, Kallman T, Sundstrom JF, Moore D, Lascoux M, Lagercrantz U. 2011. Evolution of the PEBP Gene Family in Plants: Functional Diversification in Seed Plant Evolution. Plant Physiology **156**, 1967–1977.

Korner C, Basler D. 2010. Phenology Under Global Warming. Science **327**, 1461–1462.

Koskela E a, Mouhu K, Albani MC, Kurokura T, Rantanen M, Sargent DJ, Battey NH, Coupland G, Elomaa P, Hytönen T. 2012. Mutation in TERMINAL FLOWER1 reverses the photoperiodic requirement for flowering in the wild strawberry Fragaria vesca. Plant physiology **159**, 1043–54.

Koskela EA, Sønsteby A, Flachowsky H, Heide OM, Hanke M-V, Elomaa P, Hytönen T. 2016. TERMINAL FLOWER1 is a breeding target for a novel everbearing trait and tailored flowering responses in cultivated strawberry (Fragaria × ananassa Duch.). Plant Biotechnology Journal **14**, 1852–1861.

Kurokura T, Inaba Y, Neri D, Sugiyama N. 2005. A morphological study of the development of the second infl orescences in strawberry (Fragaria × ananassa Duch.). Annals of Applied Biology **146**, 511–515.

Kurokura T, Mimida N, Battey NH, Hytönen T. 2013. The regulation of seasonal flowering in the Rosaceae. **64**, 4131–4141.

Lee J, Oh M, Park H, Lee I. 2008. SOC1 translocated to the nucleus by interaction with AGL24 directly regulates LEAFY. Plant Journal **55**, 832–843.

Lee JH, Yoo SJ, Park SH, Hwang I, Lee JS, Ahn JH. 2007. Role of SVP in the control of flowering time by ambient temperature in Arabidopsis. Genes & Development **21**, 397–402.

Legave J, Guédon Y, Malagi G, Yaacoubi A El. 2015. Differentiated Responses of Apple Tree Floral Phenology to Global Warming in Contrasting Climatic Regions. **6**.

Liao Z, Chen M, Guo L, Gong Y, Tang F, Sun X, Tang K. 2004. Rapid Isolation of High-Quality Total RNA from Taxus and Ginkgo. Preparative Biochemistry and Biotechnology **34**, 209–214.

Lièvre M, Granier C, Guédon Y. 2016. Identifying developmental phases in the Arabidopsis thaliana rosette using integrative segmentation models. New Phytologist **210**, 1466–1478.

Liu C, Teo ZWN, Bi Y, Song S, Xi W, Yang X, Yin Z, Yu H. 2013. A Conserved Genetic Pathway Determines Inflorescence Architecture in Arabidopsis and Rice. Developmental Cell **24**, 612–622.

Luedeling E, Kunz A, Blanke MM. 2013. Identification of chilling and heat requirements of cherry trees-a statistical approach. International Journal of Biometeorology **57**, 679–689.

Maltaite L, Caraglio Y. 2016. *Fragaria vesca L ., 1753 Fraisier des bois*. Montpellier.

Maltoni M, Faedi W, Simpson D, Dradi R, Persano S. 1996. No Influenza dell'ambiente sulla espressione del carattere rifiorenza in Fragola. Italus Hortus **3**, 30--36.

Manakasem Y, Goodwin PB. 1998. Floral Status of Strawberry Plants.Pdf. J. Amer. Soc. Hort. Sci. **123**, 513–519.

Massetani F, Gangatharan R, Neri D. 2011. Plant Architecture of Strawberry in Relation to Abiotic Stress , Nutrient Application and Type of Propagation System. Global Science Books **Genes**, **Gen**, 12–23.

Meier et al. 1994. Échelle BBCH des stades phénologiques de la fraise

Menzel A. 2003. Europe. In: Schwartz MD, ed. Phenology: An Integrative Environmental Science. Dordrecht: Springer Netherlands, 45–56.

Menzel A, Fabian P. 1999. Growing season extended in Europe. Nature **397**, 659–659.

de Montaigu A, Tóth R, Coupland G. 2010. Plant development goes like clockwork. Trends in Genetics **26**, 296–306.

Moon J, Suh SS, Lee H, Choi KR, Hong CB, Paek NC, Kim SG, Lee I. 2003. The SOC1 MADS-box gene integrates vernalization and gibberellin signals for flowering in Arabidopsis. Plant Journal **35**, 613–623.

Mouhu K, Kurokura T, Koskela EA, Albert VA, Elomaa P, Hytonen T. 2013. The Fragaria vesca Homolog of SUPPRESSOR OF OVEREXPRESSION OF CONSTANS1 Represses Flowering and Promotes Vegetative Growth. The Plant Cell **25**, 3296–3310.

Neri D. 2002. Tray Plant Programming Plant architecture Flower formation. Architecture, Plant.1–7.

Newstrom LE, Frankie GW, Baker HG, Jun N. 1994. A New Classification for Plant Phenology Based on Flowering Patterns in Lowland Tropical Rain Forest Trees at La Selva , Costa Rica A New Classification for Plant Phenology Based on Flowering Patterns in Lowland Tropical Rain Forest Trees at La Selva , Co. **26**, 141–159.

Ollat N, Brisson N, Denoyes B, Garcia de Cortazar-Atauri I, Goutouly J, Kleinhentz M, Launay M, Michalet R, Pieri P, Van Leeuwen C. 2013. Les Agro-Systèmes. In: Le Treut H, ed. Prevoir pour agir , la Région Aquitaine anticipe le réchauffement climatique. Presses Universitaires de Bordeaux, .

Opstad N, Sønsteby A, Myrheim U, Heide OM. 2011. Seasonal timing of floral initiation in strawberry: Effects of cultivar and geographic location. Scientia Horticulturae **129**, 127–134.

Parcy F. 2005. Flowering: A time for integration. International Journal of Developmental Biology **49**, 585–593.

Peng JR, Richards DE, Hartley NM, *et al.* 1999. 'Green revolution' genes encode mutant gibberellin response modulators. Nature **400**, 256–261.

Peñuelas J, Filella I, Comas P. 2002. Changed plant and animal life cycles from 1952-2000 in the Mediterranean region. Global Change Biology, 531–544.

Perrotte J, Guédon Y, Gaston A, Denoyes B. 2016. Identification of successive flowering phases highlights a new genetic control of the flowering pattern in strawberry. Journal of Experimental Botany **67**, 5643–5655.

Pin PA, Benlloch R, Bonnet D, Wremerth-Weich E, Kraft T, Gielen JJL, Nilsson O. 2010. An Antagonistic Pair of FT Homologs Mediates the Control of Flowering Time in Sugar Beet. Science **330**, 1397–1400.

Porter JR, Gawith M. 1999. Temperatures and the growth and development of wheat: a review. European Journal of Agronomy **10**, 23–36.

Potter D, Eriksson T, Evans RC, *et al.* 2007. *Phylogeny and classification of Rosaceae*.

Preece C, Callaghan T V., Phoenix GK. 2012. Impacts of winter icing events on the growth, phenology and physiology of sub-arctic dwarf shrubs. Physiologia Plantarum **146**, 460–472.

Prusinkiewicz P, Erasmus Y, Lane B, Harder LD, Coen E. 2007. Evolution and Development of Inflorescence Architectures. Science **316**, 1452–1456.

Rahman MM, Rahman MM, Hossain MM, Khaliq QA, Moniruzzaman M. 2014. Effect of planting time and genotypes growth, yield and quality of strawberry (Fragaria×ananassa Duch.). Scientia Horticulturae **167**, 56–62.

Rantanen M, Kurokura T, Mouhu K, Pinho P, Tetri E, Halonen L, Palonen P, Elomaa P, Hytönen T. 2014. Light quality regulates flowering in FvFT1/FvTFL1 dependent manner in the woodland strawberry Fragaria vesca. Frontiers in Plant Science **5**.

Ratcliffe OJ, Bradley DJ, Coen ES. 1999. Separation of shoot and floral identity in Arabidopsis. Development **126**, 1109–1120.

Ratcliffe OJ, Kumimoto RW, Wong BJ. 2003. Analysis of the Arabidopsis. Society **15**, 1159–1169.

Rathcke B, Lacey EP. 1985. Phenological Patterns of Terrestrial Plants. Annual Review of Ecology and Systematics **16**, 179–214.

Rigaill G, Lebarbier E, Robin S. 2012. Exact posterior distributions and model selection criteria for multiple change-point detection problems. Statistics and Computing **22**, 917–929.

Rohde A, Bastien C, Boerjan W. 2011. Temperature signals contribute to the timing of photoperiodic growth cessation and bud set in poplar. Tree Physiology **31**, 472–482.

Rousseau-Gueutin M, Gaston A, Aïnouche A, Aïnouche ML, Olbricht K, Staudt G, Richard L, Denoyes-Rothan B. 2009. Tracking the evolutionary history of polyploidy in Fragaria L. (strawberry): New insights from phylogenetic analyses of low-copy nuclear genes. Molecular Phylogenetics and Evolution **51**, 515–530.

Sabatier S, Barthelemy D. 1999. Growth dynamics and morphology of annual shoots, according to their architectural position, in young Cedrus atlantica (Endl.) Manetti ex Carriere (Pinaceae). Annals of Botany **84**, 387–392.

Savini G, Neri D, Zucconi F, Sugiyama N. 2006. Strawberry Growth and Flowering. International Journal of Fruit Science **5**, 29–50.

Searle I, He Y, Turck F, Vincent C, Fornara F, Kröber S, Amasino RA, Coupland G. 2006. The transcription factor FLC confers a flowering response to vernalization by repressing meristem competence and systemic signaling in Arabidopsis. Genes and Development **20**, 898–912.

Serce S, Hancock JF. 2005. Inheritance of day-neutrality in octoploid species of Fragaria. Journal of the American Society for Horticultural Science **130**, 580–584.

Shalit A, Rozman A, Goldshmidt A, Alvarez JP, Bowman JL, Eshed Y, Lifschitz E. 2009. The flowering hormone florigen functions as a general systemic regulator of growth and termination. Proceedings of the National Academy of Sciences **106**, 8392–8397.

Shaw D V., Famula TR. 2005. Complex segregation analysis of day-neutrality in domestic strawberry (Fragaria x ananassa Duch.). Euphytica **145**, 331–338.

Sherrard ME, Maherali H. 2006. The adaptive significance of drought escape in Avena barbata, an annual grass. Evolution; international journal of organic evolution **60**, 2478–89.

Shulaev V, Korban SS, Sosinski B, *et al.* 2008. Multiple Models for Rosaceae Genomics. Plant Physiol **147**, 985–1003.

Shulaev V, Sargent DJ, Crowhurst RN, *et al.* 2011. The genome of woodland strawberry (Fragaria vesca). Nature genetics **43**, 109–116.

Song YH, Ito S, Imaizumi T. 2013. Flowering time regulation: Photoperiod- and temperature-sensing in leaves. Trends in Plant Science **18**, 575–583.

Sonsteby A. 1997. SHORT-DAY PERIOD AND TEMPERATURE INTERACTIONS ON GROWTH AND FLOWERING OF STRAWBERRY. Acta Horticulturae, 609–616.

Sonsteby A, Heide O. 2007. Quantitative long-day flowering response in the perpetual-flowering F-1 strawberry cultivar Elan. Journal of … **82**, 266–274.

Sonsteby A, Heide O. 2008*a*. Long-day rather than autonomous control of flowering in the diploid everbearing strawberry Fragaria vesca ssp. semperflorens. Journal of Horticultural Science and … **83**, 360–366.

Sonsteby A, Heide OM. 2008*b*. Temperature responses, flowering and fruit yield of

the June-bearing strawberry cultivars Florence, Frida and Korona. Scientia Horticulturae **119**, 49–54.

Staudt G. 1962. TAXONOMIC STUDIES IN THE GENUS FRAGARIA TYPIFICATION OF FRAGARIA SPECIES KNOWN AT THE TIME OF LINNAEUS. Canadian Journal of Botany **40**, 869–886.

Staudt G. 1989. THE SPECIES OF FRAGARIA, THEIR TAXONOMY AND GEOGRAPHICAL DISTRIBUTION. Acta Horticulturae, 23–34.

Sugimoto T, Tamaki K, Matsumoto J, Yamamoto Y, Shiwaku K, Watanabe K. 2005. Detection of RAPD markers linked to the everbearing gene in Japanese cultivated strawberry. Plant Breeding **124**, 498–501.

Tanino KK, Wang R. 2008. Modeling chilling requirement and diurnal temperature differences on flowering and yield performance in strawberry crown production. HortScience **43**, 2060–2065.

Taylor ' DR, Atkey PT, Wickenden ' MF, Crisp ' CM. 1997. A morphological study of flower initiation and cryo-scanning electron microscopy velopment in strawberry (Fragaria x ananassa) using. Annals of Applied Biology **130**, 141–152.

Tenreira T, Pimenta Lange MJ, Lange T, Bres C, Labadie M, Monfort A, Hernould M, Rothan C, Denoyes B. 2017. A Specific Gibberellin 20-oxidase Dictates the Flowering-Runnering Decision in Diploid Strawberry. The Plant Cell, tpc.00949.2016.

Tomlinson PB. 1983. Tree Architecture: New approaches help to define the elusive biological property of tree form. American Scientist **71**, 141–149.

Urrutia M, Bonet J, Arús P, Monfort A. 2015. A near-isogenic line (NIL) collection in diploid strawberry and its use in the genetic analysis of morphologic, phenotypic and nutritional characters. Theoretical and Applied Genetics **128**, 1261–1275.

Verheul MJ, Sønsteby A, Grimstad SO. 2006. Interactions of photoperiod, temperature, duration of short-day treatment and plant age on flowering of Fragaria x ananassa Duch. cv. Korona. Scientia Horticulturae **107**, 164–170.

Verheul MJ, Sønsteby A, Grimstad SO. 2007. Influences of day and night temperatures on flowering of Fragaria x ananassa Duch., cvs. Korona and Elsanta, at different photoperiods. Scientia Horticulturae **112**, 200–206.

Vince-Prue D, Guttridge CG. 1973. Floral initiation in strawberry: Spectral evidence for the regulation of flowering by long-day inhibition. Planta **110**, 165–172.

Vince-prue D, Guttridge CG, Buck .M.W. 1976. Photocontrol of Petiole Elongation in Light-grown Strawberry Plants Daphne. Plant Science **114**, 109–114.

Waithaka K, Hildebrandt AC, Dana MN. 1980. Hormonal control of strawberry axillary bud development in vitro. Journal of the American Society for Horticultural Science **105**, 428–430.

Wang Y, Li J. 2006. Genes controlling plant architecture. Current Opinion in Biotechnology **17**, 123–129.

Watson R, Wright CJ, McBurney T, Taylor a J, Linforth RST. 2002. Influence of harvest date and light integral on the development of strawberry flavour compounds. Journal of experimental botany **53**, 2121–2129.

Weebadde CK, Wang D, Finn CE, Lewers KS, Luby JJ, Bushakra J, Sjulin TM, Hancock JF. 2008. Using a linkage mapping approach to identify QTL for day-neutrality in

the octoploid strawberry. Plant Breeding **127**, 94–101.

Wellmer F, Riechmann JL. 2010. Gene networks controlling the initiation of flower development. Trends in Genetics **26**, 519–527.

Wilczek AM, Burghardt LT, Cobb AR, Cooper MD, Welch SM, Schmitt J. 2010. Genetic and physiological bases for phenological responses to current and predicted climates. Philosophical Transactions of the Royal Society Biological Sciences **365**, 3129–3147.

Xu C, Park SJ, Van Eck J, Lippman ZB. 2016. Control of inflorescence architecture in tomato by BTB/POZ transcriptional regulators. Genes and Development **30**, 2048–2061.

Yasuyuki Aono, Kazui K. 2008. Phenological data series of cherry tree flowering in Kyoto, Japan, and its application to reconstruction of springtime temperatures since the 9th century. INTERNATIONAL JOURNAL OF CLIMATOLOGY **28**, 905–914.

Chapter 6: Appendices

Appendix A: Definition of categorical multiple change-point models and associated statistical methods

For a given genotype, multiple change-point models were used to delimit phases within a sample of phenological series of fixed length. Each series corresponds to a plant and may be univariate (emergence rate for a given organ) or multivariate (emergence rates for different organs such as flower, leaf and stolon in our case). These series are indexed by the successive dates of observation (with the convention that the first date of observation is 1 for notational convenience). Let θ denote the parameters of the categorical distributions attached to the successive phases (i.e. the probability masses for the possible number of weekly emerged organs). Let $f_J(\mathbf{s}, \mathbf{x}; \hat{\theta})$ denote the likelihood of the segmentation **s** of the observed series $\mathbf{x} = x_1, \ldots, x_T$. The estimation of the $J-1$ change points $\tau_1, \ldots, \tau_{J-1}$, which corresponds to the optimal segmentation $\mathbf{s}^*$ into *J* flowering phases, is obtained using a dynamic programming algorithm (Auger and Lawrence, 1989) that solves the following optimization problem:

$$\hat{\tau}_1, \ldots, \hat{\tau}_{J-1} = \arg\max_{\mathbf{s}} \log f_J\left(\mathbf{s}, \mathbf{x}; \hat{\theta}\right),$$

Regarding the inference of multiple change-point models, one key question is to select the number of phases. In a model selection context, the purpose is to estimate *J* by maximizing a penalized version of the log-likelihood defined as follows

$$\hat{J} = \arg\max_{J} \left\{\log f_J(\mathbf{x}) - \text{Penalty}(J)\right\},$$

where

$$f_J(\mathbf{x}) = \sum_{\mathbf{s}} f_J(\mathbf{s}, \mathbf{x}; \hat{\theta})$$

is the log-likelihood of all the possible segmentations in *J* phases of the phenological series **x** of length *T*. The principle of this kind of penalized likelihood criterion consists in making a trade-off between an adequate fitting of the model to the data (expressed by the log-likelihood) and a reasonable number of parameters to be estimated (controlled by the penalty term). The most popular information criteria such as AIC and BIC are not adapted in this particular context since they tend to underpenalize the log-likelihood and thus select a too large number of developmental zones (Rigaill *et al.*, 2012). We thus applied the slope heuristic (SH) given by (Guédon, 2015)

,

$$\mathrm{SH}_J = 2\{\log f_J(\mathbf{x}) - 2\,\hat{\kappa}\,\mathrm{pen}_{\mathrm{shape}}(J)\},$$

where

$$\mathrm{pen}_{\mathrm{shape}}(J) = \log\left\{\frac{T^{J-1}}{(J-1)!}\right\},$$

and $\hat{\kappa}$ is the slope of the linear relationship between $\log f_J(\mathbf{x})$ and $\mathrm{pen}_{\mathrm{shape}}(J)$ for overparameterized models estimated by the data-driven slope estimation method (Baudry *et al.*, 2012). The posterior probability of the *J*-phase model M_J, given by

$$P(M_J|\mathbf{x}) = \frac{\exp\left(\frac{1}{2}\mathrm{SH}_J\right)}{\sum_{K=1}^{J_{\max}} \exp\left(\frac{1}{2}\mathrm{SH}_K\right)},$$

can be used to assess the relative merits of the models considered.

The posterior probability of the optimal segmentation $\mathbf{s}^*$ given by

,

$$P(\mathbf{s}^*|\mathbf{x}; J) = f_J(\mathbf{s}^*, \mathbf{x}; \hat{\theta}) / \textstyle\sum_{\mathbf{s}} f_J(\mathbf{s}, \mathbf{x}; \hat{\theta}),$$

can be efficiently computed by the smoothing algorithm proposed by Guédon (2013). The assessment of multiple change-point models thus relies on two posterior probabilities:

- posterior probability of the *J*-phase model M_J, $P(M_J|\mathbf{x})$ deduced from the slope heuristic computed for a collection of multiple change-point models for $J = 1, \ldots, J_{\max}$, i.e. weight of the *J*-phase model among all the possible models between 1 and $J_{\max}$ developmental zones,
- posterior probability of the optimal segmentation $\mathbf{s}^*$ for a fixed number of phases *J* $P(\mathbf{s}^*|\mathbf{x}; J)$, i.e. weight of the optimal segmentation among all the possible segmentations for a fixed number of phases.

It is often of interest to quantify the uncertainty concerning change-point position. To this end, we computed the posterior change-point probabilities for each change point *j* and each observation date *t* using the smoothing algorithm proposed by Guédon (2013). We define the α-uncertainty interval for change point *j* as the interval such that

,

$$\alpha/2 < \sum_{t=u}^{v} P(S_t = j, S_{t-1} = j-1|\mathbf{x}; J) < 1 - \alpha/2,$$

with $\sum_{t=j+1}^{T-J+j} P(S_t = j, S_{t-1} = j-1|\mathbf{x}; J) = 1$.

Appendix B: A specific Gibberellin 20-Oxidase Dictates the Flowering-Runnering Decision in Diploid Strawberry

The Plant Cell, Vol. 29: 2168–2182, September 2017, www.plantcell.org © 2017 ASPB.

A Specific Gibberellin 20-Oxidase Dictates the Flowering-Runnering Decision in Diploid Strawberry[OPEN]

Tracey Tenreira,[a] Maria João Pimenta Lange,[b] Theo Lange,[b] Cécile Bres,[a] Marc Labadie,[a] Amparo Monfort,[c] Michel Hernould,[a] Christophe Rothan,[a,1] and Béatrice Denoyes[a,1]

[a] UMR 1332 BFP, INRA, Université Bordeaux, F-33140 Villenave d'Ornon, France
[b] TU Braunschweig, Institut für Pfanzenbiologie, 38106 Braunschweig, Germany
[c] IRTA, Center of Research in Agrigenomics CSIC-IRTA-UAB-UB, Campus UAB, Edifici CRAG, Bellaterra (Cerdanyola del Valles), 08193 Barcelona, Spain

ORCID IDs: 0000-0001-5673-7210 (T.T.); 0000-0002-3898-6130 (M.J.P.L.); 0000-0003-1294-2647 (T.L.); 0000-0001-6460-4637 (C.B.); 0000-0001-9923-8817 (M.L.); 0000-0001-7106-7745 (A.M.); 0000-0003-0676-6173 (M.H.); 0000-0002-6831-2823 (C.R.); 0000-0002-0369-9609 (B.D.)

Asexual and sexual reproduction occur jointly in many angiosperms. Stolons (elongated stems) are used for asexual reproduction in the crop species potato (*Solanum tuberosum*) and strawberry (*Fragaria* spp), where they produce tubers and clonal plants, respectively. In strawberry, stolon production is essential for vegetative propagation at the expense of fruit yield, but the underlying molecular mechanisms are unknown. Here, we show that the stolon deficiency trait of the *runnerless* (*r*) natural mutant in woodland diploid strawberry (*Fragaria vesca*) is due to a deletion in the active site of a *gibberellin 20-oxidase* (*GA20ox*) gene, which is expressed primarily in the axillary meristem dome and primordia and in developing stolons. This mutation, which is found in all *r* mutants, goes back more than three centuries. When *FveGA20ox4* is mutated, axillary meristems remain dormant or produce secondary shoots terminated by inflorescences, thus increasing the number of inflorescences in the plant. The application of bioactive gibberellin (GA) restored the runnering phenotype in the *r* mutant, indicating that GA biosynthesis in the axillary meristem is essential for inducing stolon differentiation. The possibility of regulating the runnering-flowering decision in strawberry via *FveGA20ox4* provides a path for improving productivity in strawberry by controlling the trade-off between sexual reproduction and vegetative propagation.

INTRODUCTION

Asexual and sexual reproduction are inseparable in the life history of plants and take place jointly in a large number of angiosperms (Abrahamson, 1980). Asexual reproduction produces offspring that are genetically identical to the parent. A high diversity of mechanisms is involved in this process, including the production of tubers, rhizomes, corms, bulbs, and stolons (Klimeš et al., 1997). In natural populations, clonal reproduction likely provides ecological and evolutionary benefits to flowering plants (Vallejo-Marín et al., 2010). Natural vegetative propagation has also been harnessed for food production in several crop species. A major representative of these crop species is potato (*Solanum tuberosum*), in which tubers are storage organs derived from an underground stolon (elongated stem). In strawberry (*Fragaria* spp), a major fleshy fruit-bearing crop that undergoes inbreeding depression (Darrow, 1929; Kaczmarska et al., 2016), daughter plants or ramets (clonal plants) produced from an aerial stolon (runner) are essential for the clonal propagation of commercial varieties. Notably, vegetative reproduction can occur at the expense of fruit yield (Barrett, 2015), which depends on the number of inflorescences in the plant and on the duration of the flowering period (Costes et al., 2014). Thus, new insights into the mechanisms underlying the plant decision to produce either stolons or shoots with inflorescences are crucial for improving strawberry productivity.

Strawberry is an herbaceous perennial crop species from the Rosaceae family. Natural perpetual flowering (PF) mutants in which flowering occurs all along the vegetative cycle instead of once a year in spring (seasonal flowering [SF]) have been identified in cultivated (*F. x ananassa*) and woodland (*F. vesca*) strawberries (Iwata et al., 2012; Gaston et al., 2013). This trait allows the flowering period to be extended and increases fruit yield. In *F. vesca*, this phenotype is caused by the recessive *tfl1* mutation (Brown and Wareing, 1965) in *TERMINAL FLOWER1* (*FveTFL1*), a floral repressor gene (Iwata et al., 2012). In this species, a runnerless recessive mutant (*r*) has been discovered (Brown and Wareing, 1965) and the locus was mapped onto linkage group II (Sargent et al., 2004). In *F. x ananassa*, we recently showed that the genetic control of these two major characters is different from that in *F. vesca* and that the dominant *PFRU* mutation has an opposite effect on flowering and runnering (Gaston et al., 2013; Perrotte et al., 2016a). The basis for this antagonism is poorly understood. In the two species, stolons are produced from axillary meristems (AXMs) and this process is regulated by various endogenous and environmental factors including age, daylength, temperature, and hormones (Hytönen and

[1] Address correspondence to beatrice.denoyes@inra.fr or christophe.rothan@inra.fr.
The authors responsible for distribution of materials integral to the findings presented in this article in accordance with the policy described in the Instructions for Authors (www.plantcell.org) are: Béatrice Denoyes (beatrice.denoyes@inra.fr) and Christophe Rothan (christophe.rothan@inra.fr).
[OPEN] Articles can be viewed without a subscription.
www.plantcell.org/cgi/doi/10.1105/tpc.16.00949

Elomaa, 2011). To date, the molecular mechanisms underlying the differentiation of an AXM to a stolon remain elusive.

To search for genetic factors controlling stolon induction from AXM, we investigated the *F. vesca* recessive *r* mutant. Here, we provide evidence that AXM fate is responsible for the trade-off between flowering and runnering using a population segregating for the *r* and *tfl1* mutations. We further show, using classical and mapping-by-sequencing strategies, that a deletion in a *gibberellin 20-oxidase* (*GA20ox*) gene expressed in AXM and in the developing stolon underlies the runnerless [r] phenotype in *F. vesca*. In addition, we show that stolon formation can be rescued by the exogenous application of bioactive gibberellin (GA) onto the *r* mutant. This work highlights the pivotal role of a specific AXM-expressed GA20ox enzyme, which catalyzes a rate-limiting step in the synthesis of bioactive GAs, in the induction of stolon differentiation in AXM and therefore in the trade-off between vegetative propagation and flowering in strawberry.

RESULTS

The Regulation of Axillary Meristem Fate Governs the Trade-Off between Flowering and Runnering

Strawberry is a perennial rosette-forming herbaceous plant. The primary shoot or primary crown (PC) is composed of leaves and AXMs at the axils of leaves and is terminated by an inflorescence (Figure 1A). The fate of the AXM depends on its location in the plant. When the shoot apical meristem (SAM) becomes floral, the AXM at the axil of the uppermost leaf below the terminal inflorescence develops into a shorter secondary shoot or branch crown (BC), leading to sympodial branching. AXMs along the PC can develop into either a BC (Sugiyama et al., 2004) or a stolon, which is a specialized and highly elongated stem (Savini et al., 2008), or stay dormant. This fate is controlled by genotypic and environmental factors (Hytönen et al., 2008, 2009).

Wild-type woodland strawberries such as 'Sicile' produce stolons and are seasonal flowering [SF] (Figure 1B). The 'Alpine' *r* mutant fails to produce stolons. In addition, 'Alpine' carries the natural *tfl1* allele conferring a PF phenotype (Iwata et al., 2012; Koskela et al., 2012) and therefore flowers continuously from spring to late fall. In [SF] genotypes, floral induction at the SAM is triggered in fall by short days and by low temperature (Heide et al., 2013) and, consequently, the inflorescences emerge in the following spring (Perrotte et al., 2016b). We crossed 'Alpine' *r tfl1* with 'Sicile' wild type to produce the 'Ilaria_F_2' population, which segregated for both flowering and runnering. Segregation for runnerless [r] ($\leq$3 stolons per plant per year) and runnering [R] (>3 stolons per plant per year) phenotypes was consistent with the 3:1 ([R]/[r]) ratio (Supplemental Figure 1) expected for the recessive *r* mutation (Brown and Wareing, 1965). Segregation for [PF] was consistent with the 3:1 ([SF]/[PF]) ratio expected for the recessive *tfl1* mutation (Iwata et al., 2012). In the second year after planting of the 'Ilaria_F_3' population, [SF] individuals flowered in March-April, while [PF] individuals flowered continuously from March to September. In both [SF] and [PF] subpopulations, we clearly observed an increase in the number of inflorescences produced in the *r* background (Figure 1C) that is reminiscent of the trade-off controlled by the single *PFRU* locus in cultivated strawberry *F. x ananassa* (Gaston et al., 2013). These results further suggest that the genetic regulation of AXM fate as either stolons or BCs bearing inflorescences is central for controlling strawberry productivity.

We therefore examined the fate of AXMs in the *r* and wild-type genotypes. For this purpose, we introgressed the runnering wild-type allele from *F. bucharica* into *F. vesca* 'Reine des Vallées' ('RdV') *r tfl1* to create the near-isogenic line (NIL) 'Fb2:39-63' ('Fb2') *tfl1* (Urrutia et al., 2015). In 'Fb2', AXMs at the 6th leaf and above produced stolons, while the uppermost AXM produced a BC. In 'RdV', all AXMs produced BCs or remained dormant (Figure 1D). The same effect of the *r* mutation on plant architecture was observed in 'Alpine' *r tfl1* when compared with 'Sicile' wild type (Supplemental Figure 2). We further examined AXMs in more detail in 'RdV' and 'Fb2' (Figures 1E to 1H). Regardless of their fate, AXM morphology and shape were similar between 'Fb2' and 'RdV'. Thus, in the *r* mutant, the fate of an AXM that does not produce stolon is to remain dormant or to generate a BC terminated by an inflorescence. This is likely the cause of the trade-off between runnering and flowering and, thus, of the differences in productivity observed in the 'Ilaria_F_3' population segregating for the *r* mutation (Figure 1C).

Homozygous Deletion in *FveGA20ox4* Is Strictly Linked to the [r] Phenotype

The *R* (*RUNNERING*) locus carrying the *r* mutation was previously mapped onto LGII within a 989-kb range (Sargent et al., 2004) (Figure 2A). Using microsatellites in the 'Ilaria_F_2' population enlarged with 1350 additional individuals, we mapped the *r* mutation and reduced the region to 87.5 kb (Figure 2A). Whole-genome sequencing (WGS) (Supplemental Table 1) of pools of [r] recombinants (homozygous for runnerless) allowed the identification of 23 SNPs/InDels linked to the *r* mutation in a 63.28-kb region. We further checked the status of these SNPs/InDels in two genotypes, i.e., *F. vesca* displaying either [R] ('Pawtuckaway') or [r] ('Baron Solemacher') phenotypes, using genome sequence data available in a public database (Jung et al., 2014), hypothesizing a single origin for the *r* mutation in the available *F. vesca* germplasm. We made this assumption because [r] has been used for decades in *F. vesca* breeding, like [PF] (Iwata et al., 2012). Only one deletion (DEL) and 10 SNPs are linked to the *r* mutation, encompassing a 59.11-kb region containing eight genes (Figures 2B and 2C; Supplemental Table 2). To further reduce the *R* locus, we used [R] heterozygous recombinants. We investigated the heterozygosity of the *R* locus through phenotyping of seedlings issued from selfing. Among the [R] recombinants, one named alpha5-58 was found to be informative because it was heterozygous for runnering, according to the phenotype of its progeny, and it recombined just after the DEL in *FveGA20ox4* (Figure 2D). By combining phenotyping and genotyping data from the 26 F_3 lines issued from selfing, we unambiguously identified the DEL at position 25,536,553 on chromosome 2 as the *r* mutation; it is located in a *GA20ox* gene (cited as *FveGA20ox4*; Mouhu et al., 2013) (gene09034) (Figures 2D and 2E). DEL in *FveGA20ox4* is an in-frame 9-bp deletion located in the second exon of the gene (Figure 2E) leading to the production of a shorter protein (ΔFvega20ox4) missing the $Cys^{268}Val^{269}Lys^{270}$ amino acids (Figure 2F).

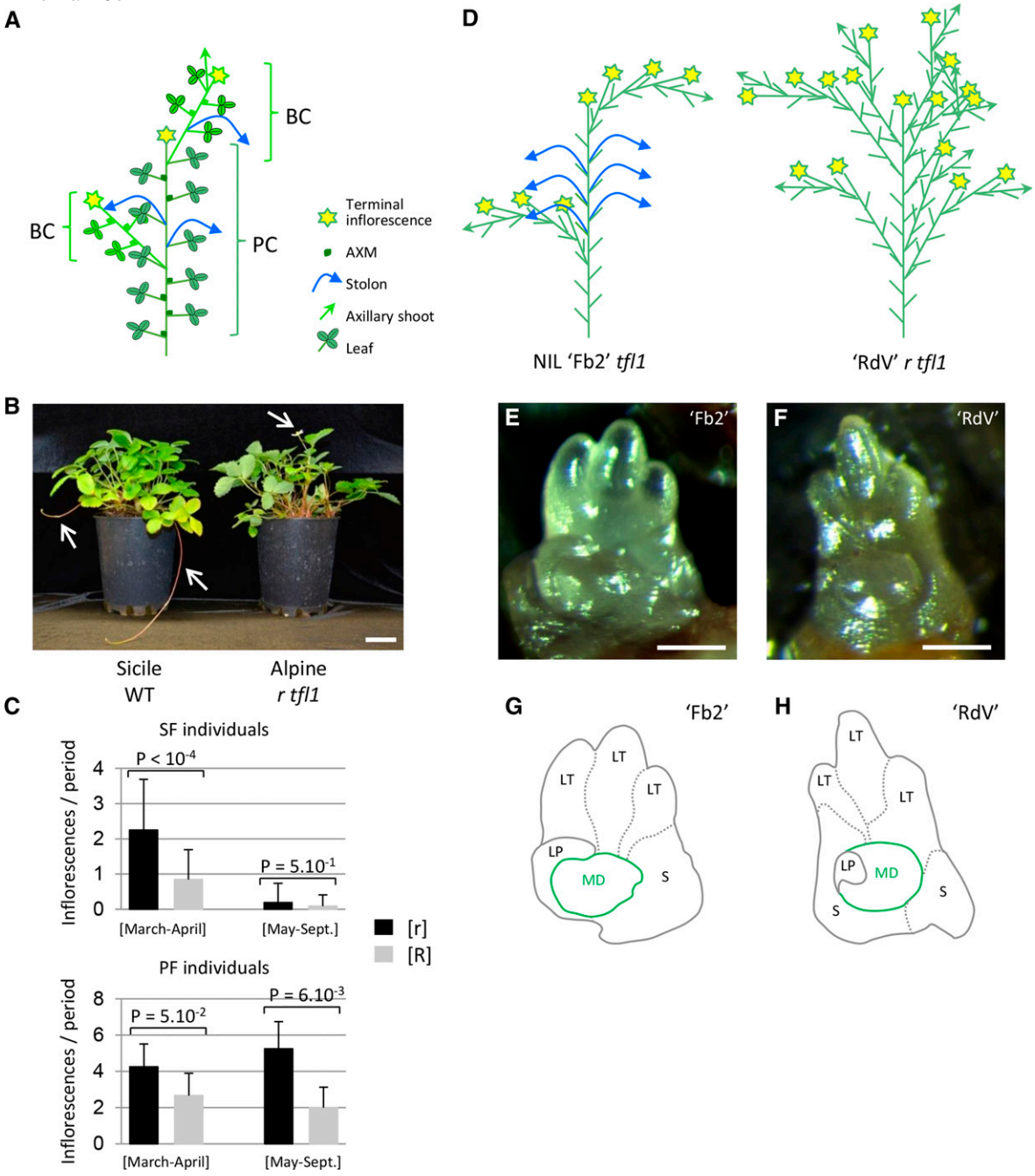

Figure 1. *r* Mutant Phenotype and Flowering/Runnering Trade-Off in *F. vesca*.

(A) Architecture of strawberry plant. The primary shoot or PC is composed of leaves, with AXMs at the axils of leaves and is terminated by an inflorescence. Along the PC, AXMs can develop in either BCs or stolons or stay dormant. Green arrow, axillary shoot; blue arrow, stolon; yellow star, inflorescence.
(B) The 'Sicile' wild type (WT) develops stolons typical of a wild-type plant ([R] phenotype). 'Alpine' is a natural runnerless *r* mutant ([r] phenotype) carrying the *tfl1* perpetual flowering mutation. Arrows, stolons and flower.
(C) Flowering/runnering trade-off in *F. vesca*. Runnering reduces the number of inflorescences in both seasonal [SF] and perpetual flowering [PF] individuals. Data are shown for the second year of phenotyping. $n = 18, 80, 5$, and 9 for [SF r], [SF R], [PF r], and [PF R], respectively, $\pm$SD. Mann-Whitney test is considered statistically significant at $P < 0.05$.
(D) Architecture of 'Reine des Vallées' ('RdV') *r tfl1* and NIL 'Fb2' *tfl1*. In 'Fb2', AXMs produce either stolons (blue arrows) or BCs (green arrows) terminated by an inflorescence (star). In 'RdV', almost all AXMs produce BCs terminated by inflorescences, leading to a bushy plant. Short green line represents developed leaf. Three 5.5-month-old plants were analyzed per genotype.
(E) to **(H)** AXMs of 'Fb2' *tfl1* **(E)** and 'RdV' *r tfl1* **(F)** and their schematic drawing (**[G]** and **[H]**). LT, leaflet; LP, leaf primordium; S, stipule; MD, meristematic dome.
Bars = 5 cm in **(B)** and 100 μm in **(E)** and **(F)**.

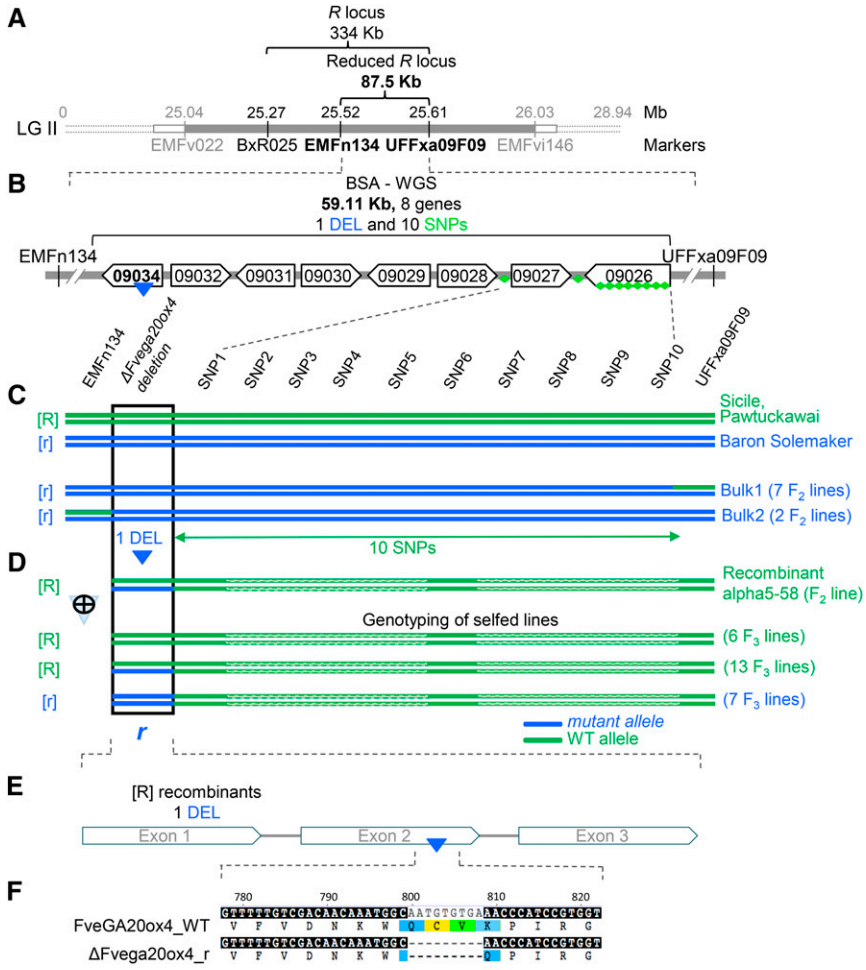

Figure 2. Mutation in *FveGA20ox4* Underlies the *R* Locus.

(A) Map-based cloning of the *R* locus (in gray) in linkage group 2 (LGII) (Sargent et al., 2004). The *R* locus was reduced to 334 kb using microsatellite markers (in black) and to 87.5 kb by recombinant analysis of 1350 individuals.

(B) *R* locus reduced to 59.11 kb by bulk segregant analysis-WGS. This region includes eight genes. Of the 11 SNPs/InDels linked to the runnerless phenotype identified, one deletion (DEL, blue triangle) is in a predicted *GA20ox* (gene09034) and 10 SNPs (green diamonds) are either in intergenic regions or in predicted genes (Supplemental Table 2).

(C) Identification of the *r* mutation responsible for the runnerless trait by screening a large number of recombinant lines (1350 individuals) from the Ilaria F_2 population to identify runnerless ([r] phenotype) lines recombining between the two markers (EMFn134 and UFFxa09F09) flanking the *r* mutation. The nine recombinant runnerless lines identified were grouped into two bulks according to the position of the breaking point: left to marker UFFxa09F09 (Bulk1 with seven F_2 lines) and right to marker EMFn134 (Bulk2 with two F_2 lines). WGS of these bulks and of Sicile (runnering [R] phenotype) (25× to 35× genome coverage) allowed the identification of all polymorphisms (23 SNPs/InDels) in the chromosomal region carrying *r*. Comparison with genome sequences of 'Pawtuckawai' ([R] phenotype) and 'Baron Solemacher' ([r] phenotype) available at https://www.rosaceae.org/ further allowed the reduction of the candidate polymorphisms to 11 SNPs/InDels. The deletion (DEL) in gene *FveGA20ox4* was the most likely candidate due to the function of the protein.

(D) Unequivocal identification of DEL in *FveGA20ox4* as the causal mutation. Recombinant lines were screened to identify one runnering line ([R] phenotype) named alpha5-58, which was heterozygous at the *FveGA20ox4* locus and recombined just after the DEL in *FveGA20ox4*. After selfing, 26 F_3 lines were obtained, seven of which displayed a runnerless [r] phenotype. All seven lines were homozygous for the DEL in *FveGA20ox4*, recombined after this mutation, and were homozygous wild type thereafter. The 10 SNPs carried by the chromosomal segment after the DEL in *FveGA20ox4* were therefore excluded as candidate polymorphisms. The recessive DEL in *FveGA20ox4* (*ΔFvega20ox4*) was confirmed as the causal mutation for the runnerless [r] phenotype.

(E) DEL of nine nucleotides occurs in exon 2 of *GA20ox* (gene09034).

(F) A shorter protein with a deletion of three amino acids ($Cys^{268}Val^{269}Lys^{270}$) is produced in the *r* mutant (ΔFvega20ox4_r) in comparison with FveGA20ox4_WT.

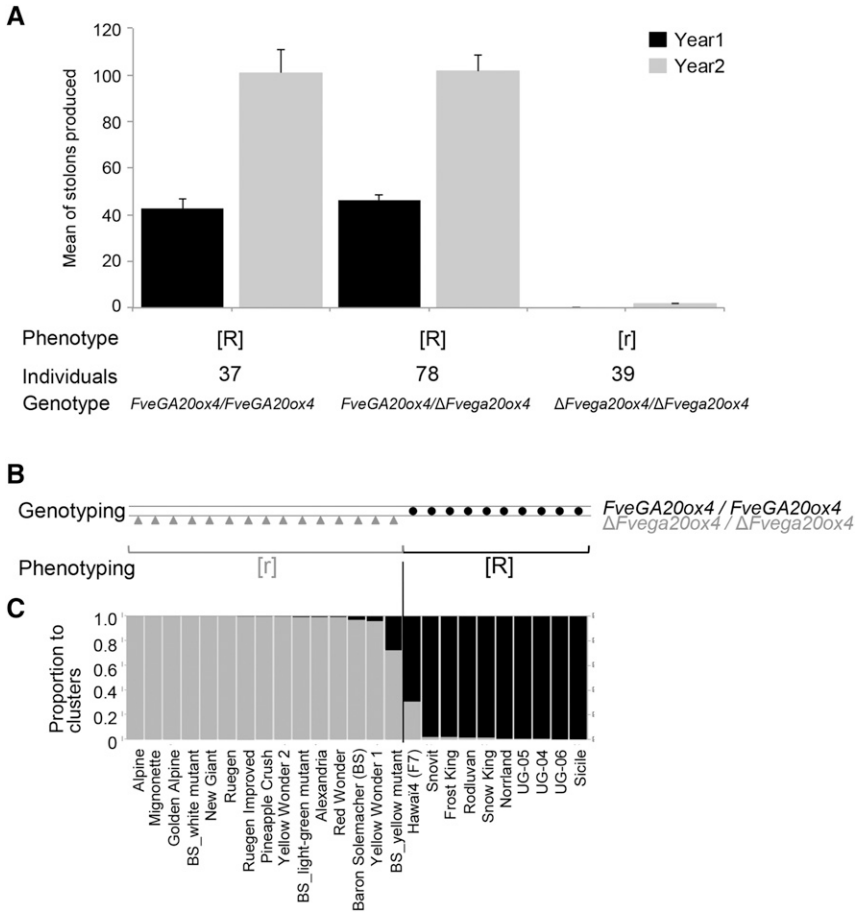

Figure 3. Distribution of *r* Mutation in Ilaria_F_2 Segregating Population and in *F. vesca* Germplasm.

(A) Allelic status of *FveGA20ox4* in the Ilaria_F_2 segregating population. The 154 plants were scored as runnering [R] or runnerless [r] when the number of stolons was >3 or ≤3, respectively. The *FveGA20ox4* wild-type allele confers [R] phenotype when present in simple or double dose. The Δ*Fvega20ox4* mutant allele confers [r] phenotype when presents in double dose. Error bars show SE.

(B) Genotyping of *FveGA20ox4* and phenotyping of runnering. *FveGA20ox4* is the wild-type gene, and *ΔFvega20ox4* is the deleted mutant version. Circle, homozygous *FveGA20ox4*/*FveGA20ox4*; triangle, homozygous *ΔFvega20ox4*/*ΔFvega20ox4*. [R], runnering phenotype; [r], runnerless phenotype.

(C) Genetic structure of 25 *F. vesca* accessions. Genetic structure was determined by examining 37 microsatellite loci distributed throughout the genome. Each accession is represented by a single vertical line, which is partitioned into gray and black segments in proportion to the estimated membership in the two clusters (K = 2).

The unequivocal genetic evidence that *FveGA20ox4* controls the decision of the AXM to generate a stolon correlates well with existing data showing that exogenously applied bioactive gibberellins (GA_3) affect stolon production in strawberry (Thompson and Guttridge, 1959; Hytönen et al., 2009). We further checked its genetic status in the Ilaria_F_2 population (Figure 3A) and confirmed that all [r] individuals were homozygous for the deleted allele, Δ*Fvega20ox4*. Plants homozygous or heterozygous for the wild-type allele were [R] (Figure 3A). Additionally, we analyzed 25 [r] and [R] accessions of *F. vesca* from different geographical origins to determine if runnering depends on the allelic status of *FveGA20ox4* (Figure 3B) and if the genetic structure of the population is linked to the runnering trait (Figure 3C). In all 25 accessions, the runnering behavior was consistent with the *FveGA20ox4* genotype: A runnering [R] phenotype was associated with a homozygous wild-type allele and runnerless [r] was associated with a homozygous mutant allele (Figure 3B). We further analyzed genome-wide population structure using Structure (Pritchard et al., 2000). The ΔK statistic (Evanno et al., 2005), designed to identify the most relevant number of clusters (K) in a population, was the highest for K = 2. By using a membership probability threshold (Q-value) of 0.7, all accessions were clearly assigned to one group that corresponds to the *FveGA20ox4* allelic status *R* or *r* (Figure 3C). This result suggests that the *r* mutation contributed to the genetic structure of these accessions. Because all runnerless mutants are arranged in a single cluster, these results are in agreement with the single origin of the mutation.

FveGA20ox4 Is Strongly Expressed in the AXM

Strawberry *GA20ox* predicted on the basis of their homology with known GA20ox include FveGA20ox1, FveGA20ox2, FveGA20ox3,

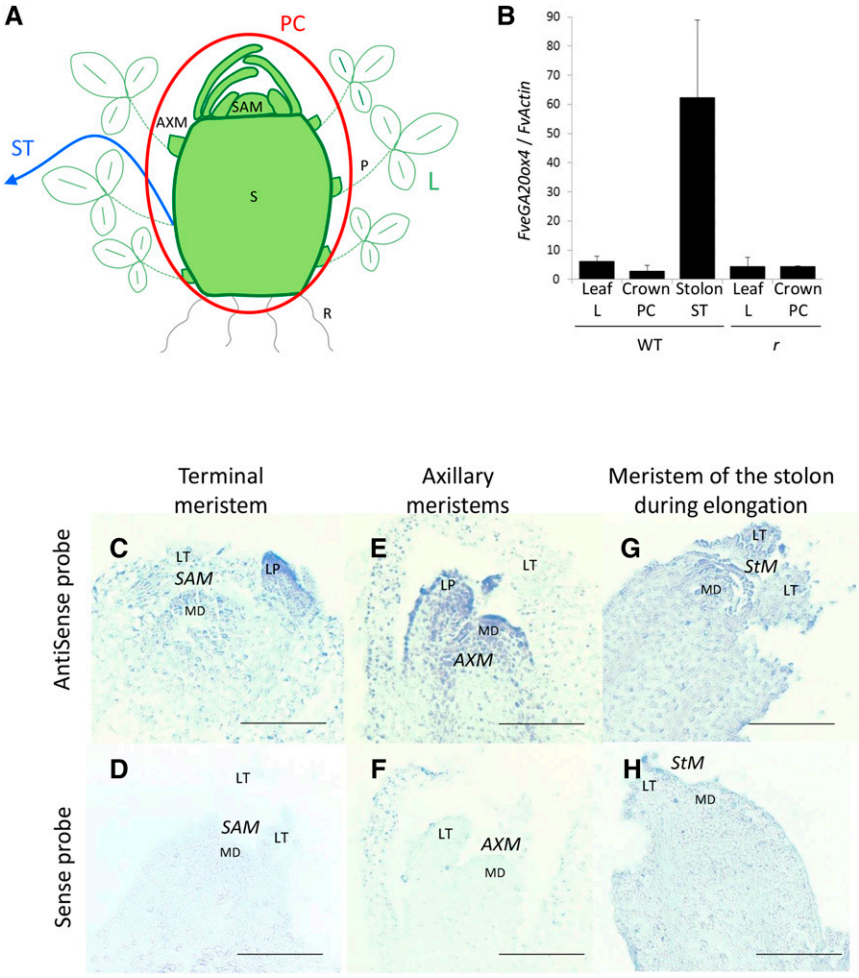

Figure 4. *FveGA20ox4* Transcripts Are Localized in the Axillary Meristem and Stolon.

(A) Tissue sampling of PC (in red circle), leaf (L), and stolon (ST; blue arrow). PC includes stem (S), SAM, and AXMs. R, roots.
(B) Relative expression of *FveGA20ox4* in leaf, PC, and stolon of 'Fb2' wild type and 'RdV' *r* mutant. Normalization with *FveActin*. $n = 3 \pm$ SE.
(C) to **(H)** In situ hybridization of *FveGA20ox4* on the 'Fb2' *tfl1* SAM (**[C]** and **[D]**), AXM (**[E]** and **[F]**), and meristem of the stolon during elongation (**[G]** and **[H]**). Upper panel of **(C)**, **(E)**, and **(G)**, antisense probe; lower panel of **(D)**, **(F)**, and **(H)**, sense probe. Samples were processed side-by-side with sense and antisense probes. MD, meristematic dome; LT, leaflet; LP, leaf primordium; ST, stolon; StM, stolon meristem. Bar = 0.1 mm.

and FveGA20ox4, as well as the more distantly related FveGA20ox5 (Kang et al., 2013; Mouhu et al., 2013). Phylogenetic analysis indicated clustering of FveGA20ox4 with AtGA20ox from *Arabidopsis thaliana* (Supplemental Figure 3A). In the 'Fb2' wild-type and 'RdV' *r* genotypes, *FveGA20ox2* and *FveGA20ox5* were preferentially expressed in the PC, *FveGA20ox3* was expressed in all vegetative aerial organs (Supplemental Figure 4), and *FveGA20ox1* was not detected. In contrast, *FveGA20ox4* was strongly and preferentially expressed in the stolon (Figures 4A and 4B). In situ hybridization of 'Fb2' wild type detected transcript accumulation in the AXM dome as well as the leaf primordia and leaflet (Figures 4E to 4H), but not in the SAM (Figures 4C and 4D).

We overexpressed *FveGA20ox4* in the Arabidopsis *Atga20ox1* single mutant and in the *Atga20ox1 Atga20ox3* double mutant, which display a dwarf phenotype (Phillips et al., 1995; Rieu et al., 2008; Plackett et al., 2012), to further explore its functional role. The expression of *FveGA20ox4* rescued the dwarf phenotype of both the single and double mutants and increased plant height in the wild type (Figures 5A and 5B), thus validating in planta the predicted gibberellin biosynthesis function of FveGA20ox4. The overexpression of Δ*Fvega20ox4* mostly produced dwarf phenotypes in the wild-type background and was unsuccessful in the single and double mutant background, i.e., no seed germination (Figure 5C), suggesting that the mutated protein has a dominant-negative effect.

Because *FveGA20ox4* transcript abundance was not affected in the *r* mutant (Figure 4B), we further investigated whether the three amino acid deletion in FveGA20ox4 protein was responsible for the loss of gibberellin biosynthetic activity. Comparison of FveGA20ox4 with other GA20ox from Arabidopsis indicated that the deletion was within the predicted catalytic domain of the enzyme (Lange et al., 1997; Huang et al., 2015), thus possibly affecting its

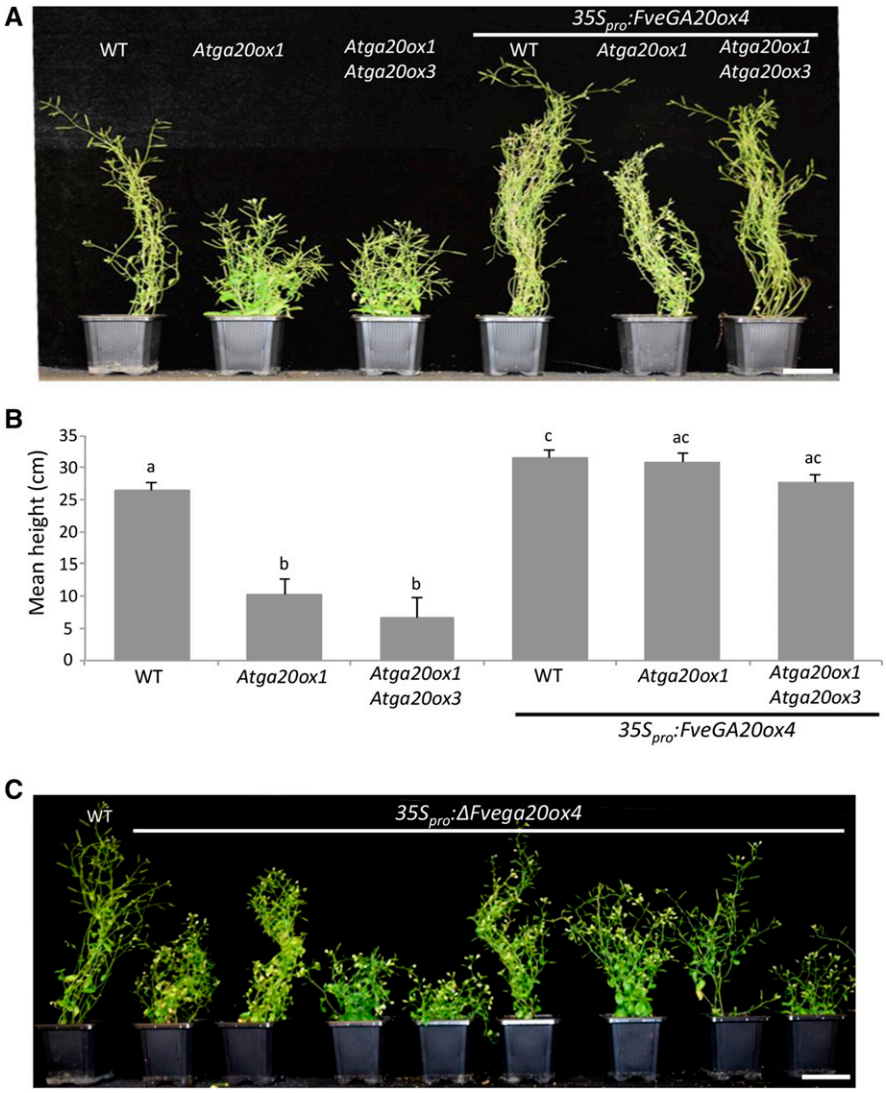

Figure 5. Overexpression of FveGA20ox4 in Dwarf Atga20ox Arabidopsis Mutants Restores Plant Growth, Whereas Overexpression of ΔFvega20ox4 Causes a Dwarf Phenotype in the Wild Type.

(A) and **(B)** Arabidopsis Colombia-0 (WT), *Atga20ox1* single mutant, and *Atga20ox1 Atga20ox3* double mutant overexpressing FveGA20ox4.
(A) Representative image of controls and transgenic plants transformed with *35S$_{pro}$:FveGA20ox4*. Bar = 5 cm.
(B) Height of the transgenic Arabidopsis lines overexpressing FveGA20ox4. *n* = 6 for controls and 10 for transgenic plants ±SE. Values with different letters differ significantly (Mann-Whitney test) ($P < 0.05$).
(C) Arabidopsis Colombia-0 (WT) overexpressing ΔFvega20ox4. Representative image of controls and transgenic plants transformed with *35S$_{pro}$:Δ Fvega20ox4*. Bar = 5 cm.

activity (Supplemental Figure 3B). GA20ox enzymes catalyze several reactions in the GA biosynthetic pathway to produce precursors that are further converted into bioactive GAs by subsequent enzymes in the pathway (Figure 6A). We produced recombinant FveGA20ox4 and ΔFvega20ox4 proteins and showed that, while wild-type FveGA20ox4 converted [^{14}C] GA_{12} to [^{14}C] GA_9 (Figure 6B), as do most other GA20ox enzymes analyzed to date (Pimenta Lange et al., 2013), the mutated ΔFvega20ox4 enzyme was not able to convert the GA_{12} substrate, indicating that the deleted version of the protein was not functional (Figure 6C).

Gibberellin Regulates AXM Fate

Because of the preferential transcript accumulation of *FveGA20ox4* in AXM and in the meristem of the stolon during elongation (Figures 4E and 4G) and the effect of its loss of function on AXM fate, we investigated the endogenous GA levels in stolon, leaf, and PC tissue from two runnering genotypes ('Sicile' and 'Fb2') and, for comparison, in leaf and PC tissue from two runnerless genotypes ('Alpine' and 'RdV'). The 13-hydroxylated pathway, which leads to the production of the biologically active

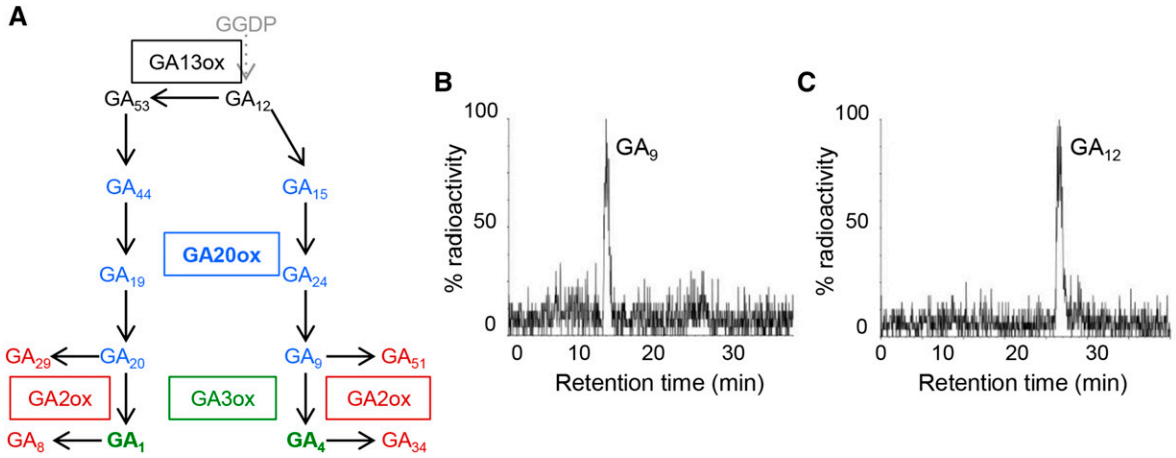

Figure 6. Deletion Leads to a Loss of FveGA20ox4 Catalytic Activity.

(A) Simplified GA biosynthetic pathway. Intermediates (blue), bioactive (green), and inactive (red) GAs are represented for the last steps of the pathway. Enzymes are framed and colored according to the product of the reaction.

(B) and **(C)** HPLC-radiochromatograms of products from incubations of recombinant FveGA20ox4 wild type **(B)** and ΔFvega20ox4 mutant **(C)** proteins with ^{14}C-labeled GA_{12}. Identities of substrate and product were confirmed as methyl esters trimethylsilyl ethers by gas chromatography-mass spectrometry by comparison of their mass spectra with published spectra.

form GA_1 and of the inactive catabolic forms GA_{29} and GA_8 (Hedden and Thomas, 2012) (Figure 6A), is the predominant GA biosynthetic pathway in strawberry (Taylor et al., 1994). GA_1 levels were higher in the leaves than in BCs and stolons (Supplemental Table 3). Strikingly, GA_8 accumulated strongly in the stolon, supporting the hypothesis of high GA20ox activity driven by the strong transcript accumulation of *FveGA20ox4* in this organ and further suggesting that the stolon should also have high GA 3-oxidase activity to produce GA_1 from GA_{20} and high GA 2-oxidase activity to fine-tune GA_1 levels via GA_1 to GA_8 catabolism (Hedden and Thomas, 2012).

As expected from these results and from previous reports (Hytönen et al., 2009), treatment of a wild-type genotype ('Rodluvan') in the spring with prohexadione-calcium (Pro-Ca), an inhibitor of GA oxidases (Rademacher, 2000), led to the severe reduction and eventually (4 weeks after treatment) the arrest of stolon emergence (Figures 7A and 7B). Stolon production resumed thereafter to its normal level 5 weeks after the last treatment. The number of inflorescences produced was unaffected in the Pro-Ca-treated 'Alpine' *r tfl1* mutant (Figures 7C and 7D). Conversely, treatment of the 'Alpine' *r tfl1* mutant with the bioactive gibberellin GA_3 restored stolon production (Guttridge and Thompson, 1964) to levels similar to those of the wild type at 4 weeks after treatment, after which the effect of GA_3 vanished (Figures 7E and 7F). Conversely, GA_3 treatment had a significant negative effect on the production of inflorescences (Figure 7G).

DISCUSSION

In plant species displaying both sexual reproduction and vegetative propagation through stolons, such as strawberry, the AXM is indeterminate and can produce a stolon or a secondary shoot and inflorescence. In this work, we show that, in the diploid strawberry *F. vesca*, a member of the GA20ox family (which catalyzes the rate-limiting steps in bioactive GA biosynthesis) is specifically expressed in the AXM where it plays a pivotal role in the decision of the meristem to produce either a stolon or an inflorescence-bearing shoot. Depending on the allelic state of *FvGA20ox4*, the AXM either produces a stolon (active allele), remains dormant, or produces a secondary branch crown terminated by an inflorescence (inactive allele). The resulting modification in strawberry architecture translates into a change in inflorescence number in both seasonal and perpetual flowering strawberry genotypes. We therefore identified a way to control the balance between flowering and runnering, both of which are essential for strawberry fruit production, by modifying a key enzyme that can switch propagation type from sexual to asexual reproduction.

Additionally, by studying the allelic status of the *FvGA20ox4* gene in runnering and runnerless *F. vesca* varieties, we provide answers to old questions on the origin of the runnerless trait in cultivated woodland strawberry. Before the breeding of the cultivated hybrid octoploid strawberry *Fragaria* x *ananassa* in the 1750s via a cross between two American species, strawberry species of wild origin were widely cultivated throughout Europe. Among these was *F. vesca*. According to Duchesne (1766), the runnerless trait in woodland strawberry was first described by Furetiere in his Dictionnaire printed in 1690. Furetiere highlighted the rare occurrence of runnerless strawberry plants at that time. Remarkably, Duchesne (1766) already confirmed the genetic origin of the runnerless trait by analyzing more than 30 plants grown from seeds and further observed that runnerless plants had more branch crowns than standard plants. He recognized the *F. vesca* origin of the runnerless mutant, named it *F. eflagellis*,

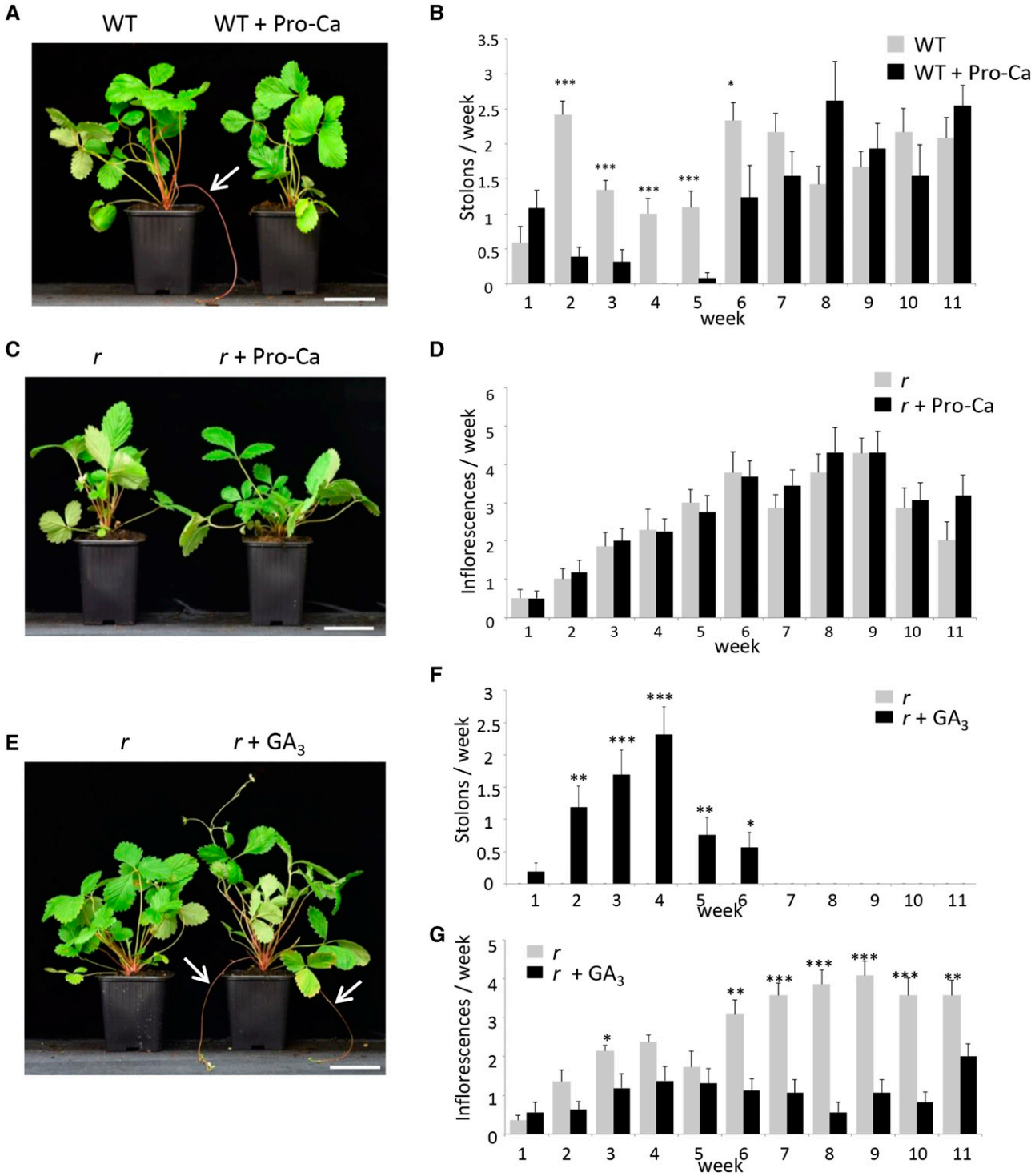

Figure 7. Treatment of the Wild Type and the *r* Mutant with GA Inhibitor (Pro-Ca) and Bioactive GA.

(A) and **(B)** Treatment of the wild type genotype with Pro-Ca.
(A) Representative image showing stolon production (white arrow) on week 3. Bar = 6.5 cm.
(B) Pro-Ca treatment significantly reduces the number of stolons produced between weeks 2 and 6. *n* = 13 or 12 ± SE.
(C) and **(D)** Treatment of the *r* mutant with Pro-Ca.
(C) Representative image on week 3. Bar = 6.5 cm.
(D) Pro-Ca treatment has no effect on the number of inflorescences. *n* = 16 or 14 ± SE.

and indicated that it spread from a garden from Burgundy province in France to several gardens in the Paris area. The runnerless trait has been retained from early varieties until today (Darrow, 1966). More recent varieties such as 'Reine des Vallées' and 'Baron Solemacher' combining runnerless and perpetual flowering traits are still successfully cultivated. We show here that the runnerless trait found in these varieties and in the other runnerless *F. vesca* varieties studied has a single origin that goes back more than three centuries.

GAs are central regulators of many developmental processes (Depuydt and Hardtke, 2011; Davière and Achard, 2013). To date, the role of GA in shoot meristems has primarily been studied in the SAM. Bioactive GAs are produced in the primordia by the key GA biosynthetic enzymes GA20ox to enable organ differentiation and growth. Because GAs promote cell differentiation and SAM indeterminacy must be maintained, bioactive GAs are excluded from the meristematic dome through several mechanisms (Galinha et al., 2009; Veit, 2009). In the cells surrounding the meristematic dome, bioactive GAs can be converted to inactive GAs by GA 2-oxidase. Depending on the species, the photoperiod, and the meristem fate, both GA20ox and GA 2-oxidase genes are further regulated by several transcription factors including KNOX (Sakamoto et al., 2001; Hay et al., 2002; Rosin et al., 2003; Jasinski et al., 2005; Bolduc and Hake, 2009), SHORT VEGETATIVE PHASE, and SOC1 (Li et al., 2008; Tao et al., 2012; Andrés et al., 2014). By contrast, the regulation of the induction of stolon differentiation in the AXM by GAs remains poorly understood (Hytönen et al., 2009). In potato, exogenous application of bioactive GAs promotes the production of stolons from AXMs, while the inactivation of bioactive GAs reduces stolon emergence (Kumar and Wareing, 1974; Kloosterman et al., 2007). In strawberry, treatment with bioactive GAs in long days (LDs) inhibits flowering but enhances stolon production (Thompson and Guttridge, 1959; Hytönen et al., 2009); inhibition of GA biosynthesis has the opposite effect (Hytönen et al., 2009). One hypothesis is that GA precursors or bioactive GAs synthesized in the leaf under LD move to the AXM to promote stolon induction (Eriksson et al., 2006; Regnault et al., 2015). This idea is further supported by the finding that overexpressing *FveSOC1* in *F. vesca* induces both stolon production and *FveGA20ox4* transcript accumulation in the leaf (Mouhu et al., 2013).

Actually, our data demonstrate that *FveGA20ox4* is strongly expressed in the AXM, whereas we detected weak transcript accumulation in other vegetative tissues. Moreover, transcriptome analysis of reproductive tissues at various developmental stages failed to detect *FveGA20ox4* transcripts in expanding fruit (Kang et al., 2013). Stolon differentiation is not induced when *FveGA20ox4* is inactivated, strongly suggesting that the bioactive GAs controlling stolon induction are specifically synthesized in the AXM and are not transported from the leaf to the AXM. Taking as model the photoperiodic activation of GA biosynthesis in the SAM during flowering in Arabidopsis (Andrés et al., 2014), which is a LD species unlike the short-day (SD) strawberry (Heide et al., 2013), it is tempting to speculate that, under inductive LD conditions, FLOWERING LOCUS T (Mouhu et al., 2013) upregulates *SOC1* expression specifically in the strawberry AXM, where in turn it induces the high *FveGA20ox4* expression required for stolon differentiation. Because *FveGA20ox4* transcript accumulation is not restricted to the flanks of the AXM but also occurs in the meristematic dome, an additional level of control would be necessary to maintain a pool of undifferentiated cells in the meristem of the growing stolon. Such control could be fulfilled by GA 2-oxidase, which converts bioactive GA_1 to the inactive GA_8 that accumulates to high levels in the stolon.

Our data further demonstrate that the production of BCs is the default developmental program of the AXMs present in the PC. When FveGA20ox4 is inactivated, the AXM eventually shifts from stolon to BC production, which is consistent with previous observations on the fate of stolon tips under LDs (i.e., stolon production) and under SDs (i.e., BC production) (Hytönen et al., 2009). As shown here, this has considerable influence on strawberry productivity in both seasonal flowering and perpetual flowering strawberry genotypes. Due to strong inbreeding depression (Kaczmarska et al., 2016), it is necessary to produce daughter plants in order to vegetatively propagate strawberry varieties, hence excluding the commercial use of strict runnerless mutants. It is technically feasible to use bioactive GAs and GA inhibitors to modulate runnering/flowering (Hytönen et al., 2008), but such products are currently not registered for commercial use for vegetative propagation in many countries. The identification of *FveGA20ox4* as a breeding target thus provides the opportunity to modulate daughter plant production/fruit yield in octoploid cultivated strawberry by screening strawberry genetic resources for weak alleles of *FveGA20ox4* and introgressing them into commercial varieties via marker-assisted selection. In addition, the newly developed CRISPR/Cas9 system for gene editing, which is well adapted for use in polyploid species (Wang et al., 2014) and has already proved its utility for improving crop yields via altering plant architecture (Krieger et al., 2010; Park et al., 2014), can be used to target one or several *FveGA20ox4* homoeoalleles of *F. x ananassa* and thus modulate the runnering/flowering balance in cultivated strawberry.

Figure 7. (continued).

(E) to **(G)** Treatment with bioactive GA restores runnering in the *r* mutant.

(E) Representative image showing stolon production (white arrows) in the *r* mutant after GA_3 treatment on week 3. Bar = 6.5 cm.

(F) Quantification of stolon production after GA_3 treatment. Mock-treated plants never produce stolon.

(G) Quantification of inflorescence production after GA_3 treatment. $n = 16$ and 14 for GA-treated and mock-treated plants ± SE. Treatments were performed twice a week during the first two weeks (last treatment on week 1). Asterisks indicate significant differences (Mann-Whitney test): *$P < 0.05$, **$P < 0.01$, and ***$P < 0.001$.

METHODS

Plant Material and Growth Conditions

Diploid strawberry (*Fragaria vesca*) genotypes were used in this study. Seeds were sown in a mixture of two-thirds loam and one-third grit and grown at 16-h/8-h day/night at 22°C/18°C using supplementary light at 150 μmol m^{-2} s^{-1} (high pressure sodium lamp; Philips 400W). Plants were transplanted to 1-liter pots containing the same mixture and were maintained in a greenhouse under natural conditions.

The wild-type 'Sicile' and 'Rodluvan' (wild type) (seasonal flowering [SF] and runnering [R] phenotypes) varieties and the 'Alpine' and 'Reine des Vallées' ('RdV') (perpetual flowering [PF] and runnerless [r] phenotypes) varieties, which carry the *r* mutation in the *tfl1* background (*r tfl1* double mutant), were used for plant architecture analysis, *r* mutation mapping, and/or hormonal treatments. For *r* mutation mapping, 'Alpine' was crossed with 'Sicile' to generate an F_2 population of 154 individuals named Ilaria_F_2. For fine mapping, 1350 additional Ilaria_F_2 individuals were produced. The trade-off between flowering and runnering was analyzed in an F_3 population of 112 individuals named Ilaria_F_3 issued from selfing of one Ilaria_F_2 individual. The segregation ratios of *r* and *tfl1* in Ilaria_F_2 and F_3 were as expected for recessive mutations.

The runnerless 'RdV' *r tfl1* genotype and the runnering NIL 'Fb2:39-63' ('Fb2') *tfl1* genotype were used for plant architecture analysis, meristem imaging, in situ hybridization, and qRT-PCR. 'Fb2' *tfl1* was obtained by introgression of the wild-type *F. bucharica* runnering locus into 'RdV'. The 3.7-Mb introgression is located between positions 18.950.307 and 22.663.853 of *F. vesca* genome v1.1 (Urrutia et al., 2015).

Seeds of the *Arabidopsis thaliana Atga20ox1* single mutant (SALK_016701C) and the *Atga20ox1-3/Atga20ox3-1* double mutant (Rieu et al., 2008; Plackett et al., 2012) were provided by The Nottingham Arabidopsis Stock Centre. Columbia-0 (Col-0) ecotype was used as a control. Plants were grown under 16-h/8-h day/night at 22°C/18°C with 70/62% humidity in a growth chamber. Light level was 100 μmol m^{-2} s^{-1} (Philips 400W).

Plant Phenotyping

Phenotyping of the Ilaria_F_2 and F_3 populations was performed during two successive years after sowing. Seeds from Ilaria_F_2 and F_3 were respectively sown in October and March and plants were grown in LD conditions under 16-h/8-h day/night and placed in a greenhouse under natural conditions in April. To quantify stolons in the Ilaria_F_2 and Ilaria_F_3 populations, the stolons in each individual were counted weekly during two successive years and were removed after counting. In addition, to analyze the trade-off between inflorescence and stolon production in the Ilaria_F_3 population, inflorescences in each individual were counted weekly from March to September during two successive years. Stolons and inflorescences were counted when they visually emerged. The seasonal flowering period occurred during March and April and was a consequence of floral initiation in the previous autumn (Perrotte et al., 2016b), whereas the perpetual flowering period occurred from May to September (end of phenotyping). The *F. vesca* genetic resources were phenotyped by the National Clonal Germplasm Repository (USDA) for the presence or absence of stolons during a 2-year period. To evaluate the impact of GA_3 and Pro-Ca on inflorescence emergence and stolon production, the number of inflorescences and stolons was counted weekly until 11 weeks after treatment in 'Rodluvan' wild type and 'Alpine' *r tfl1* at 3 months old.

Plant Architecture, Meristem Observation, and in Situ Hybridization

Plant architecture of 'Sicile' wild type, 'Alpine' and 'RdV' *r tfl1*, and 'Fb2' *tfl1* was analyzed using 5.5-month-old plants grown in the greenhouse. The plants were dissected and the different organs, including leaves, inflorescences, and stolons, were organized according to their position on the PC and its BCs.

Meristems and emerging stolons from the PCs of 4-month-old 'Fb2' *tfl1* and/or 'RdV' *r tfl1* plants were dissected under a stereomicroscope for photography and in situ hybridization. For in situ hybridization, PCs including either the SAM or AXM with two young leaves were fixed according to standard protocols (Sicard et al., 2008). In situ hybridization experiments were performed as described previously (Bisbis et al., 2006). Digoxygenin-UTP-labeled antisense RNAs for exon 1 of *FveGA20ox4* were transcribed with T7 RNA polymerase and used as probes. FveGA20ox4_ISH primers are used (forward, CATCAAAGCTTCATGCTCG; reverse, AGTATCTTCAAAACCATTCC, 5′-3′).

Map-Based Cloning of the *r* Mutation Followed by a Combination of Bulk Segregant Analysis and WGS Analyses

The *R* locus, which was previously mapped on LGII within a 989-kb region (Sargent et al., 2004), was first narrowed down to a 334-kb region between markers BxR025 (forward, TAACCGGAATCGGAGAGATG; reverse, ACAGCTTCATTTGCGCTTTT, 5′-3′) and UFFxa09F09 (Sargent et al., 2006) using new or previously developed (https://www.rosaceae.org) microsatellites in the Ilaria_F_2 population of 154 individuals. For fine mapping, the Ilaria_F_2 population was enlarged to 1350 additional individuals, which were screened for recombination between BxR025 and UFFxa09F09. Phenotyping and genotyping of the recombinants with new microsatellites allowed the *R* locus to be reduced to a region between EMFn134 and UFFxa09F09 (Sargent et al., 2006). Genotyping was performed using previously published procedures for DNA extraction (Qiagen) and microsatellite polymorphism identification (Till et al., 2003).

A strategy combining bulk segregant analysis and WGS was developed to reduce the number of SNPs/InDels linked to the *r* mutation. Nine homozygous [r] individuals recombining between markers EMFn134 and UFFxa09F09 were selected and pooled into two bulks with genotypes recombining either in the left part of the locus (seven genotypes; bulk1) or the right part of the locus (two genotypes; bulk2). Illumina paired-end shotgun indexed libraries were obtained for bulks 1 and 2 *r* mutants and 'Sicile' wild type and sequenced to a depth of 35× and 25×, respectively, on an Illumina HiSeq 2500 at GeT-PlaGe (INRA) per the manufacturer's instructions (Illumina). Raw fastq files were mapped to the strawberry reference genome sequence *F. vesca* v2.0.a1 (Shulaev et al., 2011; Tennessen et al., 2014) using BWA version 0.7.12 (Li and Durbin, 2009) (http://bio-bwa.sourceforge.net/). Variant calling (SNPs and InDels) was performed using SAMtools version 1.2 (Li et al., 2009) (http://htslib.org/). Variant analysis and comparison between *r* bulks and 'Sicile' wild type were performed as previously described (Garcia et al., 2016; Petit et al., 2016). The SNPs identified were further analyzed using WGS of one [r] genotype, 'Baron Solemacher', and one [R] genotype, 'Pawtuckaway', available in GDR (https://www.rosaceae.org/).

Genetic Structures of 25 *F. vesca* Accessions

The relatedness of 25 *F. vesca* accessions was studied with 37 neutral microsatellite loci (Supplemental Table 4) distributed throughout the genome using the Bayesian assignment approach from Structure v2.3.4 (Pritchard et al., 2000). The most relevant number of subpopulations (clusters, K) in the population was determined according to the criterion of Evanno, using the ΔK method (Evanno et al., 2005). Leaves used for DNA extraction were obtained from the National Clonal Germplasm Repository (USDA). Genotyping was performed using the KASP method (Smith and Maughan, 2015).

Phylogenetic Analysis, RNA Isolation, and qRT-PCR

Phylogenetic analysis was performed with GA20ox proteins, GA 2-oxidase proteins, and GA 3-oxidase proteins from *F. vesca* strawberry and Arabidopsis (Supplemental Table 5). The suffix used for *F. vesca* is *Fve*

according to Jung et al. (2015). GA20ox proteins included the five predicted FveGA20ox proteins already identified (http://bioinformatics.towson.edu/Strawberry/default.aspx). Multiple sequence alignments were generated via ClustalW (Supplemental File 1; Thompson et al., 1997) using BLOSUM matrix with default parameter setting (gap cost between 0.1 and 10). A phylogenetic tree was produced with the Geneious Tree Builder (http://www.geneious.com/) from 1000 bootstrap replicates by applying the neighbor-joining method with Jukes-Cantor like genetic distance model. Parameter settings were the following: no gap penalty, no outgroup, random seed of 1000, support threshold of 25%.

All tissue samples were collected at the end of April from 4-month-old 'Fb2' *tfl1* and 'RdV' *r tfl1* mutant plants. Leaves, PCs, and stolons were dissected and frozen in liquid N_2 before RNA isolation with a Spectrum Plant Total RNA kit (Sigma-Aldrich). cDNA synthesis was performed with 1 μg of total RNA with an iScript cDNA synthesis kit (Bio-Rad) following the manufacturer's instructions. RT-PCR was performed using 5 μL of the resulting cDNA product (1/10 dilution) and 10 mM of each primer in a final volume of 20 μL with GoTaq qPCR Master Mix (Promega). For each tissue sample (leaves, PCs, or stolons), three biological replicates, each resulting from the pooling of tissues from two plants, and three technical replicates per biological replicate were analyzed using a CFX96 real-time system (Bio-Rad). *FveACTIN* (gene26612) was used as a reference gene. The primers used are described in Supplemental Table 4.

Overexpression in Arabidopsis and Enzymatic Activity Assays

A 1696- and a 1687-bp DNA fragment corresponding to the open reading frame of *FveGA20ox4* and Δ*Fvega20ox4* were PCR-amplified from 'Sicile' wild type and 'Alpine' *r* mutant, respectively, using BxFveGA20ox4_C primers (forward, ATGCTTCCTATTCTTCTTTC; reverse, TCAATTGACTGATTTGGATTC, 5′-3′) and cloned through LR reaction (Gateway) into the pK7WG2D plasmid. The resulting vectors were introduced into *Agrobacterium tumefaciens* (strain GV3101) by electroporation. Five Arabidopsis plants of each genotype, Col-0, *Atga20ox1*, and *Atga20ox1-3*/*Atga20ox3-1*, were transformed by the floral dip method (Clough and Bent, 1998). For plant height measurements, six plants were phenotyped for controls and 10 for transgenic lines when possible.

The cDNAs (FveGA20ox4 gene09034-v1.0-hybrid) corresponding to the FveGA20ox4 wild-type protein (FveGA20ox4) and the mutated form (ΔFvega20ox4) were synthesized (Integrated DNA Technologies), PCR-amplified, and cloned behind a 6xHis tag into Champion pET300/NT-DEST vector through the LR reaction (Gateway). Recombinant plasmids were transformed into *Escherichia coli* strain Rosetta 2 (DE3; Novagen). Protein production was induced with 1 mM isopropyl β-D-1-thiogalactopyranoside for 2 h at 30°C in 2× YT medium.

Recombinant protein production, enzyme assays, and enzyme product purification and analysis were performed essentially as described previously (Lange, 1997; Pimenta Lange et al., 2013). The identities of substrate and products were confirmed as their methyl esters trimethylsilyl ethers by gas chromatography-mass spectrometry by comparing their mass spectra with published spectra (Gaskin and MacMillan, 1992): [1-,7-,12-,18-^{14}C]GA_{12} mass/charge (% relative abundance), M^+352(5), 344(3), 320(11), 312(6), 306(8), 298(4), 290(34), 284(20), 245(100), 239(52), 201(47), 195(22); [1-,7-,12-,18-^{14}C]GA_9, M^+338(6), 330(3), 306(75), 298(45), 276(100), 270(54), 251(60), 243(42), 233(66), 232(78), 227(38), 226(48), 189(48), 183(36).

GA Analysis and Treatments

GA content of leaves, PCs, and stolons (when present) was characterized in four genotypes: wild-type 'Sicile' and 'Fb2' and 'Alpine' and 'RdV' *r* mutants. Tissues were dissected from twelve 4-month-old plants. For 'RdV' and 'Fb2', two biological replicates (each resulting from the pooling of tissues from three plants) were analyzed for each tissue. For 'Sicile' and 'Alpine', one sample was analyzed for each tissue. GAs were analyzed using 100 mg dry weight of freeze-dried sample that was spiked with 17,17-d2-GA standards (1 ng each, from L. Mander, Canberra, Australia) as previously described (Lange et al., 2005).

For GA_3 and Pro-Ca treatments, 3-month-old 'Rodluvan' wild type and 'Alpine' *r* mutant plants were sprayed twice a week during the first 2 weeks, weeks 0 and 1, with either GA_3 (50 mg/L) or Pro-Ca (100 mg/L), as previously described (Mouhu et al., 2013). On the first day of the experiment, stolons of 'Rodluvan' wild type were removed. Plants were grown under natural conditions in the greenhouse under long days (June). Stolons were systematically removed after counting.

Statistical Analysis

When appropriate, a two-sided Mann-Whitney test was performed.

Accession Numbers

Arabidopsis Genome Initiative locus identifiers (https://www.arabidopsis.org/) used in this study are as follows: *At4G25420* (*AtGA20ox1*), *At5G51810* (*AtGA20ox2*), *At5G07200* (*AtGA20ox3*), *At1G60980* (*AtGA20ox4*), *At1G44090* (*AtGA20ox5*), *At1G78440* (*AtGA2ox1*), *At1G30040* (*AtGA2ox2*), *At2G34555* (*AtGA2ox3*), *At1G47990* (*AtGA2ox4*), *At1G02400* (*AtGA2ox6*), *At1G50960* (*AtGA2ox7*), *At4G21200* (*AtGA2ox8*), *At1G15550* (*AtGA3ox1*), *At1G80340* (*AtGA3ox2*), *At4G21690* (*AtGA3ox3*), and *At1G80330* (*AtGA3ox4*). *F. vesca* locus identifiers can be found in the Strawberry Genomic Resources database (http://bioinformatics.towson.edu/strawberry/) under the following accession numbers: *gene13360* (*FveGA20ox1*), *gene19438* (*FveGA20ox2*), *gene19437* (*FveGA20ox3*), *gene09034* (*FveGA20ox4*), *gene10825* (*FveGA20ox5*), *gene05020* (*FveGA2ox1*), *gene00852* (*FveGA2ox2*), *gene03182* (*FveGA2ox3*), *gene07935* (*FveGA2ox4*), *gene19549* (*FveGA2ox5*), *gene06004* (*FveGA3ox1*), *gene01056* (*FveGA3ox2*), *gene01058* (*FveGA3ox3*), *gene01059* (*FveGA3ox4*), *gene01060* (*FveGA3ox5*), and *gene11192* (*FveGA3ox6*).

Supplemental Data

Supplemental Figure 1. Frequency distribution of the number of stolons produced in the Ilaria_F_2 segregating population.

Supplemental Figure 2. Architecture of the wild type and *r* mutants.

Supplemental Figure 3. Comparison between FveGA20ox4 and GA oxidases of *Arabidopsis thaliana*.

Supplemental Figure 4. Expression of three additional *FveGA20ox* found in *F. vesca*.

Supplemental Table 1. Illumina paired-end shotgun indexed libraries obtained for bulks 1 and 2 *r* mutants and 'Sicile' wild type.

Supplemental Table 2. List of the 11 SNPs/InDel in linkage disequilibrium with *r* allele.

Supplemental Table 3. Endogenous GA contents of 'Sicile' and 'Fb2' wild type, 'Alpine', and 'RdV' *r*.

Supplemental Table 4. List of primers used in the manuscript.

Supplemental Table 5. Gene identifiers for phylogenetic analysis.

Supplemental File 1. Alignment used to produce the phylogenetic tree in Supplemental Figure 3.

ACKNOWLEDGMENTS

This research was funded by the French Ministry of Research. We thank Nahla Bassil (USDA-ARS, NCGR, Corvallis, OR) for diversity resources and Peter Hedden (Rothamsted Research, UK) for Arabidopsis mutant seeds.

We thank Johann Petit for photos, Frédéric Delmas for plant transformation, Norbert Bollier for recombinant protein production, Jean-Philippe Mauxion for genotyping, and Alain Bonnet for help with phenotyping. CNRGV Toulouse confirmed the sequence of *Fragaria* diploid in the *R* locus by BAC sequencing. WGS data were produced by GeT-PlaGe Toulouse, France. This work was supported by Région Aquitaine (REGAL Project) and by the French Academy of Agriculture (Dufrenoy Grant to T.T., 2015) and was carried out under the auspices of the EU-FP7-KBBE-2010-4 Project (Grant 265942).

AUTHOR CONTRIBUTIONS

T.T., C.R., and B.D. designed the experiments. C.B. performed next-generation sequencing bioinformatics analysis. M.J.P.L. and T.L. performed enzymatic activity and GA endogenous assays. A.M. produced the NIL genotype. M.L. performed architecture experiments. M.H. conducted in situ hybridization. T.T. performed all the other experiments. T.T., C.R., and B.D. wrote the manuscript. All authors discussed the results.

Received March 20, 2017; revised August 14, 2017; accepted August 31, 2017; published September 5, 2017.

REFERENCES

Abrahamson, W.G. (1980). Demography and vegetative reproduction. In Demography and Evolution in Plant Populations, O.T. Solbrig, ed (Berkeley, CA: University of California Press), pp. 89–106.

Andrés, F., Porri, A., Torti, S., Mateos, J., Romera-Branchat, M., García-Martínez, J.L., Fornara, F., Gregis, V., Kater, M.M., and Coupland, G. (2014). SHORT VEGETATIVE PHASE reduces gibberellin biosynthesis at the Arabidopsis shoot apex to regulate the floral transition. Proc. Natl. Acad. Sci. USA **111:** E2760–E2769.

Barrett, S.C.H. (2015). Influences of clonality on plant sexual reproduction. Proc. Natl. Acad. Sci. USA **112:** 8859–8866.

Bisbis, B., Delmas, F., Joubès, J., Sicard, A., Hernould, M., Inzé, D., Mouras, A., and Chevalier, C. (2006). Cyclin-dependent kinase (CDK) inhibitors regulate the CDK-cyclin complex activities in endoreduplicating cells of developing tomato fruit. J. Biol. Chem. **281:** 7374–7383.

Bolduc, N., and Hake, S. (2009). The maize transcription factor KNOTTED1 directly regulates the gibberellin catabolism gene ga2ox1. Plant Cell **21:** 1647–1658.

Brown, T., and Wareing, P.F. (1965). The genetical control of the everbearing habit and three other characters. Euphytica **14:** 97–112.

Clough, S.J., and Bent, A.F. (1998). Floral dip: a simplified method for Agrobacterium-mediated transformation of *Arabidopsis thaliana*. Plant J. **16:** 735–743.

Costes, E., Crespel, L., Denoyes, B., Morel, P., Demene, M.-N., Lauri, P.-E., and Wenden, B. (2014). Bud structure, position and fate generate various branching patterns along shoots of closely related Rosaceae species: a review. Front. Plant Sci. **5:** 666.

Darrow, G.M. (1929). Development of runners and runner plants in the strawberry. No. 157352, Technical Bulletins, USDA, Economic Research Service, http://EconPapers.repec.org/RePEc:ags:uerstb:157352.

Darrow, G.M. (1966). The Strawberry: History, Breeding and Physiology. (New York: Holt Rinehart Winston).

Davière, J.-M., and Achard, P. (2013). Gibberellin signaling in plants. Development **140:** 1147–1151.

Depuydt, S., and Hardtke, C.S. (2011). Hormone signalling crosstalk in plant growth regulation. Curr. Biol. **21:** R365–R373.

Duchesne, N. (1766) Histoire Naturelle des Fraisiers. (Paris: Didot Panckoucke).

Eriksson, S., Böhlenius, H., Moritz, T., and Nilsson, O. (2006). GA4 is the active gibberellin in the regulation of LEAFY transcription and Arabidopsis floral initiation. Plant Cell **18:** 2172–2181.

Evanno, G., Regnaut, S., and Goudet, J. (2005). Detecting the number of clusters of individuals using the software STRUCTURE: a simulation study. Mol. Ecol. **14:** 2611–2620.

Galinha, C., Bilsborough, G., and Tsiantis, M. (2009). Hormonal input in plant meristems: A balancing act. Semin. Cell Dev. Biol. **20:** 1149–1156.

Garcia, V., et al. (2016). Rapid identification of causal mutations in tomato EMS populations via mapping-by-sequencing. Nat. Protoc. **11:** 2401–2418.

Gaskin, P., and MacMillan, J. (1992). GC-MS of the Gibberellins and Related Compounds: Methodology and a Library of Spectra. (Bristol, UK: Cantock's Enterprises).

Gaston, A., Perrotte, J., Lerceteau-Köhler, E., Rousseau-Gueutin, M., Petit, A., Hernould, M., Rothan, C., and Denoyes, B. (2013). PFRU, a single dominant locus regulates the balance between sexual and asexual plant reproduction in cultivated strawberry. J. Exp. Bot. **64:** 1837–1848.

Guttridge, C.G., and Thompson, P.A. (1964). The effect of gibberellins on growth and flowering of Fragaria and Duchesnea. J. Exp. Bot. **15:** 631–646.

Hay, A., Kaur, H., Phillips, A., Hedden, P., Hake, S., and Tsiantis, M. (2002). The gibberellin pathway mediates KNOTTED1-type homeobox function in plants with different body plans. Curr. Biol. **12:** 1557–1565.

Hedden, P., and Thomas, S.G. (2012). Gibberellin biosynthesis and its regulation. Biochem. J. **444:** 11–25.

Heide, O.M., Stavang, J.A., and Sønsteby, A. (2013). Physiology and genetics of flowering in cultivated and wild strawberries - A review. J. Hortic. Sci. Biotechnol. **88:** 1–18.

Huang, Y., Wang, X., Ge, S., and Rao, G.Y. (2015). Divergence and adaptive evolution of the gibberellin oxidase genes in plants. BMC Evol. Biol. **15:** 207.

Hytönen, T., and Elomaa, P. (2011). Genetic and environmental regulation of flowering and runnering in strawberry. Genes Genomics **5:** 56–64.

Hytönen, T., Elomaa, P., Moritz, T., and Junttila, O. (2009). Gibberellin mediates daylength-controlled differentiation of vegetative meristems in strawberry (*Fragaria* x *ananassa* Duch). BMC Plant Biol. **9:** 18.

Hytönen, T., Mouhu, K., Koivu, I., and Juntilla, O. (2008). Prohexadione-calcium enhances the cropping potential and yield of strawberry. J. Hortic. Sci. **73:** 210–215.

Iwata, H., Gaston, A., Remay, A., Thouroude, T., Jeauffre, J., Kawamura, K., Oyant, L.H., Araki, T., Denoyes, B., and Foucher, F. (2012). The TFL1 homologue KSN is a regulator of continuous flowering in rose and strawberry. Plant J. **69:** 116–125.

Jasinski, S., Piazza, P., Craft, J., Hay, A., Woolley, L., Rieu, I., Phillips, A., Hedden, P., and Tsiantis, M. (2005). KNOX action in Arabidopsis is mediated by coordinate regulation of cytokinin and gibberellin activities. Curr. Biol. **15:** 1560–1565.

Jung, S., et al. (2014). The Genome Database for Rosaceae (GDR): Year 10 update. Nucleic Acids Res. **42:** 1237–1244.

Jung, S., Bassett, C., Bielenberg, D.G., Cheng, C.H., Dardick, C., Main, D., Meisel, L., Slovin, J., Troggio, M., and Schaffer, R.J. (2015). A standard nomenclature for gene designation in the Rosaceae. Tree Genet. Genomes **11:** 108.

Kaczmarska, E., Garonski, J., Jablonska-Rys, E., Zalewska-Korona, M., Radzki, W., and Slawinska, A. (2016). Hybrid

performance and heterosis in strawberry (Fragaria × ananassa Duchesne), regarding acidity, soluble solids and dry matter content in fruits. Plant Breed. **135:** 232–238.

Kang, C., Darwish, O., Geretz, A., Shahan, R., Alkharouf, N., and Liu, Z. (2013). Genome-scale transcriptomic insights into early-stage fruit development in woodland strawberry *Fragaria vesca*. Plant Cell **25:** 1960–1978.

Klimeš, L., Klimesova, J., Hendricks, R., and van Groenendael, J. (1997). Clonal plant architecture: a comparative analysis of form and function. In The Ecology and Evolution of Clonal Plants, H. de Kroon and J. van Groenendael, eds (Leiden, The Netherlands: Backhuys Publishers), pp. 1–29.

Kloosterman, B., Navarro, C., Bijsterbosch, G., Lange, T., Prat, S., Visser, R.G.F., and Bachem, C.W.B. (2007). StGA2ox1 is induced prior to stolon swelling and controls GA levels during potato tuber development. Plant J. **52:** 362–373.

Koskela, E.A., Mouhu, K., Albani, M.C., Kurokura, T., Rantanen, M., Sargent, D.J., Battey, N.H., Coupland, G., Elomaa, P., and Hytönen, T. (2012). Mutation in TERMINAL FLOWER1 reverses the photoperiodic requirement for flowering in the wild strawberry Fragaria vesca. Plant Physiol. **159:** 1043–1054.

Krieger, U., Lippman, Z.B., and Zamir, D. (2010). The flowering gene SINGLE FLOWER TRUSS drives heterosis for yield in tomato. Nat. Genet. **42:** 459–463.

Kumar, D., and Wareing, P.F. (1974). Studies on tuberization of *Solanum andigena*. New Phytol. **73:** 833–840.

Lange, T. (1997). Cloning gibberellin dioxygenase genes from pumpkin endosperm by heterologous expression of enzyme activities in Escherichia coli. Proc. Natl. Acad. Sci. USA **94:** 6553–6558.

Lange, T., Kegler, C., Hedden, P., Phillips, A.L., and Graebe, J.E. (1997). Molecular characterization of gibberellin 20-oxidases: Structure-function studies on recombinant enzymes and chimaeric proteins. Physiol. Plant. **100:** 543–549.

Lange, T., Kappler, J., Fischer, A., Frisse, A., Padeffke, T., Schmidtke, S., and Pimenta Lange, M.J. (2005). Gibberellin biosynthesis in developing pumpkin seedlings. Plant Physiol. **139:** 213–223.

Li, D., Liu, C., Shen, L., Wu, Y., Chen, H., Robertson, M., Helliwell, C.A., Ito, T., Meyerowitz, E., and Yu, H. (2008). A repressor complex governs the integration of flowering signals in Arabidopsis. Dev. Cell **15:** 110–120.

Li, H., and Durbin, R. (2009). Fast and accurate short read alignment with Burrows-Wheeler transform. Bioinformatics **25:** 1754–1760.

Li, H., Handsaker, B., Wysoker, A., Fennell, T., Ruan, J., Homer, N., Marth, G., Abecasis, G., and Durbin, R.; 1000 Genome Project Data Processing Subgroup (2009). The Sequence Alignment/Map format and SAMtools. Bioinformatics **25:** 2078–2079.

Mouhu, K., Kurokura, T., Koskela, E.A., Albert, V.A., Elomaa, P., and Hytönen, T. (2013). The Fragaria vesca homolog of suppressor of overexpression of constans1 represses flowering and promotes vegetative growth. Plant Cell **25:** 3296–3310.

Park, S.J., Jiang, K., Tal, L., Yichie, Y., Gar, O., Zamir, D., Eshed, Y., and Lippman, Z.B. (2014). Optimization of crop productivity in tomato using induced mutations in the florigen pathway. Nat. Genet. **46:** 1337–1342.

Perrotte, J., Gaston, A., Potier, A., Petit, A., Rothan, C., and Denoyes, B. (2016a). Narrowing down the single homoeologous FaPFRU locus controlling flowering in cultivated octoploid strawberry using a selective mapping strategy. Plant Biotechnol. J. **14:** 2176–2189.

Perrotte, J., Guédon, Y., Gaston, A., and Denoyes, B. (2016b). Identification of successive flowering phases highlights a new genetic control of the flowering pattern in strawberry. J. Exp. Bot. **67:** 5643–5655.

Petit, J., Bres, C., Mauxion, J.-P., Tai, F.W., Martin, L.B.B., Fich, E.A., Joubès, J., Rose, J.K.C., Domergue, F., and Rothan, C. (2016). The glycerol-3-phosphate acyltransferase GPAT6 from tomato plays a central role in fruit cutin biosynthesis. Plant Physiol. **171:** 894–913.

Phillips, A.L., Ward, D.A., Uknes, S., Appleford, N.E.J., Lange, T., Huttly, A.K., Gaskin, P., Graebe, J.E., and Hedden, P. (1995). Isolation and expression of three gibberellin 20-oxidase cDNA clones from Arabidopsis. Plant Physiol. **108:** 1049–1057.

Pimenta Lange, M.J., Liebrandt, A., Arnold, L., Chmielewska, S.-M., Felsberger, A., Freier, E., Heuer, M., Zur, D., and Lange, T. (2013). Functional characterization of gibberellin oxidases from cucumber, *Cucumis sativus* L. Phytochemistry **90:** 62–69.

Plackett, A.R., et al. (2012). Analysis of the developmental roles of the Arabidopsis gibberellin 20-oxidases demonstrates that GA20ox1, -2, and -3 are the dominant paralogs. Plant Cell **24:** 941–960.

Pritchard, J.K., Stephens, M., and Donnelly, P. (2000). Inference of population structure using multilocus genotype data. Genetics **155:** 945–959.

Rademacher, W. (2000). Growth retardants: Effects on gibberellin biosynthesis and other metabolic pathways. Annu. Rev. Plant Physiol. Plant Mol. Biol. **51:** 501–531.

Regnault, T., Davière, J.-M., Wild, M., Sakvarelidze-Achard, L., Heintz, D., Carrera Bergua, E., Lopez Diaz, I., Gong, F., Hedden, P., and Achard, P. (2015). The gibberellin precursor GA12 acts as a long-distance growth signal in Arabidopsis. Nat. Plants **1:** 15073.

Rieu, I., Ruiz-Rivero, O., Fernandez-Garcia, N., Griffiths, J., Powers, S.J., Gong, F., Linhartova, T., Eriksson, S., Nilsson, O., Thomas, S.G., Phillips, A.L., and Hedden, P. (2008). The gibberellin biosynthetic genes AtGA20ox1 and AtGA20ox2 act, partially redundantly, to promote growth and development throughout the Arabidopsis life cycle. Plant J. **53:** 488–504.

Rosin, F.M., Hart, J.K., Van Onckelen, H., and Hannapel, D.J. (2003). Suppression of a vegetative MADS box gene of potato activates axillary meristem development. Plant Physiol. **131:** 1613–1622.

Sakamoto, T., Kamiya, N., Ueguchi-Tanaka, M., Iwahori, S., and Matsuoka, M. (2001). KNOX homeodomain protein directly suppresses the expression of a gibberellin biosynthetic gene in the tobacco shoot apical meristem. Genes Dev. **15:** 581–590.

Sargent, D.J., Davis, T.M., Tobutt, K.R., Wilkinson, M.J., Battey, N.H., and Simpson, D.W. (2004). A genetic linkage map of microsatellite, gene-specific and morphological markers in diploid Fragaria. Theor. Appl. Genet. **109:** 1385–1391.

Sargent, D.J., Clarke, J., Simpson, D.W., Tobutt, K.R., Arús, P., Monfort, A., Vilanova, S., Denoyes-Rothan, B., Rousseau, M., Folta, K.M., Bassil, N.V., and Battey, N.H. (2006). An enhanced microsatellite map of diploid Fragaria. Theor. Appl. Genet. **112:** 1349–1359.

Savini, G., Giorgi, V., Scarano, E., and Neri, D. (2008). Strawberry plant relationship through the stolon. Physiol. Plant. **134:** 421–429.

Shulaev, V., et al. (2011). The genome of woodland strawberry (*Fragaria vesca*). Nat. Genet. **43:** 109–116.

Sicard, A., Petit, J., Mouras, A., Chevalier, C., and Hernould, M. (2008). Meristem activity during flower and ovule development in tomato is controlled by the mini zinc finger gene INHIBITOR OF MERISTEM ACTIVITY. Plant J. **55:** 415–427.

Smith, S.M., and Maughan, P.J. (2015). SNP genotyping using KASPar assays. Methods Mol. Biol. **1245:** 243–256.

Sugiyama, N., Iwama, T., Inaba, Y., Kurokura, T., and Neri, D. (2004). Varietal differences in the formation branch crows in strawberry plants. HortScience **73:** 216–220.

Tao, Z., Shen, L., Liu, C., Liu, L., Yan, Y., and Yu, H. (2012). Genome-wide identification of SOC1 and SVP targets during the floral transition in Arabidopsis. Plant J. **70:** 549–561.

Taylor, D.R., Blake, P.S., and Browning, G. (1994). Identification of gibberellins in leaf tissues of strawberry (*Fragaria* x *ananassa* Duch.) grown under different photoperiods. Plant Growth Regul. **15:** 235–240.

Tennessen, J.A., Govindarajulu, R., Ashman, T.L., and Liston, A. (2014). Evolutionary origins and dynamics of octoploid strawberry subgenomes revealed by dense targeted capture linkage maps. Genome Biol. Evol. **6:** 3295–3313.

Thompson, J.D., Gibson, T.J., Plewniak, F., Jeanmougin, F., and Higgins, D.G. (1997). The CLUSTAL_X windows interface: flexible strategies for multiple sequence alignment aided by quality analysis tools. Nucleic Acids Res. **25:** 4876–4882.

Thompson, P.A., and Guttridge, C.G. (1959). Effects of gibberellic acid on the initiation of flowers and runners in the strawberry. Nature **184:** 72–73.

Till, B.J., et al. (2003). Large-scale discovery of induced point mutations with high-throughput TILLING. Genome Res. **13:** 524–530.

Urrutia, M., Bonet, J., Arús, P., and Monfort, A. (2015). A near-isogenic line (NIL) collection in diploid strawberry and its use in the genetic analysis of morphologic, phenotypic and nutritional characters. Theor. Appl. Genet. **128:** 1261–1275.

Vallejo-Marín, M., Dorken, M.E., and Barrett, S.C.H. (2010). The ecological and evolutionary consequences of clonality for plant mating. Annu. Rev. Ecol. Evol. Syst. **41:** 193–213.

Veit, B. (2009). Hormone mediated regulation of the shoot apical meristem. Plant Mol. Biol. **69:** 397–408.

Wang, Y., Cheng, X., Shan, Q., Zhang, Y., Liu, J., Gao, C., and Qiu, J.-L. (2014). Simultaneous editing of three homoeoalleles in hexaploid bread wheat confers heritable resistance to powdery mildew. Nat. Biotechnol. **32:** 947–951.

A Specific Gibberellin 20-Oxidase Dictates the Flowering-Runnering Decision in Diploid Strawberry

Tracey Tenreira, Maria João Pimenta Lange, Theo Lange, Cécile Bres, Marc Labadie, Amparo Monfort, Michel Hernould, Christophe Rothan and Béatrice Denoyes

Plant Cell 2017;29;2168-2182; originally published online September 5, 2017;
DOI 10.1105/tpc.16.00949